JAR1-mediated JA-Ile accumulation: a mechanism towards drought stress resistance in *Arabidopsis thaliana*

Dissertation

zur Erlangung des Doktorgrades (Dr. rer. nat.)
der
Mathematisch–Naturwissenschaftlichen Fakultät
der
Rheinischen Friedrich–Wilhelms–Universität Bonn

vorgelegt von
Sakil Mahmud
aus Chandpur, Bangladesh

Bonn, 2021

Angefertigt mit Genehmigung der Mathematisch-Naturwissenschaftlichen Fakultät der Rheinischen Friedrich-Wilhelms-Universität Bonn

"Printed and/or published with the support of the German Academic Exchange Service"

Day of the oral examination: 12 October, 2021

Year of publication for doctoral thesis: 2021

1. Gutachterin: Prof. Dr. Ute C. Vothknecht
2. Gutachter: Prof. Dr. Gabriel Schaaf
3. Gutachter: Prof. Dr. Uwe Deppenmeier
4. Gutachterin: Prof. Dr. Dagmar Wachten

Content

Abbreviations

∞	infinity
°C	Degree Celsius
12-COOH-JA-Ile	12-carboxy-Jasmonyl-isoleucine
12-HSO_4-JA	12-*sulfo-jasmonic acid*
12-O-Glc-JA	12-O-β-D-glucopyranosyljasminic acid
12-OH-JA	hydroxyjasmonic acid
12-OH-JA-Ile	12-hydroxy-Jasmonyl-isoleucine
12,13-EOT	12,13–epoxyoctadecatrienoic acid
µ	Micro
ABA	Abscisic acid
ACX	Acyl-CoA oxidase
AGI	Arabidopsis Genome Initiative
ANOVA	Analysis of variance
AOC	Allene oxide cyclase
AOS	Allene oxide synthase
APS	Ammonium persulfate
At/AT	*Arabidopsis thaliana*
BASTA	glufosinate ammonium
bHLHzip	Basic helix-loop-helix leucine zipper
bp	Base pair
BPB	Bromophenol blue
CAM	Calmodulin
CAMTA	Ca^{2+} -calmodulin-binding transcription activator proteins
CBD	Calcineurin B like protein
cDNA	Complementary DNA
CDPK	calcium-dependent protein kinases
CDS	coding sequence
CFP	Cyan Fluorescent Protein
cm	Centi meter
CML	Calmodulin-like protein
CoA	Coenzyme A
COI1	Coronatine insensitive 1
Col-0	Arabidopsis Columbia ecotype
CYP4	Cytochrome P450
d	Day(s)
ddH_2O	Demineralized, deionized water
DEGs	Differentially Expressed Genes
dH_2O	Demineralized water
DHAR	dehydroascorbate reductase
DMSO	Dimethylsulfoxide
DNA	Deoxyribonucleic acid
dNTP	deoxynucleotide solution mix
DTT	Dithiothreitol
DW	dry weight
ECL	Enhanced Chemiluminescence
EDTA	ethylenediamine tetraacetic acid
eGSH	glutathione redox potential
JMT	JA methyltransferase
JOX	Jasmonic Acid Oxidase
KAT	L-3-ketoacyl CoA thiolase
Kb	kilobase
kDa	kilo Dalton
L	Liter
LB	“δysogeny broth” or “δuria broth”
LC-MS	Liquid chromatography mass spectrometry
LEA	Late Embryogenesis Abundant
LOX	13-Lipoxygenase
M	Molar (mol/L)
mA	milliampere
MDA	monodehydroascorbate
MDAR	monodehydroascorbate reductase
MeJA	Methyl jasmonate
MES	2-(N-morpholino)ethanesulfonic acid
MFP	Multifunctional protein
mg	Milligram
min	Minute(s)
mM	Milli Molar
mRNA	Messenger Ribonucleic acid
MS	Mass spectrometry
MS–salt	Murashige–Skoog–Medium
MYB	Myoblast
MYC2 / 3 / 4	Myogenic regulatory factor 2 / 3 / 4
NASC	Nottingham Arabidopsis Stock Centre
NES	Nuclear export signal
NGS	Next Generation Sequencing
NINJA	Novel Interactor of JAZ
nm	nano meter
OD	optical density
OPC-8:0	3-Oxo-2-(2’[Z]-pentenyl)-cyclopentan-1-octanoic acid
OPCL1	OPC-8:CoA ligase
OPDA	*cis*-12-Oxo-phytodienoic acid
OPR3	OPDA reductase 3
Orp1	peroxidase 1
PAGE	Polyacrylamide gel electrophoresis
PCA	Principle Component Analysis
PCR	Polymerase chain reaction
PDF1.2	Plant defensin 1.2
pH	Negative decimal logarithm of the H^+ concentration
PLD	Phospholipase
pro	Promoter
PS	Photosystem
PXA1	Peroxisomal ABC transporter 1
R2R3	Repeat2 Repeat3

EGTA	glycol-bis(2-aminoethylether)-N,N,N',N'-tetraacetic acid
EMBL	European Molecular Biology Laboratory (Heidelberg, Germany)
ER	Endoplasmic reticulum
et al.	et alii
EtOH	Ethanol
FC	Fold Change
FDR	False Discovery Rate
FIN219	Far-red insensitive 219
FT	Flowering locus T
FW	fresh weight
g	Gram
g	Gravity constant (9.81 ms^{-1})
GFP	Green Fluorescent Protein
GH3	Indole-3-acetic acid-amido synthetase
GIF1	GRF1-interacting factor 1
GO	Gene Ontology
GR	Glutathione reductase
GRF5	Growth-regulating factor 5
Grx1	Gtutaredoxin 1
GSH	Reduced glutathione
GSH1	γ-glutamylcysteine ligase
GSH2	glutathione synthetase
GSSG	glutathione oxidized, glutathione disulfide
GUS	β-Glucuronidase
h	Hour(s)
H_2O_2	Hydrogen peroxide
HCl	Hydrochloric acid
His–tag	histidine–affinity tag
HPLC	high performance liquid chromatography
HPOT	Hydroperoxy-octadecatrienoic acid
HSD	Honestly significant difference
ILL6	IAA-amino acid hydrolase
IPTG	Isopropyl–β–D–thiogalactopyranoside
JA	Jasmonic acid
JA-Glc	12- hydroxyjasmonoylglucoside
JA-Ile	Jasmonoyl-isoleucine JA-leucine
JAR1	Jasmonate resistant 1
JAR1-OE	35S::JAR1.1-YFP (Overexpression line of JAR1)
Jas	Jasmonate associated domain
JASSY	jasmonate precursor export transporter
JAZ	Jasmonate-ZIM-domain/ JAZ-interacting domain
RNA	Ribonucleic acid
roGFP2	Redox-sensitive GFP 2
ROS	Reactive Oxygen Species
rpm	Revolutions per minute
RT	Room Temperature
RT-PCR	Reverse transcriptase PCR
RT-qPCR	Quantitative real time polymerase chain reaction
Rubisco	Ribulose-1, 5-bisphosphate carboxylase/oxygenase
s	Second(s)
SALK	Salk–Institute (La Jolla, USA)
SCF-complex	Skp, Cullin, F-box containing complex
SDS	Sodium dodecyl sulphate
SE	Standard Error
SOT15	Sulfotransferase 2a
SWC	soil relative water content
T-20	Tween-20
T-DNA	transferred DNA used for insertional mutagenesis
TAE	tris–acetate–EDTA
TAIR	The Arabidopsis information resource
Taq	*Thermus aquaticus*
TBS	Tris-buffered saline
TCH3	Touch inducible 3
TEMED	N,N,N',N'-Tetramethylethylenediamine
TF	Transcription Factor
TLD	Thermoluminescent Dosimeter
TPL	Topless
TPM	Transcripts Per Million
Tris	2-amino-2-(hydroxymethyl)propane-1,3-diol
Ub	Ubiquitin
UV	Ultraviolet
V	voltage
vs	versus
VSP	Vvegetative Sstorage protein
w/v	Weight per volume
w/w	Weight per weight
WT	wild-type
X-Gluc	5-Bromo-4-chloro-3-indolyl-β-D-glucuronide
YC3.6	Yellow cameleon 3.6
YEB	Yeast Extract Beef
YFP	Yellow Fluorescent Protein
ZIM	Zinc-finger protein expressed in Inflorescence Meristem

List of Tables

List of Figures

1. Introduction

1.1 Drought stress impact on plants

Under the adverse climatic context of global warming, drought has been a severe problem confining plants growth and survival in several regions of the world, particularly the semi-arid and arid regions. Drought is considered as one of the foremost abiotic stresses that negatively affect plant growth and development (Gupta et al., 2020; Claeys and Inze, 2013; Harb et al., 2010). Counteracting water deficiency involves evolving mechanisms like reducing transpirational loss of water, an optimal balance of supplying water among different plant organs, etc. Some morphological adaptations such as stomatal regulation, thickening of the leaf cuticle, a shorter life cycle, limiting shoot growth, and deeper root growth will facilitate the survival of tolerant plants throughout the water deficient period. On a molecular level, plants' resistance mechanisms to drought involve global reprogramming of transcription, post-translational modifications, cellular metabolism, and hormone signaling (Yang et al., 2010). Plants synthesize a chemically diverse range of hormones such as auxins, abscisic acid (ABA), jasmonic acid (JA) etc., which regulate a wide range of functions like growth, development and response to environmental stresses. These hormones act as mediators under different stress conditions to initiate signaling cascades and subsequently transcriptional reprogramming to provide the cellular stress responses (Gupta et al., 2020; Yang et al., 2010; Claeys and Inze, 2013; Verma et al., 2016).

1.2 Jasmonic acid biosynthesis involves multiple steps within different organelles

Jasmonates refer to the multiple derivatives of jasmonic acid (JA), which are the terminal product of the octadecanoid pathway and is derived from plastidial membrane lipids (Figure 1). Jasmonates are involved in a plethora of growth and developmental processes such as flowering, seed germination, root growth inhibition, leaf senescence, fruit ripening, pollen maturation, anther dehiscence, trichome development, photosynthesis, systemic resistance (Zander et al., 2020; Wasternack and Hause, 2013; Koo, 2018). The biosynthesis of jasmonate is initiated from plastidial membrane lipids by different lipoxygenases (LOXs), which add molecular oxygen to α-linolenic acid to form hydroperoxy derivatives (HPOT) (Figure 1). Though many LOXs can be found in Arabidopsis, only LOX2, 3, 4 and 6 are to date found to be related to jasmonate signaling pathway. (Wasternack and Hause, 2013; Bell et al., 1995). The resulting HPOT is rapidly converted to an unstable epoxy derivative by allene oxide

synthase (AOS*)*. AOS is a member of the CYP74 family, which can dehydrate and direct the various pathways involved in HPOT biosynthesis towards jasmonate signaling. (Turner et al., 2002; Laudert et al., 2000; Devoto and Turner, 2005*;* Park et al., 2002). Allene oxide cyclases (AOCs) catalyze the stereospecific cyclization of the unstable epoxide to (9S,13S)-12 oxo-(10,15Z)-phytodienoic acid (*cis*-OPDA) (Wasternack and Hause, 2013). Once *cis*-OPDA is formed, it exits the chloroplast using the recently identified jasmonate precursor export (JASSY) transporter (Guan et al., 2019). The later steps of JA-biosynthesis take place in the peroxisome, where *cis*-OPDA is transported through the potential peroxisomal ABA transporter 1 (PXA1) and is reduced by oxophytodienoic acid reductase 3 (OPR3) to its reduced form 8-[(1R,2R)-3-oxo-2-{(Z)-pent-2-enyl}cyclopentyl]octanoate (OPC-8:0). Afterwards, OPC-8:0 is acetylated by the potential acetyl-CoA ligase (OPCL1/CLL5) to the CoA thioester before entering the β-oxidation cycle. Subsequent oxidation of the thioester potentially by acyl-CoA oxidase (ACX1) followed by the multifunctional protein (MFP) and 3-ketoacyl-CoA thiolase 1 (KAT1) leads to nascent (+)-7-*iso*-JA. The process by which the (+)-7-*iso*-JA is exiting the peroxisome into the cytosol is still unknown. In the cytosol, the unstable (+)-7-*iso*-JA is converted into stable (-)-7-*iso*-JA. JA is modified or conjugated to at least 12 derivatives in the cytosol, but till now the only known biologically active derivative is (+)-7-*iso*-JA-Isoleucine (JA-Ile) (Wasternack and Song, 2017; Koo, 2018; Figure 1).

1.3 JAR1 plays a critical role in the formation of the biologically active jasmonate, JA-Ile

Jasmonate resistant 1 (JAR1), a member of the GH3 gene family (AtGH3.11), is the most important regulator of jasmonate signaling because it is involved in the formation of the biologically active jasmonate, jasmonyl-isoleucine (JA-Ile) in the cytosol (Guranowski et al., 2007; Staswick and Tiryaki, 2004; Figure 1). JAR1 is one of the firefly luciferase enzyme superfamily members, which can adenylate various organic acids. Recent findings suggested that JAR1 is available in different splice variants although their specific functions have not yet been characterized (Zander et al., 2020; Howard et al., 2013). JAR1 can also conjugate jasmonates to other amino acids *in vitro* or *in planta,* but their low amount *in vivo* makes JA-Ile the prime regulator of jasmonate signaling (Staswick and Tiryaki, 2004; Suza and Staswick, 2008). JAR1-mediated synthesis of JA-Ile leads to the formation of the complex comprising JA-Ile, coronatine insensitive 1 (COI1) and the transcriptional repressor jasmonate ZIM-domain (JAZ) (Figure 2).

1.4 Diversification of JA and JA-Ile in the cytosol

In the cytosol, based on the demand of the plant, both JA and JA-Ile can be modified to multiple derivatives (Figure 1) and several of these derivatives can also interact with the coronatine insensitive 1 (COI1) receptor. Hydroxylation of JA preferably leads to 12-OH-JA (Glauser et al., 2008). Lack of knowledge on the gene/protein involved in this pathway makes it difficult to study its proper function in Arabidopsis but a recent finding suggested that jasmonic acid oxidase 3 (JOX3) is involved in this conversion (Smirnova et al., 2017). Further *O*-glycosylation and sulfation of 12-OH-JA results in two highly abundant derivatives, 12-hydroxyjasmonoylglucoside (12-*O*-Glc-JA) and 12-sulfo-jasmonic acid (12-HSO_4-JA), but their exact mode of action in a COI1-dependent manner is not yet understood (Glauser et al., 2008; Gidda et al., 2003). Hydroxylation and further carboxylation lead to the derivatives 12-OH-JA-Ile and 12-COOH-JA-Ile, respectively (Glauser et al., 2008). JA-Ile is hydroxylated to 12-OH-JA-Ile preferably by cytochrome P450 94B3 (CYP94B3) and further carboxylation of 12-OH-JA-Ile produces 12-COOH-JA-Ile by cytochrome P450 94C1(CYP94C1) (Aubert et al., 2015; Poudel et al., 2019). On the other hand, 12-OH-JA-Ile can be converted to JA-Ile by the IAA-amino acid hydrolase 6 (ILL6) (Marquis et al., 2013; Aubert et al., 2015; Wasternack and Hause, 2013; Figure 1). All in all, these derivatives can be directly or indirectly targeted to the COI1-mediated response.

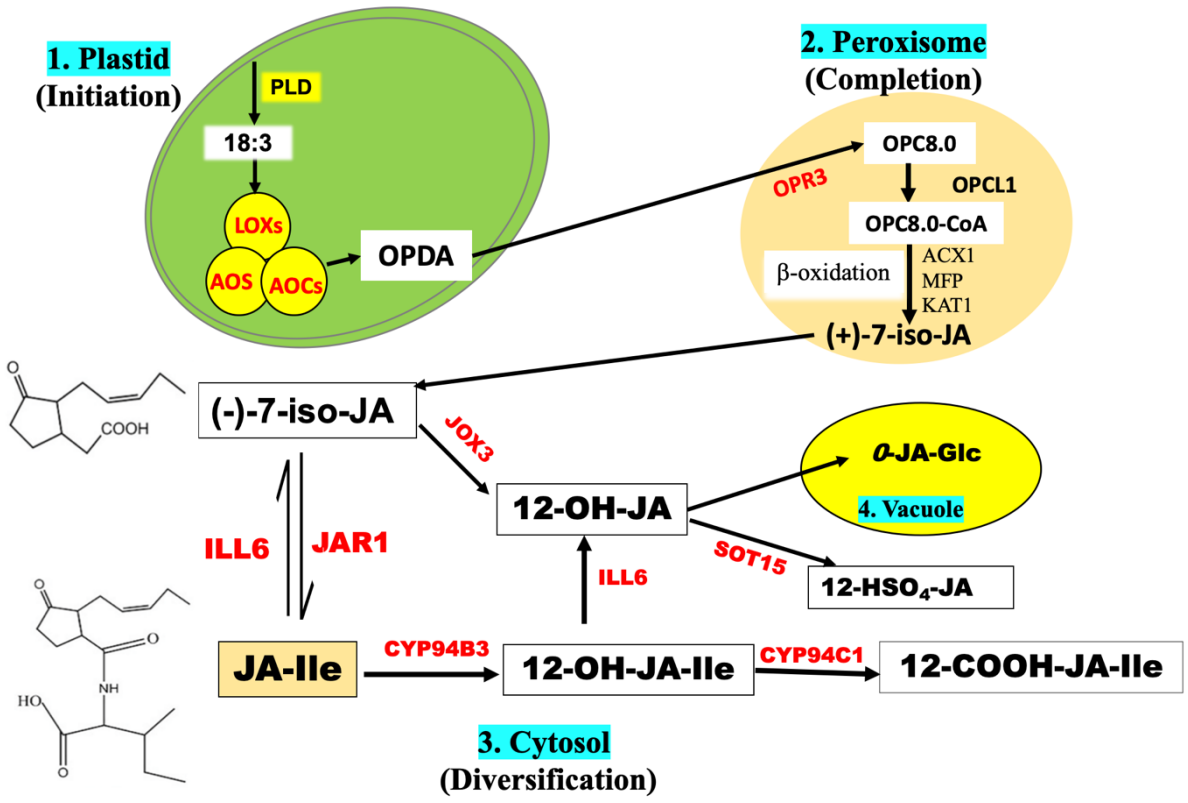

Figure 1: Pathway of jasmonate biosynthesis and diversification.
Phospholipase (PLD) releases α-linolenic acid (C18:3) from chloroplast galactolipids. Subsequent modifications by 13-lipoxygenases (LOXs), allene oxide synthase (AOS) and, allene oxide cyclases (AOCs) lead to the formation of (9S,13S)-12 oxo-(10,15Z)-phytodienoic acid (OPDA). OPDA is reduced to OPC-8.0 by OPDA reductase 3 (OPR3) in the peroxisome. OPC-8: CoA ligase (OPCL1/CLL5) allows esterification to form OPC-8: CoA. Further shortening of the carboxylic acid side chain via the fatty acid β-oxidation machinery, comprising acyl-CoA oxidase (ACX), multifunctional protein (MFP) and L-3-ketoacyl CoA thiolase (KAT). The end product is cleaved by a putative thioesterase (TE) yielding (+)-7-iso-JA, which equilibrates with the more stable (-)-JA in the cytosol. Hydroxylation of JA forms 12-OH-JA putatively by jasmonic acid oxidase 3 (JOX3) which can be further modified to 12- hydroxyjasmonoylglucoside (*O*-JA-Glc) and 12-sulfo-jasmonic acid (12-HSO_4-JA). Jasmonate resistant 1 (JAR1) catalyzes the formation of jasmonyl-isoleucine (JA-Ile). JA-Ile is hydroxylated to 12-OH-JA-Ile preferably by cytochrome CYP94B3 and further carboxylation of 12-OH-JA-Ile produces 12-COOH-JA-Ile by cytochrome CYP94C1. IAA-amino acid hydrolase 6 (ILL6) catalyzes the removal of Isoleucine from JA-Ile and 12-OH-JA-Ile. Arabidopsis enzymes that have been important for understanding jasmonate biosynthesis and diversification are indicated in red. Reaction scheme modified after (Acosta and Farmer, 2010).

1.5 The jasmonate signaling pathway

A critical step in jasmonate signaling is transcriptional regulation through the formation of the JA-Ile-COI1-JAZ complex (Figure 2). COI1 is a member of the F-box protein family and a component of the SKP1-CUL1-F-box protein (SCF) E3 ubiquitin ligase complex that can interact with the transcriptional repressor (JAZ) in the presence of JA-Ile (Wasternack and Song, 2017; Koo, 2018). In the absence of JA-Ile or at lower accumulation than the threshold amount, the C-terminal region of the JAZ protein containing the JA-associated (Jas) domain along with the general corepressor, topless (TPL) and TPL interacting partner, novel interactor of JAZ (NINJA) can bind transcription factors (TFs) and to ultimately attenuate the

transcriptional process. Accumulation of JA-Ile leads to JA-Ile-COI1-JAZ complex formation and the release of the TFs by targeting the JAZ proteins for degradation through the 26S proteasome. This process initiates the jasmonate-response, which regulates a wide range of processes spanning from biotic/abiotic stress responses to vegetative and reproductive development (Wasternack and Song, 2017; Suza and Staswick, 2008; Figure 3). Among the different TFs controlling jasmonate signaling, the bHLH group member MYC2, is considered as a master regulator since it seems to regulate most of the jasmonate-mediated transcriptional responses. Promoter analysis showed that MYC2 can bind to most of the jasmonate-biosynthetic genes, which creates a feedback loop in the jasmonate signaling process (Zander et al., 2020). MYC2 has two interacting partners, MYC3 and MYC4 (Zander et al., 2020; Fernandez-Calvo et al., 2011). A recent study showed that MYC3 shares 50% of the regulation of the genes involved in the jasmonate signaling. MYC2 and MYC3 combined regulate the transcription of 23.2 % of Arabidopsis genes (Zander et al., 2020). MYC2 is also involved in several other jasmonate and ABA-mediated responses (Yadav et al., 2005). The jasmonate signaling response is characterized by the induction of several defense genes such as vegetative storage proteins 1 and 2 (*VSP1*, *VSP2)*, plant defense protein 1.2A (*PDF1.2A)*, etc., and most of them are targets of MYC2 (Wasternack and Song, 2017; Koo, 2018; Figure 2).

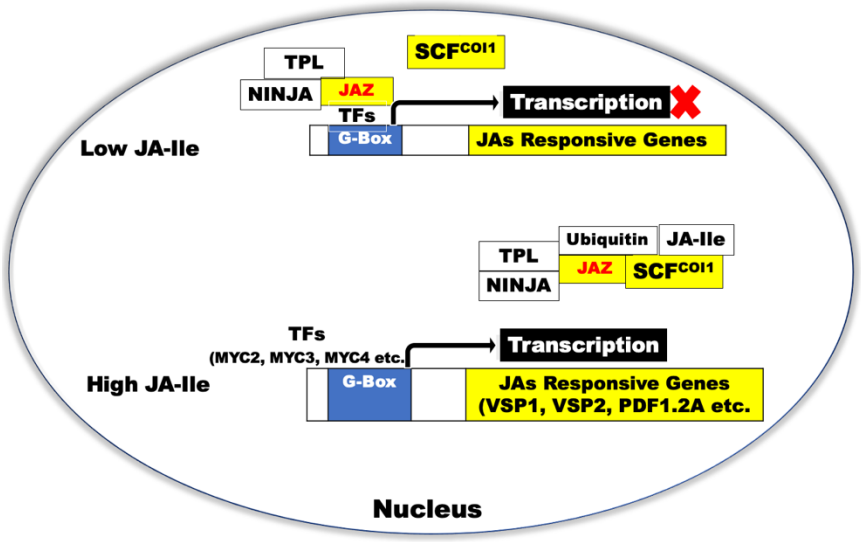

Figure 2: Model of jasmonate response of gene expression.
At the lower amount of JA-Ile under non-stress conditions, TFs (e.g. MYC2, MYC3 and MYC4) bind to their targets at the promoter region (e.g. G-box) but the transcriptional activity is suppressed by JAZ proteins along with its interacting partner, the adaptor protein NINJA and the co-repressor TPL those interact with TFs to inhibit their activity (upper panel). Upon stimuli induction or developmental cues, JA-Ile accumulates and binds to the jasmonate receptor coronatine insensitive1 (COI1), that is a part of SKP1-CUL1-F-box protein (SCF) E3 ubiquitin ligase complex. JAZ proteins recruited themselves from the TFs binding site to the JA-Ile-SCF^{COI1} complex. Further poly ubiquitination leads to degradation of JAZ proteins by 26S proteasome, thereby releasing TFs and activating the transcription of jasmonate-responsive genes (e.g. *VSP1*, *VSP*2, *PDF1.2A*) (lower panel).

1.6 JA-Ile accumulates transiently to regulate a wide range of biological processes

The first jasmonic acid mutant identified was *jar1-1*, which was identified based on root growth insensitivity upon exogenous MeJA application (Staswick et al., 1992). Later on, work on JA-Ile revealed its involvement in flowering (Zhai et al., 2015), pathogen response (Staswick et al., 1998), wounding attack (Suza and Staswick, 2008), ABA interaction (de Ollas et al., 2015a), and systemic expression of JA responsive-marker genes (Wasternack and Song, 2017; Figure 3). In addition, JAR1 is also responsible for hypocotyl elongation (Chen et al., 2018; Swain et al., 2017). Although a comparable amount of JA-Ile is found upon wounding in *jar1-1* compared to WT, a sterile flowering phenotype is not observed as seen in other jasmonate pathway mutants i.e. *aos*, *opr3* and *coi1-1* (Suza and Staswick, 2008; Koo et al., 2009). In Arabidopsis, the basal and stimuli-derived JA-Ile amount is not as high as other jasmonates, however, JA -Ile accumulates as a burst which sustained some seconds to hours after elicitor response (Glauser et al., 2008; Miersch et al., 2008; Suza and Staswick, 2008).

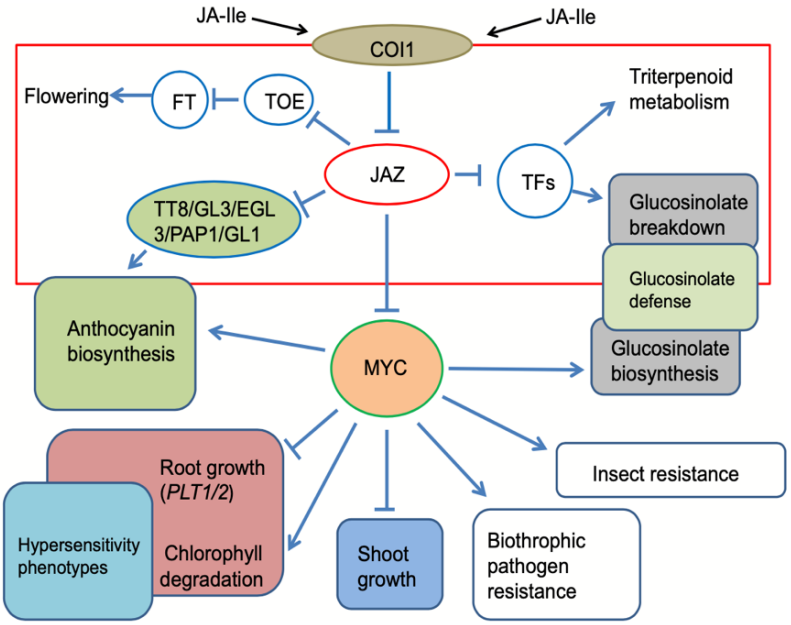

Figure 3: Model of jasmonyl-isoleucine (JA-Ile) dependent multifaceted responses in plants. FT, flowering locus T; TOE, target of eat. Collected with a permission from (Wasternack, 2017; L/C: 5075370774413).

1.7 The role of jasmonates in balancing growth-defense tradeoffs

Plants can develop various strategies of growth-defense tradeoffs to maintain their fitness when exposed to natural eco-systems (Zust and Agrawal, 2017; Claeys and Inze, 2013; Zhang and Turner, 2008). In most cases, the cost of defense is paid off as growth retardation. Jasmonates are considered as one of the prime regulators of such growth-defense tradeoffs (Howe et al., 2018; Zust and Agrawal, 2017; Guo et al., 2018; Wasternack, 2017; Figure 3). However, most work on growth regulation by jasmonate signaling was done either using exogenous MeJA application or with regard to biotic stimuli. Very little is known about the role of jasmonate signaling under soil-growth conditions and abiotic stresses.

1.8 Drought stress impacts jasmonate signaling and vice versa

Drought resistance is a cumulative mechanism involving three factors i.e. avoidance, tolerance, and escape (Claeys and Inze, 2013; Gupta et al., 2020). Avoidance involves mechanisms to increase water uptake and reduce water loss, while tolerance aims at protecting plants by enhancing anti-oxidant systems under severe drought stress. Escape comprises morphological adaptations such as changing the life cycle through early flowering and altered growth. In general, by early flowering plants adopt drought escape mechanisms, while by late flowering plants tend towards avoidance (Monorae et al., 2018; Claeys and Inze, 2013; Gupta et al., 2020). The effects of drought on plants are also dependent on their developmental stage and it

was shown that Arabidopsis is more susceptible to drought stress during the reproductive stage (Monorae et al., 2018). Drought avoidance and tolerance mechanisms are closely linked to ABA signaling. Indeed, extensive cross-talk exists between jasmonate and ABA-mediated signaling and they act both synergistically and antagonistically depending on the plant organ and stimulus (Yang et al., 2019; Daszkowska-Golec and Szarejko, 2013). Exogenous JA application can induce drought-responsive genes while exposure to drought initiates jasmonate biosynthesis leading to JA-Ile accumulation (Zander et al., 2020; Clouw et al., 2015; de Ollas et al., 2015a; de Ollas et al., 2015b). Drought tolerance includes mechanisms to alleviate reactive oxygen species (ROS) damage and JA was found to be involved in activating the anti-oxidant metabolism and in regulating the ascorbate-glutathione cycle (Dombrecht et al., 2007; Sasaki-sekimoto et al., 2005; Xiang and Oliver, 1998; Savchenko et al 2019). As mentioned above, the role of jasmonates as the prime regulators in the case of biotic stress has been well established (Howe et al., 2018; Zust and Agrawal., 2017, Guo et al., 2018; Wasternack, 2017), but much less is known in the case of abiotic stresses such as drought.

1.9 Calcium sensors and the role of Ca^{2+}-signaling in plants

Intricate mechanisms of plant signaling are mediated by different second messengers, of which calcium ions (Ca^{2+}) plays a significant role. Besides taking part in developmental processes, Ca^{2+} transduces different stimuli-derived signals to cellular responses (Kudla et al., 2018; Knight et al., 1997). These modifications occur under different biotic (wounding, pathogen, etc.) or abiotic (salt-stress, heat, drought, etc.) stimuli. Usually, the responses are dependent on certain "Ca^{2+} signatures" which are meant to be a temporary rise of cytosolic calcium $[Ca^{2+}]_{cyt}$. These signatures could be single calcium 'spikes' or different 'Ca^{2+} oscillations (Knight et al., 1997). Usually, the $[Ca^{2+}]_{cyt}$ spike is facilitated by membrane-localized channels, which are localized in the plasma membrane of the cell or in different cellular stores such as the vacuole or the endoplasmic reticulum (McCormack et al., 2005; Kudla et al., 2018; Knight et al., 1997; McAinsh and Pittman., 2009). In many cases, the rise in free Ca^{2+} is perceived by various Ca^{2+}-binding sensor proteins. Among them are Ca^{2+}-sensor decoders such as calmodulin (CAM), calmodulin-like proteins (CMLs) and CBD (calcineurin B like protein) and Ca^{2+}-sensor responders such as calcium-dependent protein kinases (CDPKs). All of them are characterized by their uniform EF-motif hand-like structures and upon binding of Ca^{2+} they undergo changes in their conformation which allowed them to interact with their target proteins and consequently to activate them (McCormack et al., 2005; Kudla et al., 2018).

1.10 Cross-talk between jasmonates and calmodulin-mediated Ca^{2+}-signaling

The dramatic increase in cytosolic Ca^{2+} is believed to act as a secondary messenger for several abiotic and biotic stresses (Dodd et al., 2010; Kurusu et al., 2013). Exogenous MeJA can stimulate the inhibition of Ca^{2+} -channel blockers and calmodulin (CaM) inhibitors to induce Ca^{2+}-mediated stomatal closure (Daszkowska-Golec Szarejko, 2013). Many Ca^{2+}-dependent kinases are potential targets of jasmonate signaling (Daszkowska-Golec Szarejko, 2013). The activity of Ca^{2+}-permeable channels was found to be suppressed in the *coi1-1* mutant (Daszkowska-Golec Szarejko, 2013; Munemasa et al., 2007). The calmodulin-like protein, CML37 has been involved in a synergistic interaction with jasmonate signaling to prevent herbivorous attack, whereas, CML42 has a negative effect on jasmonate signaling (Scholz et al., 2014; Vadassery et al., 2012). A putative link between glutamate receptor-mediated Ca^{2+}-signaling and the jasmonate response was found within the pathogen response (Förster et al., 2019).

1.11 MYB transcription factors and the role of AtMYB2

As mentioned above the jasmonate pathway is involved in transcriptional regulation and most of the advancements made on jasmonate signaling concerns bHLH group members, including the recently identified TFs ORA47, ORA59 etc., some of which function by interacting with MYC2 (Wasternack and Song, 2017; Hickman et al., 2017). Besides them, some reports made a connection between Ca^{2+} and jasmonate signaling but none reported on Ca^{2+}-mediated TFs other than the CaM-binding transcription activators (CAMTAs) (Reddy et al., 2011). In nature, the most diversified and abundant TFs are those from the MYB (myoblast) group. MYB proteins are a superfamily of transcription factors and found in abundance in all eukaryotic cells. In general, they are important in a plethora of developmental processes and defense responses in plants. The MYB proteins contain a highly conserved DNA-binding domain at the N-terminal end and a divergent functional domain at the C-terminus (Dubos et al., 2010; Ambawat et al., 2013; Baldoni et al., 2015; Figure 4). In plants, these TFs are essential in gene regulation processes and mostly belong to the R2R3 family. R2R3 family contains two repeats, each consisting of approximately 52 amino acids that form three α-helices. In the interaction with the DNA double helix, two of the helices form a helix-turn-helix structure and the last helix interacts with the major groove of the DNA. Different MYB TFs are characterized for their involvement in several molecular networks regulating different abiotic and biotic stress-responses in plants (Ambawat et al., 2013; Baldoni et al., 2015). Two important MYBs, MYB21, and MYB24 are also involved in flowering in a jasmonate-dependent manner

(Wasternack and Song, 2017). An Arabidopsis MYB factor, AtMYB2, which also belongs to the R2R3 family, was first identified in dehydrated Arabidopsis rosette leaves. AtMYB2 is characterized by the structure of its N-terminal DNA binding domain and of its catalytic C-terminal domain (Urao et al., 1993; Figure 4). The DNA binding domain interacts with CaM in a Ca^{2+}-dependent manner (Yoo et al., 2005). AtMYB2 binds to targets which carry the consensus MYB-recognition sequence (A/TAACCA and C/TA-ACG/TG). In Arabidopsis, AtMYB2 is induced by ABA treatment, salt stress, hypoxia and dehydration (Abe et al., 2003; Yamaguchi-Shinozaki et al., 1995; Hoeren et al., 1998). AtMYB2 directly controls the expression of two stress-responsive genes, *RD22 (Response to dehydration 22),* a drought responsive gene, and *ADH1 (Alcohol dehydrogenase 1)* involved in carbohydrate metabolism under low oxygen conditions (Yamaguchi-Shinozaki et al., 1995; Hoeren et al., 1998). It has been shown that AtMYB2 interacts with MYC2 in an ABA-dependent manner to control the activity of RD22 under drought stress. Overexpression lines of AtMYB2 were also found to be resistant to drought and showed the enhancement of the expression of the jasmonate-dependent gene *VSP2* (Abe et al., 2003; Yamaguchi-Shinozaki et al., 1995; Hoeren et al., 1998; Yoo et al., 2005). Despite a probability of regulating the jasmonate pathway, especially under drought, no previous study focused on the MYB2 regulatory capacity in jasmonate signaling.

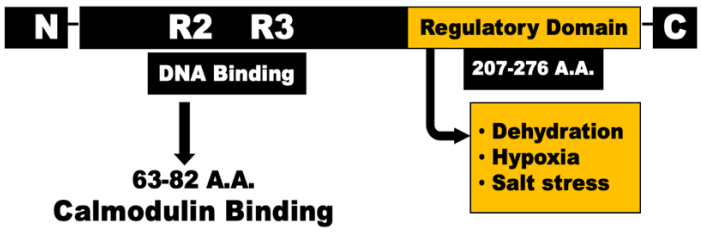

Figure 4: Schematic structural presentation of AtMYB2.
R2R3-repeat is localized at the N-terminal side with a calmodulin-binding domain consisting of 19 amino acid from the N-terminal side. Regulatory domain is characterized at the C-terminal side with 69 amino acid responsible for dehydration.

1.12 Aim of the study

Jasmonates, especially JA-Ile, have been extensively studied for their role in controlling the balance between growth and defense under biotic stress. However, no previous study focused on these processes under abiotic stresses such as drought. In the present study, the role of endogenous JA-Ile in the growth of Arabidopsis plants under normal and drought stress conditions was investigated. For this purpose, plants expressing JAR1.1-YFP under the 35S promoter (JAR1-OE) were to be developed in order to induce endogenous JA-Ile accumulation even under non-stress conditions. Together with the T-DNA insertion line *jar1-11,* the effect of differential changes in endogenous jasmonate content was analysed compared to wild type (Col-0) Arabidopsis plants with regard to growth under normal and progressive drought conditions.

On a molecular level, analysis of changes in hormone content and genes expression should provide an insight into the regulatory pathways and specific responses that are regulated by jasmonate signaling. A special focus of these analyses was placed on resistance mechanisms involving water use efficiency and ROS regulation, as well as the cross-talk with Ca^{2+}-signaling.

Furthermore, the role of transcription factors of the MYC and MYB family specific regulators of the jasmonate signaling pathway was elucidated.

2. Material and methods

2.1 Material

2.1.1 Chemicals, enzymes, and kits

If not otherwise mentioned, all chemicals were purchased from known suppliers with premium quality.

Table 1: Special chemicals/materials used in this study

Name	Company/ Brand
Complete protease inhibitor cocktail, EDTA free	Roche, Germany
Nitrocellulose membrane	Serva, Germany
Ni-NTA agarose	Qiagen, Germany
Methyl Viologen	Sigma-Aldrich, Germany
Methyl Jasmonate	Serva, Germany
Jasmonic acid	Duchefa Biochemie, Netherlands
(±)-Jasmonic Acid-Isoleucine	Cayman Chemical, USA
Medical Adhesive	Hollister, Germany
Oligonucleotides	Thermo Scientific, USA
IPTG	Duchefa Biochemie, Netherlands
Confidor WG 70	Bayer Agrar, Germany
Murashige and Skoog medium (MS) medium	Duchefa Biochemie, Netherlands
Phytagel	Sigma-Aldrich, Germany
Plant potting soil	Flora Guard, Germany

Table 2: Enzymes and kits used in this study

Name	Company/ Brand
GoTaq DNA polymerase	Promega, USA
Phusion Hi-Fidelity polymerase	Thermo Scientific, USA
FastDigest Restriction enzymes	Thermo Scientific, USA
T4-DNA ligase	Fermentas (St. Leon Roth, Germany)
Nucleospin Extract II Kit	Macherey-Nagel, Qiagen, Germany
HiYield Plasmid DNA Kit	Süd-Laborbedarf GmbH (Germany)
QuickPrep mini RNA extraction Kit	Zymo-Research, USA
RevertAid First Strand cDNA synthesis Kit	Thermo Scientific, USA
Coomassie Bradford protein assay Kit	Thermo Scientific, USA

2.1.2 Oligonucleotides

Table 3: Primers used in this study. fw – forward primer; rev- reverse primer; CDS – coding sequence

Primer name	Sequence (5'→ 3')	Purpose
LBb1.3	ATTTTGCCGATTTCGGAAC	T-DNA amplification
*jar1-11*_fw	GCTCTGGAACTAGTCAAGGCC	*jar1-11* genotyping
*jar1-11*_rev	CTGTGCAATGTGGATCAAATG	*jar1-11* genotyping
*aos*_fw	CTAACCGGAGGCTACCGTATC	*aos* genotyping
*aos*_rev	CGAGAAATTAACGGAGCTTCC	*aos* genotyping
*myb2*_fw	AAACGTGACGCAATTGAATTC	*myb2* genotyping
*myb2*_rev	ATCCACAAAACCATTCACACC	*myb2* genotyping
*cml12*_fw	CGACAAAAGCTGATCTTCAGG	*cml12-1* genotyping
*cml12*_rev	CAAGATAACAGCGCTTCGAAC	*cml12-1* genotyping
JAR1.4_fw	CTTATGGATGCTCTGAAACAAAAAG	JAR1.4 CDS amplification
JAR1.3_fw	CTTATGGTTGATGGTGACACTTCACC	JAR1.3 CDS amplification
JAR1.1_fw	CTTATGTTGGAGAAGGTTGAAAC	JAR1.1 CDS amplification
JAR1(4+3+1)_rev	CTTAAACGCTGTGCTGAAGTAGC	JAR1 splice variants amplification
JAR1.4_ ApaI	CTTGGGCCCATGGATGCTCTGAAACAT	JAR1.4 CDS with ApaI restriction site amplification
JAR1.3_ ApaI	CTTGGGCCCATGGTTGATGGTGACAC	JAR1.3 CDS with ApaI restriction site amplification
JAR1.1_ ApaI	CTTGGGCCCATGTTGGAGAAGGTTGAAAC	JAR1.1 CDS with ApaI restriction site amplification
JAR1(4+3+1) NotI	CTTGCGGCCGCCAAACGCTGTGCTG	JAR1 splice variants with NotI restriction site amplification
JAR1.1_ BamHI	CCTGGATCCCATGTTGGAGAAGGTTG	JAR1.1 CDS with BamHI restriction site amplification
JAR1.1_ NotI	CTTGCGGCCGCAAACGCTGTGC	JAR1.1 CDS with NotI restriction site amplification
ACT2 qPCR_fw	TGCCAATCTACGAGGGTTTC	RT-qPCR
ACT2 qPCR_rv	CTTACAATTTCCCGCTCTGC	RT-qPCR
JAR1 qPCR_fw	CTTCACCTATTCTCACTGGTC	RT-qPCR
JAR1 qPCR_rv	GCAAAAGCAGTGCGAAACAGT	RT-qPCR
VSP1 qPCR_fw	TACCGTCAATGTTTGGATCTTTG	RT-qPCR
VSP1 qPCR_rv	GGACTCTAACCACGACCAG	RT-qPCR
GIF1 qPCR_fw	CCTAATGTACCTAGCTGCAATAG	GIF1 qPCR_FW
GIF1 qPCR_rv	AGTCGCTTGTTGCTGCTGC	GIF1 qPCR_REV

2.1.3 Molecular weight and size markers

Table 4: Molecular weight and size markers used in this study.

Name	Company	Purpose
GeneRuler™ 1Kb Plus DNA Ladder	Thermo Scientific, USA	DNA size marker for Agarose gel electrophoresis
Peq Gold Protein-Marker IV	VWR Life Science, Germany	Protein size marker for SDS PAGE
PageRuler™ Plus Prestained Protein Ladder	Thermo Fisher Scientific, Waltham, MA, USA	Protein size marker for SDS PAGE

2.1.4 Plasmid DNA Vectors

The binary vector pBIN19-AN-YFP was applied for stable Arabidopsis (*Arabidopsis thaliana*) or transient Tobacco (*Nicotiana benthamiana)* transformation. This was supplied by Dr Norbert Mehlmer (Mehlmer et al., 2012). The protein expression vector pET21b was applied for *in vitro* protein expression in *E. coli*. This was bought from the Stratagene, USA.

Table 5: List of plasmid constructs used in this study. CDS – coding sequence

Denotation	AGI code and description	Plasmid	Purpose	Author
35S:JAR1.4-YFP	AT2G46370.4 CDS	pBIN19-AN-YFP	transient protein expression in *N. benthamiana*	self-made
35S:JAR1.3-YFP	AT2G46370.3 CDS	pBIN19-AN-YFP	transient protein expression in *N. benthamiana*	self-made
35S:JAR1.1-YFP	AT2G46370.1 CDS	pBIN19-AN-YFP	transient protein expression in *N. benthamiana* and generation of stable transgenic line	self-made
35S:CML12-YFP	AT2G41100 CDS	pBIN19-AN-YFP	transient protein expression in *N. benthamiana*	self-made
T7:JAR1.1-His	AT2G46370.1 CDS	pET21b	*in vitro* translation	self-made

2.1.5 Bacterial strains

Propagation of plasmid DNA was performed in *E. coli* strain DH10β (NEB, Boston, MD, USA), whereas protein expression was performed in BL21-CodonPlus(DE3)-RIPL cells (Agilent Technologies, Santa Clara, CA, USA). Transient transformation of Tobacco (*N. benthamiana*) plants as well as the stable transformation of Arabidopsis (*Arabidopsis thaliana)* plants was carried out with Agrobacterium (*A. tumefaciens*) strain GV3101 (Vahala et al., 1989).

2.1.6 Plant materials

Arabidopsis plants used in this study, unless otherwise stated, were in the Col-0 background except for studies relating to *opr3* which was in Wassilewskija (Ws) background. Seeds of T-DNA insertion lines, *jar1-11* (SALK_034543), *jar1-12* (SALK_011510), *aos* (SALK_017756), *cml12-1* (SALK_122731) and *myb2-1* (SALK_045455) were obtained from NASC (Nottingham Arabidopsis Stock Centre). Other lines mentioned were kind gifts from different researchers as mentioned before for *opr3* (Brioudes et al., 2009); *coi1-1* (Ralhan et al., 2012); *aba2-1* (Cheng et al., 2002); *proVSP2*-GUS; (Mousavi et al., 2013); pro*CML12::*TurboGFP-GUS (Xiao and Offringa, 2020) and *proJAZ1*-GUS (Pérezet al., 2014). Arabidopsis wild-type (WT) seed material was purchased from LEHLE SEEDS (Round Rock, TX, USA) or The European Arabidopsis Stock Centre NASC (Nottingham, UK) and *N. benthamiana* seed material was supplied by the in-house plant cultivation facility.

2.2 Methods

2.2.1 DNA methods

2.2.1.1 Screening of homozygous plants by PCR genotyping

2.2.1.1.1 Isolation of Genomic DNA

For genotyping, genomic DNA was extracted from the leaves of the 21 days old Arabidopsis plants following the modified method of (Edwards et al., 1991). Briefly, a leaf sample of about100 mg was collected in an Eppendorf tube, and immediately 400 µl of extraction buffer (200 mM Tris-HCl, 25 mM EDTA, 250 mM NaCl, and 0.5% SDS; pH 8) including a magnetic bead (100 nm) was added. Then the tube was placed in a TissueLyser II (Qiagen, produced by Retsch, Hilden, Germany) and homogenized with a 300-rpm rotation for 5 minutes. After high-speed centrifugation (14,000 *xg,* 10 min), 285 µl of supernatant was collected into a new tube, mixed with 715 ul of 70% ethanol, and vortexed vigorously. This mixture was centrifuged at

14,000 *xg* for 10 min to collect the pellet and the supernatant was discarded. The pellet was then dried at 50°C for 30 minutes followed by resuspension with 10 mM Tris-HCl (pH 8.5) and stored at -20°C for further applications. In the case of genotyping, for each mutant line, two primer combinations were used for genotyping: one containing two gene-specific primers (wild type allele) and the second comprising a gene-specific primer with an outward-facing primer for the T-DNA (mutant allele).

2.2.1.1.2 Polymerase Chain Reactions (PCR)

Standard PCR reactions were performed with extracted genomic DNA or plasmid DNA as a template using either GoTaq DNA polymerase (Promega, USA) or Phusion polymerase (Thermo Scientific, USA) according to the manufacturer's instructions, following the assay compositions displayed in Table 6.

Table 6: Composition of the standard PCR mix for GoTaq and Phusion polymerase

Components	GoTaq polymerase	Phusion polymerase
DNA template (5-50 ng/µl)	2.00 µl	2.00 µl
Forward primer (10 µM)	1.00 µl	1.00 µl
Reverse primer (10 µM)	1.00 µl	1.00 µl
dNTPs (10 mM each)	0.5 µl	0.5 µl
Buffer (5 x)	5.00 µl	5.00 µl
Polymerase	0.125 µl	0.25 µl
ddH_2O	15.375 µl	15.25 µl
Total	**25.00 µl**	**25.00 µl**

Standard PCR reactions were performed on a thermocycler set at the conditions mentioned as displayed in Table 7.

Table 7: Standard PCR protocol. * - annealing temperature depended on the primer pair applied in the reaction

PCR-steps	GoTaq polymerase	Phusion polymerase	
Initial denaturation	95°C - 120 s	98°C - 30 s	
Denaturation	95°C - 60 s	98°C - 10 s	35 cycle
Annealing	* - 60 s	* - 30 s	
Extension	72°C - 1 min / kb	72°C - 30 s / kb	
Final extension	72°C - 300 s	72°C - 300 s	
Hold	4°C - ∞	4°C - ∞	

2.2.1.1.3 Agarose gel electrophoresis

DNA samples were analysed by separation on 1 % Agarose gel (SeaKem LE Agarose, Loza, Switzerland). Nucleic acids were stained with DNA stain G (SERVA Electrophoresis GmbH, Heidelberg, Germany) according to manufacturer's instructions and separation of DNA fragments was carried out at 100 V, 100 mA for 15-30 min. Documentation was performed on a Gerix 1000 gel documentation system (biostep GmbH, Burkhardtsdorf, Germany).

2.2.1.2 Generation of vectors for *in planta* expression

For 35S-promotor driven *in planta* expression of YFP fusion proteins, it was attempted to amplify the entire coding sequences of the genes without the stop codon and clone them N-terminally to the YFP sequence into the binary plant expression vector pBIN19-YFP. PCR amplification was performed on cDNA prepared from leaf tissues of *Arabidopsis thaliana* (Col-0) using appropriate primers with ApaI and NotI restriction sites.

2.2.1.2.1 PCR amplification of the coding sequences of the gene

The entire coding sequences of the genes were first amplified from the cDNA prepared from leaf tissues of Arabidopsis thaliana (Col-0) using appropriate primers. Then a second PCR was performed using the primers with ApaI and NotI restriction sites using the first PCR product as a template.

2.2.1.2.2 PCR clean-up of the amplified PCR products

The resulting PCR product was cleaned up using the Nucleospin Extract II Kit. Briefly, it was done by mixing the PCR product with the extraction buffer, running through the filter column, and washing them with wash buffer. Finally, the dried column was eluted with the elution buffer. The eluted product was checked by running them onto a 1 % agarose gel.

2.2.1.2.3 Restriction Digestion of the amplified PCR products and the vector

Purified PCR products and the template vector pBIN19 were mixed with the restriction enzymes ApaI and NotI (Fast Digest, Thermo-scientific Research) according to manufacturer's instructions and then incubated at 37°C for 1 hour followed by 65°C for 10 minutes.

The resulting digest products were run onto a 1% agarose gel to confirm the digestion. Appropriate bands were cut out from the gel and then purified with the Nucleospin Extract II Kit.

2.2.1.2.4 Ligation of the digested PCR insert and the vector

Purified and digested inserts and vector were ligated following a vector: insert ratio of 1:3 and incubated at 22°C for 1 hour followed by 65°C for 10 min.

2.2.1.2.5 Transformation into DH10β competent cell and Colony PCR

The ligated products were transformed into *E. coli* strain DH10ß competent cells by heat shock. Briefly, it was done by mixing 10 µl of ligation product to 50 µl of the chemically competent cells in an Eppendorf tube and placing it on ice for 10 minutes. Then the tube was incubated at 42°C for 45 seconds and brought back to the ice for 2 minutes incubation. For transformation, 800 µl Luria-Bertani (LB) liquid media was added to the tube and then incubated at 37°C for 45 minutes under 400-rpm continuous shaking. The bacterial pellet was collected by centrifugation at 5,000 *xg* for 1 minute and then resuspended with the remaining 200 µl LB liquid and poured onto LB plates with Kanamycin (25 µg/ml). These transformed plates were incubated at 37°C overnight and the transformation success was measured by initial visualization of the colony formation. A colony PCR was performed using the primers designed for the known region of the PCR insert. Isolation of plasmid was performed with the plasmid-prep technique using HiYield® Plasmid Mini Kit and then the isolated plasmid was sent for sequencing.

2.2.1.3 Generation of transgenic plants by Agrobacterium-mediated transformation

2.2.1.3.1 Transformation into Agrobacterium strain GV3101 competent cells

Isolated plasmids containing the inserts in frame with the vector construct were transformed into *Agrobacterium tumefaciens* strain GV3101 by electroporation. Shortly, it was done by mixing 2 µl of the plasmid vector to 50 µl of GV3101 chemically competent cells and bringing the mixture into an electroporation cuvette (Carl Roth, Germany). Electroporation was performed by placing the cuvette in the electroporation chamber (BioRad) and then running the machine in the "**Agr**" mode. For the transformation, 800 µl of YEB media (5 g Beef extract, 5 g peptone, 5 g sucrose, 1 g yeast extract, pH 7.0) was added to the cuvette and incubated at 28°C for 2 hours under 400-rpm continuous shaking. The pellet was collected by centrifugation at 5,000-rpm at 1 min and resuspended with the remaining 200 µl of the YEB liquid. This resuspended mixture was poured onto the YEB medium containing Agar plates (YEB; Kanamycin (25 µg/ml); Rifampicin and 1M $MgCl_2$) and spread. The plates were incubated at 28°C for 48 hours for successful colony formation.

2.2.1.3.2 Floral dipping

A larger culture (100 ml/ each plant) of the YEB liquid medium containing the colonies derived from transformation was made for the transformation of the plasmid vector into plants. The culture was incubated at 28°C for 48 hours and afterward, acetosyringone (1µl/ ml of the YEB liquid) and Tween-20 (0.02%) were added to the culture and mixed by gentle shaking before dipping. The plant selected to be dipped in the culture was watered beforehand and all the developed siliques were removed keeping only the unopened buds. The whole inflorescence was dipped into the culture for 30 seconds, wrapped with plastic folium, and then kept 2 days in a dark chamber before bringing back to the growth chamber and grew until seed collection.

2.2.1.3.3 Screening of the homozygous plants

Collected F1 generation seeds were screened through BASTA selection. For screening, around 400 g of F1 generation seeds were spread on the soil, and BASTA was applied as foliar spray on the 7 days old germinated seedlings. Effect of BASTA was visible after 4-5 days where all the seeds lacking the vector constructs started dying and the resistant plants were growing normally. These resistant plants were grown until seed collection and then this F2 generation plants were grown on BASTA plates placing around 100 seeds/plate and their survival percentage was monitored. Collected homozygous seeds were further screened through RT-qPCR, Western blot, or analysing YFP fluorescence under fluorescence microscope.

2.2.2 RNA methods

2.2.2.1 RT-qPCR

2.2.2.1.1 Isolation of RNA from the leaves and cDNA synthesis

Total RNA was extracted from the whole rosettes leaves using the Quick-RNA Miniprep Kit (Zymo-Research, USA). RNA quality and quantity were determined using a Nabi UV/Vis Nano Spectrophotometer (LTF Labortechnik, Germany). For RT-qPCR analysis, cDNA was prepared from 1 µg of mRNA with RevertAid First Strand cDNA Synthesis Kit (Thermo Scientific, Thermo Fischer Scientific).

2.2.2.1.2 Quantitative Real-Time PCR (RT-qPCR)

Genes expression was quantified using the Power SYBR Green PCR Master Mix (Applied Biosystems, ThermoFisher Scientific) in 48 well-plates in a StepOne™ Real-Time PCR Thermocycler (Applied Biosystems, ThermoFisher Scientific) and the expression level was

normalized to *Actin2*. A standard thermal profile was used with 50°C for 2 min, 95°C for 10 min, followed by 40 cycles of 95°C for 15 s and 60°C for 1 min. Amplicon dissociation curves were recorded after cycle 40 by heating from 60 to 95°C with a ramp speed of 0.05°C/s. Primers used for RT-qPCR are listed in Table 3.

2.2.2.2 RNA-seq

For RNA-seq, the quality of RNA was checked by determining the RNA integrity number using a Tapestation 4200 (Agilent). RNA-seq library preparation and sequencing were performed by the NGS Core Facilities at the University of Bonn, Germany. Approximately 200 ng of RNA was used for library construction. Sequencing libraries were prepared using Lexogen‘s QuantSeq 3‘-mRNA-Seq Kit and sequenced on an Illumina HiSeq 2500 V4 platform with a read length of 1x50 bases. For each of the samples, three biological replicates were sequenced with an average sequencing depth of 10 million reads.

RNA-seq data analysis was performed in collaboration with Annika Kortz and Dr. Peng Yu, Crop Functional Genomics, INRES, University of Bonn. CLC Genomics Workbench (v.12.03, https://www.qiagenbioinformatics.com/) was used to process the raw sequencing data. Quality control and trimming were performed on the FASTQ files of the samples. Quality trimming was performed based on a quality score limit of 0.05 and a maximum number of two ambiguities. To map the additional JAR1 reads from the JAR1.1-YFP lines, an additional chromosome comprising the YFP sequence was added to the Araport 11 (Cheng et al., 2017) genome and the annotation file. The FASTQ samples were then mapped to the modified Araport 11 genome, while only classifying reads as mapped which uniquely matched with ≥ 80% of their length and shared ≥ 90% identity with the reference genome. For the mapping, to the gene models, reads had to match with ≥ 90% of their length and share ≥ 90% similarity with a maximum of one hit allowed. Subsequently, counts for JAR1.1-YFP and JAR1 were combined. Further steps were completed using the R programming language (R Core Team 2020). To test the quality of the data, samples were clustered in a multidimensional scaling plot (MDS plot) using plotMDS. To assess differential expression of the sequencing data the Bioconductor package edgeR was used (Robinson et al., 2009). First, the read counts were normalized by library sizes with the trimmed mean of M-values (TMM) method (Robinson and Oshlack, 2010). Then common and tagwise dispersion was calculated. For pairwise comparisons, the exactTest function to calculate the p-value and the log2-fold-change were used. The resulting p-values were adjusted by using the False Discovery Rate (FDR) method (Benjamini and Hochberg, 1995)

K-means clustering was performed using the kmeans function with the algorithm of Hartigan and Wong (1979) (Hartigan and Wong, 1979). The number of clusters for each clustering was estimated using the elbow method (Thorndike, 1953).

GO term enrichment analysis was performed with the topGO package (Alexa and Rahnenfuhrer, 2020). The athaliana_eg_gene dataset (Cheng et al., 2017) was downloaded from Ensembl Plants (Yates et al., 2020) via the BioMart package (Durinck et al., 2009). For this, a weighted fisher test (Fisher, 1925) was run using the weighted01 algorithm ($p \leq 0.001$). The resulting p-values were adjusted by using the BH method (Benjamini and Hochberg, 1995) filtering for an adjusted p-value ≤ 0.01.

Additionally, Transcripts Per Million (TPM) values were calculated based on the read counts. For individual genes, TPM values were compared by performing an ANOVA (Chambers et al., 1992) and a Tukey HSD test with a confidence interval of 0.95 (Tukey, 1949).

Figures and plots were created using the R packages, VennDiagram (Schwenk, 1984), pheatmap, ggpubr, and EnhancedVolcano.

2.2.3 Protein methods

2.2.3.1 Protein extraction from leaves and seedling

For protein extraction, samples or other tissues were ground to powder with liquid nitrogen (N_2). For SDS PAGE, 100 µl of 4 x solubilization buffer as mentioned in Table 8, was mixed with the ground powder, vortexed rigorously followed by heating at 95°C for 10 minutes and then centrifuged at 14000 *xg* for 10 minutes to collect the supernatant for further applications.

Table 8: Composition of the 4 x solubilization buffer

Component	Final Concentration	Amount needed to 10 ml
1M Tris, pH 6.8	(0.1M)	2 ml
1 M DTT	(0.2M)	4 ml
10% SDS	(4%)	0.8 g
BPB	(0.2%)	40 mg
100% Glycerol	(20%)	4 ml
dH2O		0

2.2.3.2 Quantification of protein content

The protein concentration of extracts or purified recombinant proteins was determined by using the Coomassie Bradford protein assay kit (Thermo Scientific) according to manufacture's instructions.

2.2.3.3 SDS-PAGE

Proteins were separated by SDS-PAGE according to Laemmli (1970) on 8% or 10% or 12% (w/v) polyacrylamide gradients.

Table 9: Composition of the SDS-PAGE.

Stacking Gel	Resolving Gel
Components	
ddH_2O	ddH_2O
30% acrylamide	30% acrylamide
1.5M Tris (pH 8.8)	1M Tris (pH 6.8)
10% SDS	10% SDS
10% APS	10% APS
TEMED	TEMED

2.2.3.4 Western blotting

Proteins separated by SDS-PAGE were transferred onto Nitrocellulose membranes according to the semi-dry blot method (Khyse-Andersen 1984). Briefly, it was done by using the semi-dry transfer unit making a sandwich of Whatman filter paper, protein gel and Nitrocellulose membrane wet through Anode buffers and cathode buffer. To confirm the blotting, the membrane was stained with Ponceau Stain (0.5 g/l Ponceau S, 25 ml/l Acetic Acid). The membrane was then blocked with 5 % milk-blocking-solution (25 g/l skim milk, 50 ml/l 20 x TBS, 1 ml/l T-20) at RT for 1 hour. The membrane was then incubated with the primary antibody for two hours at RT or overnight at 4°C, washed 3x10 minutes with 1 x TBST (50 ml/l 20 x TBS, 1 ml/l T-20), and then incubated with the secondary antibody for 1 hour at RT and again washed 3x10 minutes with 1 x TBST. For developing the membrane either alkaline phosphatase or the luminescence detection with a 1:1 mixture of H_2O_2 and luminol was used. For luminescence detection, membrane was developed with the ECL system (BioRad, Germany) using a 20 minutes exposure.

Table 10: List of primary antibodies used in this study.

Name	Dilution	Source
α-GFP (Mouse)	1:1,000	Roche, Germany
α-CML12 (Rabbit)	1:3,000	Elmore et al 2012
α-PSaB (Rabbit)	1:1,000	Agrisera, Sweden
α-JAR1.1 (Rabbit)	1:1,000	self-made
α-TKL1 (Rabbit)	1:5,000	supplied by AG Vothknecht

2.2.3.5 Polyclonal antibody generation

The entire coding sequence of *JAR1.1* was amplified by PCR using the primers designed with BamHI and NotI restriction site and then cloned into T7 promoter-driven pET- 21b vector, which fuses a 6X His-tag at the C-terminus of the insert. The procedure of cloning is the same as mentioned in the section **2.2.1.2**. The resulting vector constructs were transformed into DH10β competent cells by heat shock and plated on the LB plus Ampicillin (100µg/ml) agar plates and positive colonies were identified using colony PCR after overnight incubation at 37°C. Plasmid-DNA prepared from the positive colonies was analysed by sequencing.

2.2.3.5.1 Protein expression

The in frame insert in the vector was transformed into *E. coli* strain BL21-CodonPlus(DE3)-RIPL by heat shock and incubated overnight at 37°C. A 100 ml liquid culture was made by scraping the colonies from the plate and incubating them overnight at 37°C. 1mM IPTG was added to the culture when it reached OD_{600} to 0.5 to induce the protein expression. Then the incubation was carried out for another 4 hours for sample collection. Negative control of the culture was continued without IPTG to compare the protein overexpression. An additional aliquot of 1ml of the culture was collected besides the large culture and the pellet was collected centrifuging at 14,000 *xg* for 2 min and the pellet was resuspended with 2x SDS buffer. After the IPTG induction, the bacterial cell pellet was collected by centrifugation at 7000 *xg* for 30 min at 4°C and stored at -20°C until further use. Successful protein expression was checked by running the 1 ml resuspended pellet in 10% SDS gel and the gel was stained with Coomassie colloidal stain.

2.2.3.5.2 Purification

JAR1.1 with a C-terminal 6x- Histidine tag was purified using Ni-NTA superflow (Qiagen) and provided to David technologies, Germany to generate polyclonal antibody in the rabbit.

2.2.4 Plant methods

2.2.4.1 Growth conditions

If not otherwise stated, plants were cultured in climatized growth chambers (equipped with Philips TLD 18W of alternating 830/840 light color temperature) at 22°C under long-day conditions (16 h light/8 h dark) with 100 µmol photons m^{-2} s^{-1}. In some experiments, short-day conditions (8 h light/16 h dark) were applied.

2.2.4.2 Seed sterilization

For ½ MS medium growth, seeds were sterilized by adding 12% NaOCl (Sodium hypochlorite) followed by adding 70% ethanol and then washing by water 5 times.

2.2.4.3 Plant growth media

As indicated, plants were grown either on ½ Murashige and Skoog medium (MS) medium (Duchefa Biochemie, Netherlands) with 1% sucrose and 0.6% [w/v] phytagel (Sigma-Aldrich, Inc., Germany), or on standard plant potting soil, which was pretreated with Confidor WG 70 (Bayer Agrar, Germany).

2.2.4.4 Planting

For germination in the soil, around 50 seeds were spread out on a single pot. 5-6 days after germination, single seedlings were transplanted to another pot for experiments. Plants grown on ½ MS were stratified for 2 days at 4°C in the dark before moving them to the normal growth chamber.

2.2.4.5 Chloroplast isolation

Intact chloroplast was isolated from 32 days old *A. thaliana* plants as previously mentioned by Seigneurin-Berny et al., 2008. The plants were grown in long-day growth chambers of 16 h/8 h light/dark cycle. Leaves were harvested 2 hours after the beginning of the light cycle. The intact chloroplast samples were kept at -80°C as 50µl aliquots after direct froze using liquid nitrogen.

Chlorophyll concentration was ascertained by mixing 5µl of the sample with 5ml 80% Acetone (as previously described by Porra et al., 1989), and measured as below:

$$[(OD_{663}\text{-}OD_{750}) \times 8.2] + [(OD_{645}\text{-}OD_{750}) \times 20.2] = X\ \mu g/\mu l$$

2.2.4.6 Phenotyping under normal growth and drought stress conditions

For phenotyping under normal and drought stress conditions, seeds were directly spread in the potting soil. After 5 days of germination, seedlings (either single or 4 seedlings per pot) were transplanted to fresh pots containing 100 g potting soil. Plants were grown for 18 days with regular watering with identical volumes of tap water. Afterward, plants were watered normally or were exposed to drought stress conditions by withholding watering for up to 14 days. During the drought-stress treatment, pot weights were measured regularly, and the relative water content of soil (SWC) was calculated from the dried pot weight and adjusted among plant lines to ensure a similar drought stress level. SWC was calculated as {(pot weight at time of stress) − (empty pot weight)}/{(initial pot weight) − (empty pot weight)} × 100. After the soil water content dropped to 10% SWC, plants were watered with identical volumes of tap water and survival rates of plants were calculated 24 h and 7 d after rewatering. At least four independent experiments, each with several plants from different lines, were conducted for all experiments. All the pots were randomized throughout the experiments. Photographs were also taken at regular intervals and corresponding whole rosette leaves were collected for biochemical and RNA-seq analyses.

2.2.4.7 Stomatal aperture measurement

Stomatal apertures were measured collecting the leaf epidermis of the 21 days old Arabidopsis plants as described previously (Murata et al., 2001). Briefly, excised rosette leaves were floated on a medium containing 5 mM KCl, 50 mM $CaCl_2$, and 10 mM MES-Tris (pH 6.15) for 2 h in the light (80 µmol photons m^{-2} s^{-1}) to induce stomatal opening. The abaxial side of the excised leaf was softly attached to a glass slide using a medical adhesive (stock no. 7730; Hollister), and then adaxial epidermis and mesophyll tissues were removed carefully with a razor blade to keep the intact lower epidermis on the slide. Pictures were taken immediately using the bright field option of the confocal microscope (Leica SP8). Approximately 100 stomata were counted taking each portion maximum of 10 stomata to avoid biasness.

2.2.4.8 Stomatal density measurement

Stomatal density was measured collecting the leaf epidermis as described previously (Murata et al., 2001). Briefly, The abaxial side of the 21 days old Arabidopsis excised leaf was softly attached to a glass slide using a medical adhesive (stock no. 7730; Hollister), and then adaxial epidermis and mesophyll tissues were removed carefully with a razor blade to keep the intact lower epidermis on the slide and. Pictures were taken immediately using the bright field option of the confocal microscope (Leica SP8).

2.2.4.9 Histochemical GUS staining

For GUS staining, 32 days old plants grown under control or drought stress conditions were collected and immediately incubated in ice-cold 90% acetone for 20 min. The solution was changed to GUS staining solution containing 100 mM $NaPO_4$, pH 7.0, 0.1 mM $K_3[Fe(CN)_6]$, 0.1 mM $K_4[Fe(CN)_6]$, and 500 mg/mL 5-bromo-4-chloro-3-indolyl P-glucuronide (X-Gluc). The seedlings were infiltrated with the staining solution on ice by briefly applying and releasing a vacuum twice, followed by incubation overnight at 37°C in the dark. Then the samples were destained by repeated washing with 70 % ethanol, followed by 100 % ethanol.

2.2.4.10 Photosynthetic yield (YII) measurement

Leaf photosynthetic parameters were measured with a Junior PAM machine. Briefly, the whole apparatus was fitted into the growth chamber and the sensor nozzle was placed onto the adaxial side of the leaf and the readings were taken by using the software. Later on, the whole data sheet was extracted and analyzed in Microsoft excel sheet.

2.2.4.11 Fluorescence microscopy

2.2.4.11.1 Subcellular localization

Plasmid constructs containing splice variants JAR1.1 and JAR1.3 were transformed into *Agrobacterium tumefaciens* (GV3101) by electroporation and then infiltrated into tobacco leaves by vacuum infiltration method (Leuzinger et al., 2013). After 2-3 days, expression was checked using a confocal fluorescence microscope. Later on, the signal of the fluorescence was checked and captured with the Leica SP8 Confocal Laser Scanning Microscopy. Stably transformed plants containing GFP or GFP derivatives were also visualized in the same way.

2.2.4.11.2 *In vivo* ratio-metric imaging for redox measurements

The cytosol-targeted redox sensor lines Grx1-roGFP2 (Gutscher et al., 2008) and roGFP2-Orp1(Nietzel et al., 2019) lines were used for measuring the *in vivo* Redox measurements using the Leica SP8 confocal microscope and processed by the integrated LASX software with the **Quantify** mode. Confocal laser scanning microscopy of the leaves of 7-9 days old seedlings was performed according to Meyer et al. (2007). In short, roGFP2 was excited at wavelengths 405 and 488 nm, and the emission was detected from 505 to 530 nm. The ratiometric image of 405/488 nm, representing the GSSG/GSH (eGSH) and $H_2O_{2\ OX}$/ $H_2O_{2\ red}$ mediated redox status for Grx1-roGFP2 and roGFP2-Orp1 respectively, was calculated based on a standardization using 50 mM DTT and 10 mM H_2O_2. Leaf was incubated in the imaging buffer (10 mM MES, 10 mM $MgCl_2$, 10 mM $CaCl_2$, 5 mM KCl, pH 5.8) until the treatments were pumped through a perfusion chamber (Warner instruments). The pinhole was adjusted to 3 and 1 for roGFP2-Orp1 and Grx1-roGFP2 respectively. The ratio (0.2 and 0.6 for roGFP2-Orp1 and Grx1-roGFP2 respectively) derived from incubated sample in imaging buffer was used as control.

2.2.5 Biochemical methods

2.2.5.1 Phytohormone measurements

Phytohormone measurements were performed in collaboration with Prof. Dr. Jonathan Gershenzon, Department of Biochemistry, Max Planck Institute for Chemical Ecology, Hans-Knoell-Strasse 8, 07745 Jena, Germany.

2.2.5.1.1 Extraction of phytohormones

Flash-frozen whole rosettes of pooled Arabidopsis were ground to a fine powder under liquid N_2. Approximately 50 mg of each sample was extracted with 1 ml methanol containing 3µl phytohormone standard mix 30 ng of D_6-JA (HPC Standards GmbH, Cunnersdorf, Germany), 30 ng of D_6-ABA (Santa Cruz Biotechnology, Dallas, TX, USA), 6 ng D_6-JA-Ile (HPC Standards GmbH)) as internal standards. The contents were vortexed vigorously for 4-5 seconds, incubated for 30 min at 25°C, and agitated at 1500-rpm in a heating block. The contents were then centrifuged at 13 000 *xg* at 4°C for 5 min. Approximately 900 µl of the supernatant was transferred to new 2 ml microcentrifuge tubes. The residues were reextracted using 750 µl 100% methanol without standards. The supernatants (1650 µl in total) were completely dried over a flow N_2 at 30°C and eluted with 300 µl 100% methanol.

2.2.5.1.2 Quantification of phytohormones by LC-MS/MS

Phytohormone analysis was performed on an Agilent 1260 high-performance liquid chromatography (HPLC) system (Agilent Technologies, Santa Clara, CA, USA) attached to an API 5000 tandem mass spectrometer (AB SCIEX, Darmstadt, Germany) as described by Ullah et al. (2019). The parent ion and corresponding fragments of jasmonates, and ABA were analyzed by multiple reaction monitoring as described earlier (Vadassery et al., 2012). The concentrations of ABA, JA, and JA-Ile were determined as described previously by Ullah et al. (2019).

2.2.5.2 Anthocyanin measurements

Anthocyanin content was measured according to the modified protocol of (Neff and Chory, 1998) Briefly, whole rosettes leaves were ground with liquid N_2, 100 mg of the ground tissue were mixed with extraction buffer (methanol with 1% HCl) and the mixture was placed at 4°C in the dark overnight. After the addition of 200 µl H_2O and 500 µl chloroform, the samples were mixed thoroughly and centrifuged at 14,000 *xg* for 5 minutes. After centrifugation, 400 µl of the supernatant were collected in a new tube and re-extracted with 400 µl of 60% Methanol 1% HCl, 40%. The absorbance of the solution was taken at 530 nm (anthocyanin) and 657 nm (background) and anthocyanin content was expressed as (A530-A657) per g fresh weight.

3. Results

Previous studies done on jasmonate signaling mostly focused on biotic stimuli. JAR1-mediated accumulation of JA-Ile, the biologically active jasmonate, was proven to efficiently interact with the COI1-JAZ receptor complex as part of most of the jasmonate-mediated responses (Katsir et al., 2008; Suza and Staswick, 2008; Yan et al., 2009; Wasternack and Song, 2017). However, the role of JA-Ile in abiotic stress was only studied to a very limited extent. Therefore, this study investigated the possible involvement of JA-Ile in drought stress with a focus on the JA-Ile-mediated trade-off balance between growth and drought stress response. Additionally, investigation of some of the JA-Ile dependent targets/regulators through various phenotyping, as well as genomic and biochemical approaches was performed.

3.1 JAR1

3.1.1 Identifying the subcellular localization of JAR1 splice variants

Three different splice variants have been predicted for *JAR1*, called *JAR1.1*, *JAR1.3*, and *JAR1.4* (http://aramemnon.uni-koeln.de/; Zander et al., 2020). These isoforms vary in their exon-intron structure as depicted in Figure 5A. The longest variant, *JAR1.4*, consists of five exons, whereas both *JAR1.1* and *JAR1.3* have four exons. They both have their transcription start side localized in exon 2 of *JAR1.4* but at different positions. It should be noted that the first described/identified variant was *JAR1.1* (Staswick et al., 2002). While all proteins transcribed from these splice variants are identical from exon 3 onwards, they differ in their N-terminal sequence. To check whether this might affect the subcellular targeting of the splice variants, I cloned their entire coding sequences into the pBIN19 vector in frame with the fluorescence protein YFP (Figure 5B). After sequencing, the JAR1.4 clone was found to still retain the first intron, thus creating a frameshift and an early stop codon. I therefore discontinued the analysis of this variant and transiently expressed the other two variants in tobacco (*N. benthamiana*). Analysis of transformed leaf cells by confocal fluorescence microscopy showed a YFP signal indicative of a cytosolic localization for both JAR1.1-YFP and JAR1.3-YFP (Figure 5C). From this I assume that endogenously expressed JAR1.1 and JAR1.3 both have a cytosolic localization.

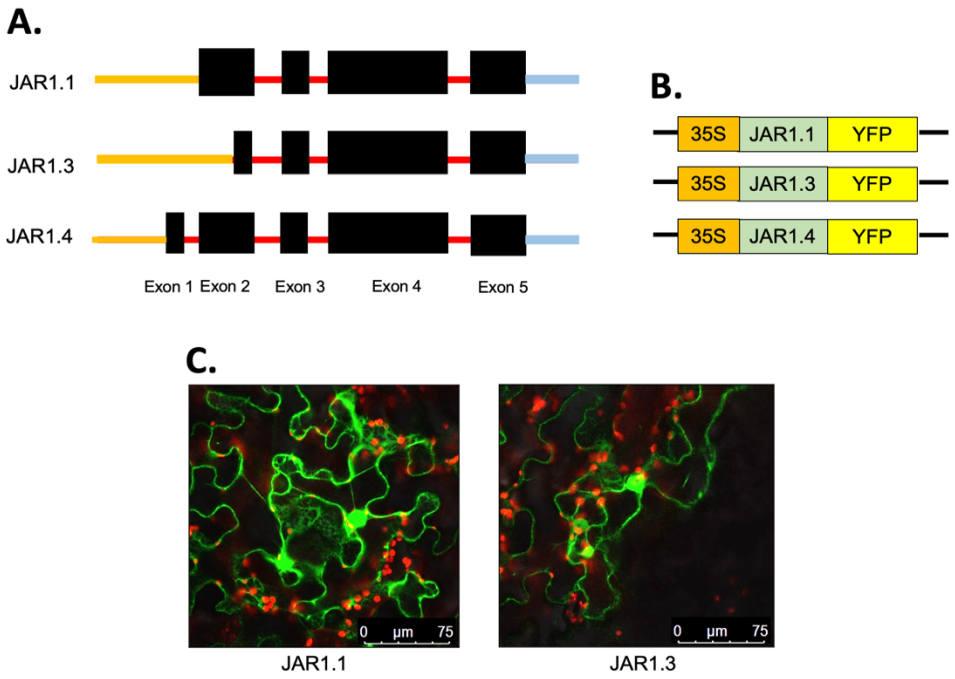

Figure 5: Subcellular localization of the JAR1 splice variants.
A. Intron-exon structure of different predicted splice variants of JAR1. Exons, introns, promoter regions including 5'-UTR and 3'-UTR are marked as black boxes, red lines, orange lines, and blue lines respectively. **B.** Schematic drawing of the vector constructs for the JAR1 splice variants. **C.** Localization of the JAR1.1-YFP and JAR1.3-YFP visualized by fluorescence microscopy in transiently transformed tobacco leaf cells. In the overlay pictures, Green fluorescence indicates the JAR1.1-YFP/JAR1.3-YFP, Red fluorescence indicates chlorophyll.

3.1.2 Generation of a stable JAR1.1-YFP line in Arabidopsis to study the effect of endogenous elevation of JA-Ile content

The first described JAR1 variant, JAR1.1 (35S::JAR1.1-YFP) was stably transformed into Arabidopsis wild-type (WT, Col-0) plants and homozygous plants were screened out. When analysed by confocal laser scanning microscopy, a cytosolic localization in Arabidopsis leaf cells similar as in tobacco was observed (Figure 6A). I further confirmed the expression of *JAR1.1-YFP* both at the transcript and protein level (Figure 6B and 6C). RT-qPCR analysis performed on rosette leaves collected from 32-day-old plants indicated that the expression level of *JAR1* in 35S::JAR1.1-YFP was more than ten times higher than in WT (Figure 6C) and more than thirteen times higher than in *jar1-11*, a T-DNA insertion mutant (Figure 6D) described previously (Suza and Staswick, 2008), which shows a strong reduction in *JAR1* expression. No knockout mutant of JAR1 is available and most of the previous mutant work on JAR1 was performed on *jar1-1,* a single amino acid point mutation line (Staswick et al., 1992). Furthermore, I identified JAR1.1-YFP at the protein level by western blot analysis using an antibody against GFP. I found a strong immunoreactive band at around 100 kDa, which fits the size of JAR1.1 (~70 kDa) tagged with YFP (~30 kDa) (Figure 6B). This immunoreaction

was observed in 35S::JAR1.1-YFP plants while it was absent in WT plants. I concluded that 35S::JAR1.1-YFP plant show expression both at transcript and protein levels and can be used as an overexpression line complementary to *jar1-11*. Thus, I termed 35::JAR1.1-YFP as JAR1-OE in further experiments.

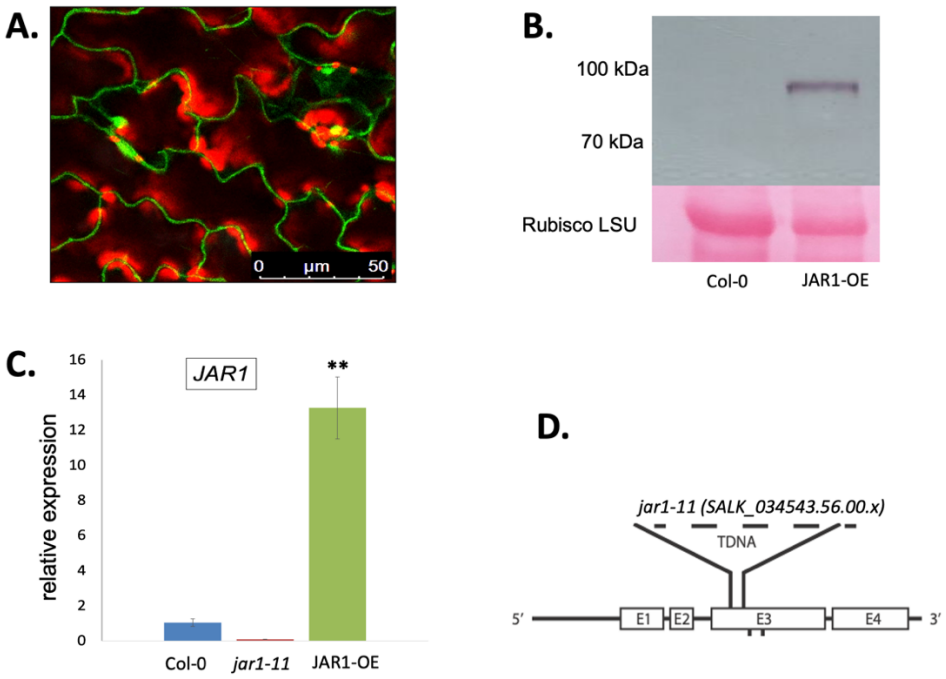

Figure 6: *JAR1* expression at the transcript and protein level.
A. Subcellular localization of the JAR1.1-YFP visualized by fluorescence microscopy in the epidermal leaf cells of the stably transformed Arabidopsis WT plants (Col-0). In the overlay picture, Green fluorescence indicates JAR1.1-YFP, Red fluorescence indicates chlorophyll. **B.** Protein Blot indicating the level of JAR1.1-YFP in the protein extract collected from the leaf tissue of the Arabidopsis plants. Upper panel; Membrane from the western blot showing the immunoreaction at around 100 kDa using the antibody against GFP in the JAR1-OE while no reaction detected in the WT, Lower panel; Ponceau stain showing the band of large subunit (LSU) of Ribulose-1,5-bisphosphate carboxylase/oxygenase (RUBISCO) used as equally loaded control. **C.** Relative expression of *JAR1* in the indicated plant genotypes. Expression was quantified by RT-qPCR from the leaves collected from 25-day-old plants. *JAR1* abundance is normalized to *Actin2* (*ACT2)* and expressed as relative quantity ($2^{-\Delta\Delta Ct}$). Data were analysed by multiple comparisons (Tukey test) followed by one-way ANOVA (**P<0.01). Error bars represent mean±SE (n = 3). JAR1-OE- 35S::JAR1.1-YFP stably transformed Arabidopsis plant. **D.** Schematic representation of the position of the T-DNA insertion at exon 3 (E3) in *jar1-11*. T-DNA insertion was confirmed with genotyping PCR.

3.1.3 Phenotypic validation of JAR1.1-YFP as overexpression line

Previous studies showed that exogenous MeJA application inhibits root and shoot growth of the plants, while jasmonic acid biosynthetic and signaling mutants remain insensitive to growth inhibition (Staswick et al., 1992; Xie et al., 1998). Thus, I assessed the root and shoot growth performance of JAR1-OE and the T-DNA insertion line, *jar1-11* according to established

protocol (Staswick et al., 1992). WT, JAR1-OE and *jar1-11* plants were grown on $^1/_2$ MS medium+sugar with or without 50 µM MeJA and root length was measured from 14-day-old seedlings, when the MeJA effect on the plants was clearly visible.

I found that the root length of JAR1-OE plants was significantly reduced even in the absence of MeJA, when no difference was found between *jar1-11* and WT (Figure 7A, - MeJA and 3B). Expectedly, after MeJA supplementation, *jar1-11* remained insensitive showing slight inhibition of root growth (Figure 7A, + MeJA and 3B). Inhibition of the shoot and root growth by MeJA was clearly visible in WT plants and both shoot and root growth of JAR1-OE was even more strongly suppressed in JAR1-OE after the MeJA application compared to WT. Overall, I conclude that ectopically expressed JAR1 can induce jasmonate signaling even without stimuli and that, with MeJA application, stunted growth through jasmonate signaling occurs even higher.

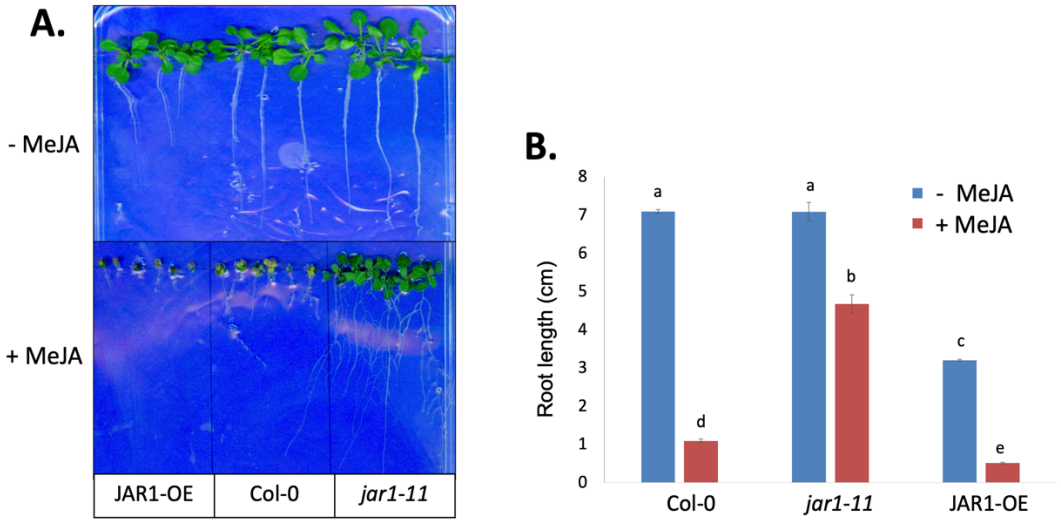

Figure 7: MeJA-mediated root and shoot growth sensitivity of the plants in $^1/_2$ MS medium.
A. Photographs were taken from 14-day-old seedlings those were grown under a long day (16 h/8 h light) condition. Upper panel- seedlings were grown on $^1/_2$ MS plate supplemented with sugar; Lower panel- Plants were grown on $^1/_2$ MS plate supplemented with sugar plus 50 µM MeJA. **B.** Bar plot showing the root length of the plants grown on $^1/_2$ MS plate with or without MeJA. Root lengths were measured using ImageJ. Data were analysed by multiple comparisons (Tukey test) followed by two-way ANOVA. Data represents mean±SE (n = 3); each replicate contained 10 seedlings at least. Bars with different letters are significantly different from each other ($P < 0.05$).

3.1.4 JA-Ile accumulation affects the growth and flowering behavior of plants under soil-grown condition

Most of the previous studies on the role of jasmonates using exogenous JA/MeJA application were performed at the seedling/initial growth stage using plant grown on media plates or cultured cells. These studies suggested that jasmonate signaling can result in arresting cell cycle processes and ultimately plant growth (Howe et al., 2018; Wasternack, 2017). When growing in nature, plants experience variable conditions that might affect their growth and flowering throughout and depending on their development. The role played by jasmonates in this variable growth pattern, especially endogenous JA-Ile in non-stressed soil growing conditions has been little studied. I thus conducted a phenotyping experiment under non-stressed soil conditions spanning from the germination stage to completion of the life cycle.

No difference in germination rate was observed on soil, whereas, a reciprocal trend in the size of both cotyledons as well as emerging true leaves was found between *jar1-11* and JAR1-OE. *jar1-11* plants had larger cotyledons, whereas JAR1-OE, had smaller cotyledons than the WT plants (Figure 8, day 11). On day 18, a distinguished rosette difference was observed between *jar1-11* and JAR1-OE. At this stage, leaf blades were narrower and longer in *jar1-11,* while the leaves were rounder and smaller in JAR1-OE (Figure 8, day 18). This difference was more visible at day 25 with an overall larger rosette shape in *jar1-11* compared to JAR1-OE where stunted growth became clearly visible (Figure 8, day 25**)**.

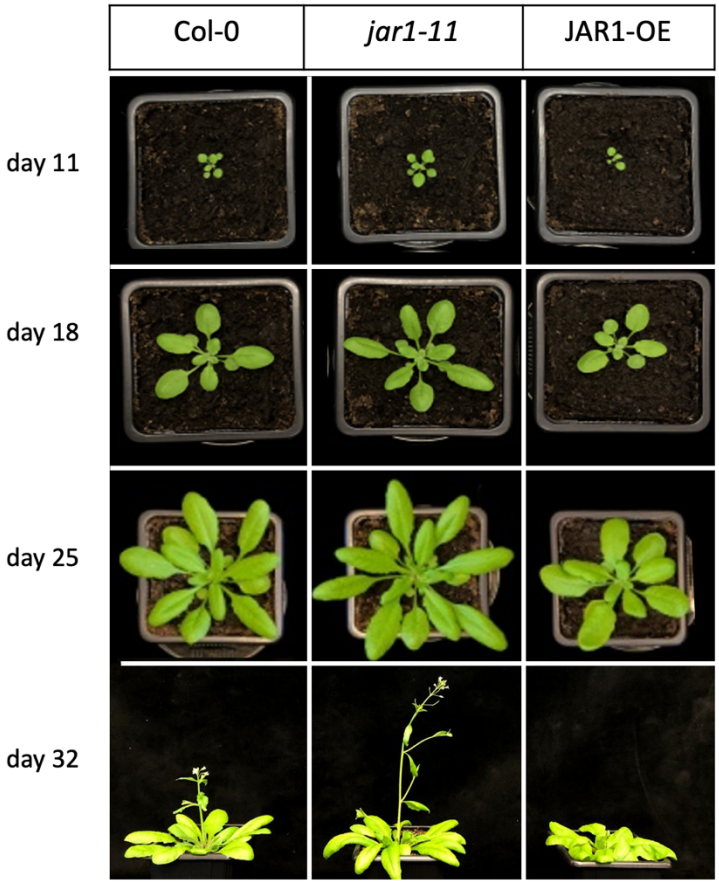

Figure 8: JAR1-dependent variation in leaf growth and flowering time.
Day-to-day variation of the leaf growth and flowering phenotype of the plant genotypes growing on soil under long-day (16 h/8 h light) condition. **Day (11-25),** Day 11 showing the 5-6-day-old seedlings 7 days after transplantation and a difference in the cotyledons are visible in the plants; Day 18 showing a distinguished narrower and longer shape of the true leaves of *jar1-11.* Day 25 showing distinguished round and smaller shapes of the true leaves of JAR1-OE. Day 32 showing the difference in flowering time between the plants. Plants were grown on the square pots with 100 g of soil placed over round Petri dishes. Every pot is watered with 50 ml of water per week. This experiment was repeated at least five times with similar results.

jar1-11 plants also initiated bolting (flower bud emergence) early (on day 25), whereas WT started bolting on day 32 and JAR1-OE bolted around 8 days after WT (Figure 9A**)**. Whereas *jar1-11* plants at their bolting stage (day 25) had around 15 true leaves, on the same day, WT had 12 and JAR1-OE only 10 leaves (Figure 9B**)**. However, even at the bolting stage, WT and JAR1-OE had a lower rosette leaf number than *jar1-11* of 13 and 11 leaves, respectively (Figure 9C**)**.

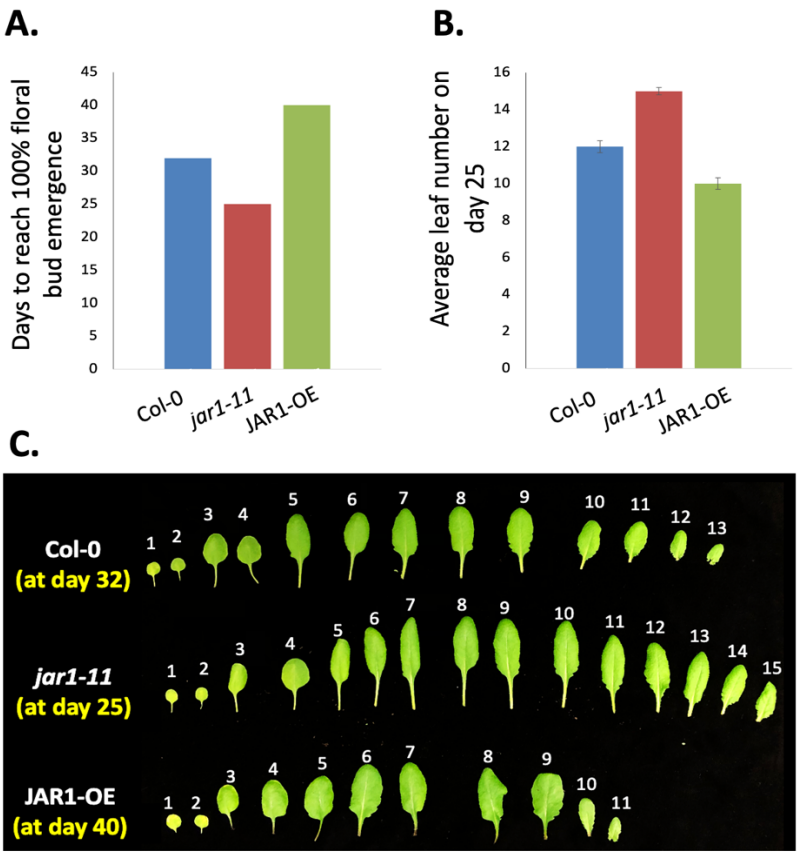

Figure 9: JAR1-dependent variation in leaf number and flowering time.
A. Time points when all the plants of the indicated plant genotypes started bolting (flower bud emerged as ~1 cm long). **B.** Rosette leaf number of the indicated plants on day 25 at the bolting stage of *jar1-11*. Data represents mean±SE (n = 3) **C.** Rosette leaf number of the indicated plants at their bolting stage grown under long-day (16 h/8 h light). Leaves were detached when the flower bud emerged as ~1 cm long.

Interestingly, JAR1-OE plants developed a broader leaf at later stages characterized by the lateral growth of the leaf blade, though their length was still shorter than that of WT and *jar1-11* (Figure 10, day 40**)**. Flowering of *jar1-11* and WT was finished around day 47 when no more apical buds emerged. In contrast, JAR1-OE plants continued flowering until day 53 (Figure 10, day 47**)**.

Figure 10. JAR1-dependent variation in leaf shape and flowering pattern at the late stage.
At the upper panel (Day 40), Leaf growth is almost to be terminated in the WT and *jar1-11* and started producing several side branches of the flowering stem. Siliques of the primary stem of *jar1-11* are matured. JAR1-OE showing lateral leaf growth with a broader shape and the bolting just initiated. At the lower panel (Day 47), a side view of the flowering stems of the indicated plant genotypes. Apical buds of all the branches of *jar1-11* matured into siliques, in WT the buds in the primary stem fully matured while in other branches are about to mature into siliques. In the JAR1-OE apical buds are still growing into siliques. Plants were grown on under long day (16 h/8 h light).

I also found that at termination of flowering the length of the primary stem in JAR1-OE was significantly shorter than its lateral stems immediately below. In contrast, the primary stem was significantly longer in *jar1-11* and in WT (Figure 11A and B**)**. Also, the overall length of both primary and lateral stems was comparatively shorter in JAR1-OE than in *jar1-11* and WT (Figure 11B**)**.

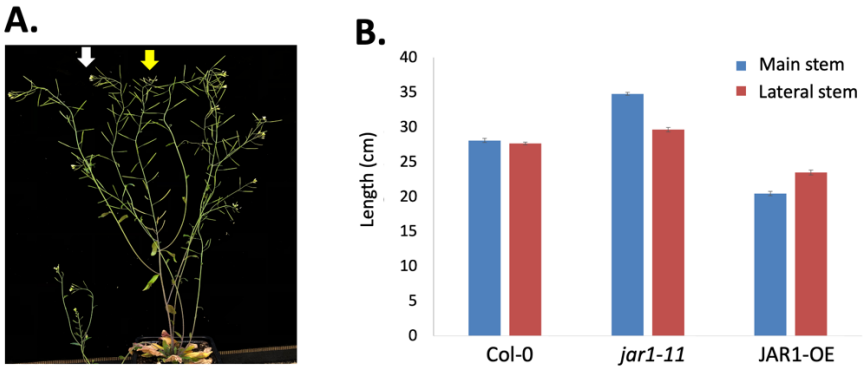

Figure 11: JAR1-dependent flowering pattern of the plants at the bolting stage.
A. Flowering pattern of JAR1-OE plants on day 53. The yellow arrow indicates the primary flowering stem which is smaller than the lateral stem (white arrow). **B.** Bar plot showing the comparison of length of primary stem and lateral stem of the inflorescence of the indicated plant genotypes. Lateral stem is considered as the stem immediately below the primary stem. Plants were grown under long day (16 h/8 h light).

Overall, I conclude that JAR1-dependent JA-Ile accumulation can affect plant leaf growth and flowering even under non-stress conditions.

3.1.5 Phenotypes of other jasmonate pathway mutants

I conducted a similar phenotypic analysis with mutants affected in enzymes/receptor localized up or down-stream of JAR1 in the jasmonate pathway. These included *aos* and *opr3,* in which the production of precursor molecules of *cis*-OPDA and JA, respectively, are blocked, as well as the jasmonate receptor mutant, *coi1-1*. In contrast to all other mutants, *opr3* was present in the Wassilewskija (Ws) ecotype background, so it was compared to a Ws wildtype (Ws).

When compared to their respective wild type, *aos* and *opr3* showed changes in leaf shape and rosette size similar to *jar1-11,* while *coi1-1,* even though it is involved in the same signaling mechanism, interestingly, showed no alterations. (Figure 12, upper panel**)**.

In the case of flowering behavior, *aos*, *opr3* and *coi1-1* all showed early flowering similarly to *jar1-11*, with *coi1-1* showing the earliest flowering (18 days) and a much more bush-like appearance (Figure 12, lower panel**)**.

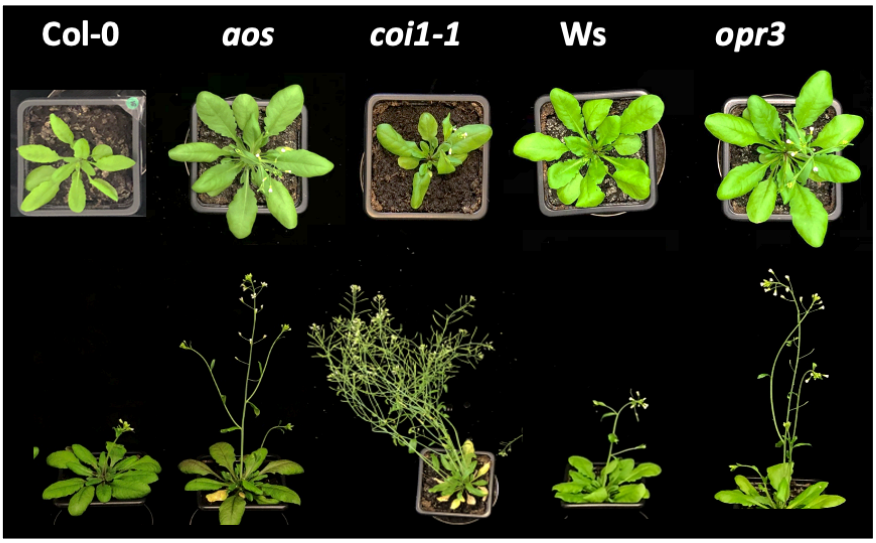

Figure 12: Phenotype of the jasmonate pathway mutants.
Upper panel showing the variation of rosette leaf between the mutant lines of jasmonate pathway and their respective WT on day 25. Lower panel showing the length of the flowering stem on day 32. *opr3* is compared to Ws (Wassilewskija) WT. Plants were grown under long day (16 h/8 h light).

Overall, I conclude that disruption of JA-Ile synthesis upstream of JAR1 produces phenotypes similar to *jar1-11*, while alterations in the receptor have differential effects on growth and flowering.

3.1.6 JAR1-mediated JA-Ile formation regulates drought stress response

With regard to jasmonate signaling, drought stress is the least well documented amongst abiotic stresses so far. A few studies showed that drought can initiate jasmonate signaling and that *vice-versa* some common drought stress-induced genes were differentially expressed after exogenous JA/MeJA application (Zander et al., 2020; Hickman et al., 2017; Huang et al., 2008; Wang et al., 2020; Clauw et al., 2016) . Though endogenous JA-Ile was found to positively regulate biotic stresses, the *jar1-1* mutant, which has a single amino acid point mutation, showed a similar phenotype to WT under moderate drought stress (Harb et al., 2010). Expression of *JAR1* under different stresses was also very transient (Hickman et al., 2017; Suza and Staswick, 2008), which made it difficult to establish the exact role of JA-Ile under drought stress. To clarify this discrepancy, phenotypic experiment with the WT, T-DNA insertion line, *jar1-11* and overexpression line- JAR1-OE under progressive drought stress was performed (Figure 13A**)**. For the initial drought stress experiment, I placed single 5-6-day old seedling in pots containing 100 g of soil and watered the plants with an identical volume of 50 ml of water until day 18. Drought was imposed by withholding irrigation until day 39, while control plants were watered regularly. Pots were weighed regularly to monitor the soil moisture. Drought

exposed plants were re-watered at day 39 and the survival rate was counted after 24 hours and 1 week (Figure 13A).

First drought stress symptoms in form of wilting were identified on day 32 when the soil relative water content (SWC) reached 40%. On day 36, when the soil water content reached 20%, severe wilting symptoms were observed in *jar1-11* plants (Figure 13B) and the WT started mild wilting. On day 39 (SWC of 10%), both *jar1-11* and WT reached a stage of unrecoverable wilting where no plants could recover 24 hours after re-watering. However, at this same stage, JAR1-OE only showed very mild symptoms of wilting, which were easily recoverable within 24 hours of re-watering (Figure 13B).

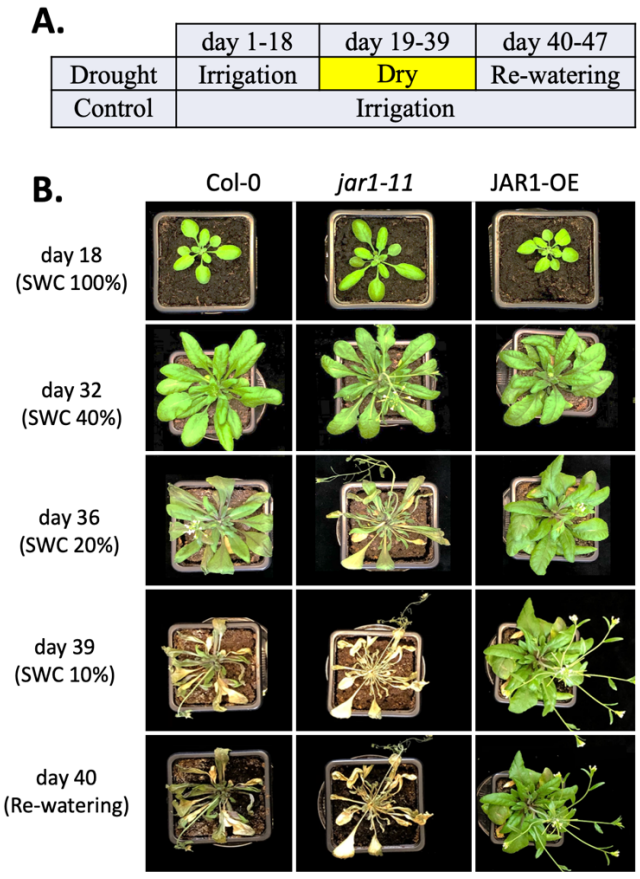

Figure 13: JAR1-dependent drought stress response under long-day conditions (16 h/8 h).
A. Schematic drawing showing the progressive drought stress time-points. The yellow box represents the time point for drought stress. **B.** Drought stress effects on the plants grown in long day (16 h/8 h light) conditions. Plants were watered regularly until day 18 and irrigation was stopped on day 18 which is discontinued until day 39. The first drought stress symptom is appeared as severe wilting of *jar1-11* on day 36. and WT started mild wilting. On day 39, an unrecoverable wilting symptom in WT and *jar1-11* while JAR1-OE showing mild wilting. On day 40 showing no recovery of the WT and *jar1-11* but JAR1-OE continued to grow as well-watered conditions. All the pots were randomized every day. This phenotyping was repeated at least five times with similar results.

To assess the physiological effect of water loss, I measured leaf relative water content (RWC) on day 32 **(**SWC 40%) and day 36 **(**SWC 20%). Leaf RWC was lowest in *jar1-11,* dropping 60% on day 32, while WT retained 80% (Figure 14**)**. At this stage, JAR1-OE still had around 100% RWC. However, after the SWC reached 20% on day 36, leaf RWC of *jar1-11* went below 30% and below 50% for WT. JAR1-OE still retained 80% RWC which would explain its resilience against drought (Figure 14**)**.

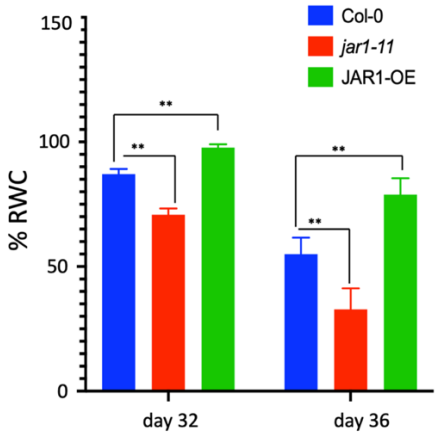

Figure 14: JAR1-dependent leaf relative water content under drought stress.
Whole rosettes of the indicated plants were collected on day 32 (SWC 40%) and day 36 (SWC 20%) for measurement. Data were analysed by multiple comparisons (Tukey test) followed by one-way ANOVA (**P<0.01). Error bars represent mean±SE (n = 3).

Under long day conditions, the plants of all genotypes would go from vegetative to reproductive stage within the time frame of the experiments. I thus performed a similar progressive drought stress experiment under short-day conditions (8 h/16 h light) to maintain all the plants in the vegetative stage since induction of flowering may affect the drought stress response. Under these conditions, when the SWC reached 40% on day 32, *jar1-11* plants again started wilting while the other two plants (WT and JAR1-OE) were still growing normally (Figure 15A). However, on day 39, all the plants including JAR1-OE showed heavy wilting symptoms and after 24 hours of re-watering, only the JAR1-OE plants could recover. After 1 week of re-watering, most of the WT but none of the *jar1-11* plants could recover (Figure 15A). After repetition of the experiment, I calculated the survival rate of the recovered plants on day 47. After 1 week of watering, 100% JAR1-OE could recover after heavy wilting, 80% of WT and 0% of *jar1-11* (Figure 15B).

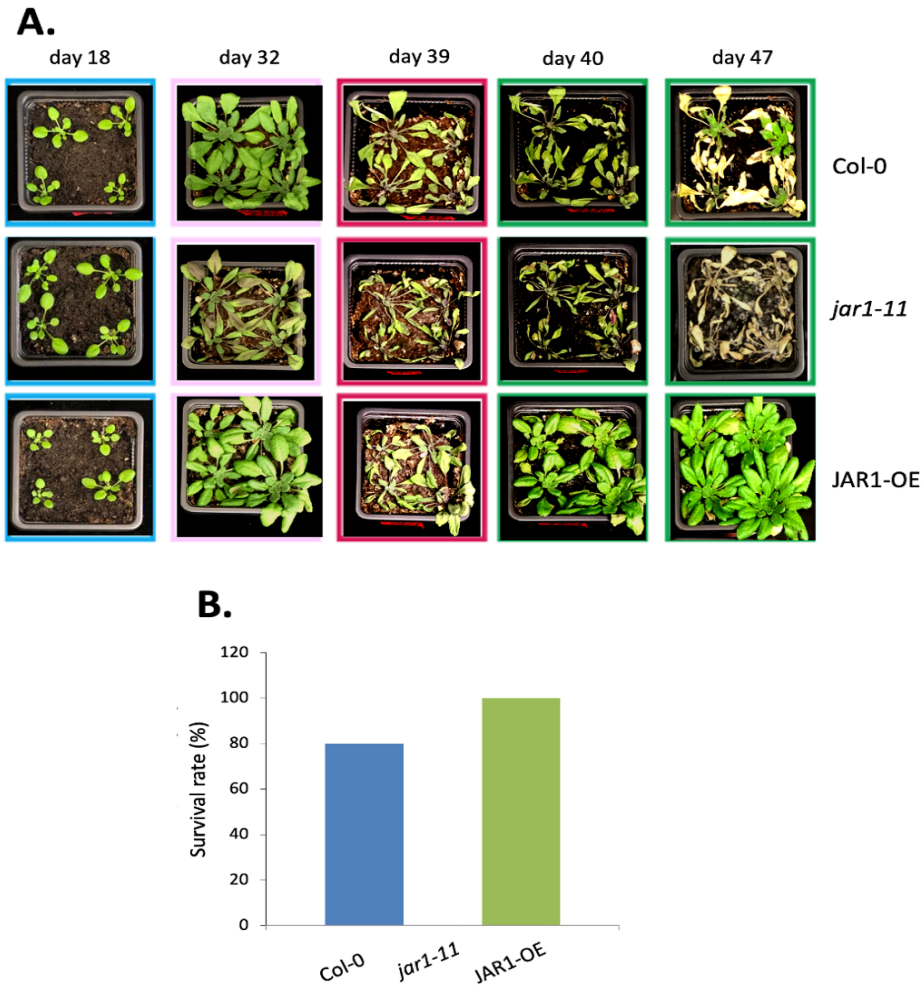

Figure 15: JAR1-dependent drought stress response under short-day (8 h/16 h light) conditions.
A. Progressive drought stress effects on the indicated plants. Four seedlings at day 7 were transplanted per pot placed on a round Petri dish and watered regularly until day 18. After the drought stress imposition, plants were randomized every day. Wilting symptom of *jar1-11* appeared on day 32. On day 39, 50 ml of water was added to the round Petri dish. This phenotyping was repeated at least twice with similar results. **B.** Survival rate of the indicated plants. Survival was calculated from two separate experiments with a total of 32 plants. This was calculated at day 47. Data are means of 2 separate experiments. The percentage was calculated based on the number of plants transplanted to the number recovered on day 47.

Taken together, I conclude that JAR1-mediated JA-Ile accumulation enhances the plants resistance against progressive drought stress irrespective of day-length and developmental stages.

3.1.7 Performance of other jasmonate pathway mutants under progressive drought stress

I also performed similar drought stress experiments with the *aos*, *opr3* and *coi1-1* mutant in the long day (16 h/8 h) conditions. As before, *opr3* was compared to the Ws background WT. Similar to *jar1-11*, both *opr3* and *aos* wilted earlier than the WT with clear signs of wilting visible on day 32 (Figure 16**)** and all plants reached unrecoverable wilting on day 39. The

wilting symptoms of *opr3* were even stronger than that of other mutants. However, I observed no difference in wilting symptoms between Ws and Col-0 background WT (Figure 16). *coi1-1*, however, with its fast flowering and early completion of the life cycle, did not display a specific phenotype under these progressive drought stress conditions.

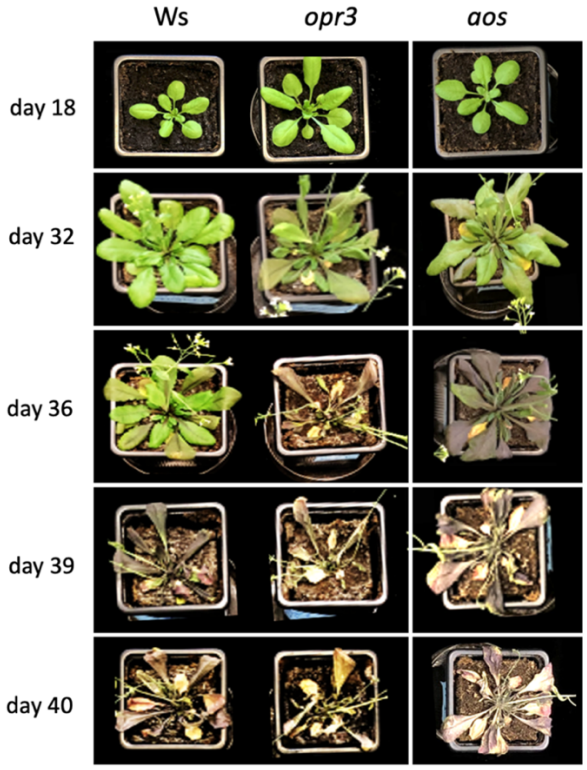

Figure 16: Drought stress-responsive phenotypes of the jasmonate pathway mutants.
Drought stress was imposed according to the scheme in Figure 13A under long-day (16 h/8 h light) conditions. *opr3* is compared to Ws (Wassilewskija) WT. *aos* is compared to Col-0 WT.

3.1.8 Effect of JAR1-mediated JA-Ile formation on anthocyanin accumulation

Anthocyanin accumulation has been an indicator for different biotic and abiotic stresses including drought (Misyura et al., 2012). Exogenous JA application enhances anthocyanin accumulation (Ai and Zhu, 2018). Thus the anthocyanin content was measured from the rosettes of 32-day-old plants under both control and drought stress conditions. On visible inspection I observed accumulation of anthocyanin in the leaf vein and leaf base of rosette leaves of 32-day-old plants in long-day conditions. Accumulation was visible as a dark brown color in the leaf base of JAR1-OE plants, while the veins of the WT appeared only light-brown dark. No accumulation was visible in *jar1-11* (Figure 17A).

When the anthocyanin content was measured from the rosettes of 32-day-old plants under both control and drought stress conditions, I could confirm a higher accumulation of anthocyanin in JAR1-OE, about three times higher compared to WT, whereas *jar1-11*, only contained about 1/10 of the content of JAR1-OE (Figure 17B).

Anthocyanin content increase in all plants upon drought stress with levels in JAR1-OE about 2 times higher than in WT and 5 times higher than in *jar1-11* (Figure17B). The increase in anthocyanin in *jar1-11* suggests that anthocyanin accumulation is also linked to processes other than JA-Ile accumulation.

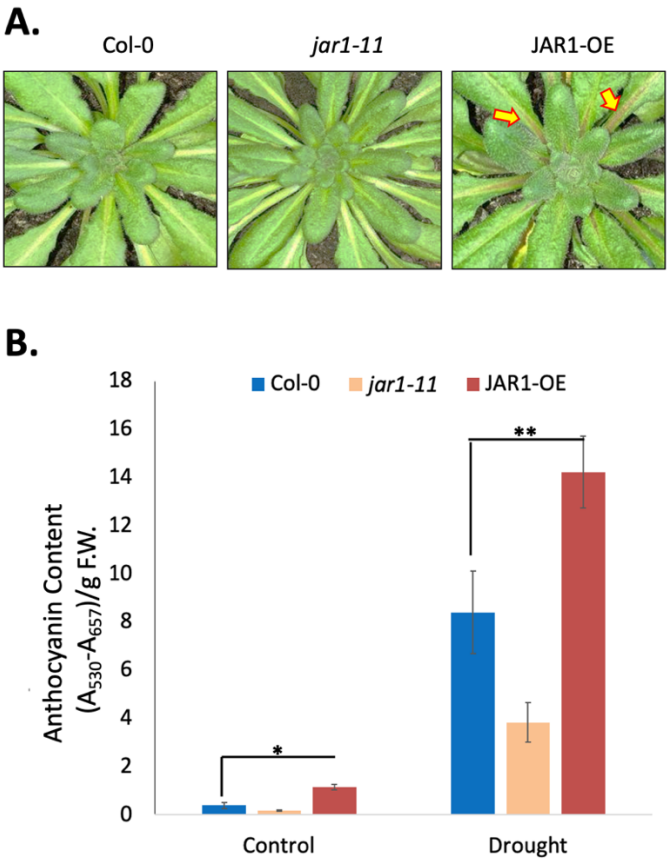

Figure 17: JAR1-mediated variation of anthocyanin accumulation.
A. Anthocyanin accumulated regions in rosette leaves. The yellow arrow indicates the anthocyanin accumulated region in JAR1-OE. The photograph was taken from the plants on day 32 growing under well-watered long day (16 h/8 h light) conditions. **B.** Bar plot indicates anthocyanin content growing under control and drought stress conditions of the indicated plant genotypes. Anthocyanin was measured from the rosette leaves of the indicated plants on day 32 under long-day conditions (16 h/8 h light). Data were analysed by multiple comparisons (Tukey test) followed by one-way ANOVA (*P<0.05, **P<0.01). Error bars represent mean±SE (n = 3).

3.1.9 JAR1-mediated regulation of jasmonates under well-watered and drought stress conditions

Phenotypic studies had shown that variation in endogenous JA-Ile content, can alter growth in soil growing conditions, and this phenotypic alteration is likely related to the homeostasis of jasmonates. Thus, an analysis of the bioactive jasmonate JA-Ile, its precursors *cis*-OPDA and JA, as well as their major catabolic products, was performed on intact rosette leaves of WT, *jar1-11* and JAR1-OE from 32 days old plants. I choose this stage since only minor wilting symptoms under progressive drought stress appeared at this stage.

In control conditions, I found that the content of both the precursor *cis*-OPDA (Figure 18A) as well as JA-Ile (Figure 18C) were highest in JAR1-OE and lowest in *jar1-11*, which only contained minute amounts of JA-Ile since the pathway to JA-Ile from JA was blocked. JA content was higher in *jar1-11* compared to WT and JAR1-OE since the blockage in conversion caused an accumulation of the unutilized JA. No significant difference was found between WT and JAR1-OE (Figure 18B) with regard to JA. I also measured the catabolic products of JA and JA-Ile and in a similar trend to JA-Ile, 12-OH-JA, 12-OH-JA-Ile and 12-COOH-JA-Ile was also enhanced in JAR1-OE compared to WT and this difference was even higher between *jar-11* and JAR1-OE (Figure 18D, F, G). I did not find any significant difference in the highest abundant derivative, JA-Glc, except for a slight increase in *jar1-11* (Figure 18E). Notably, the amount of all the precursors and catabolic derivatives were higher than JA-Ile.

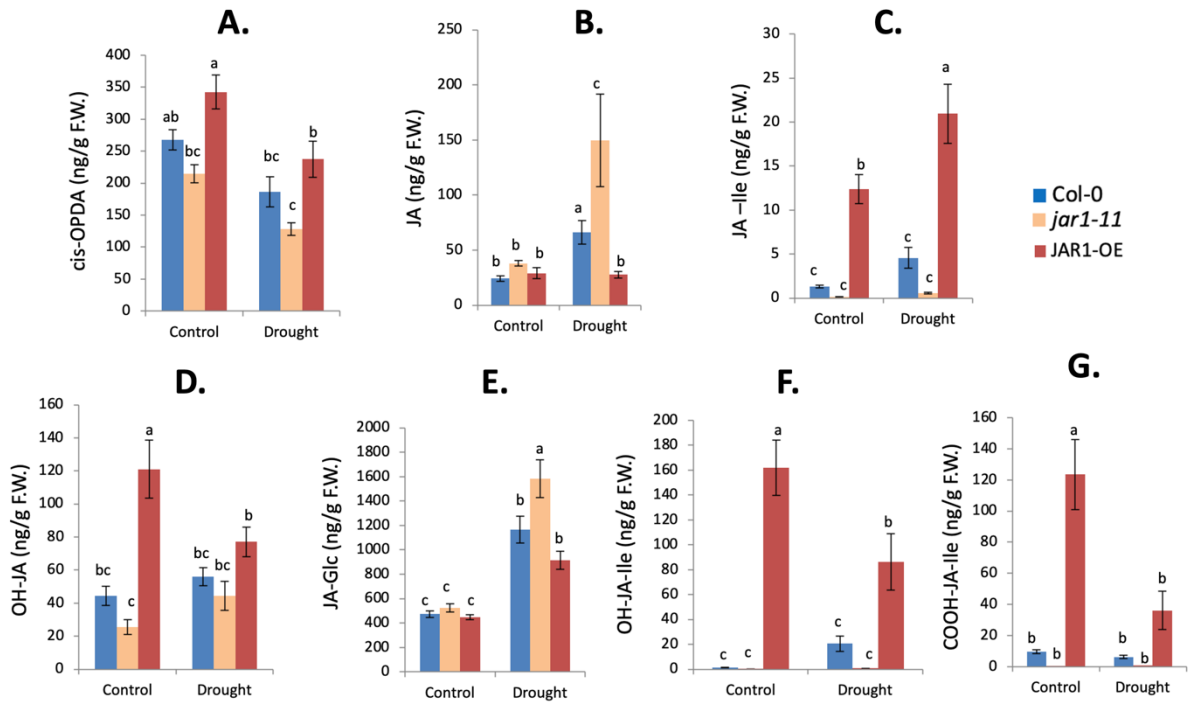

Figure 18: JAR1-mediated variation in the jasmonates under control and drought stress conditions. **(A-G)** Drought-induced variation of the content of jasmonates, **A.** *cis*-12-oxo-phytodienoic acid (*cis*-OPDA), **B.** Jasmonic acid (JA), **C.** Jasmonyl-isoleucine (JA-Ile), **D.** 12-hydroxyjasmonic acid (12-OH-JA), **E.** 12-hydroxyjasmonoylglucoside (12-*O*-Glc-JA), **F.** 12-hydroxy-Jasmonyl-isoleucine (12-OH-JA-Ile), and **G.** 12-carboxy-Jasmonyl-isoleucine (12-COOH-JA-Ile) in the indicated plant genotypes compared to control conditions. Rosette leaves of the plants were harvested on day 32 for control as well as drought stress conditions. Samples were collected from six different biological replication each with pooled three individual plants, frozen in liquid nitrogen and subjected to extraction separately as described in the Materials and Methods section. Each compound was quantified via the corresponding internal standard. Analysis was repeated twice with similar results and here one replication is presented. Data were analysed by multiple comparisons (Tukey test) followed by two-way ANOVA. Data represnt means ± SE, n = 6. F.W.- fresh weight. Bars with different letters are significantly different from each other (P <0.05).

As stated previously, both JA and JA-Ile were found to be upregulated under artificial drought stress such as letting the severed shoot dry in lab conditions (de Ollas et al., 2015b). No previous studies focused on jasmonate profiling under more natural progressive drought stress. Moreover, variation in drought response, especially for the endogenous JAR1-mediated JA-Ile, is likely linked to the regulation of other jasmonates. Thus, I further analysed the jasmonate content from the progressive drought-stressed samples and compared them with the control conditions. I collected rosette leaves from the WT, *jar1-11* and JAR1-OE plants on day 32 before the severe drought stress-induced wilting appeared. Drought stress resulted in a decrease in *cis*-OPDA in all plants albeit to a lesser extent in JAR1-OE and to the highest extent in *jar1-11*(Figure 18A). However, both JA (Figure 18B) and JA-Ile (Figure 18C) were increased under drought stress in WT which supports the previous findings that drought stress initiates JA biosynthesis. The level of JA was higher in *jar1-11,* while JA-Ile content was higher in JAR1-OE (Figure 18B and C). This is not surprising because due to lack of the JAR1 protein, the

substrate JA overaccumulated in *jar1-11* while more JAR1 could convert the substrate JA into JA-Ile in JAR1-OE. There was a slight increase of 12-OH-JA in WT, and *jar1-11* but remarkable decrease in JAR1-OE under drought stress (Figure 18D), which supports the direction of the flow towards JA-Ile. However, JA-Glc was highly up-regulated in all plants under drought (Figure 18E). Though the other catabolic products of JA-Ile, i.e. 12-OH-JA-Ile and 12-COOH-JA-Ile, were enhanced under drought stress in WT, the content of both was virtually absent in *jar1-11* and decreased in JAR1-OE (Figure 18F and G).

Overall, I conclude that drought stress enhances JA level in WT and *jar1-11*, while JA-Ile level are enhanced in WT and JAR1-OE. JAR1 overexpression enhances the upregulation of JA-Ile biosynthesis under non-stress conditions and drought stress further enhances this synthesis while disruption of JA-Ile accumulation in *jar1-11* inhibits the biosynthesis of JA-Ile as well as its catabolism.

3.1.10 JAR1-dependent global gene expression under well-watered conditions

The considerable phenotypic and hormonal differences due to the difference in JAR1-mediated JA-Ile accumulation is likely linked to the regulation of corresponding genes. An analysis of global gene expression can reveal insights into the molecular changes underpinning these differences. Thus, I performed RNA-seq to monitor global gene expression from rosette leaves of the 32-day-old well-watered WT (Col-0), *jar1-11* and JAR1-OE plants grown under long-day conditions. RNA-seq data were analysed with the help of Annika Kortz (INRES, Institute of Crop Science and Resource Conservation, Crop Functional Genomics, University of Bonn, Bonn, Germany). After performing RNA-seq, the gene clusters were analysed through PCA and I found that the deviation in each cluster was minimal (Supplementary Figure 1). Using the parameters (DESeq, adjusted FDR <0.01 and LogFC ≥ 1), I found only 4 differentially expressed genes (DEGs) between *jar1-11* and WT under control conditions, all of them downregulated. In contrast, I found 339 DEGs between JAR1-OE and the WT, of which 134 were downregulated and 205 were upregulated (Figure 19A). Among the downregulated genes in *jar1-11*, one was differentially expressed between *jar1-11* and JAR1-OE, being downregulated in *jar1-11* while upregulated in JAR1-OE. One putative phytocyanin gene (*AT1G22480)* had null expression in *jar1-11* and one gene- *PER64* was downregulated in both *jar1-11* and JAR1-OE (Figure 19B).

By looking at DEGs with potential connection to the phenotypic differences such as leaf morphology and growth regulation, I found genes related to cell formation, growth and cell

wall biosynthesis/modifications were differentially expressed between WT and JAR1-OE (Figure 19B, right and Supplemental Table 1).

Leaf morphology

Consistent with the differences in leaf morphology between WT and JAR1-OE, cell growth/cycle-related genes that are already documented or have the putative capacity to regulate cell cycle processes such as *SYP111, FBL17, CYCA3.2* and *CYCB1.2* were upregulated in JAR1-OE (Figure 19B, right and Supplemental Table 1). *CYCB1.2* was found to be involved in the G2-to-M transition of the cell cycle, regulating the mitotic cycle to produce more cells and preventing DNA damage during stress (Takahashi et al., 2019; Boruc et al., 2010), and it was also found to be sensitive to salt stress. Cell wall-related genes were mostly related to cell wall expansion and loosening. Among the upregulated genes, some were also related to the cell wall modifications such as *CSLD5* and *EXPA3*, (Bernal et al., 2007; Armezzani et al., 2018; Stamm et al., 2017), or cell wall development, such as the PEG responsive lipid transfer protein *LTP2* (Chae et al., 2010; Jacq et al., 2017) (Figure 19B, right and Supplemental Table 1). Also, consistent with the observed difference in leaf shape between *jar1-11* and JAR1-OE, I found two growth-regulating genes, *GIFI* and its interacting partner *GRF5*, to be upregulated in JAR1-OE while slightly downregulated in *jar1-11* (Supplemental Figure 2). Because of some ambiguous reads between replicates in RNA-seq, I employed RT-qPCR to monitor the difference of *GIFI* expression between *jar1-11* and JAR1-OE. Accordingly, the expression of *GIF1* was highly upregulated in JAR1-OE and slightly downregulated in *jar1-11* (Figure 19C).

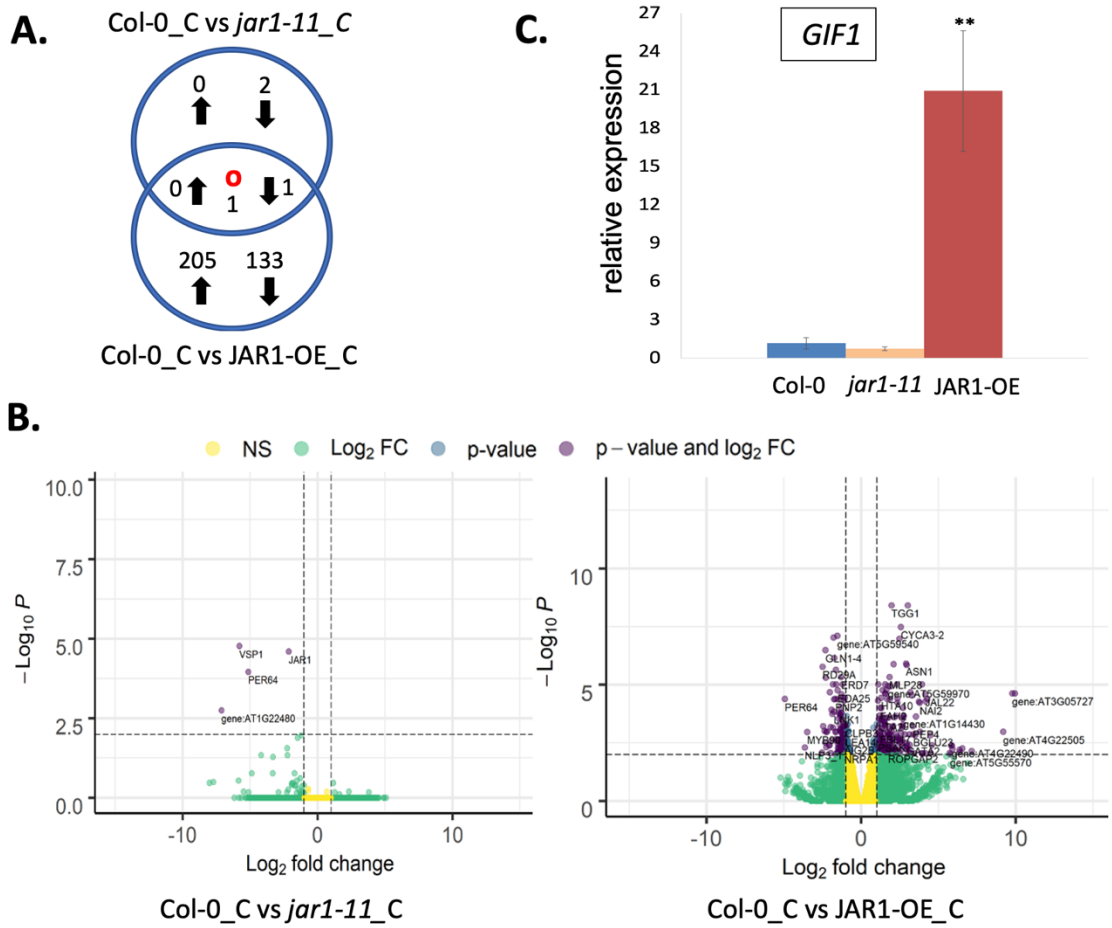

Figure 19: JAR1-dependent changes in gene expression in rosette leaves.
Rosette leaves under well-watered conditions on day 32 were collected for RNA-seq. **A.** Venn diagram showing DEGs up-and downregulated (DESeq, adjusted FDR <0.01 and LogFC ≥1) in *jar1-11* and JAR1-OE compared to WT plants. "O" indicates counter-regulated genes. "C" under control conditions. Arrows indicate up- and downregulation. **B.** Volcano plots showing statistical significance ($\log_{10}P$) versus magnitude of change (LogFC) of DEGs between WT (Col-0) and *jar1-11* (left); WT (Col-0) and JAR1-OE (right). Violet dots indicate genes that fit the DESeq criteria of FDR <0.01 and LogFC ≥1; green and blue dots represent DEGs that fit either only LogFC or FDR, respectively. **C.** Relative expression of *GIF1* in the indicated plant genotypes. Expression was quantified by RT-qPCR from the leaves on day 32. *GIF1* abundance is normalized to *ACT2* and expressed as relative quantity ($2^{-\Delta\Delta Ct}$). Data were analysed by multiple comparisons (Tukey test) followed by one-way ANOVA (**P<0.01). Error bars represent mean±SE (n = 3).

Flowering time

Although *jar-11* plants displayed early and JAR1-OE delayed flowering, there was no variation in the major flowering controller i.e. as *FT, LEAFY,* or *APETALA2.* Presumably, this can be due to sample collection from leaf samples. However, some autonomous floral responsive genes, which are mostly located in the leaf area were differentially expressed in JAR1-OE compared to WT plants though they remained unchanged in *jar1-11* as seen in the heat map (Figure 20A). The main regulator of autonomous flowering is *FLOWERING LOCUS C* (*FLC*), which inhibits the early flowering controller *SOC1* (Michaels and Amasino, 2001; Richter et al., 2019). FLC was itself increased while *SOC1* expression was decreased, which relates well

to the late flowering in JAR1-OE. Besides them, the expression of the early flowering inducers *MAF1* (Ratcliffe et al., 2001) and *SPL4* (Schmid et al., 2003; Wu and Poethig, 2006) was decreased. Expression of the *MYROSINASE BINDING PROTEIN 2 (MBP2; F-ATMBP*), related to flowering regulation through the COI1 receptor (Capella et al., 2001), on the other hand, was upregulated (Figure 20A).

Jasmonate pathway

Regarding the jasmonate pathway, I presented the genes through a heat map in three categories- biosynthesis, catabolism and signaling response (Figure 20B). Under well-watered conditions, I could not find any significant changes in the biosynthetic genes except in *JAR1,* as expected, with a reciprocal trend of downregulation in *jar1-11* and of upregulation in JAR1-OE (Figure 20B). Expression of *JAR1* was not null in *jar1-11* (Supplemental Figure 2) which supports the previous expression studies through RT-qPCR (Figure 6C). However, the effect of loss or gain of functions of JAR1 was visible from the expression of the jasmonate responsive gene- *VSP1* and *VSP2* (Figure 20B). Expression of *VSP1* was down-regulated to almost null while upregulated in JAR1-OE compared to WT. Though expression of *VSP2* in *jar1-11* remained unchanged compared to WT in the heat map, relative quantification through transcripts per million (TPM) showed slight downregulation in *jar1-11* (Supplemental Figure 2) while upregulation in JAR1-OE (Figure 20B and Supplemental Figure 2). Jasmonate-dependent master transcription factor- *MYC2,* which regulates the expression of most of the JA-responsive gene was slightly upregulated in JAR1-OE and downregulated in *jar1-11* (presented by TPM value in Supplemental Figure 2). However, *MYC4*, which is an interacting partner of MYC2, was surprisingly downregulated in JAR1-OE (Figure 20B). Two catabolic products, *ILL6*, which converts 12-OH-Ile to JA-Ile, and *JOX3*, which is involved in the hydroxylation of JA were highly upregulated in JAR-OE (Figure 20B), which is consistent with the difference in content of 12-OH-Ile and 12-OH-JA respectively (Figure 18).

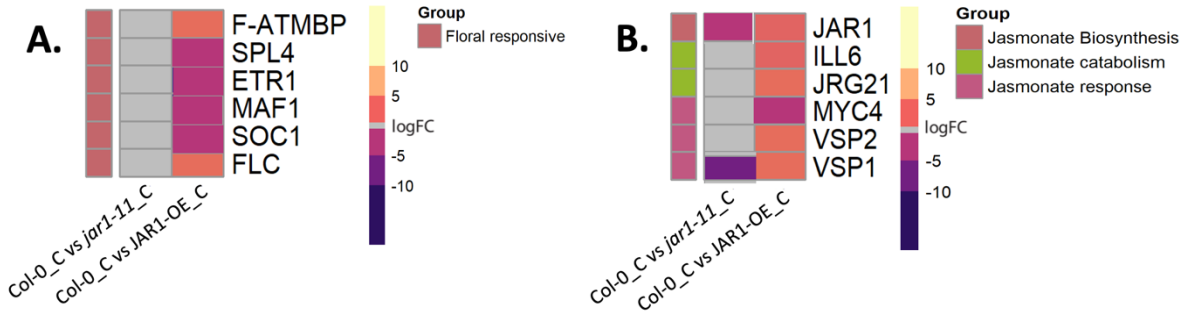

Figure 20: JAR1-dependent changes in gene expression of flowering responsive and jasmonate pathway. **A)** and **B)** Heat map showing DEGs involved in **A)** Flowering responsive and **B)** jasmonate biosynthesis, catabolism and responsive in *jar1-11* and JAR1-OE compared to WT in the rosette leaves on day 32 under well-watered condition. Data were analysed by an alternative cut off of FDR <0.05 and LogFC ≥0.5. "C" under control conditions.

Drought and ABA

Intriguingly, I found that some of the genes related to water deprivation and ABA response were downregulated in JAR1-OE. Among them are certain drought-responsive (*RD29A, ERD7, LEA14* and *GCR2*) and cold-responsive (*COR15B)* genes (Figure 19B; Supplementary Table 1). This makes us suspect that JAR1-OE could acquire a pre-stressed tolerance mechanism in normal growth conditions.

I further employed an enrichment analysis (with adjusted p-value<0.001, FDR) based on the DEGs found between *jar1-11* and JAR1-OE (Table 11). Not surprisingly, jasmonate-responsive adenylation and mycotoxin were enriched in the downregulated category in *jar1-11* (Table 11). As I did not find any DEG in the up-upregulated genes of WT and *jar1-11,* GO analysis was not possible. In the case of JAR1-OE, downregulated clusters were enriched in drought and ABA response as well as in other biotic and abiotic stress responses. This explains the downregulation of drought or other abiotic stress-related genes (Table 11). On the upregulated side, genes involved in cell cycle-related processes such as nucleosome assembly, cell cycle organization and glucosinolate catabolism were enriched (Table 11). However, it should be noted that glucosinolate catabolism is also regulated through the jasmonate signaling.

Table 11: JAR1-dependent genes expression pattern under control conditions. GO-enrichment for molecular function of significantly up-and downregulated genes in *jar1-11* and JAR1-OE plants compared to WT (Col-0) under well-watered conditions. "C" under control well-watered conditions.

Col-0_C vs *jar1-11*_C down summary

GO.ID	Term	weightFisher	p.adj
GO:0010046	response to mycotoxin	0.00017	0.5367
GO:0018117	protein adenylylation	0.00017	0.5367

Col-0_C vs JAR1-OE_C up summary

GO.ID	Term	weightFisher	p.adj
GO:0009737	response to abscisic acid	1.9E-06	0.0063
GO:0009414	response to water deprivation	2E-06	0.0063
GO:0009631	cold acclimation	1.1E-05	0.0232

Col-0_C vs JAR1-OE_C down summary

GO.ID	Term	weightFisher	p.adj
GO:0006334	nucleosome assembly	4E-18	0
GO:0019762	glucosinolate catabolic process	5.7E-06	0.018

Overall, I conclude that under non-stress conditions JAR1-mediated JA-Ile accumulation enhances growth regulation through cell cycle regulation and developmental processes as well as the autonomous flowering response. However, I observed no variation in *jar1-11* except for growth regulation. Lastly, endogenous JA-Ile accumulation induces typical stress responses.

3.1.11 Global gene expression upon progressive drought stress and its effect on the jasmonate pathway

Induction of drought can modulate the expression of genes involved in many biological processes including the jasmonate pathway. Thus, to gain a better insight into progressive drought stress-mediated global gene expression, RNA-seq analysis was performed on 32-day-old WT plants before severe wilting symptoms appeared.

Induction of progressive drought in leaf samples resulted in a total of 3401 differentially expressed genes (DEGs) in WT, of which 2023 were down- and 1378 were upregulated (Figure 21A, Supplemental Table 2). A GO enrichment analysis (with adjusted p-value<0.001, FDR) was used to identify category clusters of highest up- and downregulated genes. Not surprisingly, the upregulated genes were dominated by drought and ABA responsive genes, including those involved in osmotic or water deficient-related stresses (Table 12). The drought response is typically divided into- ABA-dependent and ABA-independent category and genes

that were upregulated under drought in the ABA-dependent category included late embryogenesis (LEA) genes *LEA7* and *LEA18*, responsive to dehydration (RD) genes *RD22*, *RD29A* and *RD29B* as well as the *RESPONSIVE TO ABA 18* (*RAB18).* ABA-independent drought-responsive upregulated genes included *DREB2A*, *LEA6* and *LEA46* (Figure 21B; Supplemental Table 2).

Downregulated genes from the enrichment analysis were mostly involved in light response as, unsurprisingly, water deficiency strongly affects phtotosynthesis (Table 12). Most of the genes involved in light-harvesting were highly downregulated, especially those of the light-harvesting complex B (LHCB) such as *LHCB1.1*, *LHCB1.4*, *LHCB2.1*, *LHCB2.2*, *LHCB2.4*, *LHCB3*, *LHCB4.1*, *LHCB5*, *LHCB6* (Figure 21B; Supplemental Table 2).

Other genes found to be downregulated, are involved in the biosynthesis/response of hormones such as auxin and salicylic acid, which suggests a cross-talk with these hormones during drought stress (Table 12). A heat map analysis of genes involved in the ABA pathway shows that most of them were either upregulated under drought or remain unchanged. As such, the biosynthetic genes- *ABA3, AAO3, NCED1, NCED3, NCED4*, the catabolic product genes- *CYP707A1* and *UGT75C1* and the responsive genes- *ABI1* and *ABI2* were all upregulated (Figure 21C).

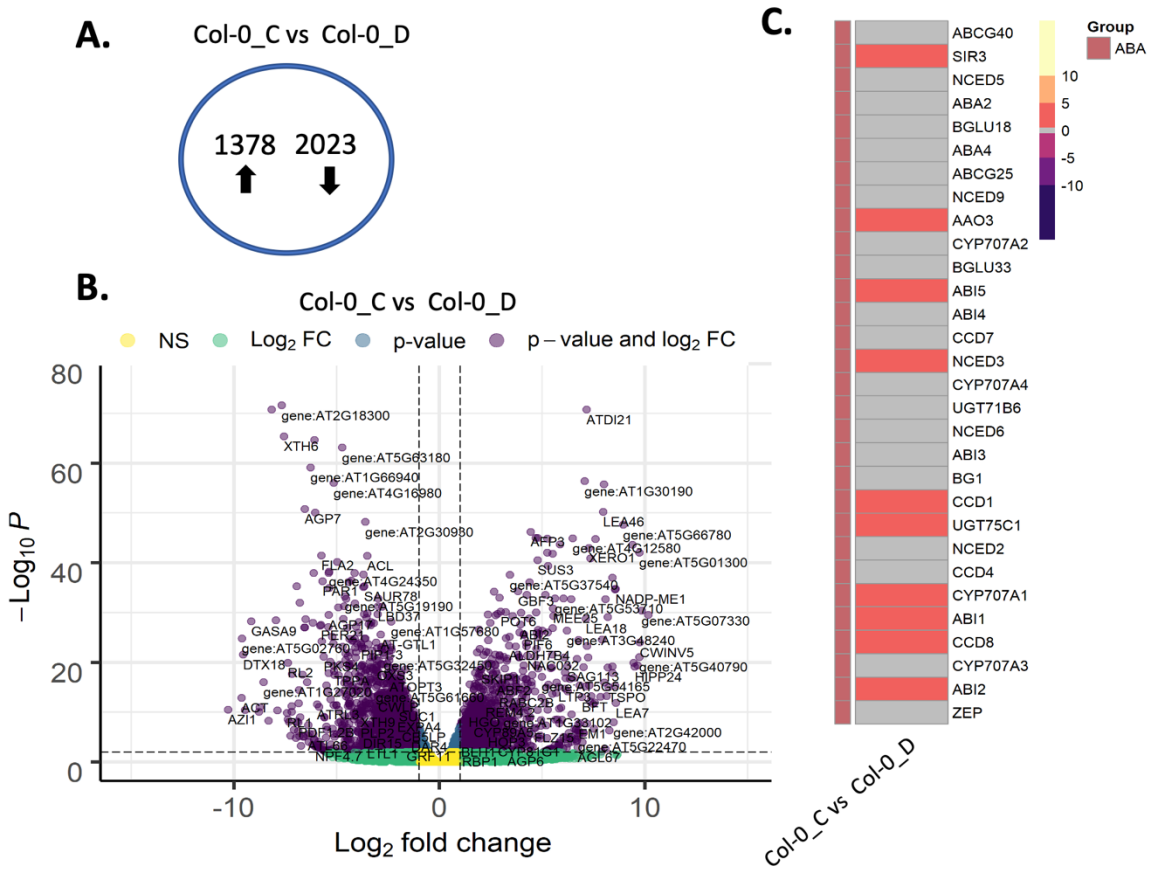

Figure 21: Transcriptional changes under progressive drought stress.
Rosette leaves of WT under drought stress on day 32 were collected for RNA-seq which was compared to well-watered conditions. **A.** DEGs up-and downregulated (DESeq, adjusted FDR <0.01 and LogFC ≥1) in WT plants under drought stress compared to well-watered conditions. Arrows indicate up- and downregulation. **B.** Volcano plot showing statistical significance ($log_{10}P$) versus magnitude of change (LogFC) of DEGs in WT plants under drought stress compared to well-watered conditions. Violet dots indicate genes that fit the DESeq criteria of FDR <0.01 and LogFC ≥1; green and blue dots represent DEGs that fit either only LogFC or FDR, respectively. **C.** Heat map showing DEGs involved in ABA-pathway in WT plants under drought stress compared to well-watered conditions. Data were analysed by an alternative cut off of FDR <0.05 and LogFC ≥0.5. "C" under control well-watered conditions and "D" under drought stress.

Table 12: Drought induced genes expression pattern. GO-enrichment for molecular function of significantly up-and downregulated genes under drought stress compared to well-watered conditions in WT (Col-0). "C" under control conditions, "D" under drought stress. Orange bar represents the jasmonate response under drought stress.

Col-0_C vs Col-0_D up summary

GO.ID	Term	weightFisher	p.adj
GO:0009414	response to water deprivation	2.9E-23	0
GO:0009737	response to abscisic acid	1.3E-19	0
GO:0009651	response to salt stress	6.5E-16	0
GO:0042542	response to hydrogen peroxide	1.6E-08	0
GO:2000143	negative regulation of DNA-templated tra...	2E-08	0
GO:0009753	response to jasmonic acid	3.7E-07	4E-04
GO:0071456	cellular response to hypoxia	6.7E-07	6E-04
GO:0009409	response to cold	4.7E-06	0.0037
GO:0042538	hyperosmotic salinity response	5.7E-06	0.004

Col-0_C vs Col-0_D down summary

GO.ID	Term	weightFisher	p.adj
GO:0009416	response to light stimulus	1.4E-09	0
GO:0010218	response to far red light	5.2E-09	0
GO:0010114	response to red light	1.2E-08	0
GO:0007623	circadian rhythm	1.8E-08	0
GO:0071456	cellular response to hypoxia	2.2E-08	0
GO:0006833	water transport	5.6E-08	1E-04
GO:0009768	photosynthesis	3.5E-07	3E-04
GO:0009751	response to salicylic acid	4.5E-07	3E-04
GO:0040008	regulation of growth	4.9E-07	3E-04
GO:0052544	defense response by callose deposition i...	7.1E-07	4E-04
GO:0006468	protein phosphorylation	7.2E-07	4E-04
GO:0019761	glucosinolate biosynthetic process	1.1E-06	6E-04
GO:0007178	transmembrane receptor protein serine/th...	5.5E-06	0.0027
GO:0010411	xyloglucan metabolic process	6E-06	0.0027
GO:0042742	defense response to bacterium	9E-06	0.0038
GO:0006949	syncytium formation	9.6E-06	0.0038
GO:0009734	auxin-activated signaling pathway	1.1E-05	0.0041
GO:0046777	protein autophosphorylation	1.2E-05	0.0042
GO:1900426	positive regulation of defense response ...	2E-05	0.0066
GO:0009409	response to cold	2.2E-05	0.0069
GO:0019253	reductive pentose-phosphate cycle	2.9E-05	0.0087
GO:0080167	response to karrikin	3.1E-05	0.0087
GO:0042546	cell wall biogenesis	3.3E-05	0.0087

Enrichment analysis further showed that, besides ABA and drought response genes, jasmonate biosynthesis and response genes were also up- and downregulated (Table 12 and Figure 22A). The chloroplast-localized gene responsible for OPDA formation, *LOX2*, was decreased, which is consistent with the decrease of *cis*-OPDA. In contrast, transcription of genes involved in later steps of jasmonate-biosynthesis in the peroxisome such as *PXG3* and *ACX1* or in cytosolic catabolism such as *CYP94B3* and *CYP94B1* were upregulated (Figure 22A). Since CYP94B3 and CYP94B1 catabolize JA-Ile to 12-OH-Ile, upregulation of both is consistent with the

increase of 12-OH-Ile observed under drought stress (Figure 18F). The impact of drought stress was also reflected through jasmonate-responsive genes. The master transcription factor *MYC2*, which is regulated through interaction between ABA and JA, was upregulated. By contrast, the *MYC2* -interacting partner, *MYC4,* was downregulated under drought stress. Two genes known for their important role in biotic attack defence, *VSP1* and *VSP2*, were also increased under drought stress (Figure 22A). To overcome some ambiguity derived for *VSP1* expression from the RNA-seq data, I confirmed the drought-induced increase in expression through RT-qPCR analysis (Figure 22C). Because a pro*VSP2::GUS* line in WT (Col-0 background) was available (Mousavi et al., 2013), drought stress-induced *VSP2* expression could also be assessed *in-situ*. Entire rosette leaves of the 32-day-old plant grown under control and drought-stressed conditions revealed a clear increase in pro*VSP2-GUS* expression under drought stress, characterized by the dark blue color of the leaf blade including the leaf base, while the expression was very weak with a mostly colorless leaf blade of the non-stressed plants (Figure 22B).

As mentioned before, JA-Ile accumulation removes the transcriptional repressor JAZ from the binding site of transcription factors in order to initiate jasmonate-mediated responses. Previously, it was shown that jasmonate signaling under biotic stress can enhance the expression of several *JAZs* such as *JAZ1, JAZ2, JAZ6, JAZ8, JAZ10,* etc. (Chung et al., 2008). However, under drought stress, only *JAZ4 (TIFY6A)* showed enhanced expression (Figure 22A). *In-situ analysis of JAZ1* expression using a pro*JAZ1::GUS* line in WT (Col-0 background) (Pérezet al., 2014), indicated a decline in the expression pro*JAZ1::GUS* in rosette leaves under drought stress (Figure 22B) not visible from the RNA-seq data.

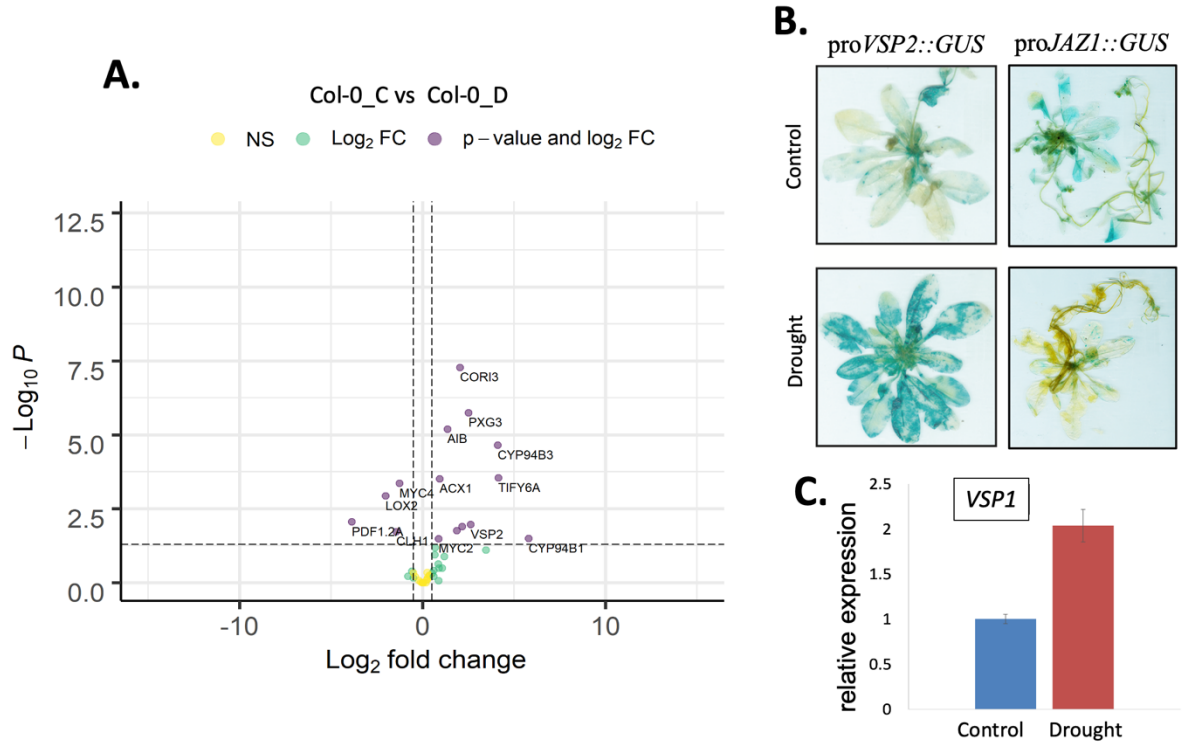

Figure 22: Drought stress-induced changes in the expression of the genes related to jasmonate pathway. **A.** Volcano plot showing statistical significance ($log_{10}P$) versus magnitude of change (LogFC) of the jasmonate pathway genes between well-watered and drought stress of WT (Col-0) plants. Violet dots indicate genes that fit the DESeq criteria of FDR <0.05 and LogFC ≥0.5; green and blue dots represent DEGs that fit either only LogFC or FDR, respectively. "Col" Col-0; "C" under control conditions, "D" under drought stress. **B.** Histochemical staining of transgenic Arabidopsis plants (Col-0) expressing the GUS reporter gene under the control of the *VSP2* promoter region (pro*VSP2*::GUS) and *JAZ1* promoter region (pro*JAZ1*::GUS) grown under control and drought stress conditions. **C.** *VSP1* transcript level in WT plants (Col-0) grown under control and drought stress conditions under long-day conditions determined by RT-qPCR using rosette leaves of 32 days old plants. *VSP1* transcript levels were normalized to *ACT2* levels and expressed as relative quantity ($2^{-\Delta\Delta Ct}$). Data were analysed by a two-tailed t-Test (*P<0.05). Error bars represent the mean ±SE of three biological replicates (n = 3).

Taken together, RNA-seq analysis support that progressive drought stress can positively regulate ABA- and jasmonate-dependent responses, while negatively affecting photosynthetic processes.

3.1.12 JAR1-dependent transcriptional changes under progressive drought stress

An opposite trend in drought response and corresponding jasmonate variation between *jar1-11* and JAR1-OE is likely to be reflected in differential gene expression. Thus, RNA-seq analysis was also performed on *jar1-11* and JAR1-OE plants under drought stress conditions. A pairwise comparison of expressed genes in different plant lines under drought conditions revealed 2411 DEGs between WT and *jar1-11*, among which 966 genes showed upregulation and 1445 genes downregulation in *jar1-11*. On the other hand, 998 DEGs were found between

WT and JAR1-OE, among which 737 genes showed upregulation and 261 genes downregulation in JAR1-OE (Figure 23A and Supplemental Table 3). Among the DEGs found both in *jar1-11* and JAR1-OE, 391 were counter-regulated in the two lines, while 10 were upregulated in both *jar1-11* and JAR1-OE and 381 showed no expression in *jar1-11* nor JAR1-OE, while being expressed in the wild type (Figure 23A and Supplemental Table 3).

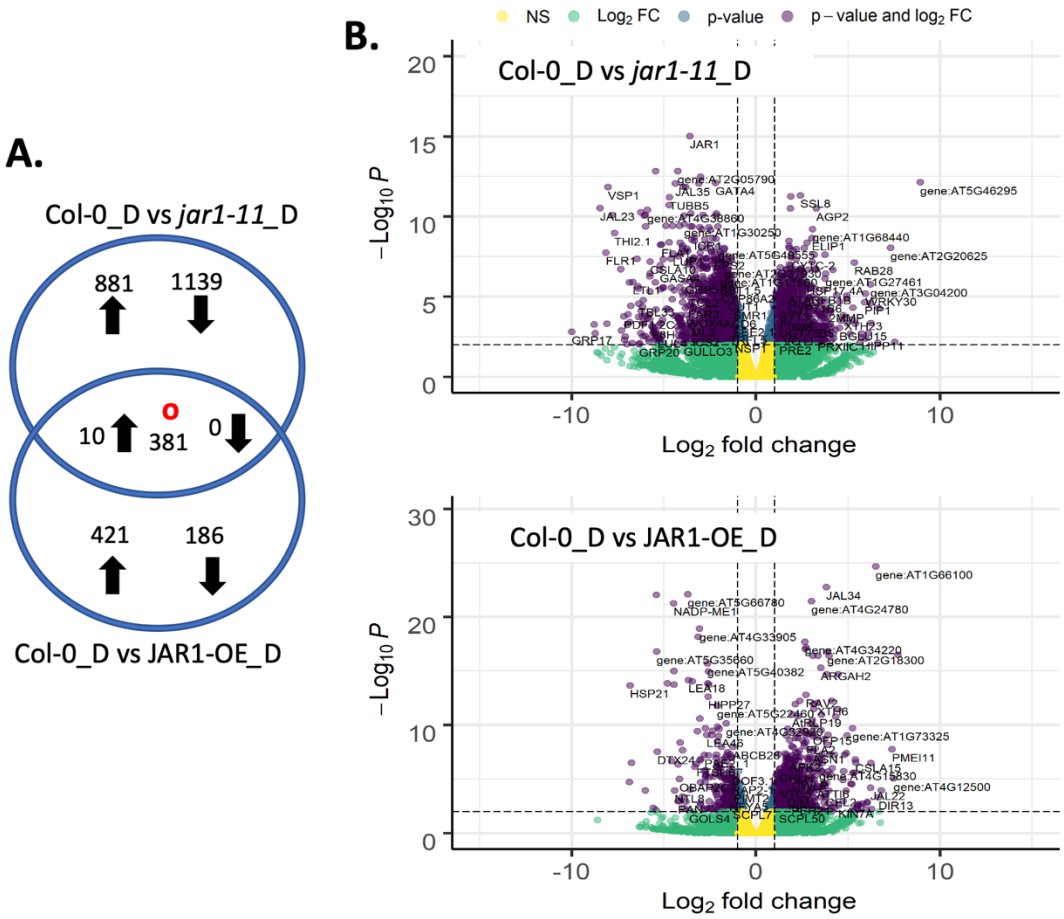

Figure 23: JAR1-dependent changes in gene expression in rosette leaves under drought stress.
Rosette leaves under drought stress on day 32 were collected for RNA-seq. **A.** Venn diagram showing DEGs up- and downregulated (DESeq, adjusted FDR <0.01 and LogFC ≥1) in *jar1-11* and JAR1-OE compared to WT plants. "O" indicates counter-regulated genes. "D" under drought stress. Arrows indicate up- and downregulation. **B.** Volcano plot showing statistical significance ($\log_{10}P$) versus magnitude of change (LogFC) of DEGs between WT (Col-0) and *jar1-11* (upper); WT (Col-0) and JAR1-OE (lower). Violet dots indicate genes that fit the DESeq criteria of FDR <0.01 and LogFC ≥1; green and blue dots represent DEGs that fit either only LogFC or FDR, respectively. "D" under drought stress.

A GO enrichment analysis on all of the DEGs found under drought stress (adjusted the p-value <0.001) confirmed the reciprocal trends between *jar1-11* and JAR1-OE for several genes groups (Table 13), such as genes involved in photosystem and light-dependent regulation. This

included, for example, the light-harvesting complex genes *LHCB6*, *LHCB2.4* and *LHCB4.2,* whose expression was lower in *jar1-11* and higher in JAR1-OE (Figure 23B, Supplemental Table 3). In line with its lower susceptibility, JAR1-OE showed downregulation of genes in drought stress response but also other abiotic stresses. In contrast, genes involved in drought stress and some other abiotic stress responses were enriched in upregulated genes in *jar1-11* (Table 13). For example, according to enrichment analysis, I observed a lower expression of several drought-responsive and ABA-responsive genes such as *LEA6*, *LEA18*, *LEA7* and *RAB18* in JAR1-OE (Figure 23B, Supplemental Table 3). These same genes were upregulated under drought stress in WT, supporting the phenotypic evidence that JAR1-OE plants did experience less drought stress after 14 days of water withholding. In contrast, transcripts of drought-responsive genes such as *DREB2A* or *RD20*, putative drought-responsive genes such as *LEA31*, and hypoxia-responsive genes such as *FMO1*, *At2g25735* and *HIGD2* had a higher expression level in the *jar1-11* line under drought conditions than in WT which is in line with the susceptibility of *jar1-11* to drought stress. The same was seen for ABA-responsive drought and cold-responsive genes such as *COR47* (Figure 23B, Supplemental Table 3).

Table 13: JAR1-dependent genes expression pattern under drought stress. GO-enrichment for molecular function of significantly up-and downregulated genes in *jar1-11* and JAR1-OE plants compared to WT under drought stress. "D" under drought stress.

Col-0_D vs *jar1-11*_D down summary

GO.ID	Term	weightFisher	p.adj
GO:0009768	photosynthesis	1.7E-12	0
GO:0009834	plant-type secondary cell wall biogenesi...	3E-10	0
GO:0018298	protein-chromophore linkage	3E-09	0
GO:0005983	starch catabolic process	9.6E-09	0
GO:0009416	response to light stimulus	1.1E-07	1E-04
GO:0015979	photosynthesis	4.7E-07	5E-04
GO:0006949	syncytium formation	1.1E-06	0.001
GO:0010218	response to far red light	1.6E-06	0.0013
GO:0071555	cell wall organization	1.9E-06	0.0013
GO:0006833	water transport	4.8E-06	0.0028
GO:0016042	lipid catabolic process	5.6E-06	0.0028
GO:0010067	procambium histogenesis	5.7E-06	0.0028
GO:0009637	response to blue light	5.8E-06	0.0028

Col-0_D vs *jar1-11*_D up summary

GO.ID	Term	weightFisher	p.adj
GO:0010200	response to chitin	1.5E-18	0
GO:0009651	response to salt stress	2.2E-11	0
GO:0042542	response to hydrogen peroxide	7.8E-11	0
GO:0009737	response to abscisic acid	2.4E-10	0
GO:0009414	response to water deprivation	3.6E-09	0
GO:0009816	defense response to bacterium	1.1E-08	0
GO:0009611	response to wounding	3.1E-08	0
GO:0042742	defense response to bacterium	2.7E-07	2E-04
GO:0006979	response to oxidative stress	5.2E-07	3E-04
GO:0080167	response to karrikin	5.2E-07	3E-04
GO:0009409	response to cold	9.7E-07	6E-04
GO:0009751	response to salicylic acid	1.8E-06	9E-04
GO:0055114	oxidation-reduction process	2.7E-06	0.0013
GO:0006749	glutathione metabolic process	1.1E-05	0.005
GO:0009408	response to heat	2.3E-05	0.0091
GO:0010112	regulation of systemic acquired resistan...	2.3E-05	0.0091

Col-0_D vs JAR1-OE_D down summary

GO.ID	Term	weightFisher	p.adj
GO:0009414	response to water deprivation	1.5E-11	0
GO:0009408	response to heat	1.6E-06	0.0051
GO:0009737	response to abscisic acid	4.5E-06	0.0095

Col-0_D vs JAR1-OE_D up summary

GO.ID	Term	weightFisher	p.adj
GO:0009768	photosynthesis	2.6E-20	0
GO:0018298	protein-chromophore linkage	1.5E-12	0
GO:0010218	response to far red light	1.9E-11	0
GO:0010114	response to red light	1.2E-10	0
GO:0009637	response to blue light	3.7E-08	0
GO:0019761	glucosinolate biosynthetic process	1.3E-07	1E-04
GO:0007018	microtubule-based movement	1.9E-07	2E-04
GO:0006949	syncytium formation	3.9E-07	3E-04
GO:0015979	photosynthesis	4.9E-07	3E-04
GO:0009769	photosynthesis	6.2E-07	4E-04
GO:0009625	response to insect	2.2E-06	0.0013
GO:0010444	guard mother cell differentiation	6.9E-06	0.0036
GO:0009611	response to wounding	8.4E-06	0.0041
GO:0007088	regulation of mitotic nuclear division	1.1E-05	0.005
GO:0030104	water homeostasis	1.2E-05	0.0051
GO:0044772	mitotic cell cycle phase transition	1.5E-05	0.0059
GO:0045490	pectin catabolic process	2.4E-05	0.0089

Irrespective of GO analysis and in line with a higher accumulation of JA-Ile in JAR1-OE under drought stress, many jasmonate-pathway genes showed a reciprocal trend between *jar1-11* and JAR1-OE under drought stress (Figure 24). Jasmonate-responsive genes such as *MYC2*, *VSP1* and *VSP2* that were upregulated under drought in WT, had even stronger upregulation in JAR1-OE but were not upregulated in *jar1-11*. This suggests the direct regulation of these genes

through JA-Ile under drought stress. However, expression of *MYC4,* which was decreased in WT under drought, further decreased in *jar1-11* though no variation was found in JAR1-OE. In addition to jasmonate responsive genes, some of the biosynthetic genes such as *LOX2, AOS (CYP74A)* showed an opposite trend between *jar1-11* and JAR1-OE, of upregulation in JAR1-OE and downregulation in *jar1-11*. This trend is consistent with the OPDA and JA-Ile accumulation in JAR1-OE (Figure 18A and C). Besides those, the expression of other biosynthetic genes such as *AOC1, AOC2, OPR3* was decreased in *jar1-11* while remaining unchanged in JAR1-OE. However, two catabolic genes, *JOX3 (JRG21)* and *ILL6* were higher expressed in JAR1-OE, which is in line with the increased content of 12-OH-JA and 12-OH-JA-Ile, respectively (Figure 18D and F).

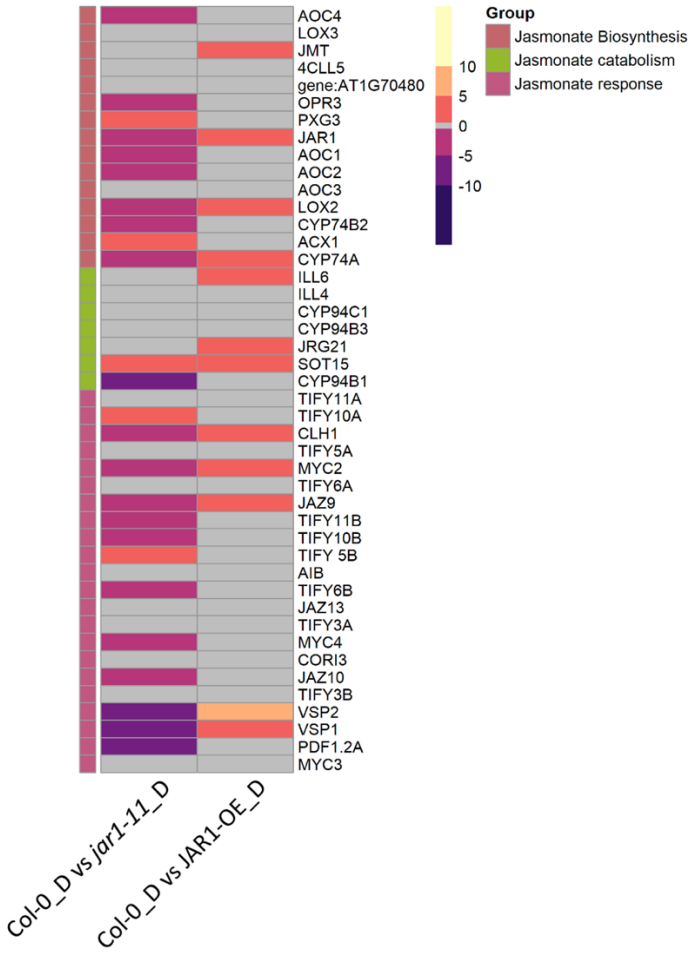

Figure 24: JAR1-dependent changes in gene expression of jasmonate pathway under drought stress.
Heat map showing DEGs involved in jasmonate-biosynthesis, catabolism and response in *jar1-11* and JAR1-OE compared to WT in the rosette leaves at day 32 under drought stress. Data were analysed by an alternative cut off of FDR <0.05 and LogFC ≥0.5. "D" under drought stress.

Overall, I conclude that JAR1-mediated JA-Ile accumulation positively regulates the jasmonate-biosynthesis under drought stress, which ultimately assists in coordinating drought stress resistance.

3.1.13 JAR1-dependent and independent regulation of jasmonate-pathway under drought stress

I have already found that the jasmonate-pathway biosynthesis, as well as response, are upregulated in JAR1-OE while being downregulated in *jar1-11* compared to WT under drought stress. I also described that the jasmonate-mediated response is upregulated but that biosynthetic genes such as *LOX2* are down-regulated in drought-stressed WT plants. To understand specifically the role of JA-Ile on the jasmonate pathway regulation under drought stress, I analysed gene expression in all lines comparing each of their drought stress responses to control conditions which I presented as a heat map in Figure 25. In the jasmonate-pathway, I found that most of the genes involved in jasmonate-biosynthesis, catabolism and response, except *PDF1.2A,* were upregulated in JAR1-OE. By contrast, in *jar1-11,* I found no variation in the major jasmonate-responsive genes such as *MYC2, VSP1* and *VSP2,* which suggests that, due to lack of JA-Ile, drought stress is unable to initiate jasmonate signaling. However, two important biosynthetic genes in the chloroplast, *LOX2* and *AOS (CYP74A),* involved in the formation of OPDA, were downregulated in *jar1-11,* correlating with the decrease of OPDA under drought stress (Figure 18A). Genes involved in the formation of catabolic products 12-OH-JA and 12-OH-JA-Ile such as *JOX3 (JRG21)*, *ILL6*, *CYP94B3* were upregulated in *jar1-11,* which suggests probable homeostasis of the upstream products due to lack of JAR1 (Figure 25).

Taken together, I conclude from the results that endogenous JA-Ile can stimulate the jasmonate pathway while lack of JA-Ile negatively regulates jasmonate-biosynthesis and response.

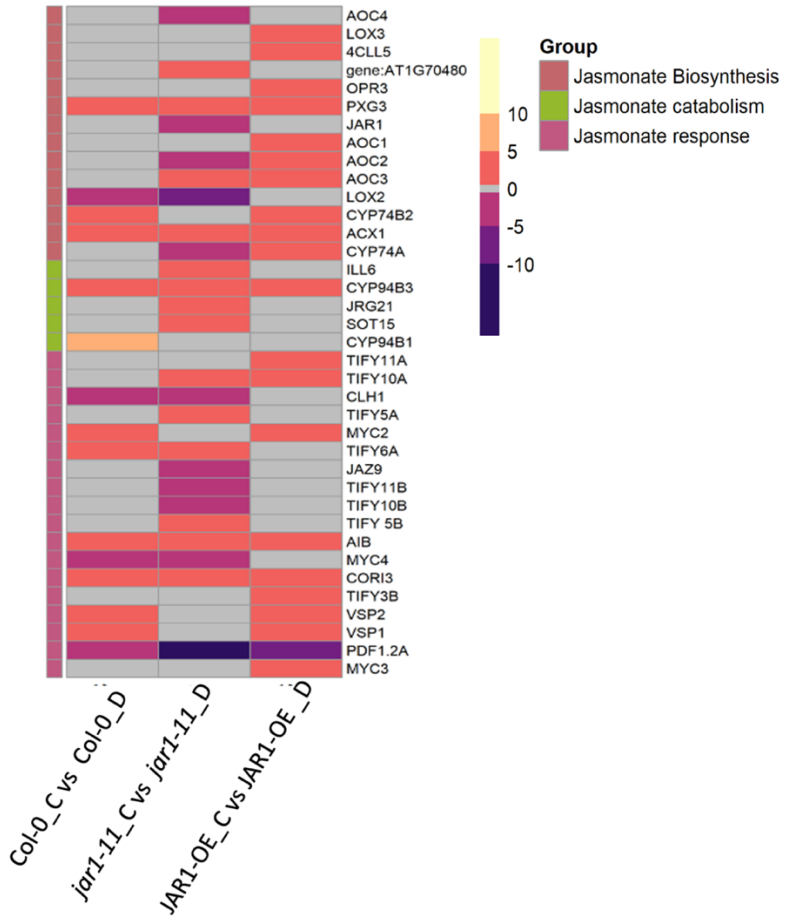

Figure 25: JAR1-dependent changes in gene expression of jasmonate pathway under drought stress compared to control conditions.
Heat map showing DEGs involved in jasmonate-biosynthesis, catabolism and signaling response in WT (Col-0) *jar1-11* and JAR1-OE under drought stress compared to each of their well-watered conditions. Data were analysed by an alternative cut off of FDR <0.05 and LogFC ≥0.5. "C" control conditions, and "D" drought stress.

3.1.14 JAR1-mediated transcriptional balance between growth and drought-mediated defence

Previous studies had suggested that jasmonate signaling is involved in keeping a balance between plant growth and biotic stimuli-induced defence (Howe et al., 2018; Züst and Agrawal, 2017, Guo et al., 2018). Thus, to elucidate the role of JAR1 in mediating growth and drought stress trade-offs hierarchical clustering was employed to all the genes differentially expressed in WT, *jar1-11* and JAR1-OE under drought stress compared to their control conditions (Figure 26). Using the K-means (K = 5) approach in the hierarchical clusters, genes were assigned to 5 clusters, which were then visualized with a heat map (Figure 26A) and centroid views (Figure 26B), revealing general patterns of transcriptomic profiles during drought treatment compared to control conditions. Figure 26C also presented two top enriched groups in each cluster (details in Supplementary Table 4).

These clusters can be categorized into two groups, where the first group includes only cluster 5, relating to drought stress effects, and clusters 1 to 4, representing drought resistance mechanisms. Clusters 1 to 4 were decreased in general (Figure 26A and Figure 26B). Clusters 1 and 3 relate to plants growth and development, including cell wall structure, which were severely affected under drought in all plant lines albeit to a higher extent in *jar1-11* and to a lesser extent in JAR1-OE. Cluster 1 also includes water transport, and, as expected, water accessibility was reduced under drought in all plant lines, though to a lower extent in JAR1-OE, in line with its resistance during drought stress. Severe drought stress effects were clearer from clusters 2 and 4, which include the downregulation of photosynthesis and its related processes, and these effects were observed to a higher extent in *jar1-11* and less so in JAR1-OE. Cluster 2 also describes the cytokinin response, suggesting a putative cross-talk between jasmonate and cytokinin signalling. Cluster 5 reflects the detrimental effect of water deficiency and other abiotic stresses, which was visible to a higher extent in *jar1-11* than in JAR1-OE.

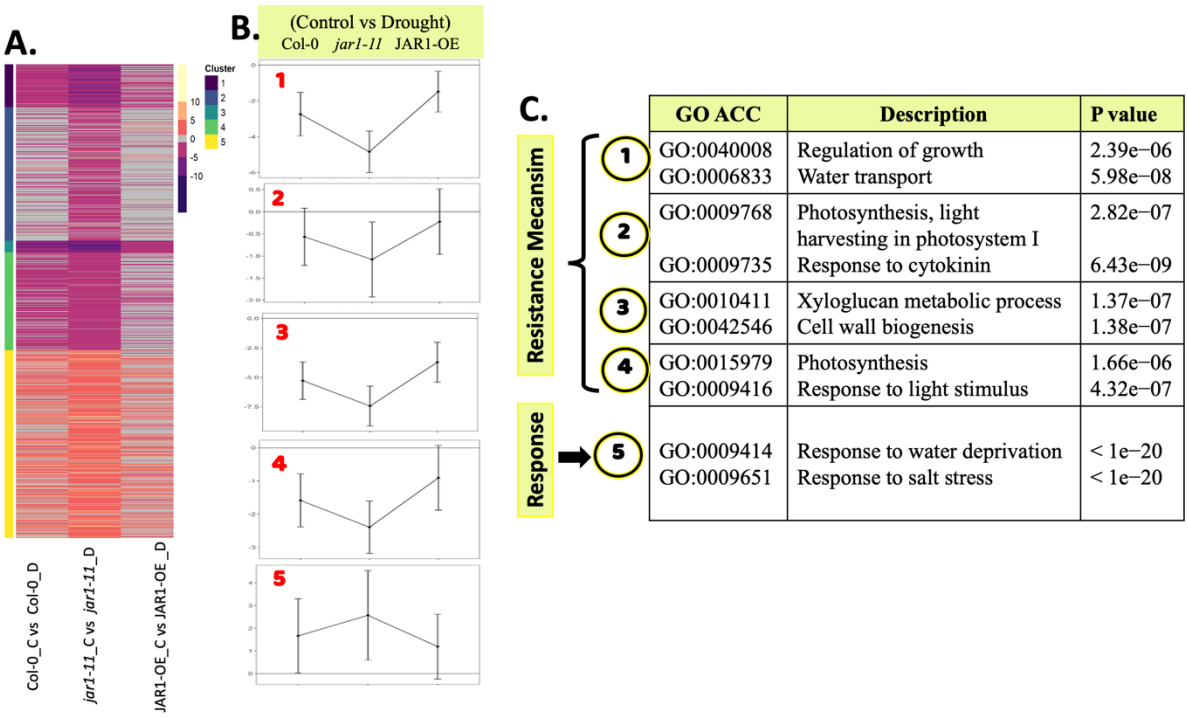

	GO ACC	Description	P value
1	GO:0040008	Regulation of growth	2.39e−06
	GO:0006833	Water transport	5.98e−08
2	GO:0009768	Photosynthesis, light harvesting in photosystem I	2.82e−07
	GO:0009735	Response to cytokinin	6.43e−09
3	GO:0010411	Xyloglucan metabolic process	1.37e−07
	GO:0042546	Cell wall biogenesis	1.38e−07
4	GO:0015979	Photosynthesis	1.66e−06
	GO:0009416	Response to light stimulus	4.32e−07
5	GO:0009414	Response to water deprivation	< 1e−20
	GO:0009651	Response to salt stress	< 1e−20

Figure 26: JAR1-mediated transcriptomic changes between drought stress and control conditions.
Heat map **(A)** and K-means clustering **(B)** of genes upregulated or downregulated under drought stress compared to control conditions in the different plant genotypes. K-means clustering was performed to produce the clusters (DESeq, adjusted FDR <0.01 and LogFC ≥1) and the thin lines represent the mean expression profiles for each cluster. "C" control conditions, and "D" drought stress. Only genes that are differentially expressed in at least one of the comparisons were used for the cluster analysis (FDR <0.01). **(C)** The top two GO terms for each cluster with p values are listed. Detailed categories are in the Supplemental Table 4.

3.1.15 Cross-talk between the jasmonate and ABA pathways

Several studies have reported the interdependency of jasmonate and ABA-signaling (Yang et al., 2019; Daszkowska-Golec and Szarejko, 2013). From the RNA-seq study, I found that both ABA and jasmonate responses were enhanced upon drought stress (Table 13). Expression of several ABA-pathway genes however, shows a reciprocal trend between *jar1-11* and JAR1-OE. Among those genes are the biosynthetic gene, *AAO3;* the catabolic gene *CYP707A1*, and the ABA-response gene *ABI2,* all of which showed higher expression in *jar1-11* and lower expression in JAR1-OE (Figure 27A). This compares well to the ABA levels, which were enhanced in all plant lines under drought albeit to a lesser extent in JAR1-OE than in *jar1-11* (Figure 27B). However, *BGLU18 (BG1),* which is involved in ABA formation from ABA-GE, was upregulated in JAR1-OE but downregulated in *jar1-11* (Figure 27A).

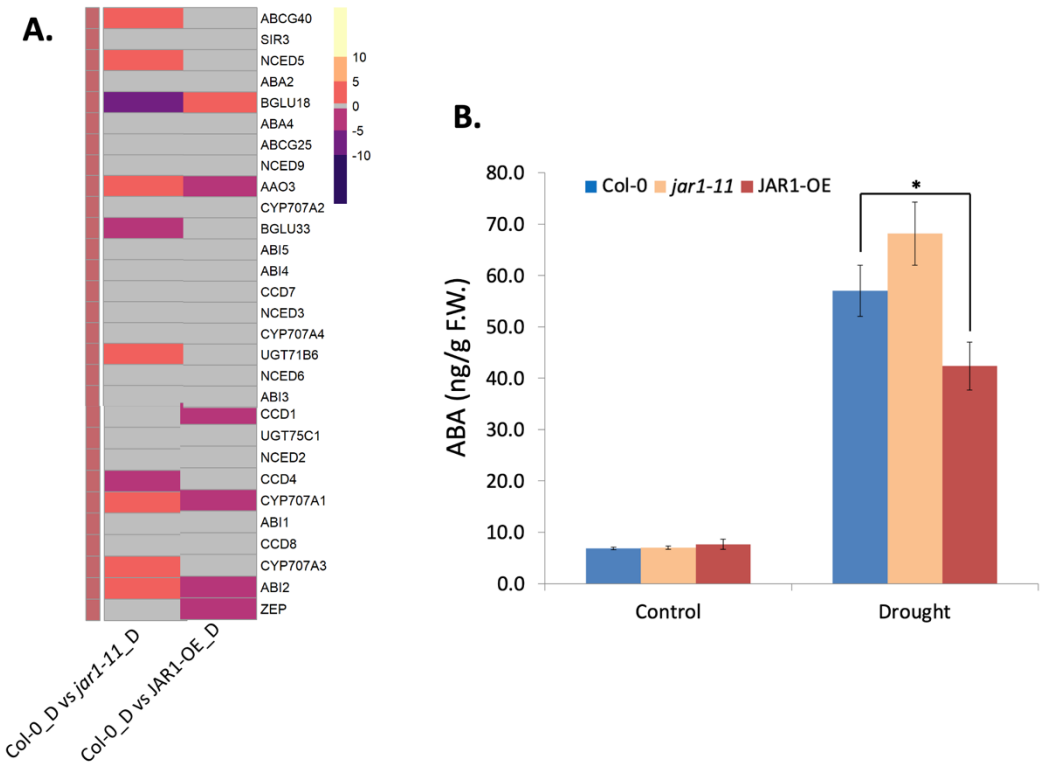

Figure 27: JAR1-dependent changes in ABA-pathway.
A. Heat map showing DEGs involved in ABA-pathway in *jar1-11* and JAR1-OE compared to WT in the rosette leaves on day 32 under drought stress. Data were analysed by an alternative cut off of FDR <0.05 and LogFC ≥0.5. "D" under drought stress. **B.** Drought-induced variation of ABA content in the indicated plant genotypes compared to control conditions. Rosette leaves of plants were harvested on day 32 for control as well as drought stress conditions. Samples were collected from six different biological replication each with pooled three individual plants, frozen in liquid nitrogen and subjected to extraction separately as described in the Materials and Methods section. ABA content was quantified via the corresponding internal standard. Analysis was repeated twice with similar results and here one replicate is presented. Data were analysed by multiple comparisons (Tukey test) followed by one-way ANOVA (*P<0.05). Data are means ± SE, *n* = 6. F.W.- fresh weight.

3.1.16 Stomatal Variation in *jar1-11* and JAR1-OE plants

Stomatal aperture and density in the leaf epidermis regulate water availability throughout the growth cycle of plants (Bertolino et al., 2019; Gupta et al., 2020). During water scarcity, tolerant plants can positively regulate stomatal closure to reduce the transpirational loss of water. However, regulation of the stomatal aperture involves an intricate mechanism. Some plants are also very effective in reducing the number of stomata to balance water usage and availability (Gupta et al., 2020). Exogenously applied MeJA was found to reduce the number of stomata in young cotyledons, while jasmonate signaling was found to modify stomatal aperture under diverse conditions (Han et al., 2018). Since cluster analysis had revealed that gain/loss of functions of JAR1 affects the water deprivation response, there is likely to be a variation in the expression of genes involved in stomatal development and function. With regard to genes related to stomatal aperture no changes in the rapidly fluctuating aperture controllers were found. However, two highly abundant Myrosinases, *TGG1* and *TGG2,* which were previously found to regulate stomatal aperture through the combined regulation of ABA and JA (Rhaman et al., 2020; Islam et al., 2009) were highly upregulated in JAR1-OE and slightly reduced in *jar1-11* (Figure 28A). Also, expression of some stomata density-related genes like *TMM*, *MYB124* (not significant), *EPF2* and *SBT1.2* was reduced in *jar1-11* while being increased in the JAR1-OE line compared to WT (Figure 28A). Measurement of the stomatal aperture and overall stomata density of the 6th rosette leaf of 21-day-old WT, *jar1-11* and JAR1-OE plants grown in long-day control conditions (Figure 28B) showed a wider stomatal aperture with a higher number of stomata in *jar1-11* compared to WT, while detecting a more narrow stomatal pore with a lower density of stomata in JAR1-OE (Figure 28B).

Taken together, these results show that JAR1-mediated JA-Ile accumulation can positively regulate stomatal aperture and density, which is reflected by a better survival during water deficiency.

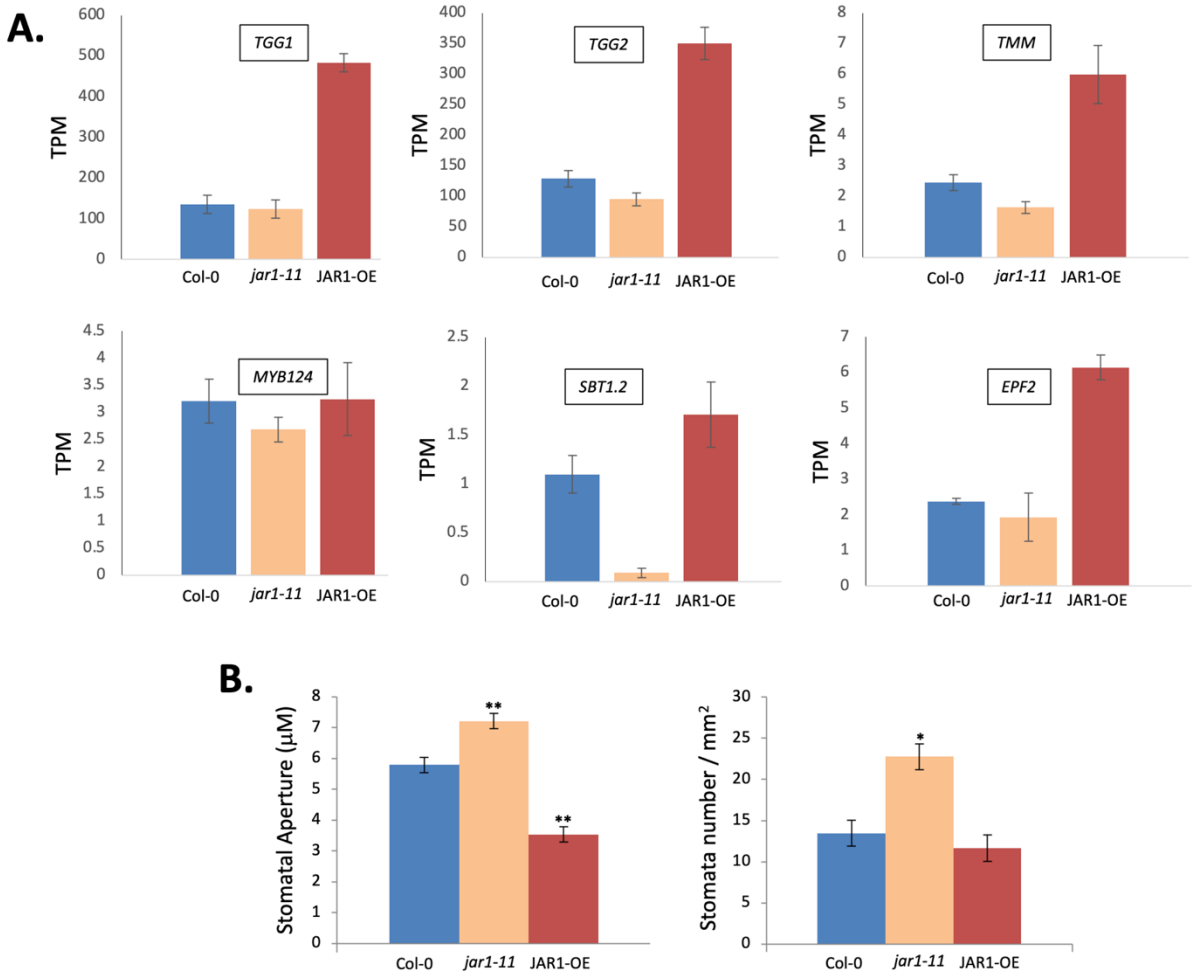

Figure 28: JAR1-dependent Stomatal regulation.
A. Relative expression of the genes controlling the stomatal intensity. Expression is presented as Transcripts per million (TPM) from the RNA-seq of the well-watered plants. Bar plot prepared with TPM values. Data represent means ± SE from 3 replicates (n=3). **B.** Size of stomatal apertures and **C.** number of stomata from indicated plant genotypes on day 21. No. 6 leaves were selected for counting. Data represent means ± SE from three individual biological replicates (n = 3). For stomatal aperture, each replicate quantified 90 to 100 stomata from 6-10 individual plants. For Stomatal density, each replicate was quantified from 5-6 individual plants. Data were analysed by multiple comparisons (Tukey test) followed by one-way ANOVA (*P<0.05, **P<0.01).

3.1.17 JA-Ile reduces cell oxidation via glutathione-mediated ROS regulation

The ascorbate-glutathione cycle plays a major role in scavenging reactive oxygen species (ROS) produced as a result of oxidative stress. As part of the cycle, glutathione, which is synthesized in its reduced form (GSH), is converted into its oxidative form (GSSG) during oxidative stress. This conversion is mostly achieved by dehydro-ascorbate reductase (DHAR1), which oxidizes ascorbate as part of its reaction. GSSG can be converted back to GSH by the enzyme glutathione reductase (GR) (Noctor et al., 2014; Marty et al., 2019; Mhamdi et al., 2010). It was previously reported that the ascorbate-glutathione cycle can act in a synergistic as well as in an antagonistic manner with jasmonate pathway. Many genes in the ascorbate-glutathione cycle are induced by external MeJA application and reduced in the jasmonate

signaling mutant *myc2.* On the other hand, the accumulation of GSH positively regulates MeJA-induced stomatal closure (Xiang and Oliver, 1998; Sasaki-Sekimoto et al., 2005; Zander et al., 2020; Akter et al., 2013). Despite this finding, no previous report was made on the effect of endogenous JA-Ile on the ascorbate-glutathione cycle-mediated ROS regulation. None of the genes involved in glutathione biosynthesis and ascorbate-glutathione cycle showed a significant difference in expression levels in WT, *jar1-11* and JAR1-OE under control conditions. However, drought stress resulted in a decrease in the biosynthetic gene *GSH2* in all lines albeit to a somewhat higher extent in *jar1-11* than in JAR1-OE compared to WT. This suggests that JA-Ile may not be important in glutathione biosynthesis during drought stress (Figure 29A). Within the ascorbate-glutathione cycle, expression of *DHAR1,* which is also MeJA induced (Xiang and Oliver, 1998), was upregulated in all plants under drought stress but to a higher extent in JAR1-OE compared to *jar1-11*. On the other hand, two glutathione reductases, *GR1* and *GR2,* were highly upregulated under drought stress in WT and the upregulation was higher in *jar1-11.* In contrast, no variation could be detected in JAR1-OE under drought stress (Figure 29A).

To gain a better insight into the JA-Ile -mediated glutathione and ROS regulation, I conducted a real-time *in vivo* redox measurement using two genetically encoded and cytosol targeted biosensor lines. One carries cyt-roGFP2-Grx1, which measures the glutathione potential (eGSH, GSSG/GSH), and the other cyt-roGFP2-Orp1 with measures the H_2O_2/H_2O ratio. Both sensors were used in the Col-0 background. To monitor JA-Ile -mediated redox regulation, these sensor lines were also crossed into *jar1-11*. Measurement was done by confocal microscopy using the leaves of 6-7-day-old seedlings. After calibration with control image buffer, 10 mM DTT or 50 mM H_2O_2, a ratio of 0.6, 0.3 and 2.5, respectively, for cyt-roGFP2-Grx1 and 0.20, 0.18 and 1.20, respectively, for cyt-roGFP2-Orp1 was found in both plant lines. This suggests no variation in redox potential due to lack of JA-Ile under control conditions. In case of cyt-roGFP2-Grx1, application of 1 mM jasmonic acid (JA) resulted in a decline of the ratio from 0.6 to 0.4 (more reduced state) within 5 minutes and later to a minimum of 0.35 in the WT, which remained the same up to 40 minutes. By contrast, the ratio remained nearly the same in *jar1-11* (Figure 29B). This is in line with the previous study that exogenous MeJA can initiate glutathione biosynthesis ((Xiang and Oliver, 1998). In case of cyt-roGFP2-Orp1 (Figure 29C), plants were treated with methyl viologen (MV) to induce gradual oxidative stress. Application of 10 mM MV shifted the ratio gradually to a more oxidized state (ratio of 0.8) within 1 hour in both plant lines with a steeper increase in *jar1-11* in the initial 20 min (Figure 29C). When 1 mM JA was given together with MV, the ratio remained well below 0.25

after 1 hour in the Col-0 background, while increasing to 0.6 in the *jar1-11* background. This suggests that endogenous JA-Ile formation by JAR1 is critical for scavenging of MV-induced H_2O_2 (Figure 29C).

Overall, I conclude that jasmonate signaling can regulate stress-induced ROS response via the ascorbate-glutathione cycle and thus H_2O_2 scavenging.

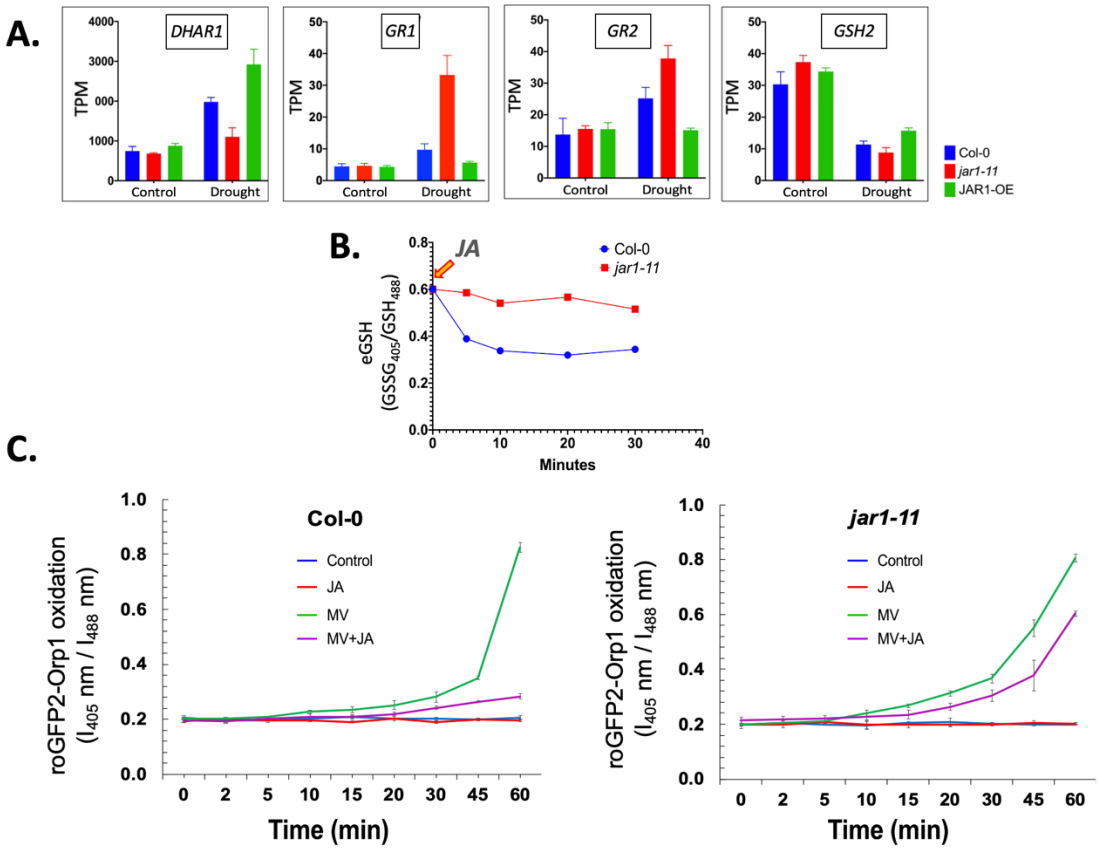

Figure 29: JAR1-dependent redox regulation.
A. Relative expression of the genes involved in the ascorbate-glutathione cycle. Expression is presented as TPM from the RNA-seq of the well-watered and drought-stressed indicated plants. Bar plot prepared with TPM. Data represent means ± SE from 3 replicates (n=3). **(B)** and **(C)**. Real-time monitoring of the **(B)** glutathione potential (eGSH, GSSG/GSH) using the cytosol targeted roGFP2-Grx1 redox sensor **(C)** H_2O_2 using the cytosol targeted roGFP2-Orp1redox sensor in the WT (Col-0) and *jar1-11* leaf cells upon different treatment. Treatments- Control-image buffer (pH 5.8); MV- 10 mM Methyl Viologen; JA- 1mM Jasmonic acid; MV+JA- 10 mM Methyl Viologen+1mM Jasmonic acid. Ratio values were calculated from the fluorescence values recorded at 535 nm after excitation at 405 nm and 488nm. Mean ratios ± SE of different time-points represent data from three replicates each including three individual seedlings.

3.1.18 Age-dependent variation of jasmonates content

It has been described that jasmonate biosynthesis in fully expanded rosette leaves of the vegetative stage is low and only increases upon external stimuli such as wounding (Glauser et al., 2008). After analysis of jasmonate dynamics under drought stress, I examined the content of various jasmonates in leaves of different ages grown under both short-day and long-day

conditions. I deemed this important because, in drought-stress experiments lasting several weeks, plants continue to grow, and depending on the start of the drought treatment and on light conditions, they might reach a different developmental stage. Wild-type (Col-0) plants grown under long-day (16 h/8 h) were analysed on day 32 and 39 and plant grown under short -day (8 h/16 h) conditions were analysed on day 32. During this time, plants grown under long-day reached the bolting and flowering stage on day 32 (LR) and 39 (LFR), respectively, while the plants grown in short-day conditions remained in the vegetative stage (SV) (Figure 30A). To avoid potential artifacts derived from day length on the vegetative stage, we also analysed plants grown in long-day (16 h/8 h) conditions on day 18 while they remained in the vegetative stage (LV) (Figure 30A).

Analysis of jasmonates confirmed the low content of several jasmonates in the rosette leaves of plants in the vegetative stage in both long- and short-day conditions. This includes the biologically active JA-Ile, its immediate precursor, JA, and the catabolic product of JA, 12-OH-JA, even though significant amounts of the OPDA precursor were present (Figure 30B). No variation of JA and JA-Ile between both vegetative stages suggests day length does not affect jasmonic acid signaling initiation. I observed a very slight increase in *cis*-OPDA, as well as in the catabolic products 12-OH-JA-Ile and 12-COOH-JA-Ile under long -day vegetative stage, which suggests some other homeostatic or regulatory functions of these compounds (Figure 30B). Interestingly, the recently described, vastly available jasmonate derivative JA-Glc was decreased in the long-day vegetative stage, which suggests a probable effect of day length on this compound. In addition, I observed a significant increase in most jasmonates in the leaves of plants at the bolting stage (Figure 30B, compare SV to LR) except for JA-Glc, which decreased slightly. In the case of *cis*-OPDA, the increase was less pronounced, consistent with the fact that its content still exceeds even the accumulated levels of all measured jasmonates (Figure 30B).

However, further growth of the plants to full flowering stage (day 39, LFR) enhanced JA and JA-Ile levels even further, while other jasmonates remained at similar levels as at the bolting stage (Figure 30B). Interestingly, JA-Glc levels which were decreased upon bolting, were enhanced in the full flowering stage.

It should be noted, as was previously found, that the amount of the bioactive jasmonate, JA-Ile was very low compared to all other jasmonates.

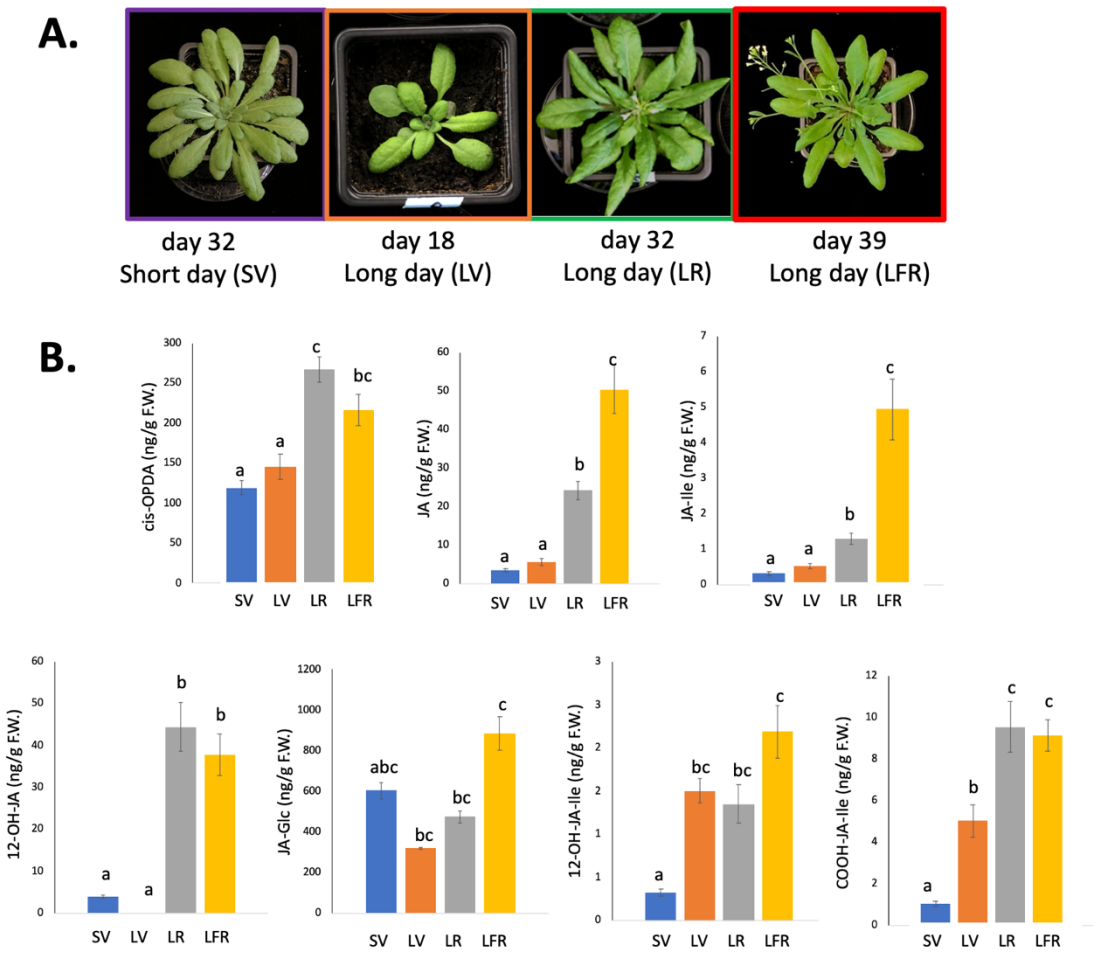

Figure 30: Age-dependent variation in jasmonates under normal growth conditions.
A. Growth stages of the WT (Col-0) plants used for measurement of jasmonates. SV, vegetative stage on day 32 under short-day; LV, vegetative stage on day 18 under long-day; LR, bolting stage on day 32 under long-day; LFR, flowering stage on day 39 under long-day. **B.** Variation of the jasmonates under different growth stages. 12-oxo-phytodienoic acid (*cis*-OPDA), Jasmonic acid (JA), Jasmonyl-isoleucine (JA-Ile), 12-hydroxyjasmonic acid (12-OH-JA), 12- hydroxyjasmonoylglucoside (12-*O*-Glc-JA), 12-hydroxy-Jasmonyl-isoleucine (12-OH-JA-Ile), and 12-carboxy-Jasmonyl-isoleucine (12-COOH-JA-Ile) content in different growth stages under well-watered conditions. Samples were collected from six different biological replication each with pooled three individual plants, frozen in liquid nitrogen and subjected to extraction separately as described in the Materials and Methods section. Each compound was quantified via the corresponding internal standard. Data were analysed by multiple comparisons (Tukey test) followed by one-way ANOVA. Data are means ± SE, $n = 6$. F.W.- fresh weight. Bars with different letters are significantly different from each other ($P < 0.05$).

With such a dramatic increase in jasmonate levels, especially in the bioactive JA-Ile in response to variation in age/growth stage, I also expected to see changes in JA-mediated gene expression. In the following experiment, I thus analysed the expression level of *VSP1* by RT-qPCR from plants at day 18 and 32 under long-day conditions (Figure 30A). Consistent with the hormonal changes, *VSP1* transcripts were upregulated in the older plants grown under long-day conditions that had reached the bolting stage, while in leaves with lower JA-Ile levels, *VSP1* transcript levels were lower as well (Figure 31).

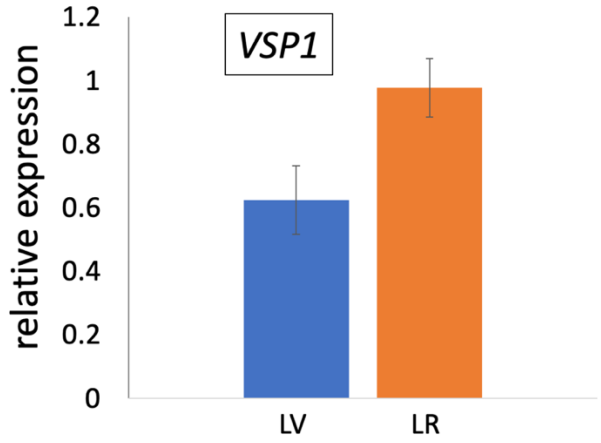

Figure 31: Age-dependent variation in *VSP1* expression.
VSP1 transcript level of the rosette leaves in WT plants (Col-0) grown until vegetative stage on day 18 (LV) and until bolting stage on day 32 (LR) under long-day conditions determined by RT-qPCR. *VSP1* transcript levels were normalized to *ACT2* levels and expressed as relative quantity ($2^{-\Delta\Delta Ct}$). Error bars represent the mean ±SE of three biological replicates (n = 3).

3.1.19 JAR1-mediated regulation of photosynthesis and chloroplast-targeted regulation

The RNA-seq analysis showed that the gain/loss-of-function of JAR1 can affect photosynthesis and light-dependent processes. It is not unlikely that JAR1 is regulated through chloroplast-derived compounds or that jasmonates could *vice versa* regulate genes coding for nuclear-encoded chloroplast proteins. A previous experiment had shown that exogenous MeJA application reduced photosynthetic activity by inhibiting RUBISCO activity (Shan et al., 2011) In this study, analysis of photosynthetic activity of the different plant lines by calculating the photosynthetic yield of photosystem II at day 25 under control conditions and drought stress showed a decline of activity in JAR1-OE under control conditions compared to WT, though I found no variation between *jar1-11* and WT (Figure 32A). However, this reduced photosynthetic activity remained unchanged in JAR1-OE after drought imposition, while being remarkably reduced in *jar1-11* and slightly reduced in WT. The amount of reduced photosynthetic activity in *jar1-11* was almost similar to the amount in JAR1-OE in both control and drought conditions (Figure 32A).

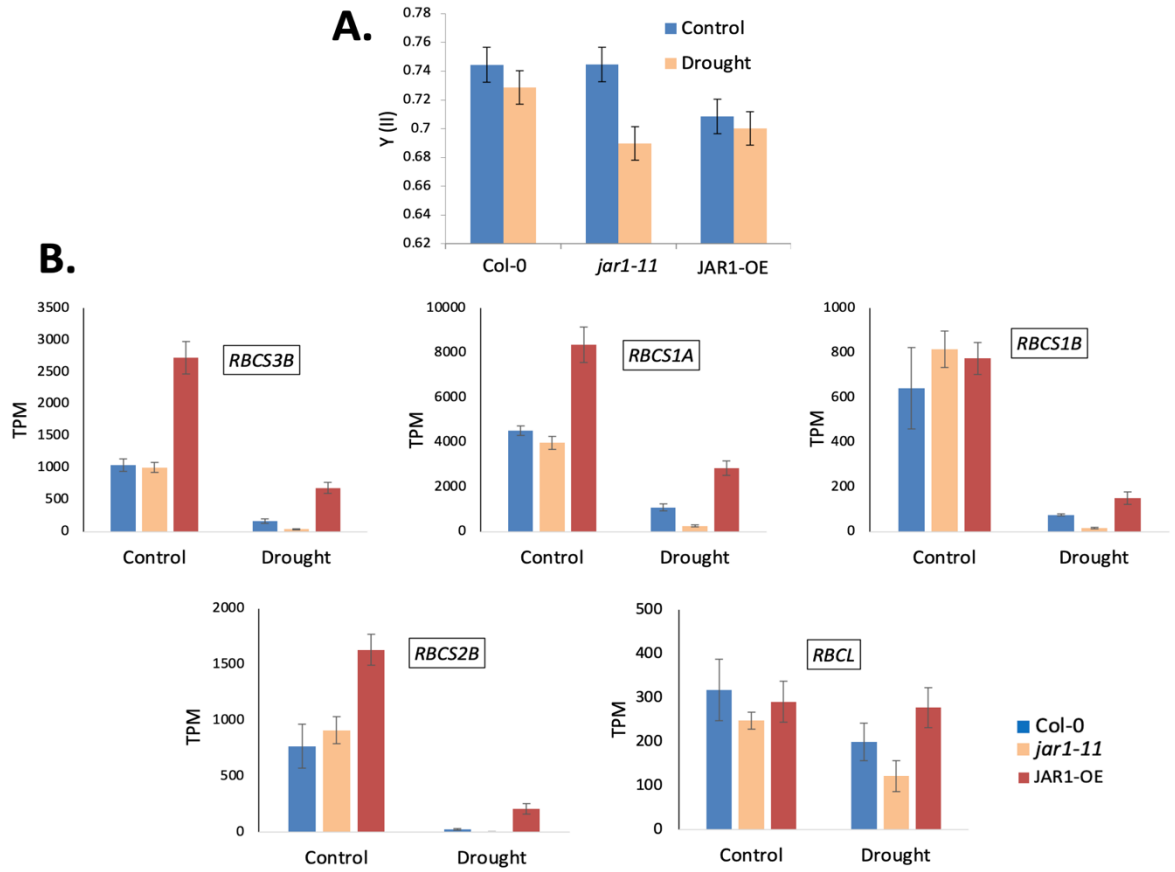

Figure 32: JAR1-dependent photosynthetic activity and RUBISCO structural genes expression.
A. Photosynthetic yield by the photosystem II, **Y(II),** in the different plant lines under well-watered and drought stress. **Y(II)** was measured by a Junior PAM from the rosette leaves on day 25 under long-day conditions (16 h/8 h). **B.** Relative expression of the genes responsible for RUBISCO-complex**.** Expression is presented as TPM from the RNA-seq of the well-watered and drought stress plants. Bar plot prepared with TPM. Data represent means ± SE from 3 replicates (n=3).

I also analysed the expression of nuclear and organelle-encoded genes of chloroplast proteins, especially related to RUBISCO activity. From the expression under normal well-watered conditions, I found that most of the RUBISCO small subunit (SSU) genes, which are nuclear-encoded, i.e. *RBCS3B, RBCS1A* and *RBCS2B* were highly upregulated in JAR1-OE and slightly downregulated or unchanged in *jar1-11* compared to WT (Figure 32B). After drought imposition, their expression was downregulated in all lines, albeit to a lesser extent in JAR1-OE which remained higher than in *jar1-11*. However, I found no significant difference in levels of the organellar encoded large subunit *RBCL* between the plants under control conditions but reduced levels in WT and *jar1-11* under drought stress. These results suggest a putative role of jasmonate signaling in regulating nuclear-encoded chloroplast-localized genes (Figure 32B).

Moreover, I looked at the expression of one important chloroplast-encoded photosystem I -related gene*, PSAB,* and found a similar expression to the SSU genes under control conditions

with lower expression in *jar1-11* and higher expression in JAR1-OE (Figure 33A). However, this expression was rather increased than decreased under drought. To confirm the JA-Ile-induced regulation of *PSAB* at the protein level, I performed western blot analysis on isolated chloroplasts from the different plant lines growing under normal well-watered conditions. Similarly, to transcript levels, I detected the lowest immunoreactivity in *jar1-11* while the difference between WT and JAR1-OE was not as pronounced on the protein level compared to the transcripts (Figure 33B).

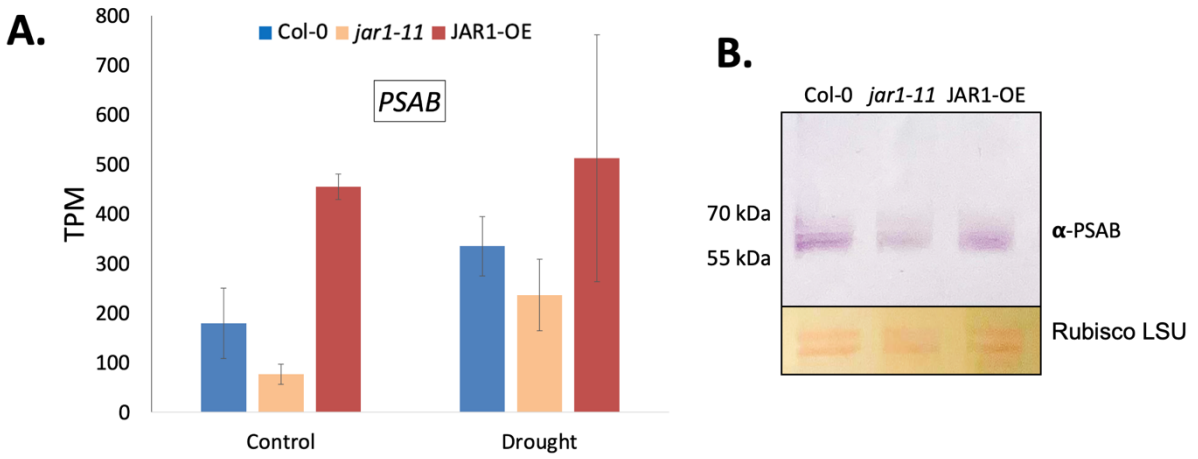

Figure 33: JAR1-dependent changes in the expression of *PSAB* and PSAB protein level.
A. Relative expression of *PSAB* in the different plant lines on day 32 under well-watered and drought stress conditions from RNA-seq data**.** Expression is presented as TPM from the RNA-seq data. Bar plot prepared with TPM. Data represent means ± SE from 3 replicates (n=3).
B. Protein Blot indicating the level of PSAB in the protein extract collected from isolated chloroplasts of the indicated plant genotypes on day 32 under well-watered conditions. Upper panel; Membrane from the Western blot showing the immuno-detecting band at around 55 kDa using the antibody against PSAB in the protein extract collected from isolated chloroplasts of the indicated plant genotypes, Lower panel; Ponceau stain showing the band of Large sub-unit (LSU) of RUBISCO used as equally loaded control.

Thus, I conclude that JAR1-mediated JA-Ile formation can regulate photosynthetic capacity probably by targeting expression of some nuclear-encoded chloroplast proteins.

3.2 CML12

3.2.1 Cross-talk between jasmonates and calmodulin-mediated Ca^{2+} signaling

Only few reports so far have addressed the cross-talk between calmodulin-mediated Ca^{2+} regulation and jasmonate signaling (Scholz et al., 2014; Vadassery et al., 2012). The RNA-seq data suggest a connection between the expression of one CML, *CML12,* and JAR1-mediated JA-Ile accumulation. Under control conditions, expression of *CML12* was higher in *jar1-11* and slightly lower in JAR1-OE compared to WT. Drought stress resulted in a remarkable

decrease of the expression of *CML12* in WT and JAR1-OE compared to their control condition, with only a slight decrease in *jar1-11* (Figure 34).

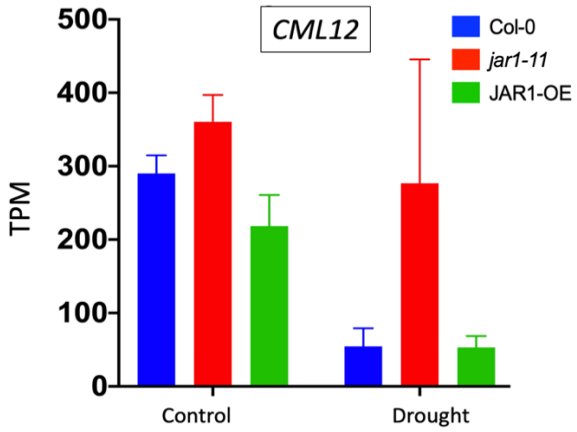

Figure 34: JAR1-dependent changes in expression of *CML12*.
Relative expression of *CML12* in different plant genotypes under well-watered conditions and drought stress on day 32. Expression is presented as TPM from the RNA-seq data. Bar plot prepared with TPM. Data represent means ± SE from 3 replicates (n=3).

This would imply that the effect of JA-Ile on *CML12* expression is dependent on the specific situation and thus probably includes other factors.

I further correlated *CML12* expression with its protein levels. I deemed this important since there are some targets of jasmonate signaling, i.e. JAZ proteins, whose transcript levels are increased upon JA-Ile accumulation, but at the protein level are reduced as JA-Ile accumulation can degrade JAZ proteins. I therefore studied the protein levels of CML12 by protein-blot using an CML12-specific antibody. For this purpose, I collected protein extracts from WT, *jar1-11* and JAR1-OE from 32-day-old well-watered and drought-stressed samples, respectively.

Surprisingly, under control conditions, the antibody reaction indicated protein levels that are directly opposite to the expression levels detected by RT-qPCR. I found a high level of CML12 as visible from the stronger immunoreactivity of the antibody in JAR1-OE, and much weaker reactivity with the WT and *jar1-11* (Figure 35). CML12 protein levels mirror the levels of JA-Ile in the plant lines, suggesting a differential role of JA-Ile the at transcriptional and translational level.

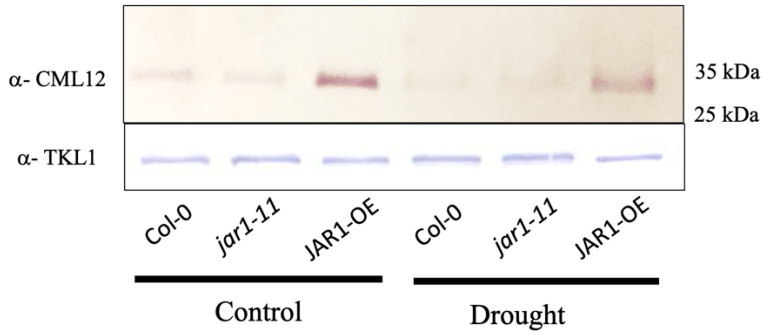

Figure 35: JAR1-dependent changes in CML12 protein level.
Protein Blot indicating the level of CML12 in the protein extract collected from the leaf tissue of the different plant genotypes under well-watered conditions and drought stress on day 32. Upper panel; Membrane from the Western blot showing the immuno-detecting band at around 33 kDa using the antibody against CML12 in the different plant genotypes. Lower panel; A protein-blot showing band with TKL1 specific antibody represents equally loaded control. Strong reaction with a thicker band in JAR1-OE under both well-watered conditions and drought stress was detected. Expression was reduced in all the lines under drought compared to well-watered conditions.

Under drought stress, CML12 were reduced in all three lines, visible by the weaker immunoreactive bands despite equal protein loading as seen from the band with TKL1-specific antibody (Figure 35). As before JAR1-OE showed the highest protein levels. This finding supports the notion that JA-Ile not only effects CML12 transcription but also proteins levels either via translation or protein degradation.

To test, whether CML12 expression and proteins levels are directly regulated by JA-Ile and not indirectly by phenotypic alterations in the different plant lines, I tested the effect of endogenous JA-Ile application. In a time-series experiment of 8 time-points, I incubated 14-day-old seedlings of the WT grown on $^1/_2$ MS medium+sugar with 100 µM JA-Ile at the indicated time-points and performed western blot analysis with protein extracts from whole shoots. I found a gradual decline in CML12 levels within 1 hour after JA-Ile treatment compared to non-treated (0 hours) WT plants (Figure 36A). I detected the lowest immunoreactivity at 30 minutes with a steady increase back to control levels after 6 hours. However, after 12 hours, expression was again strongly reduced indicating that CML12 might undergo diurnal changes in either expression or protein degradation (Figure 36A).

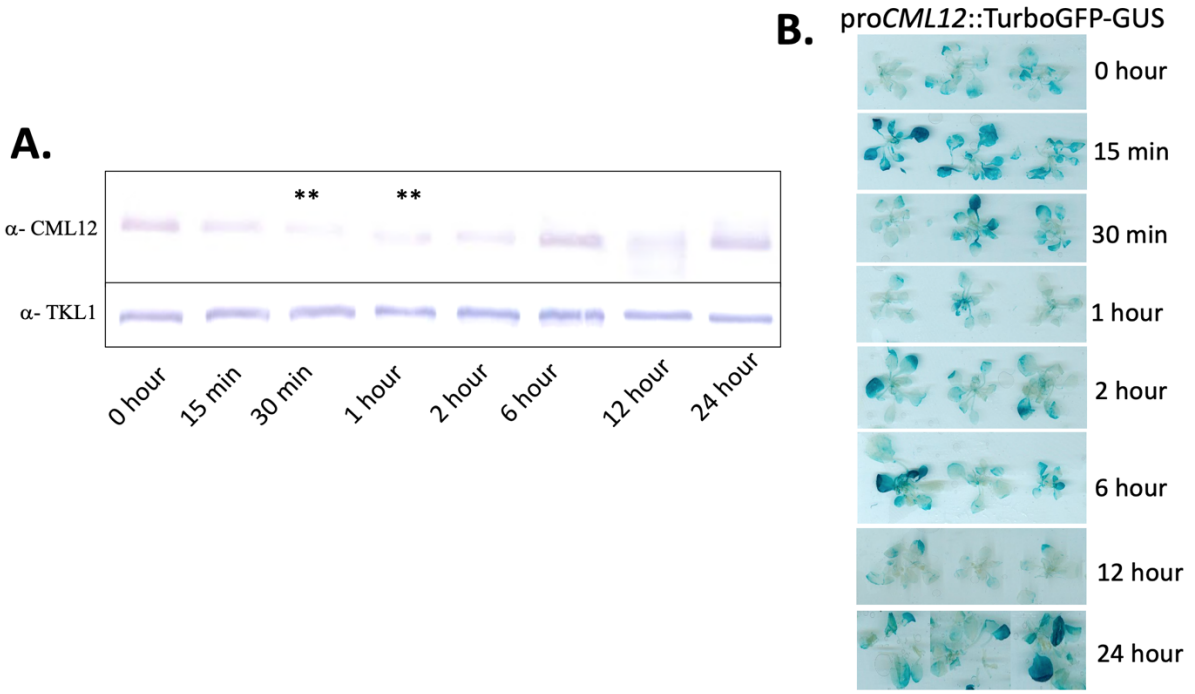

Figure 36: Exogenous JA-Ile mediated changes in CML12 protein level and the promoter activity of *CML12*.
A. Protein Blot indicating the level of CML12 in the protein extract collected from the whole shoot of the 14-day-old WT (Col-0) seedlings at indicated time-points after incubation with 100 µM JA-Ile. Upper panel; Membrane from the Western blot showing the immuno-detecting bands at around 33 kDa using the antibody against CML12 in the plant samples. Lower panel; A protein-blot showing band with TKL1 specific antibody represents equally loaded control. ** (Very weak reaction found in 30 min, 1 hour and 12 hours.) **B.** Histochemical staining of transgenic Arabidopsis 14-days-old WT (Col-0) seedlings expressing the GUS reporter gene under the control of the *CML12* promoter region (pro*CML12*::Turbo-GFP-GUS) collected at indicated time-points after incubation with 100 µM JA-Ile. The highest expression was found at 15 min while the lowest at 12 hours. Plants were grown on $^{1}/_{2}$ MS plate supplemented with sugar.

Since I previously found a differential behavior between of JAR1-dependent *CML12* expression and protein levels, I also tried to characterize the promoter activity of *CML12*. Thus, I analysed the *in-situ* expression of *CML12* using a pro*CML12::*TurboGFP-GUS line in WT (Col-0) background (Xiao and Offringa, 2020). Plants were treated as before for the western blot analysis at the same time points and immediately dipped them into GUS staining solution for expression study. Interestingly, the expression of GUS was strongly enhanced after 15 minutes compared to non-treated (0 hour) plants (Figure 36B). Expression then declined after 1 hour but increased toward the 6 hours time point. Similar to protein levels GUS expression was again strongly reduced after 12 hours and increased after 24 hours (Figure 36B).

Overall, the data suggest that CML12 is regulated in a complex manner, potentially combining a diurnal expression rhythm with differential regulation by JA-Ile on an expression and protein level.

3.2.2 ABA-dependent regulation of CML12

I found previously that the expression of *CML12,* was reduced under drought stress both at the transcriptional and translational level. And that drought stress likely induces ABA accumulation (Gupta et al., 2020; Yan et al., 2010). Thus, I investigated the direct role of ABA on the CML12 level. For this purpose, I incubated 14-day-old seedlings of the WT grown on $^1/_2$ MS medium+sugar for 24 hours with 1 mM ABA, collected their shoots for protein extraction and performed a protein-blot using the antibody against CML12. Interestingly, ABA treatment also reduced CML12 level compared to non-treated plants similarly to drought stress as I observed a very light band with low immunoreactivity even though I loaded more protein extracts in the case of ABA-treated plants of WT (Figure 37A).

To confirm the endogenous effect of ABA on CML12, I collected the *aba2-1* mutant, where ABA is less produced compared to WT (Cheng et al., 2002). I collected protein extracts from the rosette leaves of WT, *jar1-11*, JAR1-OE and *aba2-1* lines at day 32 under drought stress. After performing a protein-blot using the antibody against CML12 with an equally loaded protein amount, I found a stronger immunoreactivity of the CML12 antibody in *aba2-1* compared to all other lines presented as a thick band which is even stronger than the band found in JAR1-OE (Figure 37B).

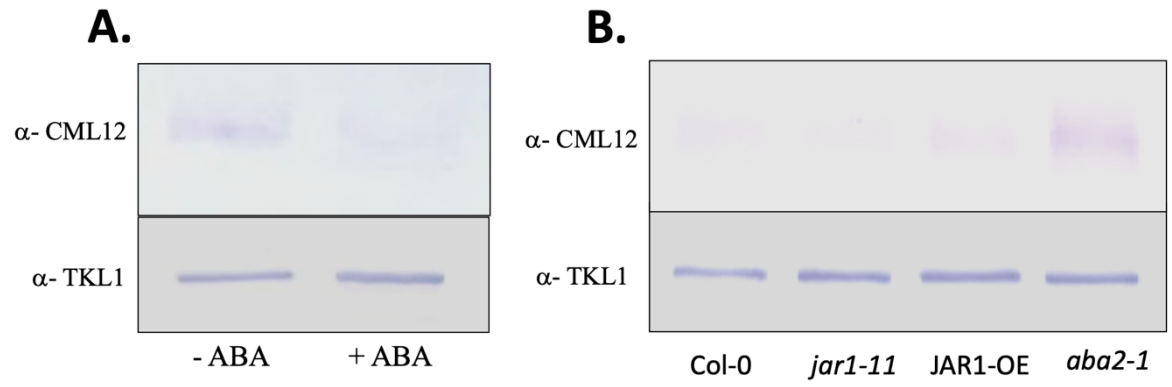

Figure 37: ABA-mediated regulation of CML12 protein level.
A) and **B)** Protein Blot indicating the level of CML12 in the protein extract collected from the **A.** whole shoot of the 14-day-old WT (Col-0) seedlings after incubation with or without 1 mM ABA for 24 hours. Plants were grown on $^{1}/_{2}$ MS plate supplemented with sugar. Clear reduction of the immuno-reaction was detected in the ABA-treated sample **B.** leaf tissue of the indicated plant genotypes under drought stress on day 32. The highest immuno-reaction was detected in the *aba2-1* line. Upper panel; Membrane from the Western blot showing the immuno-detecting band at around 33 kDa using the antibody against CML12 in the different plant genotypes. (Upper panel). A protein-blot showing band with TKL1 specific antibody represents equally loaded control (Lower panel).

Thus, I conclude that drought-induced ABA accumulation can negatively affect CML12 level.

3.2.3 Growth phenotype of a *cml12* knockout line

CML12, was firstly reported as TOUCH INDUCIBLE 3 (TCH3) to be induced upon wounding, rain or wind stress (Braam and Davis, 1990; Braam et al., 1992). However, no previous studies focused on the general growth performance of loss-of-function mutants of CML12 in soil. I thus analysed the T-DNA insertion line *cml12-1* (SALK_122731.26.30.x), which carries the T-DNA insertion in the third exon as confirmed by PCR (Figure 38A). The lack of an immunoreactive band in western blot analysis further establishes *cml12-1* as a real knockout line (Figure 38B).

Figure 38: Genotypic and phenotypic screening of *CML12* knockout line.
A. Schematic representation of the position of the T-DNA insertion at exons 3 (E3) in *cml12-1*. T-DNA insertion was confirmed by genotyping PCR. **B.** Protein Blot indicating the level of CML12 in the protein extract collected from the leaf tissue of the WT and *cml12-1*. Upper panel; Membrane from the Western blot showing the immuno-detecting band at around 33 kDa using the antibody against CML12 in WT while missing in *cml12-1*, Lower panel; Ponceau stain showing the band of Large sub-unit (LSU) of RUBISCO used as equally loaded control. **C.** Phenotyping differences, leaf morphology (upper panel) and flowering pattern (lower panel) between WT and *cml12-1*. No difference in the leaf morphology was detected. Lateral stems of *cml12-1* inflorescence bend downward while they move upwards in WT under well-watered conditions.

Under normal growth conditions, no variation in rosette shape or leaf morphology was visible between WT and *cml12-1* (Figure 38C, upper panel). Later during development, *cml12-1* plants displayed a downward bending of the laterally-flowering stems during their initial emergence while the WT stems moved upwards (Figure 38C, lower panel).

When analysed under progression drought conditions *cml12-1* showed similar wilting as the WT, but the *cml12-1* plant showed a better recovery after re-watering, indicating that CML12 enhances the drought resistance of plants to a certain extent (Figure 39).

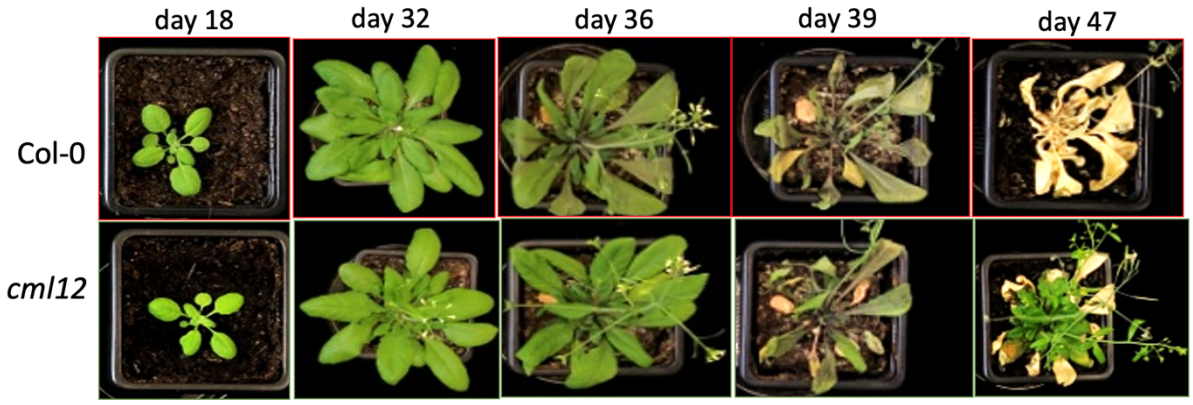

Figure 39: CML12-dependent drought stress response.
Progressive drought stress was performed with WT and *cml12-1* plants in the long-day conditions (16 h/8 h) according to the scheme mentioned in Figure 13A. No visible differences were found between WT and *cml12-1* until day 39 as both started wilting on day 36, reached unrecoverable wilting on day 39. Visible differences appeared on day 47 with re-emergence of the leaves in *cml12-1* while nothing emerged in WT. All the pots were randomized every day. This phenotyping was repeated at least three times with similar results.

3.3 AtMYB2

3.3.1 MYB2-mediated drought stress response

Jasmonate signaling is mostly regulated through bHLH group transcription factors, especially through MYC2 and its interacting partners such as MYC3, MYC4 etc. Another transcription factor, ORA59, is controlled through both ABA and jasmonate interactions (Chen et al., 2016). Additionally, several jasmonate related genes, i.e. *LOX2 AOS* and *CYP94B3,* have the recognition sequence for MYB2 in their promoter region (Figure 40A) and it previously has been reported that *MYB2* is drought inducible and that an overexpression line of MYB2 is resistant against drought stress. However, no previous studies focused on the general growth performance of loss-of-function mutants of MYB2 in soil. I thus analysed the T-DNA insertion line *myb2* (SALK_045455), which carries the T-DNA insertion in the third exon as confirmed by PCR (Figure 40B). Initially, I tried to grow the *myb2* plants in a similar pattern as done for jasmonate pathway mutants but I could not find any significant difference in the rosette shape, leaf morphology or flowering pattern under well-watered conditions compared to WT (Figure 40C).

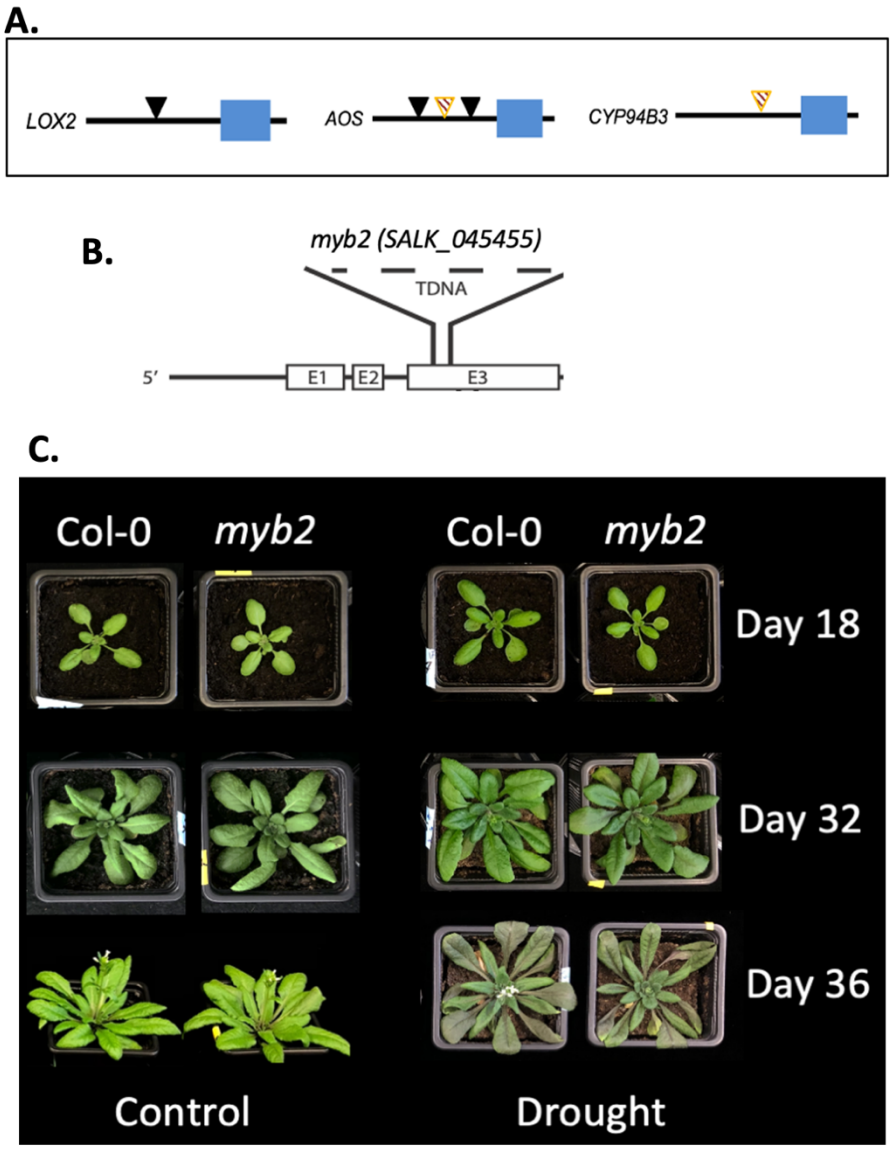

Figure 40: MYB2-dependent phneotypic variation.
A. Schematic drawing of the MYB-recognition sites TAACTG (Black arrow) and CAGTTA (yellow arrow) on the promoter region of some jasmonate pathway genes. Black line before the blue box (First exon) indicates promoter region. **B.** Schematic representation of the position of the T-DNA insertion at exons 3 (E3) in *myb2.* T-DNA insertion was confirmed with genotyping PCR. **C.** Leaf morphology and flowering pattern of WT and *myb2* under normal grwoth condition (left) and drought stress (right). A progressive drought stress was performed with WT and *myb2* plants in the long-day conditions (16 h/8 h) according to the scheme mentioned in Figure 13A. No visible differences were found between WT and *myb2* until day 36 as they started showing wilting symptoms on day 36, All the pots were randomized every day. This phenotyping was repeated at least twice with similar results.

I then performed a progressive drought stress experiment as described in Figure 13A but again, no phenotypic difference between *myb2* and WT plants could be observed (Figure 40C). I therefore concluded that loss of function of MYB2 does not have a visible effect on leaf/flowering morphology under control conditions or on the plant's susceptibility to progressive drought stress.

3.3.2 MYB2-mediated regulation of jasmonate levels

To gain a better insight into potential MYB2-mediated regulation of the jasmonate-pathway, I measured the jasmonate content in rosette leaves of WT and *myb2* plants on day 32 in well-watered control conditions and after imposing progressive drought stress as described previously.

In control conditions, the amount of the precursor *cis*-OPDA was decreased in *myb2* plants (Figure 41), but the amount of JA and JA-Ile was slightly increased. This increase was also observed with 12-OH-JA-Ile, while 12-OH-JA was decreased (Figure 41). The decrease in *cis*-OPDA thus might co-relate with a slight increase in JA, JA-Ile and their catabolic products in control conditions.

While levels of the precursor molecule *cis*-OPDA decreased upon drought stress in the WT (Figure 41), no significant changes occurred in *myb2*. In a similar manner, JA, JA-Ile and 12-OH-JA-Ile were increased in the WT under drought stress but remained unchanged in *myb2* plants. Levels of hydroxylated JA, 12-OH-JA were a bit lower in *myb2* plants but showed a similar trend as WT with regard to a slight increase under drought. (Figure 41).

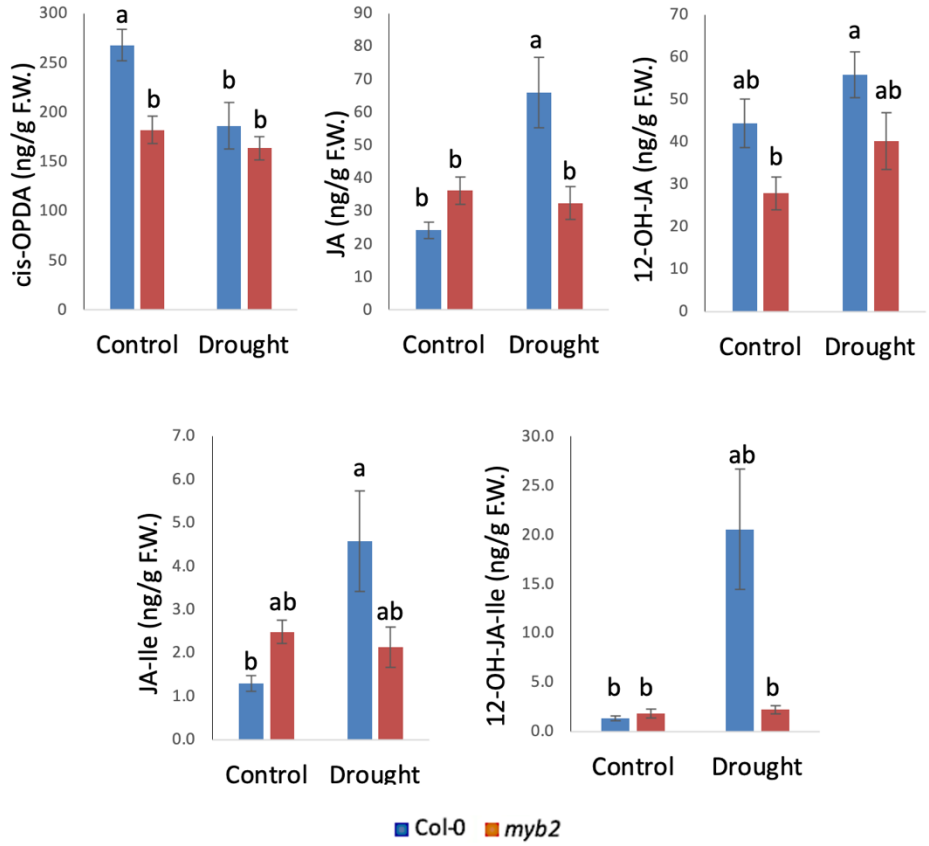

Figure 41: MYB2-mediated variation in the jasmonates under control and drought stress conditions. Drought-induced variation of the jasmonates, *cis*-12-oxo-phytodienoic acid (*cis*-OPDA), Jasmonic acid (JA), Jasmonyl-isoleucine (JA-Ile), 12-hydroxyjasmonic acid (12-OH-JA) 12- hydroxyjasmonoylglucoside (12-*O*-Glc-JA), 12-hydroxy-Jasmonyl-isoleucine (12-OH-JA-Ile) and 12-carboxy-Jasmonyl-isoleucine (12-COOH-JA-Ile) content in WT and *myb2* compared to control conditions. Rosette leaves of the plants were harvested on day 32 for control as well as drought stress conditions. Samples were collected from six different biological replication each with pooled three individual plants, frozen in liquid nitrogen and subjected to extraction separately as described in the Materials and Methods section. Each compound was quantified via the corresponding internal standard. Analysis was repeated twice with similar results and here one replication is presented. Data were analysed by multiple comparisons (Tukey test) followed by one-way ANOVA (*P<0.05, **P<0.01). Data are means ± SE, n = 6. F.W.- fresh weight.

3.3.3 MYB2-mediated transcriptional regulation with a focus on jasmonate signaling

RNA-seq was used to further assess MYB2-related changes in global gene expression in rosette leaf samples at day 32 in well-watered control conditions and after imposing progressive drought stress as described previously in Figure 13A.

Under control conditions, only three DEGs were found between WT and *myb2*, all of which were reduced (Figure 42A, left). Under drought stress, a total of twenty DEGs were identified between WT and *myb2*, among which seventeen were downregulated and three were upregulated (Figure 42A, right).

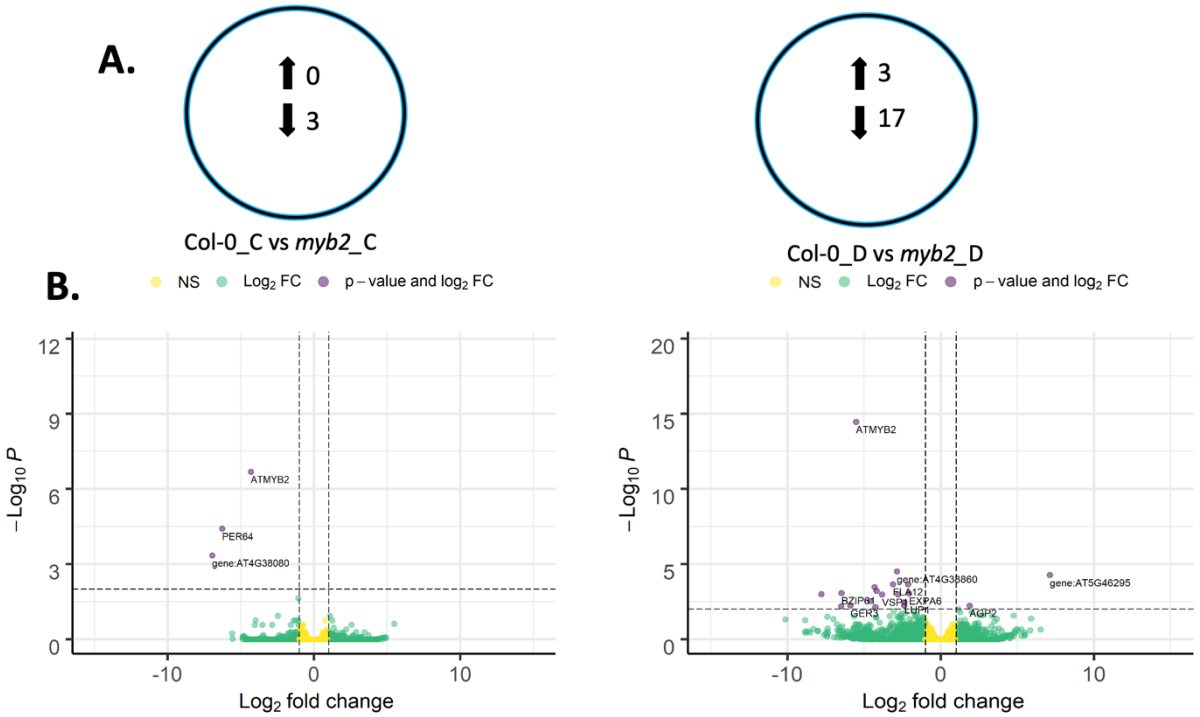

Figure 42: MYB2-dependent changes in gene expression in rosette leaves under well-watered and drought stress conditions.
Rosette leaves under well-watered conditions and drought stress on day 32 were collected for RNA-seq from WT and *myb2* for RNA-seq. **A.** DEGs up-and downregulated (DESeq, adjusted FDR <0.01 and LogFC ≥1) in *myb2* compared to WT plants. "C" under control conditions; "D" under drought stress. Arrows indicate up- and downregulation. **B.** Volcano plot showing statistical significance ($log_{10}P$) versus magnitude of change (LogFC) of DEGs between WT (Col-0) and *myb2* under control conditions (left) and under drought stress (right). Violet dots indicate genes that fit the DESeq criteria of FDR <0.01 and LogFC ≥1; green and blue dots represent DEGs that fit either only LogFC or FDR, respectively.

Among the genes that were downregulated in control conditions, one is non-characterized (*AT4G38080)* and one was identified as PEROXIDASE GENE 64, *PER64,* which has a role in root cell wall biosynthesis (Rojas-Murcia et al., 2020). This suggests a probable role of MYB2 in cell wall biosynthesis. I also found null expression of *MYB2* which supports *myb2* as being a proper knock-out line (Figure 42B, left, Supplemental Figure 5).

Moreover, under drought stress, I could not find any genes that were directly related to drought response despite finding some genes directly or indirectly related to cell wall formation such as *FLA12*, *EXPA6* and *EXPA8.* These genes were downregulated in *myb2* compared to WT under drought stress, which further supports that MYB2 might play a role in cell wall formation under drought stress (Figure 42B, right). Additionally, downregulation of one auxin responsive gene, *SAUR16,* and one gibberellic acid responsive gene, *GASA4,* suggests the involvement of MYB2 in hormonal regulation (Figure 42B, left and Supplemental Table 5).

With regard to jasmonate signaling, I found the jasmonate-responsive genes *VSP1 and VSP2* to be downregulated in *myb2* plants compared to WT (Figure 43) under drought, which correlates with the decreased amount of JA and JA-Ile in *myb2* plants found under drought stress compared to WT. I could not see any significant difference in jasmonic acid biosynthetic genes with exception of the catabolic gene, *CYP94B3,* which converts JA-Ile to 12-OH-JA-Ile, and whose expression was slightly higher in *myb2* compared to WT under control and specially under drought stress conditions (Figure 43). Interestingly, expression of the jasmonate/ethylene-dependent defense gene, *PDF1.2A,* was significantly decreased in *myb2* under control and drought stress conditions compared to WT (Figure 43).

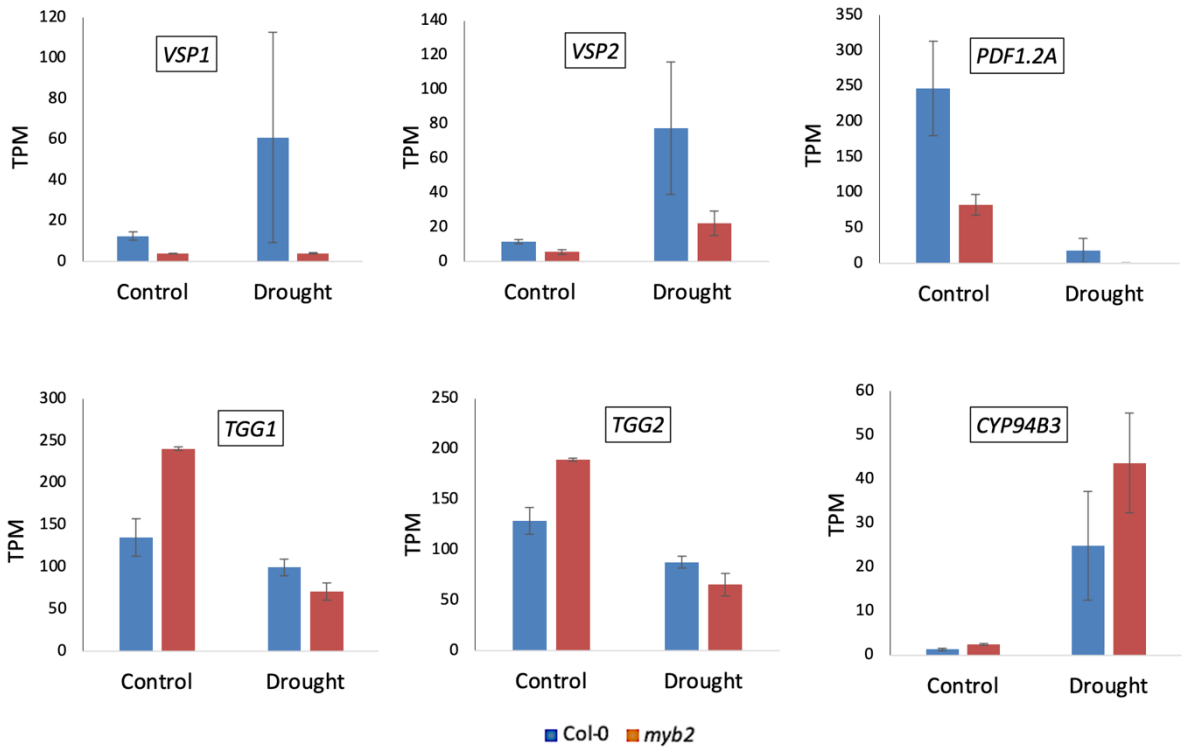

Figure 43: MYB2-dependent changes in jasmonate-responsive genes expression.
Expression is presented as TPM from the RNA-seq of the well-watered and drought-stressed WT and *myb2* plants. Bar plot prepared with TPM. Data represent means ± SE from 3 replicates (n=3).

Noteworthily, expression of the two stomata-related myrosinases *TGG1* and *TGG2,* which were found upregulated in JAR1-OE (Figure 28), was also increased in *myb2* (Figure 43).

When I analysed the expression of jasmonate related genes between WT and *myb2* under each of the two conditions (WT control vs. drought and *myb2* control vs. drought), I found that many genes showed differential changes in expression. In the biosynthetic pathway, I found the expression of some genes such as *LOX3*, *OPCL1* (*4CLL5), AOC3* or *ILL4* to be increased in

myb2 under drought and to remain unchanged in WT (Figure 44). Besides, *JMT,* which is responsible for methylation of JA, was slightly enhanced in *myb2*. As already shown above (Figure 43), the expression of JA-Ile-responsive genes such as *VSP1* and *VSP2* but also *MYC2,* which was enhanced in WT under drought, showed no variation in *myb2* plants. And while the expression of some JAZ genes such as *JAZ1 (TIFY10A)*, *JAZ11(TIFY3A)* and *JAZ12 (TIFY3B)* was enhanced in *myb2* but not WT under drought, expression of *JAZ6 (TIFY11B)* in *myb2* plants was reduced. (Figure 44).

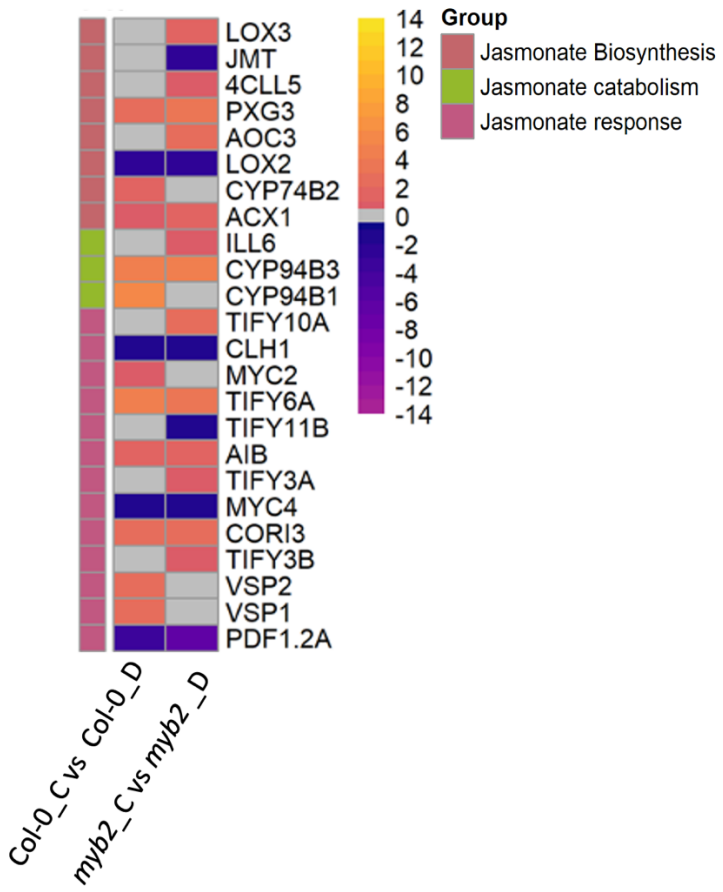

Figure 44: MYB2-dependent changes in gene expression of jasmonate pathway under drought stress compared to control conditions.
Heat map showing DEGs involved in jasmonate-biosynthesis, catabolism and signaling response in WT (Col-0) and *myb2* plants in the drought stress compared to each of their well-watered conditions. Data were analysed by an alternative cut off of FDR <0.05 and LogFC ≥0.5. C- control conditions, and D- drought stress.

No variation was found in *JAR1* expression in *myb2* plants compared to WT under any conditions (Supplementalal Figure 3). However, western blot analysis on extracts from rosette leaves using an antibody against JAR1.1 revealed a higher JAR1 content in WT compared to

myb2 plants (Figure 45). This result is consistent with the trend of decreasing JA and JA-Ile levels in *myb2* plants compared to WT.

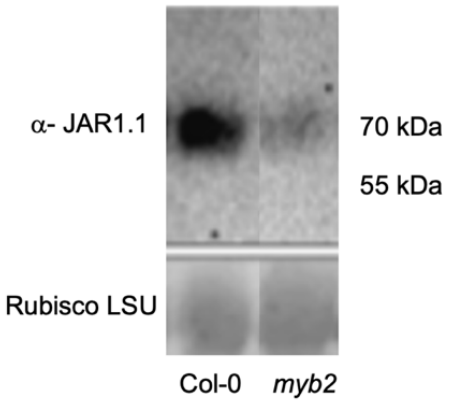

Figure 45: MYB2-mediated regulation of JAR1 protein level.
Protein Blot indicating the expression of JAR1.1 in the protein extract collected from the leaf tissue of the WT and *myb2* under well-watered conditions on day 32. Upper panel; Membrane from the Western blot showing the immuno-detecting band at around 70 kDa using the antibody against JAR1.1 in the plant genotypes. Lower panel; Ponceau stain showing the band of Large sub-unit (LSU) of RUBISCO used as equally loaded control. Strong reaction with a thicker band in WT while less reaction with a light band in *myb2* plants is visible.

I then analysed the shoot and root growth of WT, *myb2* and *jar1-11* plants on $^1/_2$ MS medium+sugar with and without 50 μM MeJA supplement to monitor the effect of exogenous MeJA on *myb2* plants. As found previously, exogenous MeJA inhibited the growth of the WT plants. And while *jar1-11* plants were insensitive to MeJA application, *myb2* plants showed a similar growth inhibition as WT (Figure 46).

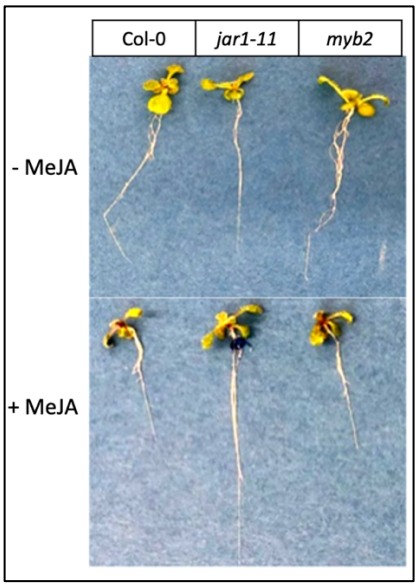

Figure 46: MeJA-mediated root and shoot growth sensitivity of the plants in $^{1}/_{2}$ MS medium.
Photographs were taken from 14-day-old seedlings under a long day (16 h/8 h light) condition. Upper panel- seedlings were grown on $^{1}/_{2}$ MS plate supplemented with sugar; Lower panel- Plants were grown on $^{1}/_{2}$ MS plate supplemented with sugar and 50 μM MeJA.

Overall, I therefore conclude that MYB2 can regulate the jasmonate pathway under specific conditions in both a positive and negative manner.

4. Discussion

The response of plants to drought stress involves an intricate interplay of different signaling pathways, which includes hormonal regulation. ABA is the canonical stress hormone that is typically accumulated under drought as a means to counteract early stage stress (Yang et al., 2019; Daszkowska-Golec and Szarejko, 2013). However, recent studies are focusing on the role of other hormones besides ABA in drought stress adaptation and recovery.

Jasmonates have been studied for the last two decades for their involvement in regulating biotic stress such as in counteracting wounding and pathogen-associated defenses (Wasternack and Song, 2017; Wasternack and Hause, 2013; Koo, 2018). JA-Ile is the bioactive jasmonate that can mediate most of the jasmonate-related defense responses. The role of JAR1-mediated JA-Ile accumulation and its regulation through the COI1 receptor under biotic stimuli is well described (Katsir et al., 2008; Suza and Staswick, 2008; Yan et al., 2009; Wasternack and Song, 2017), but the exact role of JA-Ile in abiotic stresses such as drought is an emerging area of plant biology. It was reported several times that exogenous JA/MeJA application results in growth retardation at early stages of growth (Noir et al., 2013; Pauwels et al., 2008; Zhang and Turner, 2008; Brioudes et al., 2009; Świątek et al., 2004). However, the role of jasmonate signaling in soil-grown growth regulation and drought stress-mediated defense mechanisms throughout the life-cycle of plants has not been studied.

4.1 JAR1.1 is the active splice variant of *JAR1*

Describing the role of endogenous JA-Ile production has always been hampered by the unavailability of a proper *JAR1* knockout. Phenotypic analysis was limited to a few types of stress and could not readily be accomplished with the point mutation line *jar1-1*. To overcome those limitations, researchers were mostly focusing on the COI1 receptor mutant *coi1-1*. However, the use of this line became controversial when several reports suggested that the JA precursor OPDA could regulate biotic and abiotic stress independently of COI1 and that some catabolic products could interact with COI1 (Savchenko et al., 2014; Gheysen and Mitchum, 2019; Smirnova et al., 2017, Aubert et al., 2015; Poudel et al., 2019). In this study, a substantial progress was made by using the T-DNA insertion line *jar1-11,* where *JAR1* expression was remarkably reduced. Downregulation of master transcription factor *MYC2* and nearly null expression of the marker genes *VSP1* and *VSP2* supported the reduction of JA-Ile activity in this mutant line. However, using only the *jar1-11* line to study the role of JA-Ile during normal growth conditions-was problematic because it still produces some amount of *JAR1* transcript.

This challenge might be overcome by an ectopically expressing JAR1-line, where endogenous JA-Ile is upregulated even under normal growth conditions. Recent findings suggested that JAR1 is available as three splice variants (Zander et al., 2020; Howard et al., 2013), of which JAR1.1 was the first to be described (Staswick et al., 2002). This variant was thus chosen for the overexpression line. Recent findings from Zander and co-authors suggested that the most abundant splice variant of JAR1 is indeed JAR1.4 (Zander et al., 2020), however, retention of the first intron after PCR amplification (Figure 5A) limited the use of this splice variant for this study. Moreover, JAR1-OE (35S:JAR1.1-YFP) plants showed a phenotype opposite of that observed in *jar1-11* with higher accumulation of JA-Ile even under non-stress conditions. Together with upregulation of the marker genes *MYC2*, *VSP1* and *VSP2* this supports JAR1-OE as a functional overexpression line. Therefore, the T-DNA insertion line *jar1-11* and the JAR1.1 overexpression line (JAR1-OE) were deemed very useful tools in the analysis of the proper role of JA-Ile in growth, development and drought stress.

4.2 Variation in leaf morphology and flowering time is regulated through altered jasmonates

Exogenous MeJA arrests the cell cycle and mitotic regulation to ultimately suppress growth (Noir et al., 2013; Pauwels et al., 2008; Zhang and Turner, 2008; Brioudes et al., 2009; Świątek et al., 2004). In this study, overexpression of JAR1 constitutively increases JA-Ile accumulation even in non-stress conditions which is likely to regulate the morphological growth of plants. When grown on ½ MS medium, differences were observed in form of reduced root length and somewhat smaller leaf sizes of JAR1-OE. By contrast, the variation in *jar1-11* was not very pronounced. Inhibition of growth of JAR1-OE was even stronger than WT after addition of MeJA to the medium. In soil-growing conditions, the differential growth between *jar1-11* and JAR1-OE became more pronounced with larger rosette leaf sizes in *jar1-11* compared to JAR1-OE. This is the first indication of complementary growth difference related to gain or loss of JAR1-mediated endogenous JA-Ile accumulation. Moreover, similar growth phenotype of *aos* and *opr3* mutant to *jar1-11* supported the role of JA-Ile on leaf growth in soil grown conditions. This is also consistent with the growth suppressing nature of the recently described jasmonate-signaling mutant, *jazD*, where almost all the important JAZ repressors are knocked out or expressed at low levels (Guo et al., 2018). It is also consistent with the previous findings that JA-Ile accumulation can degrade JAZ repressors and thereby inhibit plant growth (Thines et al., 2007; Wasternack and Song, 2017).

JAR1-OE plants also showed a delay in flowering compared to WT, while *jar1-11* plants flowered earlier. Interestingly, genes which are directly related to floral response i.e. *FT*, *CO* and, *LEAFY* etc. do not differ in expression levels between the different plant lines even though it had been shown previously that COI1 inhibits *FT* expression (Zhai et al., 2015). Instead, this difference was related to vernalization and the autonomous flowering-time pathway, as evidenced by upregulation of the flowering repressor *FLC* and downregulation of the FLC-repressed transcriptional activator *SOC1* in JAR1-OE (Michaels and Amasino, 2001; Richter et al., 2019). Early flowering with higher leaf number in *jar1-11* plants led to a faster completion of their life cycle. By contrast, in JAR1-OE, even at the time of flowering, leaf number was a lot lower than in both WT and *jar1-11* that suggested the direct role of JA-Ile in regulating the duration of the life-cycle of plants by controlling leaf growth and flowering time.

4.2.1 Jasmonate-dependent stunted growth is overcome at later growth stages

Intriguingly, the initial stunted growth of JAR1-OE was overcome at later stages characterized by increased lateral leaf growth. From RNA-seq data, which were obtained on day 32, i.e. at a later stage of development, cell cycle-related genes like *CYCB1.2,* which was shown to be induced during cell proliferation (Takahashi et al., 2019; Boruc et al., 2010), were enhanced in JAR1-OE. *CYCB1.2* expression is reduced by treating cell cultures with exogenous JA/MeJA (Zhang and Turner, 2008). However, enhanced expression of *CYCB1.2* in JAR1-OE suggested that cell cycle and development-related processes are not under direct regulation of jasmonate-signaling and that some mediators play a role in transmitting the jasmonate-response. Two growth-regulating transcriptional regulators, *GIF1* and its interacting partner *GRF5,* showed enhanced expression in JAR1-OE while being reduced in *jar1-11*. A mutant of the *GIF1* locus, *gif1,* had narrower leaf blades (Kim et al., 2004; Lee et al., 2009) similarly to *jar1-11,* which supports its role in promoting lateral leaf growth in JAR1-OE. *GIF1* expression has been recently found to be repressed by the MYC2 interaction partner, MYC4 (Liu et al., 2020), which itself was decreased in JAR1-OE. Thus JA-Ile dependent decrease of *MYC4* expression in JAR1-OE would lead to the release of *GIF1* repression. The subsequent increase in *GIF1* expression would then cause enhanced lateral leaf growth as observed for JAR1-OE. From this, it is clear that the inhibitory nature of jasmonate-signaling during early growth can be recovered in later stages under non-stress conditions. This also indicates the onset of further development in JAR1-OE at the time when the growth of leaves is almost terminated in WT and *jar1-11*.

Interestingly, the primary flowering stem in *jar1-11* and WT was taller than secondary stems, while JAR1-OE displayed an opposite pattern (Figure 11). Thus, it appears that jasmonate-

signaling also affects stem growth in a differential manner. Detailed analysis of gene expression in the stems apical meristems would be required to understand the JAR1-dependent changes in expression pattern that are behind this unusual growth pattern.

4.3 JA-Ile plays a role in drought stress priming

Modifications of growth pattern and morphology are some of the typical mechanisms that plants use to counteract water deficiency. Flowering is accelerated by severe drought stress to complete the life cycle (Kazan and Lyons, 2016; Kenney et al., 2014), while mild drought stress is characterized by stunted growth and delayed flowering (Clauw et al., 2016; Claeys and Inze, 2013; Schmalenbach et al., 2014). In this study, *jar1-11* plants displayed greater susceptibility to progressive drought but JAR1-OE plants only displayed a mild drought stress phenotype. Stunted growth of JAR1-OE plants likely reduces transpirational loss of water due to reduced surface area, while delayed flowering helps them to extend the duration of carbon and nitrogen assimilation. Later increased development of radial leave blades might either be part of a potential mechanism of drought stress resistance by unknown means or is simply made possible by better water usage efficiency due to drought induced adaptations (see below). Overexpression of *JAR1* led to the downregulation of drought-responsive genes even under normal growth conditions. Assumingly, this primes the plants for a better drought stress response. Indeed, it was demonstrated previously, that in the case of repetitive drought exposure, jasmonates are part of the memory system that enhances drought resistance during a second exposure (Liu and Avramova, 2016). In the case of progressive drought, overexpression of JAR1 already under control conditions, likely provides a memory-like response that ultimately provides resistance against severe drought. This might involve the prime target of drought stress response, *RD29A*, whose expression was downregulated in JAR1-OE. A similar finding suggested that exogenous MeJA priming led to MYC2-mediated regulation of the drought stress-responsive gene *RD29B* (Liu and Avramova, 2016). This is further supported by the recent finding whereby JA-treated plants reduced *RD29A* expression after 24 hours (Zander et al., 2020).

4.4 JA-Ile regulates the intricate anti-oxidant and physiological systems to combat drought stress

Drought stress resistance involves intricate mechanisms such as the reduction of transpirational loss of water through the regulation of stomatal density and aperture, the upregulation of the anti-oxidant system, etc. JAR1-OE plants retained high relative water content even under

severe drought stress, suggesting that they can lower transpirational loss by positively regulating stomatal aperture and density. A previous study on cotyledons showed that exogenous MeJA application could reduce stomata number in the epidermis (Han et al., 2018). This correlates with a lower number of stomata in JAR1-OE compared to WT and an even greater difference between JAR1-OE and *jar1-11*. This stomata density regulation by JAR1-OE is supported by the expression of several density-related genes such as *TMM*, *MYB124*, *EPF2* etc. Also, a relatively smaller stomatal aperture was found in JAR1-OE than in *jar1-11*. However, regulating stomatal aperture is an intricate mechanism which depends on various stimuli and regulators. Though no variation in common regulators of stomatal aperture was seen in the RNA-seq data, higher expression of two myrosinases, *TGG1* and *TGG2,* was found in JAR1-OE compared to *jar1-11,* underpinning their potential role in the regulation of stomata. These two myrosinases were previously found to induce stomatal closure through the combined regulation of ABA and JA (Rhaman et al., 2020; Islam et al., 2009).

Very commonly, drought stress leads to the production of ROS and drought-resistant plants have developed anti-oxidant mechanisms to scavenge the toxic hydroxy-radicals (Noctor et al., 2014). Plants can accumulate flavonoids such as anthocyanin to combat drought stress induced ROS formation (Misyura et al., 2012). JAR1-OE plants did show a higher amount of anthocyanin even in control conditions compared to other plants. This is in line with the previous finding that exogenous JA application enhances anthocyanin accumulation (Ai and Zhu, 2018). However, under drought stress, all three plants lines accumulated anthocyanin, the highest levels being found in JAR1-OE and the lowest ones in *jar1-11.* This suggests jasmonate-signaling upregulates the anthocyanin process but is not its sole regulator.

The ascorbate-glutathione cycle plays a major role in scavenging ROS generated during oxidative stress. However, this current study could not find any variation in the genes of the ascorbate-glutathione cycle under control conditions suggesting no specific regulation of JA-Ile on the ascorbate-glutathione pathway in well-watered conditions even though JA-treated young seedlings decreased the GSH::GSSG ratio to favor the GSH state in WT (Figure 29B). While, several previous findings suggested that exogenous MeJA treatment can enhance the expression of the glutathione biosynthetic genes (Xiang and Oliver, 1998; Sasaki-Sekimoto et al., 2005; Zander et al., 2020), However, in our study, drought stress (which resulted in increased JA-Ile formation, resulted in a decrease in glutathione biosynthetic genes in all plant lines. Despite not finding any variation of the biosynthetic genes among the plant lines, a reciprocal trend in the expression of the genes inside the cycle, *GR1/GR2* and *DHAR1,* was found between JAR1-OE and *jar1-11* under drought stress. This suggested a putative

mechanism to scavenge ROS under oxidative stress which is further supported by the successful recovery of oxidative stress induced by MV upon exogenous JA application in WT but not in *jar1-11*. Thus alteration with the cycle rather than altered expression of biosynthetic genes seems to the target of JA-Ile mediated ROS regulation during drought. Further detailed studies are required to address this regulation.

4.5 Jasmonate homeostasis beyond JA-Ile is involved in the regulation of the jasmonate-mediated drought response

The content of the bioactive jasmonate, JA-Ile, in the aerial part is typically low under normal growth conditions (de Ollas et al., 2015; de Ollas et al., 2015b; Figure 18). The content of JA and JA-Ile increased under drought stress in WT (Figure 18) and thus the expression of known jasmonate-dependent genes. The amount of the precursor *cis*-OPDA was almost 200 times higher than that of JA-Ile under control conditions and remained higher also under drought stress despite the reciprocal trend with an increase in JA-Ile and a decrease in *cis*-OPDA. This suggests that *cis*-OPDA formation is not a limiting factor in JA-Ile mediated signaling. The decrease in *cis*-OPDA under drought was equal to the net increase of JA, JA-Ile and several of their derivatives such as 12-OH-JA, 12-OH-JA-Ile, etc. However, the increase in JA, JA-Ile, and other derivatives could also come from other sources such as JA-Glc. Vice versa, excess JA could be converted first to 12-OH-JA and then to JA-Glc after imposing drought stress, to remove excess JA that is not used for JA-Ile production. Other regulatory pathways could be leading from JA-Ile to JA-Glc to remove excess JA-Ile. The extreme high content of JA-Glc under all conditions is indeed very remarkable. A high concentration of JA-Glc was also found recently in Poplar (Ullah et al., 2019), although it was comparatively lower in the Arabidopsis Ws background (Miersch et al., 2008). JA-Glc can be a precursor for JA and JA-Ile through 12-OH-JA back-conversion but this idea is still little explored due to the lack of knowledge on the enzyme regulating the conversion from JA-Glc to 12-OH-JA. In rice, OsTGG1, which is predicted to be a homolog of Arabidopsis BGLU18, can convert JA-Glc to 12-OH-JA through hydrolyzation (Wakuta et al., 2010). Arabidopsis BLU18 was previously shown to hydrolyze abscisic acid glucose ester (ABA-GE) to ABA (Lee et al., 2006). In this current experiment, expression of *BGLU18* was reduced in *jar1-11* and increased in JAR1-OE under drought stress which mirrors the reduction of JA-Glc level in JAR1-OE and increase in *jar1-11* (Figure 18). This suggested a potential role of BGLU18 in the hydrolyzation of JA-Glc. Overall these results suggest that a careful balance in the amount of jasmonates, including JA-Ile, is important jasmonate-dependent regulation of plant stress response.

4.6 MYC2 is a target of both JA and ABA signaling to initiate jasmonate-biosynthesis

Several studies reported both positive and negative interactions between ABA and jasmonate-signaling (Yang et al., 2019; Daszkowska-Golec and Szarejko, 2013). Under control conditions, no great variation in ABA content was found between the three plant lines investigated in this current study. By contrast, under drought stress the ABA amount increased in all lines, especially in *jar1-11* when compared to JAR1-OE. MYC2 was found to be a target of jasmonate-signaling in response to most biotic stimuli, while it is a target for ABA-signaling only under drought stress (Wasternack and Song, 2017; Koo, 2018; Abe et al, 2003). In this current study, the expression of *MYC2* was slightly increased in JAR1-OE compared to WT under control conditions even though MYC2-dependent marker genes were highly upregulated. This trend of slight increase of *MYC2* might be due to the low ABA content in the mutant.

Under drought stress, even though ABA content in *jar1-11* was higher than in the other two lines, the expression of *MYC2* was downregulated compared to WT and even more to JAR1-OE. This suggests that *MYC2* expression is dependent on the combined effect of both ABA and jasmonate and reduction of at least one of them contributes to decrease in *MYC2* expression. The combined effect of ABA and jasmonate is more reflected in JAR1-OE plants under drought stress, in which not only *MYC2* but also the jasmonate biosynthetic as well as responsive genes were highly up-regulated. Recent findings form Liu and co-workers (Liu et al., 2016.) suggested that ABA and jasmonate signaling together are perceived by MYC2 more efficiently rather than single exposure of either ABA or JA. MYC2 ultimately acts as a memory factor to initiate jasmonate-biosynthesis under drought stress as feedback regulation and results in a higher expression of jasmonate-responsive genes underpinning findings of this current study. Thus, it appears likely that ABA and JA-mediated regulation of MYC2 is required during drought stress for initiating the jasmonate-response. Interestingly, expression of *MYC4*, an interacting partner of MYC2, behaved opposite under drought stress suggesting it might have a different but not an additive role to MYC2.

Similarly to the observed ABA content, ABA-related genes were decreased in JAR1-OE under drought but increased in *jar1-11* compared to WT. This included genes involved in biosynthesis and catabolism, as well as genes involved in ABA-mediated response, such as-*ABI2*. Recent studies also found that the ABA-responsive gene *ABI2*, was decreased upon exogenous JA-priming (Zander et al., 2020). This observation was more pronounced in the expression of the ABA-mediated responsive gene *RD29A*, since it is a prime target of ABA accumulation. Though the ABA-mediated response is directly related to drought stress, this

trend is biased between *jar1-11* and JAR1-OE in terms of *RD29A* expression. This suggests the ability of jasmonate-signaling to reduce the overaccumulation of ABA under drought stress and to balance ABA levels before they reach unfavorable levels. This is also supported by the lower expression of the receptor-like *GCR2* in JAR1-OE, which is involved in initiating ABA biosynthesis (Liu et al., 2007). The cross-talk between jasmonates and ABA was observed for common transcription factor regulation (Chen et al., 2016) and activation of the ABA receptor (Lackman et al., 2011).

4.7 Jasmonate-signaling targets nuclear and chloroplast-encoded chloroplast-localized genes

In the current study, it has been shown that endogenous JA-Ile accumulation can affect photosynthesis related genes expression under drought stress. Photosynthetic processes involve nuclear-encoded but chloroplast-localized proteins of the photosystem (PSI and PSII) and related processes. Several genes involved in the light-harvesting complexes showed differential expression between *jar1-11* and JAR1-OE under drought stress. Also expression of several genes coding for isoforms of the RUBISCO small subunits were upregulated in JAR1-OE and downregulated in *jar1-11*. It came as a piece of evidence from Zander et al. (2020) that these genes are also upregulated with exogenous JA treatment. Therefore, it is likely that jasmonate-signaling targets nuclear-encoded chloroplast genes, which then modify the photosynthetic machinery. Moreover, the upregulation of the chloroplast-encoded *PSAB* gene in JAR1-OE suggests that jasmonate-signaling might also target chloroplast-encoded genes, which is in line with finding by Zander et al. (2020) regarding JA priming. How the expression of chloroplast encoded genes is regulated by jasmonates, is not known. This regulation could happen i) via nuclear-encoded regulatory factors regulated themselves by JA-Ile, or ii) chloroplast-localized targets of jasmonate-signaling such as LOX2, and AOS, responsible for biosynthesis of *cis*-OPDA, or iii) by a chloroplast-localized biosynthesis intermediate such as *cis*-OPDA directly. More investigation is required for a better understanding of the role of jasmonate signaling in chloroplast gene expression.

4.8 Jasmonate-signaling regulates the expression of *CML12* differentially at the transcriptomic and protein level

In this study, a reciprocal trend of *CML12* expression between *jar1-11* and JAR1-OE was found from RNA-seq data with a higher expression in *jar1-11* and a lower one in JAR1-OE compared to WT. Surprisingly, at the protein level, an opposite trend was found compared to transcript

level. Previous studies on *CML12* suggested that its expression could be induced by touch and wounding attack (Braam and Davis, 1990; Braam et al., 1992). Jasmonate-signaling was also initiated upon these same stimuli (Suza and Staswick, 2008). So, jasmonate-signaling is likely to induce *CML12* expression. A similar finding from dehydrated leaves showed upregulation of transcript level of *CML12* in *coi1-1* mutants (Reymond et al., 2000), which underpins its upregulation at the transcript level in *jar1-11*. One possibility for this differential trend between transcript and protein levels could be a regulation similar to that of the transcriptional repressors JAZs. The latter's expression is enhanced at the transcriptomic level but due to its JA-Ile-mediated degradation, protein levels are reduced. Moreover, CML12 protein levels indicated a potential diurnal rhythm, which would further complicate the picture. More detailed analysis covering longer time frames and more time points are required to address the effect of JAR1-mediated JA-Ile formation on *CML12* expression and protein homeostasis.

4.8.1 *CML12* expression as well as CML12 protein level is reduced under drought stress in an ABA-dependent manner

Calmodulin-like proteins are a family of plant specific calcium sensor proteins (Zeng et al., 2015; Kim et al., 2009) and previous studies had confirmed the capacity of CML12 to bind Ca^{2+} (Sistrunk et al., 1994; Antosiewicz et al., 1995). Drought stress induces a temporary increase of cytosolic Ca^{2+} (Reddy et al., 2010) and ABA induces stomatal closure by increasing the amount of guard cell cytosolic Ca^{2+} (Daszkowska-Golec and Szarejko, 2013). In this current study, drought stress resulted in a decrease in transcript level of *CML12* as well as CML12 protein level. A previous study done on dehydrated leaves showed a reduced transcript level of *CML12* (Reymond et al, 2000), which is in line with the decrease of *CML12* expression under drought stress. ABA-treatment reduced CML12 protein levels, suggesting endogenous ABA can be a negative regulator of CML12, which is further evidenced by higher CML12 levels in the *aba2-1* line compared to WT under drought stress. During water deficiency, the plant response is likely to be linked to Ca^{2+}signaling. but no previous study was focused on the involvement of CML12 in this process but only in hypoxia stress (Lee and Bailey-Serres, 2019). Strong reduction of CML12 level in the WT under drought as well as ABA-treatment and survival of *cml12-1* under severe drought further suggested that CML12 can be involved in the regulation of drought stress resistance and that is function might be controlled by endogenous ABA accumulation.

4.9 AtMYB2 is a potential regulator of jasmonate-signaling

JA-Ile accumulation leads to the formation of the JA-Ile-COI1-JAZ receptor complex and releases repression by transcriptional repressors to initiate transcription of jasmonate-mediated responsive genes. Among the different transcription factors described previously as involved in jasmonate signaling, bHLH group members, especially MYC-group TFs, are the best-characterized (Wasternack and Song, 2017; Koo, 2018). However, other TFs can work independently of MYC2 or interact with MYC2 in a jasmonate-dependent manner (Chen et al., 2016). One of the important drought stress-responsive TFs, MYB2 was shown previously to interact with MYC2 in an ABA-dependent manner (Abe et al., 2003). Also, drought-responsive *RD29A*, which is downregulated in JAR1-OE, carries a MYB-recognition sequence at the promoter region. However, very low number of DEGs were found between WT and *myb2* plants (compared to *jar1-11* or JAR1-OE) under both control as well as drought conditions that strongly indicates that MYB2 does not play such a dominant regulatory role under either condition.

In control conditions, the jasmonate precursor *cis*-OPDA was remarkably decreased in *myb2*. By contrast, JA and JA-Ile content were slightly increased while the JA-Ile-mediated response genes *VSP1*, *VSP2* and *PDF1.2A* were slightly decreased. This suggests that the increase in JA-Ile alone is not sufficient to initiate jasmonate-responses in *myb2*. The process behind the increase in JA and JA-Ile could be the back-conversion of some catabolic products like 12-OH-JA, which itself decreased in control conditions. The two myroinases TGG1 and TGG2, which are targets of both ABA and jasmonate-mediated stomatal closure, seem to be negatively controlled by MYB2 in normal conditions since their expression is remarkably increased in *myb2* compared to WT. These myrosinases also have a role in the defense against insects and pathogens (Barth and Jander, 2006). Thus, MYB2 might be a potential mediator of the jasmonate and myrosinase-regulated defense response.

Under drought conditions, the level of all jasmonates remained unchanged in *myb2*, which was also seen through the almost unchanged expression of *VSP1* and *VSP2*. A previous finding showed that overexpression of MYB2 resulted in higher expression of *VSP2* under drought stress (Abe et al., 2003), which is in line with the unchanged amount of *VSP1* and *VSP2* in *myb2* under drought stress. Considering that i) jasmoante-biosynthesis is under feedback regulation of JAR1-mediated JA-Ile accumulation, ii) the release of the transcription factor MYC2 plays a major role in jasmonate-signaling-mediated feedback regulation and iii) MYB2 was previously found to interact with MYC2 under drought stress, it could be speculated that

when MYB2 is absent, the regulation of MYC2 in the jasmonate-mediated response is also diminished. Further studies on this regulation pathway may provide a clearer explanation.

4.10 Conclusion and future perspectives

In conclusion, this work has established a concrete approach to elucidate the specific role of endogenous JA-Ile in balancing shoot growth and drought stress response. It has specially described the regulatory capacity of jasmonate signaling under drought stress which is a novel finding in our understanding of the relation between jasmonate signaling and abiotic stress. Future studies in this field will help elucidate how plants, upon stimuli, balance growth and defenses in response to a manifold of other environmental conditions such as heat-stress, salinity, hypoxia, etc. As a feedback mechanism, it has been shown that a higher JA-Ile accumulation enhances a positive feedback of jasmonate biosynthesis under drought stress. However, it is known that *cis*-OPDA can also work independently (Savchenko et al., 2014). Thus, characterizing other metabolites of the jasmonate pathway in the same manner would provide a holistic understanding of the role of the jasmonate pathway in drought stress regulation. Previously, the jasmonate signaling receptor mutant *coi1-1* was used to describe the activity of JA-Ile but COI1 can be a target for other signaling responses, which is clear from the non-similar phenotypes to other biosynthetic mutants of the jasmonate pathway (Figure 12). Moreover, there is another limitation to the utilization of the *coi1-1* mutant since plants do not produce seed and have to be maintained as a heterozygous parental line. Using another mutant line in the *COI1* locus, such as *coi1-30*, which shows a similar phenotype to *jar1-11* (Yang et al., 2012), may be a better choice to analyses the growth and drought stress-mediated regulation of jasmonate signaling. Moreover, further characterization of other jasmonate signaling mutants e.g. *jazD*, *jazQ*, *myc2* etc. in soil growing conditions can also provide insight into the signaling response. In the context of drought stress, some potential targets of jasmonate signaling such as RD29A, LEA14, GCR2, etc. were found. It would be sensible to characterize them in more detail in their relationship to jasmonate. One approach is the characterization of the promoter activity of e.g. RD29A in the *jar1-11* and JAR1-OE backgrounds. Additional post-translational approaches are needed to support the transcriptomic data. A good example is CML12, which was identified here as being connected to jasmonate signaling pathway and which showed a differential regulation at the transcriptional and translational levels. Further studies in this area should be performed to better understand the relationship between Ca^{2+} sensing proteins such as CMLs and JA-Ile signaling.

Under the context of global warming, it is now imperative to develop more drought-resistant crop varieties. This study has described in detail the importance of JA-Ile in drought stress recovery in Arabidopsis. Applying similar approaches, validation of the increase in endogenous JA-Ile in field crops could lead to the development of more drought-resistant crops, especially useful in areas which face longer periods of progressive drought or shorter periods of repetitive drought.

Summary

In the present work, the regulatory capacity of biologically active jasmonate, jasmonyl-isoleucine (JA-Ile), under normal and progressive drought stress conditions throughout a plant's life-cycle was investigated. To alter endogenous JA-Ile levels, two different plant lines were used: i) the T-DNA insertion line *jar1-11,* which contains significantly reduced amount of JA-Ile and ii) complementary to this, a T-DNA insertion line (JAR1-OE) expressing *JAR1.1-YFP* under the control of the 35S promoter, which results in *JAR1* overexpression and enhanced endogenous JA-Ile levels. This line was newly developed within this work. Both lines displayed difference in growth and stress resistance compared to the wild type and each other. Under normal growth conditions *jar1-11* plants displayed a larger rosette with narrower leaf blades, while JAR1-OE plants had stunted growth with lateral leaves. And while JAR1-OE was late in flowering, a reciprocal trend was observed in *jar1-11*. Furthermore, *jar1-11* plants were more susceptible to drought stress, while JAR1-OE plants were highly resistant. In line with the difference in JAR1, hormone analysis revealed increased accumulation of JA-Ile in JAR1-OE under drought, while *jar1-11* accumulated JA that could not be converted to JA-Ile. In addition, the homeostasis of some precursors and highly abundant catabolic products of JA and JA-Ile were differentially affected in these lines. Global gene expression analysis by RNA-seq revealed a reprogramming of the jasmonate signaling pathway with a positive feedback upregulation in JAR1-OE under drought stress. By contrast, in *jar1-11* the biosynthesis of jasmonates was inhibited. Positive feedback in JAR1-OE helps plants to acquire pre-stress tolerance with positive stomatal regulation, anti-oxidant activity and modulation of ABA biosynthesis. This ultimately helps the plants in coping with subsequent drought stress through regulation of the photosynthetic machinery and other biological processes. Furthermore, calmodulin-like protein 12 (CML12) was identified as a potential target of jasmonate signaling. Intriguingly, CML12 behaves differentially at the transcriptional and translational levels to the presence or absence of JAR1 or endogenously added JA-Ile supporting a potential cross-talk between jasmonate and Ca^{2+}-signaling. Finally, the transcription factor AtMYB2 was found to be a regulator of jasmonate signaling as it could control the accumulation of JA and JA-Ile under normal growth as well as drought stress conditions.

Zusammenfassung

In der vorliegenden Arbeit wurde die Rolle des biologisch aktiven Jasmonats, Jasmonyl-Isoleucin (JA-Ile), in der Regulation von Wachstumsprozessen und Trockenstresstoleranz von *Arabidosis thaliana* untersucht. Um den endogenen JA-Ile-Spiegel zu verändern, wurde eine T-DNA-Insertionslinie im *JAR1*-Locus, *jar1-11*, verwendet, welche einen reduziertem JA-Ile Gehalt aufweist. Komplementär zu dieser T-DNA-Insertionslinie wurde eine Linie entwickelt, die die *JAR1.1*-Spleißvariante unter der Kontrolle des 35S-Promotors (JAR1-OE) exprimiert. Diese Linie besaß eine erhöhte *JAR1* Expression und JA-Ile Gehalt bereits unter nicht-Stress Bedingungen im Vergleich zum Wildtyp (Col-0). Unter normalen Wachstumsbedingungen unterschieden sich *jar1-11*-Pflanzen vom Wildtyp durch eine größere Blattrosette mit schmaleren Blattspreiten, während JAR1-OE-Pflanzen ein reduziertes Wachstum mit späterhin verbreiteten Blattspreiten aufwiesen. Zudem blühten JAR1-OE Pflanzen später als der Wildtyp und der primäre Blütenstiel war im Vergleich zu den sekundären Blütenstielen verkürzt, während in *jar1-11* ein reziproker Trend zu beobachten war. Eine detailierte Phänotypisierung ergab, dass *jar1-11*-Pflanzen anfälliger für und JAR1-OE-Pflanzen deutlich resistenter gegen Trockenstress waren. Eine Hormonanalyse zeigte, dass die Erhöhung des JAR1 Gehaltes in JAR1-OE zu einer verstärkten Akkumulation von JA-Ile unter Trockenstress führte, während JA in *jar1-11* nicht zu JA-Ile umgewandelt werden konnte und akkumulierte. Auch die Homöostase von Vorstufen und katabolen Produkten von JA und JA-Ile war betroffen. Globale Expressionstudien durch RNA-seq zeigten eine Reprogrammierung des Jasmonat-Signalwegs mit einer positiven Rückkopplung in JAR1-OE unter Trockenstress, welche den JAR-OE Pflanzen ermöglicht, eine Vorstresstoleranz mit positiver stomataler Regulation, antioxidativer Aktivität und Modulation der ABA-Biosynthese zu entwickeln. Dies hilft letztendlich bei der Bewältigung von Trockenstress durch die positive Regulierung der Photosynthesemaschinerie und anderer biologischer Prozesse. Darüber hinaus konnte das Calmodulin-ähnliche Proteins 12 (CML12) als potentielles Ziel einer Regulation durch Jasmonate identifiziert werden. Interessanterweise verhält sich CML12 in Gegenwart oder Abwesenheit von JAR1 auf transkriptomischer und translationaler Ebene unterschiedlich. Weitere Studien zu CML12 zeigten seine verringerte Expression unter Dürre und ergaben Hinweise auf eine ABA-vermittelte Regulation. Zudem wurde festgestellt, dass der Transkriptionsfactor ATMYB2 ein Regulator des Jasmonat-Signalweges ist, da er die Akkumulation von JA und JA-Ile sowohl unter Kontroll- als auch unter Trockenstressbedingungen regulieren kann.

Supplementary information

Figures

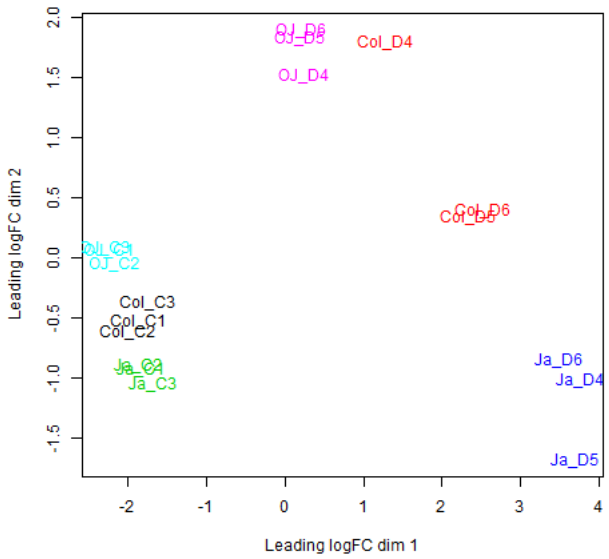

Supplemental Figure 1: Multidimensional scaling (MDS) plot of the indicated samples in the RNA-seq. The MDS represents clustering of the similar samples those are close to each other in the genes expression, while different samples are distant. MDS is adjusted at FDR < 0.01 and LogFC ≥1). Col- Col-0 WT, Ja- *jar1-11*, OJ- JAR1-OE, 1,2 and are the replicates. "C" control and "D" drought stress samples.

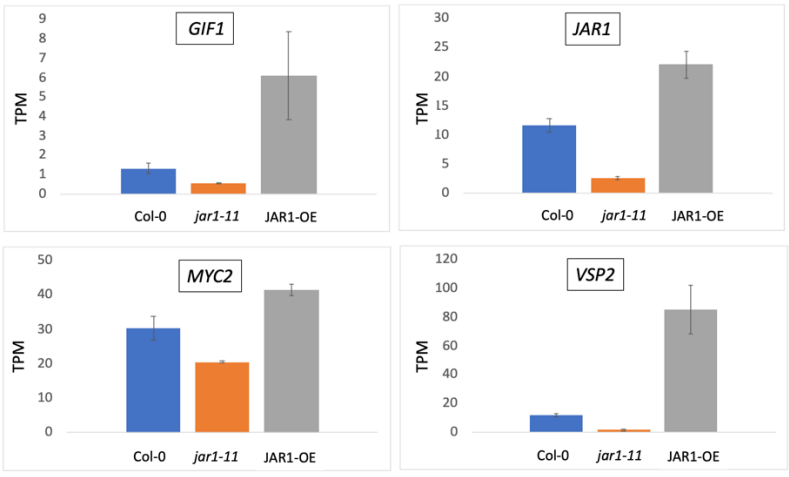

Supplemental Figure 2: JAR1-dependent changes in genes expression. Expression is presented as TPM from the RNA-seq of the well-watered WT and *myb2* plants. Bar plot prepared with TPM. Data represent means ± SE from 3 replicates (n=3).

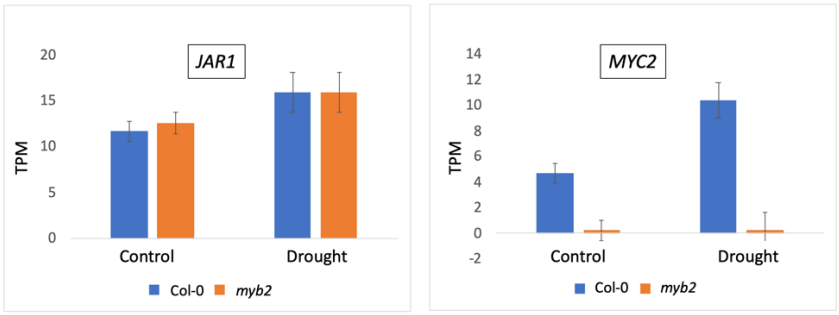

Supplemental Figure 3: MYB2-dependent changes in genes expression. Expression is presented as TPM from the RNA-seq of the well-watered WT and *myb2* plants. Bar plot prepared with TPM. Data represent means ± SE from 3 replicates (n=3).

Tables

Supplemental Table 1: List of DEGs up-and downregulated in *jar1-11* and JAR1-OE compared to WT plants in the control conditions. (DESeq, adjusted FDR < 0.01 and LogFC ≥ 1)**;** logFC with "+" or "-" sign indicates up- or downregulation respectively. "C" under control conditions

Col-0_C vs *jar1-11*_C		**Col-0_C vs JAR1-OE_C**		**Col-0_C vs JAR1-OE_C**		**Col-0_C vs JAR1-OE_C**	
AGI code	**logFC**	**AGI code**	**logFC**	**AGI code**	**logFC**	**AGI code**	**logFC**
AT5G24780	-5.7904643	AT1G04350	-1.3295151	AT4G31840	2.70096194	AT1G74780	1.53552097
AT2G46370	-2.1427345	AT1G32700	-1.05856	AT4G32460	1.30456539	AT2G17880	1.90817918
AT5G42180	-5.135911	AT2G42530	-1.5081723	AT5G59690	1.21409126	AT4G22490	5.85730209
AT1G22480	-7.123115	AT3G14020	-1.3000878	AT1G14430	2.73687821	AT5G47920	5.804205
Col-0_C vs JAR1-OE_C		AT5G55660	-1.0292944	AT2G28790	2.753305	AT1G64510	1.40119912
AGI code	**logFC**	AT4G23050	-1.2078141	AT5G08000	2.27156832	AT1G62520	1.57111362
AT5G59540	-1.5371764	AT1G12480	-2.045449	AT2G06925	1.39092527	AT2G26180	2.39888035
AT3G20100	-1.7971029	AT1G28660	-1.3973692	AT5G47500	3.54360593	AT1G15580	2.7177142
AT5G16570	-2.3143142	AT2G20560	-2.0667454	AT5G07030	2.15021616	AT3G23110	2.97791888
AT1G72416	-1.7293925	AT4G13550	-1.1451615	AT5G10390	1.67262098	AT5G07660	2.02802009
AT5G52310	-2.5043886	AT3G58660	-1.0718873	AT5G10400	1.76422117	AT4G02530	1.04275519
AT1G13930	-1.6473044	AT3G07730	-1.2011418	AT3G02120	2.69203649	AT5G07440	1.8962776
AT2G17840	-1.2968873	AT2G11810	-2.2526622	AT3G25860	1.1347011	AT1G43790	1.05432395
AT1G51090	-2.2980322	AT1G08610	-1.2820256	AT5G06290	1.3244988	AT5G24780	2.9386208
AT1G78930	-1.613872	AT4G38340	-3.6441943	AT5G59570	1.33625124	AT3G22070	1.74745591
AT1G53590	-1.2135431	AT3G46130	-1.4946247	AT5G35360	1.25745864	AT3G06130	1.3074308
AT1G78070	-1.8306452	AT1G56170	-1.2398123	AT1G64660	1.49905535	AT3G16400	1.32842261
AT1G72440	-1.5201425	AT1G65800	-1.0049083	AT3G46320	1.53390013	AT4G22513	6.54483687
AT2G37460	-2.0372345	AT5G48570	-1.2483245	AT3G21390	1.52313102	AT3G07320	1.72459802
AT5G58070	-1.2829096	AT1G62570	-1.4975019	AT2G30620	1.22924014	AT3G53380	1.83018322
AT2G42600	-1.193992	AT4G17550	-1.338233	AT1G02730	2.69311114	AT4G28310	1.99910397
AT2G45660	-1.062876	AT5G15970	-1.370677	AT1G14890	1.5244844	AT1G54840	5.90937644
AT5G14580	-1.6715125	AT4G19520	-1.2160443	AT1G33170	2.07375475	AT2G34560	1.00108032
AT5G42180	-4.9459136	AT4G26600	-1.0409844	AT5G09980	3.34164105	AT2G30200	1.14437416
AT2G38640	-1.7488306	AT2G15480	-1.347657	AT5G24420	2.64668899	AT5G18670	1.150677
AT4G04020	-1.5018447	AT1G27200	-1.0371441	AT4G25260	1.767059	AT5G50930	2.93888357
AT4G13010	-1.1196392	AT1G45332	-1.2211656	AT1G66100	2.01964016	AT1G72260	3.09223913
AT1G76955	-1.3336769	AT2G39920	-1.1346234	AT4G16140	2.64043078	ATCG00810	1.31770891
AT2G17710	-1.9245913	AT4G18210	-1.2303504	AT4G21280	1.33544087	AT1G50790	2.16839601
AT5G64170	-1.7708462	AT4G10120	-1.3024479	AT3G56940	1.04167704	ATCG00650	1.32825069
AT2G33770	-1.4560909	AT5G26860	-1.0366101	AT3G20670	1.46359894	AT3G23890	2.26471803
AT4G12290	-1.2954162	AT4G02280	-1.4474829	AT5G23530	1.9590487	AT4G12520	6.346444
AT1G06720	-1.2891636	AT3G57660	-1.0958031	AT3G54650	1.2296254	AT5G38410	1.50098136
AT3G05660	-1.866296	AT1G70420	-1.120166	AT3G51280	3.79502516	AT3G13175	2.53568802
AT1G20450	-1.4040217	AT5G56150	-1.0128584	AT4G22505	9.18296568	AT4G03100	1.74215893
AT3G49240	-1.3482052	AT3G59410	-1.1661763	AT3G53190	1.70124757	AT5G27450	1.57763799
AT2G34660	-1.4472089	AT5G51220	-1.1938366	AT3G21770	1.87529573	AT5G65360	1.10449971
AT4G01037	-1.2421817	AT4G32940	-1.3519534	AT1G04730	2.58586361	AT5G01870	7.13724141
AT4G29210	-1.2586228	AT1G76820	-1.1428315	AT3G15520	1.47103007	ATCG00790	1.04947414
AT2G15970	-1.06193	AT1G71140	-1.4321858	AT1G06760	1.03292473	AT4G31290	1.06721446
AT5G09590	-1.4008532	AT5G59050	-1.2824109	AT2G38530	2.25373091	AT1G18250	2.26224472
AT5G15450	-1.0482701	AT5G45380	-1.5468734	AT1G17650	1.76666081	AT3G25920	1.23035477
AT5G22300	-2.4567037	AT1G20440	-1.1335038	AT5G47190	1.23976182	AT5G45680	1.41854361
AT5G11680	-1.1389204	AT1G68990	-1.0450699	AT1G66760	2.83167781	AT3G50820	1.45532155
AT4G33950	-1.191346	AT3G50970	-1.5139224	AT3G09260	3.36892928	AT2G45970	1.13322779
AT5G55860	-1.0024138	AT5G56030	-1.1028257	AT1G66280	3.12085676	AT1G62770	1.83376145
AT1G73810	-1.9757537	AT1G17744	-2.5460383	AT5G15780	1.789664	AT2G42570	1.38934405
AT3G07770	-1.0261786	AT2G02955	-1.4464431	AT1G18140	4.47632697	AT1G52245	3.05935075
AT5G45820	-1.8190359	AT4G18830	-1.275881	AT1G21810	3.49805827	AT1G09750	1.15944443
AT5G15700	-1.336353	AT1G32270	-1.9809065	AT1G09200	1.71092995	AT5G11550	1.82451689
AT3G59670	-1.1810179	AT5G24655	-1.5132353	AT1G03090	1.27493198	AT2G37470	1.09259118
AT3G01060	-1.3789721	AT1G52080	-1.6807475	AT5G16190	1.93399233	AT1G53520	1.84934416
AT5G45650	-1.3241134	AT1G10270	-1.1090305	AT5G66750	2.30519085	AT3G11630	1.64601395
AT1G80130	-2.377952	AT5G26000	1.96079806	AT1G44350	1.32706883	AT5G25090	2.46697996
AT5G52640	-2.2048391	AT5G06150	3.01574495	AT1G76310	1.8226841	AT1G29930	1.14289035
AT1G64600	-1.6601299	AT1G47210	2.55698388	ATCG01130	1.37082455	AT5G38940	6.38976666
AT4G27300	-1.6528879	AT5G23820	2.47119913	AT1G67630	2.43186441	AT1G50490	1.729289
AT3G55760	-1.3085368	AT3G47340	2.89256378	AT5G45490	1.11944427	AT5G06870	1.56123419
AT1G66390	-3.4956913	AT5G59870	2.1022696	AT2G29980	1.4124118	AT2G14900	2.11608757
AT3G22840	-2.2620192	AT2G34430	2.939845	AT2G25060	2.428408	AT3G56130	1.38107368
AT1G34260	-1.3067122	AT1G70830	1.83836197	AT3G05730	2.00067058	AT2G27130	1.32323152
AT1G01470	-1.0123699	AT3G53730	1.10805452	AT3G01500	1.99529533	AT1G21740	1.90996904
AT5G55920	-1.1787465	AT5G25980	1.5595634	AT2G18969	2.64126746	AT3G54560	1.87192793
AT1G69760	-1.1871286	AT1G54010	2.29605032	AT1G30380	1.09607407	AT1G04020	1.71440966

AT1G74250	-1.1439384	AT1G14250	3.93015543	AT5G22880	1.33926655	AT3G06160	5.71074053
AT3G44450	-1.2308473	AT5G59970	1.74645274	AT1G14290	1.34447061	AT2G42840	3.22017415
AT3G15890	-1.193256	AT4G18670	1.89727014	AT4G26660	2.44955606	AT3G27920	4.50359362
AT1G70580	-1.0453401	AT3G18280	1.61853984	AT1G70370	1.19250467	AT5G21920	1.3262925
AT5G04230	-1.1327165	AT2G28740	1.38158854	AT5G24580	1.75768401	AT2G44450	3.42970545
AT5G66540	-1.2805401	AT1G08560	3.17947979	AT3G58650	2.26725218	AT1G11820	1.13065825
AT5G10770	-1.2887833	AT3G05727	9.77122327	AT5G45040	1.50820162	AT2G29710	4.16065098
AT1G55760	-1.6344768	AT5G10160	1.57158502	AT1G03600	1.31498533	AT5G61000	2.05944017
AT1G56110	-1.302683	AT3G27360	1.54839542	AT1G78630	1.29151433	AT3G25900	1.71629297
AT1G11210	-1.5140602	AT4G22517	9.94478033	AT1G44110	1.98122131	AT5G12920	3.91060541
AT1G14200	-1.0516046	AT2G39310	4.14862837	AT1G31690	2.48596314	AT1G66620	2.19877407
AT4G26780	-1.3299916	AT5G36910	3.27427708	AT3G12145	2.65744786	AT3G53232	1.84517814
AT5G17460	-1.6485639	AT1G51060	1.28973	AT2G32380	1.16460162	AT2G37560	3.97943382
AT1G02460	-1.9433784	AT2G25270	2.33547559	AT2G45050	2.92981738	AT5G28290	1.42291802
AT4G03400	-1.2830874	AT2G37640	1.84851401	AT2G04780	1.41330336	AT1G02720	1.35328837
AT3G57540	-1.2382313	AT3G27060	1.68521632	AT3G62030	1.49124163	AT1G63310	1.26386374
AT2G45820	-1.1250553	AT5G19110	4.27805406	AT5G16390	1.13009532	AT1G26770	1.3761133
AT2G46450	-1.1738864	AT1G07790	1.07244183	AT3G46940	1.43831964	AT5G01930	1.91168407
AT3G28940	-1.0781964	AT4G37410	4.15153773	AT5G39320	1.70256378	AT1G29980	1.35868664
AT5G39020	-1.1822184	AT2G05440	3.7267913	AT1G80280	1.05546374	AT5G55570	5.7494321
AT5G25110	-2.328586	AT3G15950	3.77742909	AT3G01710	3.14726581		
AT1G65490	-1.238964	AT3G07350	2.33889926	AT4G11190	4.57323898		
AT3G19000	-1.1127096	AT4G20870	1.23138085	AT1G50010	1.22187228		

Supplemental Table 2: List of DEGs up-and downregulated in WT (Col-0) plants under drought stress compared to well-watered conditions. (DESeq, adjusted FDR < 0.01 and LogFC ≥ 1)**;** logFC with "+" or "-" sign indicates up- or downregulation respectively. "C" under control conditions; "D" under drought stress

Col-0_C vs Col-0_D		**Col-0_C vs Col-0_D**		**Col-0_C vs Col-0_D**		**Col-0_C vs Col-0_D**	
AGI code	**logFC**	**AGI code**	**logFC**	**AGI code**	**logFC**	**AGI code**	**logFC**
AT2G18300	-7.6830159	AT1G67810	-2.9374827	AT4G24670	-1.9438795	AT1G58520	2.86161659
AT5G44020	-8.1700576	AT1G52342	-1.866325	AT3G61380	-1.4922201	AT3G51610	1.12994231
AT5G65730	-7.5652187	AT3G27090	-1.170296	AT3G16620	-1.1457853	AT4G29400	1.34340486
AT1G72416	-6.0958241	AT4G29140	-2.5129253	AT4G12310	-1.3805658	AT4G17840	1.63716317
AT5G63180	-4.732946	AT4G25890	-1.6550149	AT1G78110	-1.0516241	AT1G53100	2.06338848
AT1G66940	-6.2757076	AT4G37080	-1.4208274	AT4G10770	-1.1775289	AT5G16360	2.27282201
AT4G16980	-5.1493833	AT2G37640	-2.5059715	AT5G52100	-1.3989845	AT1G51130	2.31607668
AT5G65390	-6.5649299	AT1G50010	-1.643296	AT1G31860	-1.0966258	AT3G17790	2.4883381
AT2G38310	-6.0442253	AT3G49680	-1.018943	AT4G08870	-1.3791199	AT4G36700	7.52272683
AT2G30930	-3.6188486	AT5G14730	-3.9602184	AT2G35650	-1.6011186	AT1G03070	6.58124631
AT4G12730	-5.7411872	AT2G27050	-1.0344099	AT5G27330	-1.8119283	AT5G03204	6.66378475
AT2G23600	-3.5080686	AT3G49580	-3.392592	AT2G28080	-1.1694299	AT5G16980	2.40058378
AT1G68840	-4.9737233	AT2G38650	-1.1447564	AT3G49290	-1.2890602	AT1G32560	3.49121022
AT4G24350	-5.3788726	AT1G22882	-1.2319627	AT1G62480	-2.5471342	AT3G49210	1.62539039
AT1G10020	-4.1295475	AT5G18030	-1.9082974	AT3G05800	-1.6403526	AT1G60710	1.19122653
AT1G06160	-6.1184698	AT1G52200	-3.7715009	AT4G11000	-2.3963413	AT4G16190	1.55369507
AT4G08950	-5.39153	AT1G62630	-1.7515365	AT1G51400	-1.0495996	AT5G54160	1.13411199
AT3G49670	-3.7045726	AT5G67480	-1.8841142	AT1G32190	-1.7189766	AT2G28840	1.17905225
AT5G23210	-4.2780169	AT5G12170	-1.5836278	AT1G73020	-1.4708639	AT5G14530	1.26102871
AT2G42870	-5.6853529	AT3G24050	-1.0442687	AT4G11850	-1.2908585	AT5G10410	1.83985814
AT1G29660	-4.419998	AT5G01015	-4.4738984	AT4G37750	-2.1142019	AT5G16840	1.09402986
AT1G72610	-6.9505237	AT3G48040	-1.936013	AT5G44585	-4.5699027	AT1G75400	1.44274373
AT1G72430	-3.6709089	AT1G79720	-2.0489803	AT3G28960	-1.9501235	AT5G50170	1.7857708
AT4G24780	-3.7084291	AT4G31800	-2.2163912	AT4G18480	-1.0964479	AT5G67245	1.3165273
AT5G62280	-5.3765326	AT1G57990	-2.755578	AT2G45470	-1.32515	AT2G19810	1.72316564
AT5G19190	-4.6108933	AT1G21520	-1.6241414	AT1G48260	-3.0084114	AT1G07870	1.46073828
AT3G19680	-2.9812647	AT5G43870	-1.930677	AT4G38825	-2.6616743	AT3G18420	1.1050575
AT2G32100	-4.5435115	AT5G14740	-2.5777147	AT3G62860	-1.4557546	AT2G17680	6.65453468
AT5G25190	-6.8035152	AT4G13050	-1.3140022	AT4G38420	-1.6906908	AT5G27660	1.23774779
AT5G45650	-4.1240916	AT3G16250	-1.5607859	AT5G14360	-3.0183048	AT1G48840	1.32575277
AT5G67420	-2.9839123	AT1G28400	-1.6481229	AT4G20940	-1.9620435	AT1G33260	2.1997986
AT2G34510	-4.6432886	AT5G02120	-1.3718329	AT5G43500	-1.1219975	AT3G03480	4.08063143
AT4G16990	-2.7768194	AT3G52520	-3.5323713	AT4G02075	-1.2818632	AT3G13910	1.27409087
AT2G36050	-4.9236321	AT1G11860	-1.6798992	AT1G11303	-1.787783	AT5G24670	1.12264702
AT3G14840	-3.5143982	AT3G49930	-2.3983741	AT5G61270	-1.3373487	AT1G03220	2.71968345
AT3G07470	-3.0085601	AT2G21060	-1.1935094	AT4G35380	-2.3952762	AT1G56600	3.38523164
AT3G07010	-3.6689692	AT5G66770	-1.862034	AT1G14380	-1.0491305	AT4G36630	1.26444972
AT2G23130	-5.3951228	AT1G04250	-1.8105031	AT4G24970	-1.4051675	AT2G40350	1.97385805
AT1G18620	-3.556994	AT3G54880	-3.107768	AT1G65481	-4.5346828	AT2G47870	2.22964173
AT2G16660	-4.6846837	AT2G37080	-1.4031896	AT1G30520	-1.7646394	AT4G27840	1.25515225
AT4G04840	-6.5173705	AT3G15060	-1.7333028	AT3G28420	-1.9079365	AT1G64810	1.15381441
AT5G56840	-7.9568517	AT5G66210	-1.2461652	AT4G13345	-1.0391049	AT1G25530	2.3940251
AT1G22690	-9.1635082	AT1G64980	-1.112878	AT5G35740	-3.8457757	AT1G72100	6.77466416
AT1G57680	-2.3611041	AT5G48460	-2.147265	AT4G23440	-1.1289646	AT4G22590	2.05049845

AT1G35350	-3.327331	AT1G76680	-1.4183119	AT3G55060	-1.6905022	AT5G24150	2.7471296
AT5G49630	-3.9324361	AT2G29980	-1.8591255	AT4G02810	-5.8374221	AT1G78610	1.40598764
AT2G30010	-6.164371	AT3G13510	-1.8334418	AT5G26850	-1.4229745	AT1G65660	1.18799314
AT4G34220	-3.1920455	AT5G60800	-3.3785001	AT4G03190	-1.1259642	AT2G29380	8.26085022
AT3G28040	-3.4471581	AT2G42070	-1.116657	AT3G19030	-1.2431338	AT1G20490	4.2651127
AT2G37130	-5.7640347	AT2G16280	-1.1498415	AT5G15970	-1.2450224	AT5G28080	3.24810925
AT1G49750	-3.3462904	AT3G50060	-2.436405	AT1G12940	-2.8703528	AT3G25400	1.65255891
AT1G22330	-5.8065767	AT4G25110	-3.4155366	AT1G35260	-2.0123171	AT3G26290	1.79827907
AT1G09750	-4.054716	AT5G20950	-1.1394087	AT1G76240	-3.2947758	AT2G42540	2.09378846
AT3G06770	-5.4175776	AT4G31850	-1.2572519	AT5G48450	-2.1085403	AT5G56160	2.28573549
AT1G66100	-6.5762564	AT5G37770	-1.8232279	AT5G17400	-1.340108	AT4G02380	2.33002279
AT1G03870	-6.564332	AT1G05210	-2.7449319	AT2G32400	-1.1925943	AT4G07408	2.21809161
AT1G13260	-4.485232	AT1G68400	-2.0759325	AT5G49360	-1.534099	AT5G08380	1.23336467
AT2G37170	-3.9453571	AT1G58602	-1.1700863	AT2G02450	-1.125214	AT5G04010	4.10143139
AT1G33240	-2.8641675	AT1G23870	-2.4472662	AT5G54300	-1.6067442	AT5G50100	1.46886264
AT5G40450	-5.2193177	AT1G22280	-1.2943203	AT3G11720	-1.2330738	AT5G49700	2.79060444
AT4G25050	-3.6413996	AT5G23510	-1.2557303	AT3G60580	-2.2686625	AT3G21670	2.4220505
AT1G31580	-4.1339034	AT4G38700	-3.7300107	AT3G54830	-5.1901912	AT5G17210	2.3207377
AT5G02760	-9.608042	AT1G65390	-6.3268033	AT4G39640	-1.5813824	AT4G03200	1.47726393
AT2G17230	-3.6137415	AT1G30280	-2.5909103	AT1G10130	-1.1031889	AT2G25625	2.75760513
AT1G12110	-4.3783848	AT1G53800	-1.1779193	AT2G43745	-1.4496617	AT2G04350	1.29477111
AT4G00400	-4.2106118	AT5G22930	-4.8443724	AT1G47480	-2.6947303	AT5G66460	1.684024
AT1G04800	-4.2567343	AT5G64120	-5.003574	AT4G00880	-1.0349993	AT1G55280	1.53911557
AT4G13340	-5.7258199	AT4G18250	-3.4600814	AT1G27960	-1.3137945	AT2G28500	2.19588464
AT3G22210	-3.0795026	AT3G01290	-2.6615427	AT4G15630	-1.0830352	AT1G15960	1.86093206
AT5G67385	-3.8330678	AT3G47570	-1.3176402	AT3G47340	-1.6667099	AT1G03940	3.54213566
AT2G45180	-5.1761339	AT2G44240	-6.1362964	AT3G49570	-2.2853152	AT3G61960	1.14285444
AT4G15800	-2.5398566	AT5G23280	-1.6503525	AT1G73330	-2.8973482	AT3G15790	1.26925693
AT5G14120	-3.9978411	AT4G00970	-3.1388661	AT4G23800	-1.8085236	AT4G21910	2.15059755
AT2G15090	-3.4554943	AT1G15820	-1.6077916	AT2G27810	-1.1692181	AT4G19960	1.29376327
AT1G01620	-3.8204957	AT3G26320	-5.1337861	AT3G02020	-1.7640461	AT2G34450	2.10781073
AT2G30520	-2.8016439	AT5G52120	-2.6956021	AT4G21903	-2.882164	AT1G15230	1.09041637
AT5G44680	-3.7739225	AT1G49230	-1.7113322	AT5G37600	-1.2386232	AT4G34540	1.37130855
AT1G23480	-4.7104532	AT5G43170	-4.4126947	AT3G13780	-1.0985917	AT3G62740	3.2241118
AT3G45860	-4.102424	AT3G18780	-1.0507616	AT2G19620	-1.1625024	AT4G15780	1.24256386
AT1G66150	-2.3456979	AT1G70470	-2.5897372	AT2G05100	-1.0179704	AT1G75370	1.01206568
AT5G08330	-2.8449451	AT4G38620	-1.8750073	AT4G30410	-1.7033827	AT5G59720	2.77030743
AT5G04230	-3.0370297	AT2G25900	-1.4754605	AT2G03550	-1.0797494	AT2G43590	2.19535985
AT4G38860	-3.7789969	AT1G09390	-2.3225183	AT1G11850	-1.7080228	AT4G12400	2.3494791
AT4G30270	-3.6530717	AT1G59930	-3.7692729	AT3G05625	-1.2872874	AT4G23050	1.43325365
AT4G19530	-2.8165627	AT1G72930	-2.5360539	AT1G36675	-2.8294365	AT1G47710	1.14194756
AT3G06080	-2.6393965	AT5G59920	-1.9722515	AT3G09940	-3.2317878	AT3G48390	1.14802517
AT3G10520	-2.3271126	AT5G45480	-1.8475018	AT5G44572	-1.6129691	AT2G38270	1.12432781
AT2G46630	-3.2668268	AT5G16000	-1.6806332	AT1G48770	-1.2229861	AT1G10865	1.03482426
AT3G43800	-2.4552856	AT4G31500	-1.6601722	AT5G48380	-1.1556822	AT5G04530	2.81424312
AT3G06145	-4.0617058	AT1G14920	-1.1860246	AT1G55120	-1.0941227	AT5G04750	1.25506014
AT3G26520	-4.3883335	AT3G01750	-1.5959182	AT4G24275	-1.4867605	AT1G52855	1.53113052
AT4G03110	-2.7645047	AT2G24550	-1.4684689	AT1G70890	-1.5916021	AT2G01890	3.37750622
AT5G54380	-4.5593088	AT2G18890	-1.8712399	AT3G63200	-1.5125404	AT1G59640	2.25597805
AT3G23550	-9.5582948	AT5G06870	-2.3121285	AT2G44790	-3.1236979	AT3G58150	2.38208617
AT5G32450	-2.707823	AT3G16770	-1.7446416	AT1G02460	-1.5904796	AT1G58270	2.82725617
AT5G02890	-4.4508721	AT3G58620	-1.8672545	AT2G46710	-1.1300104	AT4G35300	1.41207175
AT1G01790	-2.4306162	AT5G57490	-1.430113	AT5G38980	-1.0643069	AT4G34000	1.96360891
AT5G04190	-5.6335314	AT4G20270	-1.9279929	AT5G03670	-2.4998949	AT2G05440	3.76145725
AT1G70090	-3.2165614	AT5G14090	-2.4003334	AT3G48970	-2.4569566	AT2G32300	6.82106282
AT5G22390	-3.350384	AT3G01450	-2.1709416	AT4G22305	-1.6054445	AT1G80160	3.67398028
AT4G14400	-4.0853999	AT3G06370	-1.7951753	AT2G39900	-1.2158615	AT4G15490	1.42508586
AT5G09440	-3.0646441	AT5G50210	-1.2602002	AT2G41950	-1.1076957	AT4G21580	1.17364233
AT5G52882	-4.5714671	AT3G25690	-1.4767226	AT5G50450	-1.5019913	AT4G17550	1.74743051
AT4G04570	-2.9682642	AT1G59960	-1.8623567	AT1G71140	-1.2919405	AT5G54840	2.14339862
AT5G60710	-2.4498721	AT4G13510	-1.7800724	AT2G38480	-1.2285277	AT1G44760	1.88613815
AT5G44568	-5.315264	AT2G42300	-1.1077634	AT5G55730	-1.7066184	AT5G16960	7.00468051
AT2G43150	-3.3893238	AT4G24230	-1.9296688	AT5G57630	-1.2916121	AT5G09640	7.01478007
AT2G21650	-7.386452	AT4G11100	-1.6449034	AT1G74750	-1.1230855	AT3G47600	1.57651533
AT4G16563	-4.4006295	AT5G56860	-1.2489507	AT5G36940	-1.1989034	AT2G36640	6.30232063
AT2G38120	-2.5334117	AT2G31010	-2.3226909	AT2G26980	-1.4007907	AT4G38020	1.39043561
AT4G38660	-4.2754965	AT2G32380	-1.6432614	AT1G27480	-1.1333002	AT5G47880	1.95119609
AT2G31750	-2.844277	AT1G74690	-1.3803944	AT4G37110	-1.5300401	AT1G11910	1.13655098
AT1G51805	-2.7198054	AT3G17390	-1.6209905	AT4G11080	-1.5285847	AT2G36750	6.71477791
AT3G12150	-2.8216002	AT5G19160	-1.5402864	AT1G09310	-1.1914134	AT1G17530	1.79328756
AT3G13437	-4.8406375	AT2G48020	-1.1321761	AT5G54970	-1.4681533	AT5G48655	1.02031695
AT3G10720	-3.7606606	AT1G69900	-2.8548883	AT5G15840	-2.4651854	AT5G06190	1.98927614
AT5G56550	-3.0507691	AT5G10520	-3.5577473	AT2G07680	-1.5833789	AT4G33540	1.26119635
AT4G36670	-3.7898921	AT3G24550	-1.0239707	AT3G21770	-1.808345	AT3G19580	1.85653552
AT5G44130	-4.3734929	AT1G76080	-1.2795107	AT1G01110	-1.5637561	AT1G17744	2.26357617
AT4G36540	-4.3791757	AT1G28110	-2.1165095	AT5G10200	-1.4796255	AT5G37550	3.36598298

AT5G23020	-5.1491732	AT3G18930	-1.0374012	AT5G10250	-3.6681522	AT5G02640	3.28341151
AT2G44740	-4.4087087	AT3G25600	-1.8309267	AT1G51800	-4.0294421	AT2G33380	2.50971555
AT5G16570	-3.8254854	AT5G04160	-1.3371691	AT5G40830	-1.0879385	AT2G43080	1.38728743
AT2G42580	-3.6669104	AT5G22140	-2.3160266	AT1G69810	-2.6609755	AT1G73010	2.69477115
AT3G07460	-3.0618872	AT4G14680	-1.787574	AT5G20630	-3.7987368	AT5G37720	1.07036437
AT3G14310	-3.3486807	AT1G51570	-1.072022	AT3G20470	-2.1165112	AT5G47020	1.10736818
AT5G49730	-2.4423444	AT5G09240	-1.4058639	AT3G59570	-1.4070132	AT1G48750	2.22790721
AT5G16030	-3.2438203	AT1G75440	-1.0341828	AT1G70370	-1.0239083	AT5G57910	1.82446145
AT4G38840	-3.0593927	AT1G35140	-4.6073808	AT2G16850	-2.0068084	AT1G53030	1.30729501
AT1G12500	-2.2518845	AT5G08520	-1.0469802	AT2G41010	-1.4775681	AT1G34340	1.18397862
AT3G04910	-2.0928133	AT1G22885	-1.1887954	AT2G30500	-1.0143011	AT5G46830	4.49395229
AT4G12390	-3.2487624	AT1G58080	-1.1856702	AT3G57800	-1.2516919	AT5G15260	1.67095049
AT1G65190	-1.6600129	AT1G32470	-1.5731589	AT3G52450	-4.2825378	AT2G34460	1.11796041
AT4G00950	-3.2382031	AT1G02640	-3.7724097	AT5G24270	-1.2329259	AT5G08400	1.22233926
AT2G18328	-3.562081	AT1G31330	-1.2656248	AT4G01460	-1.2581552	AT1G52565	3.87173149
AT5G03120	-3.5643845	AT5G44070	-1.3579016	AT2G35190	-1.561088	AT1G54830	1.07590324
AT5G15350	-3.0263801	AT1G65250	-1.1441131	AT3G13730	-1.7804524	AT1G32860	1.55703349
AT5G10770	-3.0788875	AT5G57030	-1.2312476	AT2G38640	-1.1016322	AT4G22950	3.06984774
AT5G51460	-5.1204935	AT3G11110	-6.4005792	AT1G47670	-1.3748923	AT3G03640	1.32124153
AT4G18760	-3.4062615	AT1G26570	-2.6268797	AT1G20823	-1.2870714	AT4G11960	1.3802177
AT5G64410	-3.8169341	AT2G17710	-1.899243	AT1G01120	-1.4350421	AT4G23630	1.18504093
AT5G46330	-2.4749888	AT1G49730	-2.1348913	AT5G20410	-1.3842698	AT3G54440	1.3700837
AT1G22530	-2.9459209	AT1G29280	-2.8813257	AT1G62520	-1.6676205	AT5G41960	1.22517744
AT2G23290	-3.03976	AT4G12500	-7.2469793	AT3G59310	-1.0768601	AT4G01870	2.8087371
AT1G20330	-1.8706663	AT3G15356	-3.3875772	AT5G15830	-3.5292854	AT3G57680	2.3234867
AT2G37950	-4.0981886	AT1G80920	-1.3124759	AT1G23080	-1.0561521	AT4G39140	1.15201789
AT3G19850	-3.6343315	AT5G50810	-1.3471145	AT2G27770	-1.4729308	AT1G48370	1.86596854
AT1G75250	-5.3950702	AT1G75450	-2.862261	AT3G28930	-1.008264	AT4G23670	2.21944543
AT2G01420	-2.3296259	AT3G60750	-1.0108195	AT1G54385	-4.031736	AT5G14680	1.05557254
AT1G15125	-7.1810766	AT5G22050	-1.0979874	AT5G14690	-2.4043922	AT4G31860	1.2306527
AT1G66200	-2.1556806	AT4G34750	-2.3170899	AT3G12110	-1.9483035	AT5G57790	1.89645215
AT5G10170	-3.1415477	AT1G74730	-1.0875112	AT5G54148	-4.2932019	AT4G23920	1.66505687
AT5G05440	-6.6622714	AT5G57800	-1.4000528	AT2G36200	-2.6715963	AT3G61220	1.80075211
AT5G58670	-2.5172184	AT1G55160	-1.3410256	AT2G05160	-1.454081	AT1G07530	1.09384026
AT5G03380	-2.570245	AT5G51670	-1.8361855	AT4G02060	-1.3864109	AT3G44100	1.10702622
AT3G13750	-5.1034637	AT5G18970	-1.4617097	AT2G14890	-1.3013931	AT3G10450	1.72063885
AT4G29310	-4.4440231	AT5G40010	-6.8249481	AT2G37030	-5.3649104	AT2G27150	1.51501112
AT5G38420	-4.9133483	AT5G47770	-1.193874	AT2G04790	-1.1927857	AT1G65890	3.13434686
AT1G67910	-3.0438672	AT3G07270	-1.1307198	AT2G27040	-1.1403124	AT4G16690	2.47401002
AT5G28770	-3.9373056	AT5G18690	-2.1656547	AT1G64390	-1.5130263	AT1G22160	2.30491707
AT3G14415	-1.8762314	AT2G31810	-1.2596235	AT1G78320	-2.0229553	AT2G38400	1.53494286
AT4G28780	-3.870768	AT2G39870	-1.3865735	AT3G02885	-2.5095004	AT2G46280	1.08344947
AT4G16370	-2.4304901	AT3G52500	-2.0826073	AT2G46225	-1.1685529	AT5G58770	1.81064754
AT1G70410	-1.9707184	AT5G51720	-2.1744202	AT3G51740	-2.5216307	AT3G49130	4.88859376
AT3G09035	-2.5013734	AT2G41100	-2.4706762	AT1G14810	-1.0072061	AT4G28830	1.29367631
AT4G17340	-3.3751935	AT2G42610	-1.7159749	AT4G20430	-1.5108585	AT4G23450	2.04010813
AT2G31110	-3.0029991	AT1G32700	-1.2670081	AT3G63088	-5.6881578	AT3G23490	1.24538323
AT5G46790	-2.2633651	AT2G34680	-1.3034658	AT1G76880	-1.0370005	AT4G36900	1.33483162
AT1G80280	-3.3701884	AT1G04110	-6.6185451	AT1G75690	-1.1163705	AT1G07910	1.15749985
AT3G63440	-4.5685234	AT5G63020	-1.0308338	AT2G28140	-4.1952696	AT3G04040	1.67901386
AT1G09340	-2.3760138	AT3G02050	-1.1838307	AT4G39900	-1.3303149	AT3G55910	3.11565443
AT2G44210	-2.3772254	AT2G28460	-2.2483864	AT4G19380	-2.1136682	AT5G19440	1.35613418
AT1G29430	-3.3830852	AT1G53510	-1.0146558	AT3G21080	-5.6641967	AT1G11170	2.36794142
AT1G66970	-2.4024971	AT5G17890	-1.3727098	AT5G52190	-1.0693259	AT4G05100	4.03519912
AT3G29670	-2.3882596	AT1G31690	-6.6074484	AT1G09970	-1.0155455	AT3G09390	1.22477475
AT5G19140	-1.8504227	AT5G59750	-1.3555031	AT3G25020	-1.4765109	AT1G28960	1.03846816
AT1G69530	-4.3981795	AT4G26530	-1.9691612	AT1G73620	-5.3636542	AT1G43160	4.33550664
AT4G26150	-2.3520664	AT5G10290	-1.1572961	AT2G46140	-1.2473164	AT1G17460	1.56530728
AT2G03350	-2.2771786	AT5G21160	-1.085926	AT1G17700	-2.2946266	AT1G04990	1.10887381
AT3G55630	-2.1225157	AT5G06720	-5.1170827	AT3G07580	-1.3049495	AT3G11410	2.00279129
AT5G11420	-2.3812997	AT1G05850	-1.2963399	AT3G46320	-1.1077546	AT3G53970	1.22611647
AT1G78460	-3.0892883	AT3G62410	-1.3201305	AT1G29510	-1.7368741	AT3G29090	1.03161205
AT1G58440	-1.9939464	AT4G00180	-1.1974224	AT1G68780	-1.7800232	AT4G13990	2.0306799
AT4G17460	-2.9953496	AT4G38970	-1.0732584	AT5G66330	-1.8177264	AT3G30460	3.23190358
AT1G04040	-3.8544002	AT3G02140	-2.8031573	AT1G72940	-1.4939754	AT2G46510	1.35567929
AT4G32800	-3.569491	AT3G20570	-1.5978804	AT1G20020	-1.109766	AT5G14800	1.14969461
AT5G51550	-3.7456515	AT3G06140	-2.5315976	AT3G15115	-1.0792965	AT1G36070	1.1664431
AT1G27020	-8.5642412	AT5G41790	-1.0517196	AT1G11580	-1.1636549	AT4G09750	2.15236309
AT4G23400	-3.2843096	AT4G37580	-1.9409971	AT1G52270	-1.1557451	AT1G10660	1.34018116
AT1G56430	-6.4418232	AT3G48550	-2.1310392	AT1G74030	-1.5970458	AT1G70160	1.02772418
AT2G15620	-2.8942189	AT2G34010	-2.4352959	AT3G61760	-2.7732356	AT3G15400	1.73584069
AT3G06070	-4.6224279	AT1G22610	-1.0653636	AT3G46780	-1.1807738	AT2G38540	1.50535301
AT2G18910	-2.0948803	AT4G16950	-1.1965024	AT4G28230	-1.1502161	AT5G04080	1.10629794
AT1G72150	-1.8973709	AT5G54710	-2.8073187	AT4G17243	-5.5852739	AT5G67330	1.1667391
AT1G78270	-2.5165445	AT3G56760	-1.0991346	AT1G77060	-1.1355775	AT3G21790	1.18873719
AT1G14460	-2.5725668	AT4G07400	-1.7436084	AT4G10120	-1.0956812	AT1G75170	1.80991466

AT1G08930	-2.701704	AT5G44040	-2.1147082	AT5G25250	-1.8781048	AT5G65110	1.27296076
AT5G04140	-1.8956882	AT1G09430	-1.0025378	AT2G19990	-5.6343968	AT1G32450	1.68783412
AT1G53230	-2.1654443	AT1G29160	-1.6043903	AT3G18130	-1.1211723	AT5G22470	6.74305744
AT5G13710	-2.7215929	AT4G04220	-2.9335072	AT5G54770	-1.0047981	AT5G43260	1.4067659
AT2G41940	-1.888673	AT5G23920	-1.2119921	AT2G22140	-2.1244772	AT3G63000	1.35471395
AT3G18773	-4.4410394	AT1G21100	-3.4626295	AT3G51080	-1.8191137	AT3G58070	2.01426507
AT5G12470	-2.0412279	AT4G12980	-1.6739483	AT3G42800	-5.2400732	AT1G19490	2.49414762
AT1G53430	-2.2534837	AT1G01430	-1.0952831	AT1G03457	-2.9895806	AT1G71910	1.22109409
AT1G48480	-4.2241976	AT5G45470	-1.762132	AT1G12520	-1.1931931	AT2G38820	1.24793619
AT2G28950	-3.0347801	AT4G25080	-1.3409218	AT4G27730	-2.2635463	AT5G42825	1.37132861
AT2G15080	-2.2226076	AT2G34490	-2.3510402	AT4G00670	-1.6383656	AT3G53880	1.4414749
AT1G75750	-5.4977322	AT1G07650	-1.0938732	AT2G39410	-3.280728	AT2G37200	1.19723487
AT3G02170	-3.4784829	AT1G33770	-2.9500378	AT2G40620	-1.3866354	AT3G27180	1.22905816
AT4G12320	-3.5114489	AT4G11290	-5.5314038	AT5G57760	-1.303758	AT2G36270	2.06002529
AT1G52190	-4.3077585	AT3G52060	-1.0909259	AT4G02130	-1.2120866	AT1G72260	3.93555287
AT2G33330	-3.9557642	AT5G35200	-1.2233291	AT1G61900	-1.0290516	AT1G65980	1.04380088
AT5G61660	-3.0783784	AT3G45160	-2.1433298	AT1G62400	-1.8157997	AT1G02700	6.0335829
AT5G55620	-2.5556954	AT5G54510	-1.979425	AT1G06960	-1.1255184	AT5G12840	1.15367421
AT5G62630	-2.0929148	AT5G36120	-1.2424268	AT3G59080	-1.4108325	AT3G47590	1.13544234
AT1G76990	-2.3005824	AT5G36930	-1.470994	AT1G65450	-2.404124	AT2G40080	1.38195331
AT3G04210	-3.5553712	AT5G59380	-1.3776169	AT2G03505	-1.795482	AT3G20810	1.45199739
AT2G30990	-1.8857058	AT3G19380	-2.2002734	AT1G74940	-1.0998421	AT1G04970	1.02419708
AT5G18650	-1.596511	AT4G06746	-3.7156767	AT5G41180	-1.1645461	AT3G28840	3.27236125
AT1G52230	-2.2862636	AT2G36400	-1.7385304	AT1G67720	-1.4452602	AT5G51990	3.36310655
AT3G22142	-4.0337148	AT1G70820	-1.5607897	AT1G18250	-2.5296138	AT2G18240	1.37414299
AT3G63110	-6.8282725	AT4G35900	-2.5785844	AT5G11070	-1.0351968	AT2G18100	2.73937475
AT5G21430	-2.0454008	AT5G03720	-2.5324119	AT3G50570	-5.4730148	AT3G15940	1.00951941
AT3G29631	-4.0390252	AT5G62670	-1.6176967	AT1G35710	-1.4957083	AT4G01060	3.16221457
AT2G31070	-1.6825016	AT2G40820	-1.6667271	AT1G51920	-5.3983215	AT3G05880	1.01184284
AT3G05730	-4.6157183	AT5G57700	-1.6947477	AT5G20640	-5.3503162	AT5G11390	1.02625961
AT3G19540	-1.8942411	AT2G06520	-1.1682046	AT2G37590	-1.7862064	AT5G62490	6.40939383
AT3G58120	-4.3524323	AT1G29920	-2.0764276	AT5G48900	-1.32609	AT4G25580	6.18106955
AT4G21870	-5.4494399	AT3G28080	-1.9697029	AT1G29980	-1.2826275	AT1G48320	1.70122858
AT1G64170	-4.0189834	AT5G09650	-1.2560845	AT1G78530	-5.39032	AT5G21020	1.47100235
AT3G62110	-1.6540629	AT1G22360	-1.4683215	AT3G20350	-1.0261966	AT1G45230	1.0288421
AT3G25070	-1.7642074	AT2G46440	-1.532986	AT1G68130	-1.0542642	AT3G16170	1.62310193
AT5G19770	-2.0666415	AT2G19110	-1.545224	AT5G55480	-1.3141524	AT3G03470	1.4765669
AT5G27290	-3.7105345	AT4G13770	-1.9289251	AT1G18590	-1.0269208	AT5G40800	4.02315129
AT2G01910	-2.4025402	AT2G36830	-2.4811526	AT3G16670	-4.4251888	AT4G09820	4.77816075
AT5G21170	-2.6483032	AT3G16420	-1.7800765	AT4G21880	-1.496563	AT5G05750	1.2791346
AT3G01860	-2.3724213	AT3G50740	-1.6986906	AT1G63180	-1.3063967	AT4G08540	1.14391796
AT1G61100	-2.0800247	AT1G63690	-1.1649304	AT1G29530	-1.0423362	AT3G21390	1.54070216
AT1G74670	-4.8698529	AT1G64670	-2.1709563	AT4G31840	-1.8631369	AT1G73880	1.67583625
AT4G12420	-3.4587232	AT3G51600	-1.1546136	AT1G11670	-1.7311015	AT3G55840	2.38533223
AT1G10470	-2.7350737	AT1G78995	-1.3062961	AT4G16141	-1.2407119	AT5G42280	3.47784659
AT1G15000	-2.8021611	AT1G70280	-1.6211263	AT5G05860	-2.1436038	AT5G51680	4.26177954
AT3G50270	-2.8531472	AT1G21050	-2.1766835	AT1G56210	-1.0917928	AT5G17600	2.03734532
AT3G10120	-2.2368451	AT5G01240	-1.1543637	AT5G10760	-1.8677524	AT4G11910	1.70950271
AT4G37260	-2.3635847	AT1G05385	-1.2749504	AT4G25830	-1.1164986	AT4G23490	2.04563326
AT1G10990	-3.4855878	AT2G22125	-1.1024412	AT3G50280	-1.8705554	AT4G14385	1.17379764
AT1G21500	-2.2128082	AT1G16390	-6.9912932	AT5G18470	-1.9390855	AT5G62800	5.22481704
AT1G67740	-2.1060562	AT3G06300	-1.1533777	AT4G35030	-1.5387997	AT5G61510	1.19712711
AT2G41090	-2.9420124	AT3G55420	-1.4965716	AT3G47090	-1.3106773	AT4G32770	1.4113991
AT5G45820	-4.145838	AT5G19240	-2.0394327	AT5G04950	-1.5247861	AT2G19860	1.20877029
AT1G67480	-1.9690336	AT5G54270	-1.456354	AT5G06430	-1.040574	AT1G62810	1.17363202
AT1G52290	-2.6766006	AT1G19050	-3.8077317	AT5G43060	-1.0581212	AT5G62540	1.03372137
AT3G07340	-4.4934139	AT3G59840	-1.0664277	AT3G09260	-5.4022424	AT3G52340	1.53262124
AT1G62380	-2.85526	AT5G57220	-3.4528093	AT3G47560	-1.0947292	AT1G26450	2.31916966
AT4G33220	-3.0014602	AT3G06740	-1.7073147	AT1G56720	-1.023064	AT1G56170	1.33485823
AT3G50750	-2.2613894	AT5G09660	-1.2058149	AT5G16023	-5.3190783	AT2G45920	1.31398918
AT2G24150	-1.7366315	AT4G37520	-2.3713577	AT3G48360	-3.5130918	AT1G23330	1.33377017
AT2G02950	-2.592566	AT3G54690	-1.4190357	AT4G29360	-1.5911073	AT5G03180	1.39012007
AT3G44450	-2.3876355	AT4G18370	-1.0286953	AT3G09920	-1.0178962	AT5G49525	2.3375035
AT5G19780	-2.276819	AT3G45780	-1.132414	AT2G44930	-5.0359503	AT3G27330	2.39742648
AT1G76110	-1.8647127	AT3G27020	-1.2021741	AT2G14560	-1.9065882	AT3G22565	6.35286801
AT1G05300	-2.98276	AT1G72920	-2.3639803	AT1G77855	-2.4049667	AT1G55310	1.03265375
AT4G37800	-4.5453744	AT2G31790	-1.2812027	AT5G56230	-2.0146634	AT1G23800	1.63008398
AT4G01330	-2.0216189	AT5G22310	-1.7071704	AT4G29700	-2.2824269	AT5G01720	1.24078603
AT1G65486	-3.2800025	AT1G67325	-1.151249	AT3G50630	-1.0741933	AT3G22200	1.16374589
AT1G32060	-1.8790331	AT1G23880	-1.8436796	AT5G07571	-3.0187973	AT4G13560	1.16681582
AT3G22890	-1.5596405	AT2G19880	-1.1844263	AT2G41610	-2.6391342	AT2G35730	4.91286926
AT2G37460	-3.176581	AT1G17140	-1.8103746	AT1G62930	-1.1515137	AT5G51890	2.03164536
AT3G22120	-2.9921594	AT1G48610	-1.4594608	AT1G66380	-5.2404269	AT3G03320	1.45555456
AT5G44340	-1.8619509	AT1G03820	-2.0544518	AT4G10340	-1.1372724	AT5G13930	2.39950983
AT1G10960	-1.6757784	AT3G16240	-3.388602	AT3G15354	-1.005286	AT5G23460	1.25012627
AT3G23820	-1.8510887	AT3G53130	-1.282359	AT5G59050	-1.0625753	AT5G13210	1.33105141

AT3G54920	-2.6516362	AT4G37930	-1.2249301	AT1G17060	-1.1425962	AT2G28320	1.41262258
AT5G61160	-9.6261491	AT1G70100	-1.0807616	AT4G32830	-3.1734587	AT1G49560	1.16819233
AT1G51940	-2.1882812	AT4G17490	-2.3519876	AT1G09440	-1.2609711	AT1G72120	1.77523601
AT3G52720	-4.4155713	AT3G60290	-4.4908106	AT1G33960	-3.3910688	AT1G11785	1.66382497
AT1G69850	-1.9220306	AT4G35950	-1.1956682	AT5G51465	-3.2362017	AT3G48520	4.09950091
AT5G11000	-2.051829	AT1G55450	-1.4740296	AT1G07610	-1.8253721	AT3G27460	1.08714815
AT3G60320	-2.5697178	AT2G40460	-1.5274584	AT1G43910	-1.9824933	AT3G47510	1.32680246
AT4G38470	-2.0878555	AT3G59010	-1.6818475	AT1G60960	-1.3783263	AT5G09980	3.36810855
AT4G39400	-1.6896365	AT3G11170	-1.2396979	AT4G39720	-1.7260436	AT3G58170	1.0883068
AT2G10940	-5.307664	AT3G14020	-1.512803	AT3G46090	-2.9895476	AT5G24080	6.16499355
AT2G47440	-2.1518024	AT3G50070	-2.1697408	AT5G62920	-2.9134692	AT3G19910	1.11426831
AT3G19550	-3.4584131	AT3G03000	-1.7175731	AT5G05320	-1.3207835	AT5G19660	1.02085152
AT5G60200	-2.3360472	AT3G43600	-1.6780619	AT3G14740	-5.2838145	AT3G48330	1.19113913
AT3G19450	-1.9485243	AT2G14660	-1.4185323	AT3G04420	-2.2502336	AT1G11840	1.24203937
AT1G11260	-3.7491927	AT5G06800	-4.4413383	AT3G23880	-1.8148943	AT5G13310	1.09233472
AT5G21930	-2.3355708	AT2G35960	-1.5458534	AT5G50443	-2.9732249	AT1G19970	1.55360934
AT1G63090	-1.6513338	AT2G41880	-1.0672351	AT1G24150	-1.1657484	AT3G60810	1.00593667
AT5G24660	-2.4352827	AT2G18560	-1.5137257	AT5G40140	-1.2851567	AT4G01280	1.01004983
AT3G28180	-2.4162853	AT4G23130	-2.1135689	AT4G04610	-1.2413618	AT1G47980	6.60559829
AT2G29970	-1.5647706	AT3G57040	-1.6004501	AT1G51850	-5.5863533	AT3G57520	1.69075588
AT1G04530	-1.9184352	AT1G16170	-1.5268633	AT4G30280	-2.9332099	AT3G49760	3.80745342
AT1G75820	-2.3534392	AT1G55360	-1.5661662	AT4G11211	-1.4779613	AT3G60670	3.06054402
AT1G18400	-4.3654417	AT3G06020	-3.1311949	AT1G18670	-1.0117251	AT1G67370	1.86083849
AT1G23390	-2.3729798	AT5G41060	-1.9815234	AT5G44420	-3.8654615	AT3G14690	1.18593932
AT5G23860	-2.3720822	AT5G22400	-1.2154536	AT3G14940	-1.5584396	AT1G19680	1.15341063
AT5G18060	-3.5843919	AT5G45490	-1.319871	AT5G45740	-1.6098648	AT4G22240	1.15430996
AT2G33050	-1.9045575	AT2G26640	-1.3869754	AT1G08090	-5.3151889	AT1G49200	2.01306953
AT2G39730	-1.798839	AT5G55230	-1.3169993	AT3G20015	-1.3116737	AT1G61800	3.38218725
AT3G30180	-3.1011445	AT5G63470	-1.3303074	AT4G16780	-1.2870011	AT5G67620	2.02250269
AT1G31420	-1.7494414	AT3G46130	-1.8106265	AT4G26760	-1.6905383	AT1G18710	2.6273909
AT5G15580	-2.9137174	AT1G72440	-1.2765236	AT4G02100	-1.3869375	AT1G71695	1.12525354
AT4G18205	-2.7677234	AT1G02380	-2.4463242	AT2G46640	-1.3806509	AT3G23240	2.69092937
AT1G14345	-1.9343659	AT1G70290	-1.2604581	AT4G24570	-1.9821845	AT3G61450	3.49714908
AT4G39770	-3.5851446	AT5G39210	-1.1816966	AT1G68810	-1.1329975	AT1G62045	1.84518621
AT3G48720	-4.0464864	AT3G27770	-1.1362294	AT4G18440	-1.0156937	AT3G14060	3.11812137
AT1G68238	-6.8581494	AT3G26470	-3.3719233	AT5G23010	-1.2495623	AT5G55700	1.3405128
AT4G17870	-1.6224258	AT4G04700	-3.1053471	AT5G40460	-3.7919009	AT4G17530	1.35017111
AT1G63360	-1.4138437	AT4G00760	-1.1017475	AT3G15450	-1.8116732	AT4G05020	1.7054848
AT5G18500	-2.2764253	AT4G25940	-1.1445928	AT5G49560	-2.10939	AT3G19390	3.11464032
AT2G06850	-3.4181917	AT4G29110	-1.2468096	AT4G32480	-1.2316773	AT2G22900	1.75838125
AT5G42530	-3.3819158	AT1G76870	-1.9204398	AT1G17860	-1.4267805	AT3G24800	1.09915281
AT3G11700	-2.143019	AT1G05590	-1.1655939	AT2G24395	-1.4710495	AT3G10815	3.40052532
AT1G23090	-4.4244195	AT3G53420	-1.7097245	AT2G19590	-3.6772477	AT4G17650	1.5121584
AT1G65490	-2.406673	AT2G01850	-1.4650935	AT3G56200	-1.1818288	AT3G20300	1.45723333
AT3G53190	-4.3868695	AT1G72880	-1.0063369	AT3G17626	-1.1150257	AT1G71260	1.0250774
AT1G53440	-1.9488453	AT1G21920	-1.1439294	AT1G66980	-1.6655273	AT2G16700	1.12720171
AT5G46240	-2.6234184	AT5G35630	-1.0133822	AT1G25510	-2.2069344	AT2G04190	6.70128168
AT4G03400	-2.3597233	AT4G38520	-1.1922268	AT4G23550	-5.142778	AT1G25422	2.55504544
AT3G62720	-2.5999065	AT5G42680	-1.5624652	AT2G46530	-1.0123274	AT5G16760	1.19596171
AT3G56060	-3.2563463	AT4G21850	-3.4363253	AT4G36770	-4.9000874	AT5G67180	1.53964686
AT2G42040	-2.7831424	AT3G02110	-1.4891432	AT3G49340	-2.1457021	AT3G17800	1.07586436
AT2G46330	-3.1889139	AT4G32000	-1.825066	AT4G15910	7.1529744	AT2G25820	3.86756079
AT3G28860	-2.1870688	AT1G52140	-2.3011389	AT1G30190	7.07517486	AT1G78850	1.87411997
AT2G03440	-1.3108135	AT5G18020	-2.0567538	AT4G09600	8.00500902	AT2G46660	2.1960003
AT4G36570	-5.9500045	AT1G24147	-2.5549184	AT5G06760	7.97124781	AT1G33700	1.60787135
AT1G03010	-3.8160127	AT1G10120	-1.3441152	AT5G66780	8.93557047	AT2G46910	1.04352111
AT1G29450	-3.0435577	AT4G34160	-2.6012705	AT3G29575	4.44157624	AT1G02470	2.1998625
AT2G29290	-2.7475181	AT5G23760	-1.2830843	AT4G36240	4.6911589	AT1G07390	1.91274859
AT4G27300	-2.8287548	AT1G65960	-1.1448614	AT4G33150	4.78569636	AT2G21940	1.25283995
AT4G37240	-5.1484415	AT5G58360	-6.0917522	AT4G12580	6.47742075	AT2G01540	1.17260797
AT4G14750	-5.010076	AT2G20670	-2.6921873	AT1G69260	5.25537164	AT5G43430	1.03601075
AT1G12020	-2.1617488	AT3G49060	-1.2015505	AT4G33905	7.5965473	AT1G49660	1.53246285
AT5G43270	-2.061052	AT4G00300	-1.3465697	AT5G40382	5.85928799	AT2G31350	1.35581305
AT1G26761	-2.2582242	AT1G03130	-1.1012862	AT5G13170	9.39384772	AT2G16770	1.5477224
AT3G09580	-1.7545575	AT2G37050	-1.3091517	AT3G50980	7.26450232	AT3G05650	1.51261688
AT5G65700	-2.2058727	AT2G23100	-2.1064941	AT5G01300	9.74075614	AT1G50260	1.73215044
AT4G02330	-5.0208133	AT1G63480	-1.5970828	AT4G02360	5.24737823	AT4G37980	1.6132367
AT1G02705	-3.6166394	AT2G24580	-2.0751753	AT2G46940	5.51667231	AT1G13360	1.26873726
AT1G76890	-1.9578384	AT1G18880	-1.9331249	AT3G02480	7.35791171	AT4G12130	1.69189719
AT1G16880	-1.6892705	AT1G77460	-1.307608	AT4G02280	4.77993725	AT1G80610	1.42517868
AT3G15630	-3.7071797	AT1G47400	-6.1127495	AT3G03341	5.2808582	AT5G14590	1.00005199
AT5G03995	-4.3719611	AT1G74440	-1.7514306	AT5G37540	3.42741607	AT3G20910	1.36954536
AT3G13062	-1.4717274	AT3G15620	-2.9559958	AT4G25433	8.41840029	AT4G35050	1.23378774
AT5G67190	-1.8883673	AT1G02360	-3.4606459	AT2G21590	4.39009078	AT2G18600	1.64021711
AT2G02070	-1.7620718	AT5G01740	-2.6926783	AT2G19900	8.55920798	AT4G18400	1.48233566
AT1G73600	-4.4470846	AT4G01720	-2.5267365	AT5G43840	8.54330318	AT4G37295	3.83911753

AT2G17740	-7.1931421	AT4G15270	-2.5118033	AT2G46270	3.82300452	AT1G72690	1.12431226
AT2G23770	-2.4617603	AT1G77640	-4.3479991	AT3G14560	2.65832811	AT5G58700	1.55079603
AT1G71030	-1.9115647	AT2G44490	-1.0573831	AT3G61890	5.14955042	AT2G30550	1.37287997
AT1G65295	-2.2845576	AT4G02770	-1.044695	AT3G24520	4.26148359	AT3G61530	1.20164908
AT3G18080	-2.3347241	AT1G30250	-2.0743178	AT4G27520	2.92702311	AT1G06090	4.05039693
AT1G61667	-1.7802038	AT5G12900	-1.6778183	AT5G53710	5.63092186	AT1G32870	1.38166536
AT2G30766	-4.2770615	AT4G14360	-1.0427741	AT1G05340	6.04201833	AT3G17820	1.3790121
AT1G71880	-1.9700837	AT5G39760	-1.6118545	AT2G41190	6.40809327	AT3G50910	1.06318697
AT5G19250	-1.3762567	AT5G61590	-1.0747741	AT5G50360	8.08444352	AT5G43770	5.88449616
AT1G66140	-1.6511426	AT4G05130	-1.4107274	AT2G34850	5.52928573	AT2G18050	2.72381174
AT3G50560	-5.8621964	AT2G05790	-1.6323227	AT5G07330	9.85163955	AT3G02875	1.34394868
AT2G19670	-2.5837113	AT1G69160	-2.0474719	AT1G70300	2.98018829	AT2G19350	1.08452762
AT1G52220	-1.6724568	AT1G59950	-4.4465817	AT1G35720	3.21661827	AT4G18270	2.47142845
AT4G31360	-2.2246861	AT3G16460	-1.5830337	AT5G66110	4.70763764	AT5G16380	1.26502299
AT1G75190	-2.5355355	AT5G12880	-3.5210867	AT1G64660	3.96718818	AT3G03440	2.26542324
AT1G33811	-3.0951176	AT5G58310	-2.7206705	AT2G12400	2.83175431	AT1G23960	1.06187038
AT5G49215	-2.4429197	AT5G64300	-1.2081468	AT4G19390	2.36275556	AT5G01990	1.6349866
AT2G40330	-8.7533056	AT1G72910	-2.0311591	AT4G31830	10.1667626	AT1G61255	3.06892682
AT1G27210	-2.2670198	AT5G39860	-2.8746483	AT3G19960	2.72844004	AT1G50630	1.27385907
AT3G26700	-2.6827739	AT3G26760	-4.1563688	AT2G39800	5.54849679	AT5G56520	1.47347386
AT5G56850	-1.9161918	AT3G25130	-2.5532329	AT2G33590	3.56368255	AT2G21780	4.26600487
AT5G07580	-2.5782414	AT3G18390	-1.5592582	AT5G35660	8.19629296	AT5G23750	1.86164464
AT3G16660	-3.7866605	AT4G27240	-1.4396453	AT4G35560	4.37103383	AT5G37670	1.46803455
AT1G16640	-3.8401322	AT1G08510	-1.0081124	AT2G35300	7.12389258	AT1G53780	1.06470905
AT2G18730	-2.340512	AT2G47160	-1.5735116	AT2G04240	2.47703633	AT4G13790	6.6735153
AT5G22920	-2.7463895	AT1G07090	-1.3744453	AT5G57050	3.92501351	AT3G15352	1.73182105
AT1G04680	-3.4479048	AT1G67260	-2.4224521	AT1G22990	5.50920248	AT5G17850	1.48725496
AT3G54400	-3.5464563	AT2G35620	-1.4637251	AT5G42570	1.93303304	AT3G02990	1.98154742
AT1G75380	-1.540556	AT5G65810	-1.2315933	AT5G15190	4.8018981	AT1G27170	1.71563016
AT5G23870	-2.8230263	AT5G16590	-2.2529331	AT1G16850	5.00359281	AT1G57540	1.030481
AT2G32080	-1.5350043	AT2G23680	-1.4423965	AT3G48240	6.21174099	AT1G61890	1.52072021
AT5G63850	-2.1778242	AT1G55910	-1.4815365	AT4G21320	3.89939134	AT5G20150	1.53640422
AT1G28670	-2.286082	AT2G39360	-1.0589801	AT5G63350	5.26331374	AT5G25130	2.02523263
AT4G34760	-2.878098	AT5G06980	-1.3791268	AT4G24000	4.7436758	AT1G08650	1.43547696
AT4G34740	-1.7842701	AT3G26490	-1.7784573	AT3G22560	4.85866303	AT3G51895	1.4211793
AT5G06790	-2.6561032	AT1G22900	-3.1906848	AT3G28007	4.10614962	AT5G17490	2.16014166
AT4G08300	-3.5514626	AT1G29440	-2.4763151	AT3G62090	4.1101649	AT5G67310	2.84276497
AT1G02340	-3.990982	AT2G24600	-1.9384695	AT4G30450	3.41460513	AT5G63000	1.03667888
AT5G14200	-2.312734	AT3G52360	-1.6228559	AT3G14360	4.79652763	AT3G62290	1.29486043
AT5G40850	-2.6454188	AT3G13000	-1.9309777	AT2G41210	3.23728006	AT1G21650	1.05713102
AT5G06560	-1.4692801	AT3G21950	-2.4464795	AT5G66400	7.91635566	AT1G12845	1.35728567
AT3G12700	-2.6007969	AT2G05070	-1.7449423	AT1G07985	6.76814571	AT2G18550	6.43776212
AT2G17550	-2.2297768	AT1G69040	-1.8665011	AT3G15350	2.37169075	AT1G52080	1.59251586
AT4G30110	-3.1644652	AT1G78970	-1.963309	AT3G13784	9.74558086	AT4G15530	1.51084103
AT2G47930	-3.1693845	AT4G15920	-1.155863	AT5G65280	4.22297246	AT2G35940	1.06153842
AT1G80440	-1.8210641	AT3G11402	-2.3812787	AT1G54100	3.39420414	AT3G14960	1.02154782
AT3G16530	-4.9095243	AT5G10240	-1.8339862	AT5G44310	7.18634831	AT1G01480	3.15083538
AT4G12470	-10.298452	AT2G39880	-4.5982302	AT3G13672	3.71615349	AT3G20660	1.3030167
AT1G59970	-1.6363226	AT2G34060	-3.0234141	AT1G16515	4.23896051	AT3G23260	1.90419067
AT1G63260	-2.9946661	AT5G50335	-2.5710554	AT1G17870	4.72431055	AT2G44750	1.50373757
AT1G06830	-9.4684106	AT2G11810	-2.6709601	AT5G09620	1.9610024	AT1G73080	1.23794649
AT2G23690	-7.8812547	AT2G28085	-3.7063804	AT5G60580	2.26839622	AT4G01550	1.22774937
AT1G76160	-2.5365862	AT2G30420	-2.6691137	AT5G05110	1.83395233	AT1G63850	1.83951977
AT5G66920	-3.0792121	AT2G38290	-1.4563496	AT4G21570	2.37047305	AT1G64970	1.5806452
AT1G14290	-2.5560194	AT3G27400	-2.4312847	AT3G57010	3.81746209	AT2G34610	6.96174082
AT3G12750	-2.4991124	AT2G01755	-1.7418473	AT4G01985	5.48629245	AT3G62650	1.47444181
AT4G20780	-2.2260331	AT3G53750	-1.4183478	AT4G18280	2.72085813	AT2G16595	1.46764153
AT2G15760	-3.8501252	AT2G04780	-1.7077971	AT5G65990	2.15388049	AT2G46000	1.40973059
AT4G26540	-2.5858535	AT1G33610	-3.1556248	AT5G22460	2.92797834	AT5G62020	1.65875215
AT2G32690	-2.3436045	AT5G07460	-1.8788498	AT1G77450	4.26210914	AT5G61880	1.21518349
AT5G49910	-1.9357048	AT5G14230	-2.2951263	AT2G20770	2.91308071	AT5G12140	1.0765353
AT5G38430	-3.1442483	AT1G29520	-1.5960632	AT2G43580	4.64618472	AT5G06510	2.01151848
AT3G18050	-2.4145849	AT5G56030	-1.3135085	AT2G16720	3.13384158	AT1G27900	1.30319244
AT5G59030	-1.2499182	AT4G29610	-3.4629841	AT5G40790	9.73273902	AT3G17950	1.01771557
AT5G53500	-1.8808789	AT2G28930	-1.0100503	AT1G68500	3.87748295	AT4G24010	2.32989197
AT2G40670	-3.7532917	AT2G01670	-1.2947441	AT5G05220	7.23309854	AT3G15280	4.10180464
AT1G13110	-1.8466125	AT5G23820	-2.0622479	AT1G29640	6.07678011	AT5G47570	1.00007313
AT5G59080	-2.7668865	AT4G36120	-2.5011049	AT4G30460	3.88146986	AT3G21250	1.48027365
AT1G23030	-3.0543673	AT3G61430	-1.0084465	AT1G72770	3.28786878	AT2G38530	2.17825758
AT2G22122	-4.05685	AT1G78040	-1.0986909	AT5G42290	6.69743269	AT5G45130	1.04207461
AT3G15530	-1.5066971	AT1G75780	-2.1812181	AT1G21400	2.55421658	AT1G30640	1.11311898
AT3G01490	-2.3917448	AT1G68800	-3.1895505	AT5G61820	2.93850302	AT1G29810	1.17381322
AT1G50040	-8.7906957	AT3G11850	-1.1348673	AT5G10300	3.27096791	AT3G57590	1.09605788
AT1G17560	-3.9156943	AT1G08380	-1.0137156	AT1G24580	9.44225959	AT5G59700	1.73593497
AT5G46220	-7.2020152	AT4G14960	-1.0232553	AT4G34710	2.37711724	AT4G32510	5.83296907
AT2G42530	-2.6083502	AT5G13100	-1.2726193	AT1G67300	2.51876658	AT3G06420	1.44982866

AT4G12690	-2.9591241	AT1G10200	-1.1680483	AT5G47550	2.71888751	AT1G62370	2.75962515
AT4G30190	-1.9879924	AT5G49100	-1.6787776	AT1G01470	2.25350217	AT4G23910	1.04478761
AT5G58900	-2.2413204	AT1G71970	-1.0344139	AT1G30220	4.72745613	AT1G47820	1.13129078
AT4G14040	-1.824594	AT3G48200	-1.3046542	AT1G31750	4.1008322	AT1G74780	1.56944831
AT5G56870	-4.1634016	AT1G80180	-1.3869605	AT1G07720	2.71422296	AT5G47640	1.47555225
AT5G65010	-2.5054325	AT5G57460	-1.0432924	AT3G46230	9.63649226	AT4G30960	1.62361753
AT5G10180	-1.8677144	AT1G29470	-1.1857346	AT3G17520	8.40978633	AT2G32090	1.05685892
AT1G75180	-2.0094157	AT5G04020	-1.3749536	AT5G59220	6.22548215	AT1G08230	1.37822745
AT5G46450	-1.7530979	AT2G31880	-1.9590316	AT4G08570	9.49840019	AT5G42510	5.80768091
AT4G03210	-3.8363049	AT1G72060	-2.7122671	AT2G37770	7.01746489	AT1G72660	3.7977257
AT2G32487	-3.7338462	AT1G09810	-1.197284	AT5G52300	8.18795621	AT1G43790	1.11750193
AT1G26960	-2.3912119	AT5G65660	-1.150371	AT3G62990	5.47262013	AT1G67265	1.31236978
AT1G11350	-1.5245711	AT4G33530	-1.328443	AT2G47780	5.41765601	AT5G47810	1.26924747
AT1G69780	-2.9158836	AT4G37820	-1.0381328	AT1G57590	4.79769707	AT3G25290	1.75300057
AT1G77990	-2.1624185	AT3G50140	-3.6967175	AT1G70640	3.1844806	AT1G28540	1.1999077
AT4G39250	-7.4237136	AT5G41140	-1.3454372	AT5G57900	2.03076828	AT1G62770	2.01580221
AT3G06750	-3.1222167	AT1G12160	-2.047821	AT2G25620	2.01472715	AT1G10585	3.17335071
AT3G49940	-3.2209006	AT1G27050	-1.0833792	AT5G62530	1.9449345	AT5G53830	1.47627547
AT5G38410	-2.7556761	AT3G52840	-1.641695	AT1G09530	2.48226245	AT2G37300	2.30463825
AT5G16650	-1.4306754	AT1G31320	-2.7711828	AT3G50970	4.06005006	AT4G34412	1.12541911
AT3G10050	-1.8443171	AT1G73830	-2.3668889	AT3G18280	2.7540362	AT5G48180	1.7322449
AT1G72180	-1.5787153	AT1G53520	-2.9260006	AT1G64110	6.11284951	AT3G27870	1.43667299
AT2G25200	-2.2112905	AT4G02520	-2.5752071	AT3G15670	8.4189306	AT5G55750	6.2667564
AT1G53730	-2.0107936	AT1G75960	-3.2302534	AT5G06370	1.7398132	AT5G40960	1.24359499
AT3G51910	-3.4721323	AT5G03040	-1.0001758	AT1G06570	2.59333329	AT5G07990	2.50385354
AT2G39890	-1.8089962	AT4G04890	-1.0915009	AT3G55880	2.79445543	AT1G19570	1.33758688
AT5G08150	-4.1807139	AT4G05180	-1.5102206	AT4G22820	1.92827088	AT1G23040	1.36725469
AT5G57660	-1.9323742	AT1G80850	-1.9162575	AT3G55610	2.59557183	AT1G15100	1.13243644
AT3G17330	-1.5703288	AT2G37380	-3.8658419	AT1G51140	4.5115944	AT1G69800	1.34972414
AT5G60270	-4.0530184	AT3G04720	-2.7156953	AT4G26080	2.06985284	AT5G20510	1.25684506
AT5G46780	-1.793342	AT4G13930	-1.0658661	AT4G34860	3.60388065	AT5G15740	1.4668586
AT2G45850	-1.6570606	AT3G05910	-1.4460418	AT5G07920	1.94211083	AT3G10940	1.37187148
AT5G28020	-2.2156229	AT5G14210	-1.1649765	AT5G54165	4.98666519	AT2G32870	1.22608838
AT4G17810	-2.7583248	AT4G32330	-1.0061961	AT5G54585	3.4703789	AT5G39050	1.87181258
AT5G22090	-1.5495775	AT1G13250	-1.7693767	AT1G58360	1.85438672	AT4G18372	1.41886011
AT5G22580	-3.8468136	AT5G51480	-4.529283	AT1G48000	3.34135568	AT3G54390	1.75515442
AT4G32790	-1.6450974	AT3G10610	-1.3736565	AT4G17030	4.06821078	AT4G34990	1.29803798
AT2G26910	-1.6380461	AT5G55960	-1.0191551	AT4G10250	6.53509337	AT4G23000	2.0303479
AT5G49980	-1.2488477	AT2G41800	-2.774896	AT4G20320	3.69103388	AT5G65470	1.00100798
AT2G04795	-2.2869147	AT1G15085	-3.4671049	AT4G33467	6.14757193	AT5G03080	1.1555368
AT5G10560	-1.2636895	AT2G34070	-1.5386227	AT1G20160	2.37567882	AT2G37900	2.46654825
AT5G18600	-1.4273206	AT3G01680	-1.4845133	AT3G05640	3.08115564	AT2G24260	1.43747643
AT5G14060	-1.7837957	AT3G56360	-1.4628418	AT3G22840	4.22836751	AT4G21610	1.38844073
AT3G15850	-2.0286229	AT2G21840	-5.8754548	AT5G03210	6.35648009	AT1G74020	1.82584716
AT1G24170	-2.0995828	AT5G16400	-1.1470489	AT1G17830	4.20059701	AT3G22420	1.01047745
AT5G24520	-1.3078941	AT5G37740	-1.2246044	AT3G03170	3.72888574	AT1G48500	4.14308521
AT5G50740	-3.024057	AT3G12600	-1.2056595	AT3G47080	2.24927275	AT3G16030	1.2844818
AT4G38550	-1.6189342	AT3G56170	-1.0682946	AT1G45249	2.78015692	AT2G23110	4.05387703
AT1G24100	-1.503969	AT3G15820	-1.1656364	AT5G50240	2.47478406	AT5G23050	1.02866737
AT3G23730	-3.7512421	AT4G21750	-1.1237998	AT1G77120	3.42697264	AT3G06240	1.03601469
AT1G13210	-1.9633386	AT1G49470	-1.2415181	AT5G15960	4.48386518	AT3G62590	1.46789671
AT4G19420	-2.3406807	AT5G66560	-1.6254223	AT3G22830	5.69260336	AT5G25610	1.11058349
AT3G03850	-4.3407175	AT2G01870	-1.1690741	AT2G42560	8.03237848	AT3G27270	1.54786899
AT5G49170	-4.5992954	AT5G48220	-1.1153468	AT3G17000	1.9351552	AT1G61340	2.41785749
AT5G25460	-2.3844291	AT1G21130	-1.2821181	AT3G15780	2.37469928	AT5G01200	1.34674951
AT2G32240	-1.5232307	AT4G18030	-1.243545	AT1G67920	3.06265807	AT3G14067	1.06048321
AT4G20260	-1.3048973	AT3G54470	-1.2206446	AT1G08630	4.28871794	AT5G49280	1.32866091
AT4G12480	-4.0724709	AT3G04730	-1.0850917	AT4G25450	1.73464119	AT2G35060	1.12617858
AT1G62790	-1.6509849	AT3G54050	-1.0688476	AT1G17020	3.72467774	AT5G09990	1.42047705
AT5G28630	-5.6226573	AT5G10570	-3.4604094	AT4G12000	2.71442368	AT4G34131	1.91359384
AT3G15680	-2.7745761	AT2G16050	-1.8588259	AT1G49450	3.2258726	AT5G49650	1.05270543
AT1G55330	-3.6692312	AT2G30570	-1.0838809	AT4G27410	2.95283786	AT2G44300	1.54179997
AT3G05320	-3.0101699	AT1G74450	-1.0552538	AT3G48000	1.48001828	AT3G10620	1.03940058
AT2G39700	-2.0522358	AT5G06850	-1.2202599	AT4G18422	5.30416419	AT1G20440	1.21641051
AT5G52900	-1.6922331	AT1G66350	-1.5498958	AT1G69295	1.81542885	AT4G37970	2.72947351
AT3G61260	-1.5761171	AT5G20160	-1.0703892	AT1G62290	4.4758842	AT2G18230	1.1964787
AT1G68585	-2.4062949	AT1G66920	-1.6423571	AT4G23493	2.51925508	AT5G02420	2.56824967
AT4G31820	-2.3219825	AT5G38990	-1.289972	AT4G33550	6.8188355	AT2G47630	1.4299589
AT4G12490	-6.7751265	AT5G45500	-1.2101494	AT3G44290	7.29332354	AT5G51640	1.18731132
AT1G06410	-1.4958516	AT4G09420	-6.3762037	AT4G13800	4.14371218	AT4G21550	1.61700521
AT5G27380	-1.4848009	AT3G52400	-1.8575912	AT4G27670	8.55860816	AT3G12120	1.05991935
AT2G45960	-1.4301924	AT1G51790	-2.4525338	AT1G02205	3.06722594	AT5G03230	1.70966728
AT4G39940	-1.9768589	AT5G24920	-1.680201	AT5G04660	3.73053612	AT5G60760	2.03232478
AT5G40150	-2.0880063	AT1G73660	-1.0921812	AT1G17940	2.11403677	AT1G67360	1.52556189
AT3G15030	-1.3175817	AT5G25265	-1.2335565	AT2G21820	7.09762051	AT1G28370	1.74738317
AT5G20400	-2.2720381	AT1G31350	-1.4487656	AT1G24600	3.72593377	AT4G18465	1.47468746

AT1G25230	-2.2023069	AT2G39180	-3.7093189	AT1G71360	1.70747808	AT1G54570	1.0675866
AT5G20250	-5.5947288	AT1G22740	-1.5533517	AT5G59320	5.78899752	AT4G08170	1.19916062
AT4G08920	-1.1674571	AT1G55850	-1.3897996	AT5G17460	3.43463666	AT1G17630	3.62554872
AT1G19990	-1.8897527	AT1G34315	-1.9776316	AT3G49120	2.79836878	AT5G49330	1.88709879
AT4G33565	-1.5549547	AT5G23300	-1.431001	AT4G32920	1.9120665	AT2G47180	1.47796993
AT3G62390	-2.8315689	AT4G31890	-2.8072532	AT2G47770	8.23232892	AT1G24070	3.12372953
AT5G10150	-2.9426915	AT1G26220	-1.2990856	AT1G07430	5.1915811	AT1G03550	1.26464815
AT5G51560	-3.1315548	AT4G23460	-1.1894374	AT3G21270	2.06199852	AT5G58980	1.43377623
AT4G04630	-2.2702378	AT4G21760	-3.6059455	AT5G45310	3.04676557	AT3G56260	1.61358577
AT1G20840	-1.802851	AT1G16630	-3.7834435	AT1G60190	6.10859221	AT4G14950	1.10845789
AT3G54600	-2.4301	AT1G04520	-2.725546	AT2G29300	3.36930254	AT5G03190	2.25922438
AT4G25620	-1.5101496	AT1G78290	-2.5108345	AT5G57350	1.6850263	AT5G23190	5.80126181
AT3G15540	-2.6341628	AT1G63860	-1.2311385	AT5G22545	3.94990161	AT5G54230	4.02621667
AT5G18080	-2.298906	AT1G65930	-1.0931591	AT1G70800	2.12681116	AT4G36830	2.04694965
AT5G11670	-1.4786762	AT2G29550	-1.2533236	AT3G52850	1.65950213	AT4G36010	1.63633287
AT2G30424	-2.3867701	AT1G56110	-1.3195954	AT1G52890	2.97444795	AT1G10530	3.84448041
AT3G01690	-1.643591	AT5G04930	-1.2358391	AT3G55940	3.04177276	AT4G15248	4.43145237
AT2G25510	-2.5316689	AT1G45474	-1.0441861	AT3G54680	2.47112272	AT3G47420	1.83904494
AT1G71020	-1.8580069	AT1G29670	-1.7663683	AT1G01250	3.93792743	AT4G32460	1.02512667
AT3G16180	-2.4843677	AT5G04310	-3.7454887	AT4G16000	2.60347973	AT3G03240	5.8536374
AT4G09000	-1.2220613	AT1G05010	-1.708943	AT2G46680	4.31412012	AT1G12064	5.61771895
AT3G61310	-1.8762994	AT3G06868	-2.6177224	AT4G15990	4.26204944	AT2G14110	1.18473801
AT2G33480	-1.575449	AT5G51840	-1.3331585	AT1G66390	4.64170696	AT2G46980	1.97862071
AT3G57870	-1.3691596	AT4G17900	-1.0000658	AT3G44880	2.06449051	AT1G69210	1.58024378
AT5G55990	-1.3633148	AT3G01810	-1.1526201	AT4G09610	6.2417287	AT3G16400	1.32157155
AT5G43750	-1.9137317	AT3G51710	-2.17445	AT5G43150	3.21170582	AT3G54320	1.04142239
AT3G08600	-2.210425	AT5G04470	-1.0231816	AT5G53660	3.67952217	AT2G29525	1.38837627
AT5G61440	-3.0779475	AT1G06680	-1.1311184	AT3G09910	2.89470328	AT5G20380	1.04655363
AT1G09160	-1.5136071	AT1G15530	-1.410879	AT4G14819	5.68150292	AT5G56180	1.22901223
AT2G38970	-1.6205816	AT4G24810	-1.1930971	AT5G53870	3.53298222	AT1G74010	2.3628218
AT1G50460	-1.7889485	AT1G14180	-2.7860797	AT2G39250	2.68691562	AT5G02880	1.29227783
AT5G44565	-2.0976505	AT2G46890	-1.3551837	AT4G36600	5.49785317	AT5G13490	1.62141937
AT5G58390	-2.7670596	AT3G19710	-1.7805074	AT2G16990	4.06249931	AT5G14285	1.28200039
AT3G47380	-7.3735165	AT4G23170	-1.2590949	AT1G73390	2.60124067	AT5G24120	1.52186925
AT2G42380	-4.1550697	AT4G38540	-1.5648921	AT1G21790	2.20773327	AT4G28340	3.25105439
AT2G42320	-1.7525652	AT4G37650	-1.0982648	AT1G02310	7.39423582	AT2G20560	1.66659538
AT1G31710	-3.099401	AT5G67390	-2.1469563	AT4G21060	3.08268006	AT3G50000	1.08053493
AT5G28840	-1.1979372	AT4G00335	-1.0409226	AT3G12960	8.12835042	AT2G30790	1.41384471
AT3G23050	-2.1307483	AT4G37040	-1.0515348	AT1G69410	1.67593642	AT4G24530	1.15639043
AT2G15050	-2.0984748	AT4G31620	-2.7590638	AT2G18540	7.8330371	AT1G78560	1.0461701
AT5G66640	-2.6561506	AT3G50010	-3.0074004	AT4G06536	4.22232143	AT3G55640	1.00929075
AT3G16370	-2.1909574	AT4G35685	-1.5534481	AT1G04220	4.01786052	AT1G64900	1.17250585
AT5G07100	-2.5654842	AT2G15390	-2.2482185	AT5G62040	6.92975115	AT4G16540	1.75550633
AT1G54740	-1.9880289	AT2G29180	-1.2192486	AT1G51090	2.89850793	AT3G51090	1.53911408
AT5G65430	-1.2475478	AT2G46450	-1.1938252	AT4G34650	3.38500608	AT5G01260	1.20417394
AT1G54460	-1.2815644	AT1G18570	-1.8081814	AT2G02120	4.9708883	AT5G24030	1.71177367
AT3G56480	-2.1822997	AT1G70070	-1.1522763	AT3G03310	2.4085408	AT3G04530	4.17506303
AT4G16380	-1.3111006	AT4G23790	-1.2412302	AT1G79260	1.81172399	AT1G66760	2.48866776
AT1G65985	-2.9521357	AT2G40530	-1.7372156	AT5G22290	2.10935226	AT3G27880	1.38944899
AT1G68520	-2.112546	AT3G52480	-1.4967855	AT3G57540	2.11895733	AT3G53210	1.34507412
AT1G05805	-1.4941218	AT1G28390	-2.4923208	AT4G30470	2.1185548	AT5G65300	1.48278325
AT1G75840	-1.4607338	AT2G16400	-1.0077775	AT3G53370	1.8492037	AT5G23310	1.19184241
AT1G77690	-3.8672567	AT3G46550	-1.237017	AT1G54120	3.32857862	AT1G03760	1.12338735
AT4G13500	-1.8529411	AT1G69910	-1.2414152	AT5G09225	1.85428686	AT3G47620	1.00158582
AT5G21482	-1.9903785	AT4G32340	-1.6126432	AT5G03560	1.63505471	AT4G33040	2.37303275
AT4G34770	-4.6371747	AT1G01080	-1.1332274	AT1G79520	1.90286509	AT5G03200	1.01901888
AT4G03390	-1.2647754	AT3G55500	-1.5416677	AT5G43850	1.90160873	AT1G68340	1.33468516
AT1G48600	-2.071165	AT5G55530	-1.0318501	AT2G37760	2.69654114	AT3G22430	1.00359487
AT5G53880	-2.2391475	AT4G24026	-2.0311452	AT5G44670	2.30971279	AT2G36800	1.47847905
AT4G38850	-3.2508693	AT3G15570	-1.3304411	AT5G47610	2.5033338	AT1G63720	1.5167871
AT1G09250	-2.0830477	AT3G15640	-1.294855	AT5G22860	2.87287463	AT1G11210	1.34938989
AT3G46820	-2.2893172	AT3G04290	-3.5065278	AT1G28260	1.85537734	AT5G53120	1.2374291
AT5G53160	-1.9981084	AT1G08980	-1.2158576	AT5G04760	1.72403368	AT3G53780	1.24227892
AT4G19120	-2.027127	AT1G29720	-1.2364481	AT2G37870	7.32222298	AT5G24860	4.53495182
AT1G10550	-8.3278263	AT1G70880	-3.5878345	AT5G24090	3.96015416	AT3G05660	1.34841417
AT4G04830	-2.4915172	AT4G18010	-1.1671425	AT5G10930	3.74935176	AT5G12930	1.73822965
AT1G60800	-1.9294046	AT4G39795	-2.7195243	AT2G41200	1.43215447	AT3G14280	1.78680793
AT1G19450	-3.0336911	AT4G11521	-2.2491491	AT2G41870	2.24998564	AT2G22190	1.61078066
AT3G14870	-2.2857949	AT1G18650	-1.5346696	AT5G15250	7.55423481	AT3G56240	1.17112648
AT2G36120	-2.9635186	AT1G70520	-1.086272	AT1G01720	2.72258995	AT4G23250	1.37931084
AT4G16983	-6.9326996	AT1G26770	-1.9725795	AT1G62570	2.54614639	AT3G60040	1.59578037
AT1G61190	-1.3132791	AT5G17870	-1.312977	AT1G03106	5.12545287	AT1G49900	2.98173316
AT2G02020	-2.7104628	AT3G10230	-1.1043905	AT1G52690	8.58109843	AT3G09560	1.35581052
AT5G51850	-4.807509	AT3G07540	-2.0484175	AT3G54820	2.75163234	AT1G70830	1.18598018
AT4G39990	-1.3163054	AT5G25240	-1.8604134	AT1G14730	2.46596079	AT1G66500	1.28196726
AT4G00165	-1.6602375	AT2G40000	-1.642135	AT3G43520	1.32883057	AT3G13130	3.22635952

AT5G49740	-1.6148555	AT2G39795	-1.2615856	AT5G19875	3.09471975	AT1G09280	1.10593271
AT4G34790	-7.3329166	AT5G61190	-1.011084	AT5G25560	1.56254083	AT4G40010	1.49838681
AT2G26530	-3.0411682	AT2G02820	-1.6585255	AT3G23920	1.81086302	AT5G10080	2.71685093
AT2G30960	-1.5588242	AT5G06570	-3.2373412	AT1G50930	7.47988372	AT1G53580	1.04775801
AT5G19230	-3.0454168	AT1G34260	-1.2163923	AT3G23910	2.12239832	AT4G35480	1.26142263
AT1G57980	-2.3815548	AT5G13180	-1.3621184	AT5G24800	1.85098443	AT5G14700	1.19777082
AT3G49260	-1.9075155	AT3G56590	-1.1766577	AT5G04250	2.51189055	AT2G30540	1.70162074
AT1G20010	-2.9379635	AT5G07000	-1.8085738	AT5G01670	1.99989287	AT3G24170	1.04885165
AT4G16860	-1.5574979	AT2G13820	-2.5225519	AT2G22470	3.33038123	AT3G03230	5.74054953
AT3G59670	-1.6328879	AT4G37610	-4.3197648	AT3G19100	1.83529919	AT4G13180	1.18172398
AT2G47730	-1.720838	AT3G50240	-1.1841079	AT1G47570	1.54030475	AT2G43240	1.53151443
AT3G26510	-1.3281583	AT1G73110	-1.5035463	AT3G16990	1.989597	AT3G51240	2.03057869
AT2G26020	-6.8687441	AT2G43110	-1.3845196	AT1G21410	2.24025864	AT1G23550	1.89617468
AT4G04955	-2.0933942	AT1G79670	-1.0001887	AT1G63010	1.59892849	AT1G21750	1.20358099
AT1G30690	-1.6506368	AT2G46250	-1.1157644	AT1G76980	2.11923452	AT5G45275	1.36403924
AT1G12090	-1.8721232	AT5G11410	-5.8783126	AT1G62710	2.83430169	AT1G11190	2.19485171
AT2G31730	-4.9096644	AT3G02640	-2.3942749	AT1G80300	1.68648253	AT4G19645	1.72505589
AT2G18290	-1.540157	AT2G40750	-2.0971451	AT4G25480	3.6516291	AT1G76960	1.49590549
AT5G16720	-2.0182489	AT4G32030	-1.2892621	AT5G58380	1.75640814	AT4G19810	2.68568127
AT1G19510	-2.7444869	AT2G25220	-2.3696073	AT5G02020	3.58025027	AT1G73210	1.61646565
AT4G24240	-2.3569284	AT3G57560	-1.0184613	AT2G34790	2.40070568	AT1G69270	1.00973948
AT1G01490	-1.3567544	AT4G03510	-1.0005037	AT3G27250	4.1750984	AT5G05380	1.10918444
AT4G36810	-1.2434519	AT1G30840	-1.5279973	AT5G47060	2.05962624	AT4G38960	2.17075286
AT3G05220	-1.2924546	AT2G34300	-1.3495863	AT3G53980	5.92885892	AT1G77950	6.72541599
AT2G26560	-3.8288924	AT4G36030	-3.2327425	AT5G25110	3.91740717	AT1G60680	1.82170044
AT5G12420	-2.2331753	AT5G59010	-1.1601858	AT5G48480	1.48754805	AT1G73177	1.57704143
AT4G33666	-2.0483361	AT3G45930	-1.1708064	AT4G39730	1.66138124	AT3G10200	3.04682059
AT3G01480	-1.4964215	AT5G58260	-1.244781	AT2G15480	2.33897794	AT1G56650	3.05358601
AT3G27960	-1.9020409	AT5G45840	-2.8057598	AT4G39210	2.37984599	AT3G60300	1.25752481
AT2G23700	-2.1137414	AT5G57130	-2.0307312	AT5G43400	3.63026681	AT4G30080	1.08105198
AT2G21140	-3.9303447	AT4G27450	-1.3226283	AT5G15860	1.98018691	AT5G22540	1.92792003
AT2G28630	-4.6172178	AT4G14130	-5.2782873	AT1G05100	5.82555384	AT4G37550	1.25947748
AT5G61570	-2.6614473	AT1G67980	-3.354731	AT5G26770	1.55891008	AT2G16530	1.18235154
AT1G24530	-2.7976033	AT4G01950	-1.7578465	AT1G54575	3.28382072	AT5G57480	1.7619446
AT4G01750	-2.6312901	AT4G18253	-3.2470327	AT1G18840	1.7874175	AT2G05185	3.17946202
AT2G26975	-1.436871	AT4G23260	-1.1210987	AT2G36220	1.58765747	AT2G22570	1.07140376
AT5G06530	-1.7198805	AT1G13100	-1.4041311	AT5G02550	3.69556446	AT1G77810	1.02855845
AT5G58150	-2.0026186	AT3G06470	-1.101459	AT3G01520	1.19434604	AT3G51990	1.05873449
AT2G40610	-4.3955966	AT5G11740	-1.08263	AT3G11420	1.81414301	AT3G11020	1.40326808
AT2G03750	-1.4875178	AT1G21910	-2.9129794	AT1G47960	2.98636138	AT1G50970	2.23735671
AT4G27310	-2.0155238	AT1G31970	-1.009653	AT3G28270	5.26085715	AT3G51440	1.70990095
AT2G17705	-1.4477576	AT1G78370	-1.5494275	AT1G60970	4.77436162	AT2G32510	2.74646587
AT2G22990	-1.6175756	AT1G56120	-1.7931582	AT5G01600	2.40386274	AT1G29240	1.34911255
AT5G14920	-2.5309741	AT4G12030	-1.7537767	AT2G28400	2.20369707	AT4G24130	1.81276984
AT4G04340	-1.5486106	AT5G07860	-1.4422889	AT5G37300	4.28920903	AT1G12050	1.00185522
AT5G59540	-1.3766729	AT4G33000	-1.4753167	AT5G04000	2.76282597	AT5G02040	1.15008888
AT1G75500	-2.1566123	AT3G45260	-1.2887387	AT1G78070	2.23425293	AT5G09315	1.53933573
AT4G39710	-1.8421966	AT3G02880	-1.1864426	AT1G05870	2.57216195	AT1G04560	6.19230812
AT2G35880	-1.8627413	AT1G20780	-1.3342507	AT1G54160	2.53126047	AT1G19200	2.82159726
AT2G44500	-2.7150144	AT3G28200	-1.1569715	AT3G10340	3.8779023	AT1G62620	2.04795742
AT4G12830	-2.2411462	AT4G02420	-1.4296454	AT5G37500	2.63409836	AT5G37260	1.4598923
AT5G47780	-1.5539652	AT3G10540	-1.13179	AT1G13990	1.88015173	AT1G63240	1.35997416
AT4G01900	-1.4716681	AT3G23750	-1.099183	AT2G45380	1.39697251	AT2G20400	1.23967135
AT5G22940	-3.1772268	AT5G15310	-1.4962808	AT2G16890	2.2004092	AT5G25390	2.10971941
AT5G18050	-2.4438591	AT1G76190	-6.1768322	AT1G27150	1.8117159	AT2G25590	1.04095812
AT5G18170	-1.3545856	AT4G36500	-1.2526007	AT3G51960	2.32421196	AT3G15150	1.54855499
AT4G27740	-1.8277649	AT1G56520	-1.5033848	AT4G03820	2.65768958	AT4G39670	3.29560109
AT2G37180	-3.4947822	AT3G23090	-1.4502209	AT1G20450	1.98280101	AT3G63010	1.06847247
AT3G26200	-2.6906433	AT3G62960	-2.2072967	AT1G46768	1.86921583	AT2G34720	1.16949013
AT3G02700	-1.2518474	AT1G19950	-2.7176921	AT4G36195	1.24619805	AT2G43800	1.54327697
AT5G64040	-1.6027161	AT2G26760	-3.7046081	AT3G57020	3.04378267	AT4G28590	1.03306652
AT4G28080	-1.4186866	AT5G01530	-1.1111806	AT1G76590	1.68096254	AT2G46950	5.7836976
AT1G65845	-3.8100703	AT4G27440	-1.0017346	AT2G22080	1.53389953	AT4G36950	3.36346583
AT5G19120	-3.4167251	AT1G69570	-1.6399115	AT5G54080	1.41930454	AT5G47650	1.04710332
AT4G38680	-1.236636	AT4G18970	-2.0598351	AT5G16200	2.18625295	AT1G54870	6.00957364
AT1G17970	-1.4802953	AT5G46270	-1.007627	AT4G30830	2.48085636	AT1G06180	1.39918206
AT5G12050	-2.3158585	AT4G23060	-1.2821822	AT1G33102	3.13569034	AT1G08570	1.16816891
AT1G53390	-1.2660039	AT4G15233	-1.6956673	AT1G68570	1.99758485	AT5G66480	1.71534699
AT4G29080	-2.1788611	AT2G35860	-1.4697125	AT4G01610	1.48398665	AT3G14070	1.62124363
AT5G18840	-4.7382058	AT1G80560	-1.2457789	AT4G12410	4.14308591	AT1G68360	2.43050699
AT3G13690	-1.4548892	AT4G36410	-2.6499448	AT1G21680	1.42481467	AT3G18680	1.0426849
AT1G70270	-6.3836756	AT3G13470	-1.2852914	AT5G27670	1.53360309	AT1G52920	1.93499024
AT5G09870	-1.5094919	AT3G29035	-1.7346684	AT4G30710	1.75174607	AT1G30300	1.17920944
AT5G64850	-1.9191874	AT1G49130	-1.2633972	AT2G29500	2.34536975	AT5G67080	2.62473307
AT5G39020	-1.7241311	AT5G26220	-5.9855058	AT5G43330	1.78686407	AT3G08505	1.75054205
AT2G16060	-3.0552	AT4G23470	-1.37038	AT1G29330	2.2714085	AT4G14220	1.18057855

AT1G01300	-2.0183702	AT3G04770	-1.0962554	AT4G12430	2.67098812	AT3G18950	2.02469361
AT2G17820	-1.7316168	AT2G24762	-1.483247	AT1G30500	2.33449355	AT5G05880	5.4536186
AT5G63780	-2.160047	AT4G34810	-5.7919251	AT4G16750	2.79758159	AT1G12672	3.75506176
AT5G17920	-1.1181883	AT4G33400	-1.5361635	AT3G14595	2.36260886	AT1G71340	1.20554178
AT1G76090	-2.5289954	AT5G43020	-1.8712584	AT5G16550	1.32732701	AT3G11670	1.09509473
AT2G26650	-2.1467266	AT3G52430	-2.4473018	AT1G79270	2.85010127	AT5G28350	2.54554914
AT2G25735	-3.5799587	AT2G01860	-1.4657966	AT3G03620	6.43046711	AT1G45145	1.21375028
AT1G21270	-1.7831435	AT5G61420	-1.8270071	AT4G24960	1.74460238	AT5G49665	1.57985399
AT5G10450	-1.2715535	AT4G03100	-2.6178196	AT5G62150	3.85430125	AT5G02065	1.83796728
AT5G08760	-2.4539149	AT3G19930	-1.4787155	AT3G27210	1.43304488	AT3G62260	1.04439996
AT1G22650	-3.2198494	AT1G32460	-1.1040149	AT3G14720	1.80290371	AT2G26660	1.03969687
AT3G28910	-1.8024342	AT4G32140	-1.1683067	AT5G05410	2.38076606	AT4G40070	1.74280939
AT3G58850	-2.3842586	AT5G59680	-2.1996432	AT4G01120	1.27256049	AT1G18750	1.00373009
AT5G43310	-1.638824	AT1G47290	-1.1114772	AT5G07470	1.32441485	AT5G56100	1.33207428
AT3G21055	-1.7608098	AT4G17880	-1.252772	AT5G53590	2.0130667	AT1G08500	1.61914626
AT1G61300	-1.2505518	AT3G50470	-2.38814	AT4G34230	1.82955279	AT1G02390	2.0194138
AT1G28660	-2.0629405	AT5G13280	-1.0332131	AT5G13330	2.87573026	AT5G61930	1.12962334
AT4G08930	-1.4906683	AT5G46050	-1.8053529	AT3G46450	1.39442936	AT5G42900	1.01279753
AT1G20340	-1.5586245	AT3G17640	-2.7670667	AT1G73040	2.80612148	AT4G18130	1.25433352
AT3G29034	-3.0696566	AT4G35270	-1.1134131	AT3G25870	1.75246384	AT2G39030	1.84337273
AT5G47250	-2.1587585	AT3G61820	-1.3148904	AT1G71110	1.98483306	AT3G27900	3.53267705
AT2G18860	-1.4055225	AT2G01990	-1.2546745	AT3G12490	1.42790412	AT1G64690	1.72191742
AT1G13245	-1.5531207	AT5G63140	-1.9904157	AT2G23910	3.1613487	AT1G22065	1.73940736
AT1G75680	-1.5863855	AT4G17070	-1.5533035	AT3G08590	1.43355485	AT3G29180	1.20677328
AT1G67090	-2.132774	AT5G48830	-1.2517654	AT1G79900	3.51704735	AT5G07530	8.07782114
AT4G39050	-1.179761	AT2G19460	-1.2497889	AT2G46610	1.42229522	AT1G35320	1.28936396
AT5G42180	-5.5032135	AT2G28510	-1.1235181	AT4G23680	3.21216858	AT1G01640	1.19141214
AT2G45170	-1.4478057	AT2G34360	-4.051737	AT3G11050	4.41634775	AT4G39360	3.1679297
AT3G55330	-2.0410198	AT5G65925	-2.1160506	AT2G42790	1.43376173	AT3G24750	5.34970028
AT3G54810	-1.5906466	AT2G32560	-1.1222904	AT3G06810	1.49985178	AT1G22985	1.29157706
AT3G14240	-1.8680118	AT5G56040	-1.6397596	AT1G17550	1.45882457	AT3G14440	1.29604127
AT1G37130	-2.5009907	AT5G23100	-1.3333407	AT1G32100	2.40707046	AT4G30720	1.00140097
AT5G67560	-1.469389	AT2G31020	-3.4949958	AT1G04830	1.65375317	AT3G07350	1.57495536
AT4G16880	-2.7866499	AT2G15790	-1.1173569	AT4G14010	2.07150733	AT1G07290	2.58705365
AT5G20110	-1.4923296	AT1G35560	-1.1804209	AT4G18980	1.9749053	AT5G05840	1.91610861
AT4G09160	-1.9569698	AT2G40095	-2.1746559	AT1G15310	2.21022739	AT4G21020	5.4992646
AT1G30440	-1.2993833	AT4G25835	-1.6586575	AT3G20500	1.7127646	AT4G14090	2.28324196
AT3G06150	-1.3394432	AT5G35490	-1.1363802	AT4G02880	1.2977087	AT1G02335	1.26027753
AT1G44920	-1.6257534	AT3G54640	-1.0931167	AT3G12955	4.38716079	AT1G03790	5.56111294
AT1G60660	-1.8305721	AT3G42670	-1.4050904	AT3G61420	1.8685274	AT1G32900	1.88104221
AT1G11380	-1.9903021	AT5G07590	-1.5210237	AT4G03960	1.63813102	AT4G27530	5.3291296
AT1G78450	-3.3394873	AT3G10010	-1.4374411	AT3G01100	1.48126591	AT5G64310	1.64687258
AT5G06930	-3.4945783	AT4G39190	-1.267677	AT2G45600	1.82735034	AT1G05560	1.02919102
AT1G66190	-2.2775567	AT5G18240	-1.5214549	AT3G24730	1.73382295	AT5G11350	1.05846148
AT1G65860	-2.3774409	AT2G42690	-1.3249202	AT1G08040	1.24908858	AT5G01940	1.16994865
AT5G65450	-1.9000007	AT5G59360	-2.8360908	AT2G43540	1.27689582	AT3G52180	1.16881966
AT4G26690	-1.6360292	AT3G26670	-1.3058444	AT1G62510	3.350375	AT1G73810	1.36434221
AT5G18590	-1.7590601	AT1G22550	-1.5654231	AT2G35070	4.25208584	AT3G01430	1.09997316
AT3G62150	-3.0579269	AT4G33360	-1.3679089	AT5G18040	1.78959045	AT3G50760	1.7635059
AT3G27030	-2.1459131	AT1G15260	-1.2904254	AT3G56270	2.36168369	AT5G42200	1.19603965
AT5G35750	-1.8738933	AT5G12860	-1.2332323	AT5G64080	2.09246554	AT4G11660	1.0674801
AT4G15760	-1.9437024	AT1G66465	-2.8034383	AT3G17180	5.74234371	AT5G16140	1.20373489
AT2G01290	-1.3842176	AT5G62710	-1.6157606	AT4G29820	1.37708045	AT5G24155	3.22824992
AT3G49790	-1.7038249	AT4G10800	-1.5853567	AT4G23880	2.07291971	AT4G02410	1.04332822
AT4G38770	-2.5578419	AT2G02930	-2.5679612	AT5G47560	1.61604664	AT3G10070	1.24811512
AT5G18290	-4.683481	AT3G04860	-1.5671915	AT5G59310	5.95449394	AT4G25180	1.01211906
AT1G54010	-4.4977332	AT4G00360	-1.3434121	AT3G51750	2.41454357	AT4G09589	5.30552668
AT5G35732	-2.4383676	AT2G01260	-1.0472257	AT2G45570	5.63647144	AT3G13210	1.60024081
AT4G37450	-2.3664774	AT1G16650	-1.5422006	AT3G53230	1.69494512	AT5G37530	1.97116024
AT2G30600	-2.4123637	AT3G25597	-2.2787087	AT5G15240	3.40078989	AT4G26055	1.11462409
AT4G18570	-1.5257881	AT5G22300	-2.000584	AT1G14720	1.37924361	AT5G58660	2.56743785
AT1G55670	-1.7093777	AT5G54630	-1.1603629	AT3G24500	2.17601144	AT2G29460	2.20217887
AT1G68330	-2.9541768	AT3G62820	-1.0371965	AT4G37430	3.01524869	AT4G36050	1.03433881
AT3G09980	-1.1900063	AT4G03140	-3.8707943	AT4G17280	4.94725411	AT1G69480	2.35027483
AT3G23805	-1.8930496	AT4G22120	-1.2469381	AT5G40390	2.53737773	AT1G68880	3.72938479
AT3G49720	-1.4709478	AT5G60400	-1.0573067	AT1G04570	3.5201696	AT1G22180	1.05961314
AT1G45180	-2.5720231	AT4G23180	-1.2558068	AT1G34630	1.59201052	AT5G13200	1.11711045
AT4G39970	-1.6236682	AT5G39380	-1.2005525	AT3G16190	1.43478616	AT3G17030	2.94979603
AT4G23820	-2.9973062	AT3G12710	-1.877031	AT1G66890	1.80206501	AT3G27290	5.27368395
AT3G04140	-2.6203816	AT2G22170	-1.5253636	AT5G66170	3.03406518	AT1G07745	1.2795207
AT2G21210	-2.5541639	AT4G36920	-1.0640388	AT1G30820	1.83456636	AT2G22690	1.14397117
AT3G05900	-1.7866211	AT1G43670	-1.0237277	AT5G16120	1.4468373	AT3G61990	1.18921385
AT5G49760	-1.3406256	AT2G41990	-6.7452612	AT5G59845	3.5636348	AT1G05450	5.27605138
AT3G13520	-2.1081609	AT2G32010	-1.6150654	AT2G32120	1.86580745	AT3G16610	3.73854727
AT4G27260	-2.145484	AT5G10020	-1.1881482	AT5G13370	2.12136951	AT4G10180	1.00548111
AT1G77760	-2.825396	AT5G27690	-1.0028741	AT5G49990	2.15176449	AT1G74458	1.14149231

AT4G37770	-4.7441315	AT1G04180	-3.3645895	AT1G08460	1.18476485	AT2G42950	1.32092251
AT4G24015	-1.9353638	AT2G28190	-2.354587	AT4G29070	1.35854619	AT4G28390	1.14573063
AT5G59670	-2.8711918	AT2G05810	-1.7487755	AT5G20280	1.1754098	AT5G41860	1.20830627
AT3G22060	-3.2722082	AT1G30040	-2.8757388	AT3G22740	2.36508005	AT5G60910	1.11228423
AT1G63220	-1.9632542	AT4G15830	-2.6686858	AT1G06110	1.37241906	AT1G22490	1.84398238
AT1G22590	-1.3354842	AT5G57685	-1.8069292	AT1G69430	3.27595645	AT1G07900	1.7777801
AT2G34930	-2.5917811	AT4G21430	-1.0621012	AT5G64430	1.9907317	AT1G62050	1.08019337
AT3G57240	-5.1981003	AT2G28660	-1.1492117	AT1G61620	1.09225357	AT1G63420	1.02517699
AT1G14280	-1.5536787	AT1G63750	-1.141984	AT3G12580	3.68427608	AT1G55760	1.13308782
AT4G23290	-2.7963382	AT2G43100	-1.6262049	AT2G46800	1.07458414	AT4G09900	1.10717823
AT3G56370	-2.3218108	AT2G20570	-1.1935243	AT4G19230	2.53801853	AT1G52570	1.34468599
AT4G18710	-1.1435965	AT1G54217	-2.1253284	AT3G14130	1.84319174	AT1G61065	1.04232827
AT5G65310	-1.6516396	AT1G34010	-1.3469356	AT1G63840	1.89118101	AT5G17050	1.21941963
AT5G19260	-2.400903	AT5G46690	-2.0280793	AT2G37340	1.17457105	AT4G18220	1.48537165
AT1G59710	-1.6871779	AT2G18700	-1.4076257	AT3G02620	2.98953265	AT3G60140	4.44987715
AT2G25480	-1.784696	AT5G14930	-1.0778363	AT2G42000	8.47522063	AT3G50440	1.40167256
AT3G63140	-1.4981573	AT2G27970	-1.1862173	AT1G64950	1.66599528	AT1G72680	1.280476
AT1G60950	-1.4188013	AT5G22640	-1.0439827	AT3G15020	1.65292614	AT5G51760	5.62713776
AT1G16410	-2.3967753	AT5G24570	-1.3199664	AT1G20030	2.26939915	AT2G21180	1.11733957
AT3G55240	-2.6888043	AT2G13790	-1.2051607	AT2G35343	2.97292539	AT2G34810	1.15142282
AT4G21280	-1.6549156	AT5G62140	-1.534143	AT3G26380	1.52904447	AT3G52820	3.00611438
AT2G45590	-1.2199688	AT2G16380	-1.1740441	AT2G25950	1.25935372	AT2G21350	1.25039778
AT1G61740	-1.94147	AT2G01760	-1.326485	AT4G00430	1.2480842	AT3G08880	1.03035268
AT1G36940	-3.2445205	AT5G57780	-2.5777025	AT1G62305	2.05365008	AT5G46395	3.85241739
AT3G12610	-2.9155734	AT2G37540	-1.0819171	AT1G10070	1.78394835	AT3G03900	1.01697163
AT1G21110	-3.4768434	AT2G14247	-4.8426917	AT5G53360	1.22068048	AT1G69540	3.91356848
AT1G02610	-2.082948	AT1G77620	-1.4094733	AT3G54200	1.41010028	AT4G31354	1.55723884
AT3G57410	-1.246217	AT3G46490	-3.3321241	AT3G48510	6.83472512	AT2G36770	2.19318266
AT1G54820	-2.6094212	AT3G12220	-3.5463809	AT1G22370	1.98273084	AT3G16175	3.78335855
AT1G01180	-2.0328085	AT1G50900	-1.0291105	AT1G09500	5.83148587	AT5G24460	1.1110517
AT1G15830	-2.8339404	AT1G34760	-1.5999769	AT5G63030	1.08635553	AT5G55400	1.56972705
AT4G19410	-1.593029	AT3G13450	-1.0395867	AT3G14590	2.78398188	AT5G14640	1.05035042
AT1G58100	-1.2742477	AT1G67750	-2.2706624	AT1G29680	7.17552188	AT3G15534	2.73095249
AT4G38690	-1.5650397	AT1G06640	-1.1675862	AT5G52310	2.49421073	AT1G72210	1.72256917
AT3G58990	-2.4469548	AT1G75335	-1.1196579	AT3G03270	1.51623358	AT3G12460	2.12238405
AT5G35790	-1.2185988	AT5G62730	-6.0409051	AT5G63130	2.82933433	AT3G15740	5.4736315
AT3G28650	-3.9170789	AT4G28190	-2.4786354	AT1G07040	1.49379935	AT2G37970	1.11909275
AT3G17650	-1.2913306	AT3G07195	-1.9179085	AT5G57610	1.52060037	AT1G53540	5.1502594
AT1G19380	-3.0279219	AT1G06360	-2.4735919	AT3G51810	6.76452967	AT2G25940	2.86235134
AT1G61170	-1.8074274	AT1G03740	-1.1625682	AT5G59570	1.65235834	AT5G04200	1.34133418
AT1G33790	-4.2438357	AT5G18430	-2.7585098	AT1G60420	1.16318769	AT2G46735	1.16375424
AT5G65440	-1.4838148	AT1G15410	-1.4352638	AT2G22420	1.64404652	AT1G24265	2.06499458
AT3G27830	-1.6991433	AT5G62350	-1.2147325	AT1G06430	1.35016263	AT3G57380	2.36593461
AT4G21445	-2.1234213	AT2G44830	-1.8496338	AT5G25450	2.43162169	AT1G52030	2.07445681
AT5G62360	-5.4796756	AT5G03150	-1.5418707	AT2G47890	1.34730572	AT2G14825	1.06168496
AT1G55370	-1.4129144	AT3G06060	-1.1631852	AT1G33480	2.63133707	AT1G73066	3.81272618
AT3G43720	-1.4903216	AT1G31490	-3.9520238	AT5G14960	2.56791706	AT2G01175	1.51059722
AT2G13610	-2.1051901	AT3G23940	-1.2023864	AT5G60360	1.31797502	AT2G35075	5.20603023
AT3G10985	-1.4647407	AT5G05180	-1.4826038	AT4G31290	1.67047531	AT3G02210	2.36936121
AT1G14200	-1.3894698	AT1G77660	-1.3568241	AT1G72700	1.52873199	AT1G01520	3.80279754
AT1G65010	-1.6682759	AT3G17470	-1.0951173	AT2G43500	2.09880907	AT1G67340	1.05213124
AT5G03355	-7.0752752	AT5G48540	-2.0230147	AT4G27657	2.19324381	AT1G16520	1.20466424
AT2G39000	-1.1154109	AT3G22231	-2.5392492	AT3G23000	1.38572596	AT1G05490	2.10416175
AT1G12440	-1.0211907	AT3G09470	-1.0768499	AT4G14615	1.07318241	AT3G52740	1.04013357
AT4G34950	-2.7389158	AT2G39470	-1.2480164	AT5G64350	1.05584087	AT2G40900	1.34012341
AT3G27690	-2.1581388	AT1G02620	-5.9949556	AT1G69360	1.54885865	AT2G37580	1.8811295
AT1G44000	-1.5419007	AT5G06290	-1.0662564	AT2G25964	1.65784958	AT5G50110	1.125774
AT4G22010	-2.9069323	AT3G24420	-1.4146888	AT4G14270	1.67074824	AT3G06160	5.21613926
AT4G30250	-3.1504676	AT2G33400	-1.8170077	AT5G53970	1.8578948	AT5G19740	1.37278379
AT2G43910	-1.4836198	AT3G50350	-1.2512506	AT4G32910	1.21525107	AT1G76570	1.15996114
AT3G29639	-2.9861788	AT5G13000	-1.1679849	AT1G62610	1.70152802	AT1G07500	5.25547627
AT3G10060	-1.4685539	AT4G03270	-5.6695756	AT5G65380	1.76292468	AT2G33070	3.76410748
AT5G40670	-1.0558205	AT2G28620	-2.9638933	AT5G15500	3.96163019	AT1G71000	2.87805973
AT1G12900	-1.5137717	AT1G03850	-2.9330459	AT4G22270	1.60142909	AT5G41315	2.75658306
AT1G69760	-1.4963005	AT1G27460	-1.7323927	AT5G10730	1.95072537	AT1G33110	1.07245274
AT1G52510	-1.3434234	AT1G07370	-2.0932579	AT5G20010	1.02038513	AT4G37220	5.56467384
AT2G35390	-1.3365096	AT2G36010	-1.8096765	AT4G32250	1.54299492	AT5G67090	1.61676184
AT5G13610	-1.3871089	AT5G55920	-1.00315	AT3G16120	5.18261144	AT5G19850	1.21192233
AT3G19553	-1.0281197	AT1G35580	-1.1787309	AT5G11110	1.62304554	AT1G68640	2.70698019
AT2G39705	-1.506621	AT1G70690	-1.7876121	AT5G52420	1.35087916	AT1G55590	1.05834881
AT1G74070	-1.6720928	AT1G07135	-2.5958249	AT5G57040	1.2052675	AT3G20130	1.83602273
AT2G46820	-1.3788396	AT1G53840	-1.0365766	AT4G20170	1.77944991	AT1G07540	5.27728377
AT2G48030	-2.1141089	AT1G04430	-1.2650101	AT5G62480	2.7714212	AT1G32350	2.52929083
AT3G01500	-2.6273933	AT5G27390	-1.2986562	AT4G23600	2.05136091	AT1G13195	1.00952763
AT5G44580	-1.129303	AT3G49110	-2.7657296	AT3G46660	4.91928407	AT5G62210	1.81702395
AT1G64200	-2.1599905	AT1G63470	-1.320508	AT4G11350	2.35213354	AT5G28910	1.41952643

AT5G05250	-3.5584318	AT2G34620	-1.5188734	AT5G40640	1.82000711	AT3G15357	1.83669845
AT1G77630	-1.7837835	AT1G30720	-5.9161203	AT3G61900	3.10898065	AT5G24380	1.73552239
AT5G50000	-1.2513194	AT2G18210	-4.1087907	AT1G69790	3.06901645	AT2G27300	2.54904038
AT1G65590	-2.5191274	AT1G30420	-1.9086732	AT4G10960	2.2857399	AT4G05110	5.49674668
AT3G30775	-4.0016657	AT1G57560	-4.5475244	AT1G33265	1.59392062	AT3G21600	1.27914317
AT4G04745	-4.7758673	AT2G22330	-1.5437568	AT2G39050	2.32775316	AT4G28820	1.36136873
AT1G62750	-1.2323907	AT3G56650	-1.0008146	AT3G48020	2.72938188	AT5G08510	1.24722886
AT5G56610	-1.5433721	AT3G45140	-2.0235078	AT5G02280	1.52661071	AT1G74700	1.5440844
AT1G65230	-1.2683941	AT2G40010	-2.3577782	AT5G16600	2.54082492	AT1G22640	1.00126929
AT1G09415	-1.2502648	AT2G45970	-1.3215074	AT1G06210	1.15917842	AT3G20865	4.35303978
AT3G08670	-1.4662009	AT5G13140	-1.8857383	AT3G23400	1.17265567	AT2G33585	1.07841819
AT4G08850	-2.0737105	AT1G21830	-1.0294003	AT4G37320	1.44655899	AT3G10550	1.12366169
AT1G12010	-2.3815748	AT2G43060	-1.1257295	AT1G17470	1.04194151	AT5G14380	3.31506312
AT1G67050	-1.6426862	AT1G48210	-1.149439	AT3G19500	2.95385793	AT4G25700	1.0323902
AT4G29740	-6.87935	AT4G01380	-3.6441067	AT5G46825	3.59850189	AT1G02770	1.60398722
AT5G60490	-2.469224	AT5G52830	-2.42598	AT4G27560	1.45398568	AT5G64230	1.2147073
AT4G27430	-1.186056	AT1G13170	-1.0475859	AT1G80110	2.66147951	AT4G22250	1.4695225
AT2G34430	-2.5774763	AT1G76530	-3.1797172	AT3G48690	1.46873136	AT1G02850	1.2994512
AT2G27402	-3.6593335	AT3G08920	-1.0476586	AT2G33080	2.8383016	AT1G49700	1.06694471
AT3G03990	-1.1946108	AT2G24645	-1.4720697	AT1G27200	1.46590518	AT3G07850	7.89439214
AT3G05490	-2.0252527	AT2G39330	-1.9932639	AT5G62610	1.36687133	AT2G37150	1.08678197
AT5G11920	-3.2888689	AT5G16250	-1.9275004	AT3G63520	1.11093566	AT5G62100	1.18173747
AT1G20090	-1.3971799	AT1G64625	-2.037569	AT3G05890	3.33901363	AT4G23870	1.06394001
AT2G01950	-2.3258239	AT5G25440	-1.2113772	AT2G41905	2.23522459	AT5G41460	1.37923441
AT1G11545	-3.6987301	AT4G35770	-2.1952515	AT3G10740	1.32377084	AT1G04490	5.76970688
AT3G13560	-1.926353	AT3G25730	-4.2543288	AT1G79970	1.24695953	AT1G19250	3.46781927
AT5G56530	-1.9696512	AT4G15975	-2.276721	AT1G79160	1.26208161	AT1G55020	1.2445316
AT5G52780	-1.3883106	AT2G30575	-1.3122975	AT5G42050	1.7961805	AT4G27830	1.12697338
AT1G74910	-1.4982734	AT2G38230	-1.2031842	AT5G01520	2.00469205	AT2G44260	1.47434096
AT3G47070	-1.5568512	AT1G47370	-1.9957857	AT2G12190	1.86496576	AT4G18890	1.02631887
AT1G32170	-2.4097956	AT1G12430	-1.0443454	AT1G21460	2.03999388	AT3G22410	1.86191958
AT4G05120	-2.3466359	AT2G38170	-1.0591399	AT3G20250	1.41788258	AT1G79450	1.75952322
AT1G25450	-2.6084082	AT2G23560	-5.8663	AT3G47360	2.1014756	AT1G58470	1.09349495
AT4G13840	-1.092506	AT1G62180	-1.1169177	AT3G59280	1.37978532	AT5G52390	1.26404947
AT1G68560	-1.4132782	AT5G64900	-2.0909925	AT5G02560	1.775368	AT1G18100	5.06088984
AT3G22970	-1.6596424	AT4G30560	-1.487944	AT5G07080	2.459327	AT3G27200	1.39692174
AT2G43340	-2.1322944	AT5G60210	-1.0439074	AT5G01880	1.91313475	AT3G29590	3.41862651
AT2G15890	-1.9432035	AT4G19370	-1.7618841	AT1G69610	1.62901047	AT5G13360	1.21393654
AT1G19840	-2.9770828	AT3G09020	-1.583264	AT4G30490	1.68328667	AT3G21700	1.13539526
AT5G46710	-1.7998903	AT5G17630	-1.0096218	AT1G70920	3.85888342	AT5G17220	2.9999555
AT1G47395	-3.9710928	AT5G42720	-1.2629165	AT5G45630	4.66269161	AT3G07255	5.43538389
AT4G35100	-2.087337	AT4G36550	-1.7152942	AT5G49120	4.60674112	AT5G13880	1.31269216
AT1G66180	-2.0935381	AT3G01440	-1.4632815	AT3G60690	1.40602466	AT5G41040	2.94803219
AT3G57070	-1.4757318	AT5G16170	-2.401204	AT4G39955	1.42851559	AT5G42800	2.72509971
AT5G02160	-1.8855443	AT3G19820	-1.3870225	AT3G04240	1.44768086	AT3G20340	1.23248238
AT1G67470	-1.9537941	AT3G50700	-1.0273212	AT1G67856	2.73797373	AT3G10190	1.07837743

Supplemental Table 3: List of DEGs up-and downregulated in *jar1-11* and JAR1-OE compared to Col-0 WT plants under drought stress. (DESeq, adjusted FDR < 0.01 and LogFC ≥ 1)**;** logFC with "+" or"-" sign indicates up- or downregulation respectively. "D" Drought stress

Col-0_D vs *jar1-11*_D		**Col-0_D vs *jar1-11*_D**		**Col-0_D vs *jar1-11*_D**		**Col-0_D vs *jar1-11*_D**	
AGI code	**logFC**	**AGI code**	**logFC**	**AGI code**	**logFC**	**AGI code**	**logFC**
AT2G46370	-3.5995822	AT3G15095	-1.5201846	AT3G52155	-1.1683069	AT1G21110	2.77998189
AT2G05790	-4.252827	AT3G05130	-1.4224663	AT4G20270	-2.000891	AT5G62770	1.81917452
AT3G19850	-5.4500444	AT4G03415	-1.1804923	AT5G66920	-3.0012587	AT5G66850	1.21576819
AT1G28400	-3.0171852	AT3G53260	-1.0302	AT5G67200	-2.5591253	AT3G22420	1.0327158
AT3G60530	-2.200308	AT2G47940	-1.1831484	AT4G17340	-1.8053902	AT1G63450	2.59724773
AT3G16470	-4.3880099	AT1G75460	-1.0173685	AT1G30530	-2.2659598	AT4G33150	1.24431126
AT3G18050	-3.0975452	AT2G22450	-1.0197646	AT3G63200	-2.3754573	AT3G04640	1.83394453
AT4G17460	-3.9467422	AT4G33960	-2.0499514	AT4G32890	-3.2471348	AT3G05890	2.08309973
AT4G38770	-3.8193528	AT3G45780	-1.0867231	AT5G22310	-1.5142858	AT3G16785	1.10851846
AT5G24780	-8.0421215	AT5G01740	-6.1589302	AT4G13810	-1.2578531	AT3G60130	2.24639542
AT1G20010	-4.7051394	AT5G44430	-7.1808033	AT1G65590	-2.9422401	AT5G54165	1.88868781
AT3G45140	-4.708952	AT5G40830	-1.4966022	AT3G10940	-1.1425712	AT2G30250	1.32224728
AT2G39330	-8.4782028	AT5G61660	-1.6236273	AT5G56850	-1.1468359	AT1G03370	1.39633354
AT4G38860	-5.8932868	AT1G47740	-1.2846844	AT1G49470	-1.2574278	AT3G12700	1.72108046
AT1G52400	-6.2596469	AT2G39705	-1.4903033	AT1G70370	-1.1177381	AT4G24160	1.02504434
AT3G45310	-2.1471848	AT1G76100	-1.0843443	AT1G72510	-1.3793507	AT1G64500	1.63538805
AT3G14210	-3.5413109	AT3G16140	-1.1056449	AT5G60980	-1.0337262	AT3G62260	1.24989808
AT5G60490	-7.8217422	AT3G05800	-2.4327125	AT3G25130	-5.177759	AT4G09750	1.74777645
AT5G25460	-2.8749923	AT2G40610	-6.3764333	AT3G16050	-1.1615481	AT5G51760	3.65420994
AT5G16250	-6.0170354	AT1G80640	-1.3008407	AT2G22170	-1.3633354	AT3G26200	1.94303671
AT5G10430	-3.9180239	AT2G38750	-4.2107728	AT1G29520	-1.5524854	AT3G16530	2.8136457

AT1G52030	-6.065958	AT2G41940	-1.001492	AT2G43800	-1.4796686	AT3G21305	3.88147167
AT5G01240	-2.175298	AT5G50375	-2.2656663	AT5G35930	-1.2399053	AT1G01060	2.06260939
AT1G30250	-3.8930625	AT5G20700	-1.8725998	AT2G27040	-1.2290719	AT5G25450	1.55885185
AT5G22580	-4.5374038	AT3G17040	-1.01453	AT5G10460	-1.0549687	AT4G12250	1.2010256
AT1G49430	-4.1556548	AT3G19720	-1.0939469	AT4G07995	-2.0988494	AT3G18830	1.51096667
AT1G52410	-4.8894908	AT2G22330	-2.0473484	AT1G17700	-5.4125771	AT3G26210	1.86324867
AT2G39700	-3.4657738	AT1G74470	-1.1761927	AT2G27060	-1.5449265	AT5G27420	2.35859158
AT2G28950	-3.5570804	AT1G12080	-4.1128487	AT5G27300	-1.18216	AT5G39660	1.27842016
AT5G49730	-2.0685458	AT5G64330	-1.3651818	AT5G18030	-1.9581867	AT5G40780	1.56058537
AT3G28220	-5.9924102	AT1G02290	-1.3449747	AT4G12420	-1.8093434	AT4G08555	3.53269998
AT2G24762	-3.0495487	AT1G78170	-2.1212979	AT5G24920	-1.8074814	AT3G49780	2.26230959
AT2G38120	-2.5655329	AT2G37090	-2.8868137	AT1G65860	-1.9691739	AT5G44310	1.91305009
AT4G39710	-2.9427727	AT5G11790	-1.1054369	AT3G61880	-1.8688918	AT1G60470	3.76872049
AT1G76800	-2.4563146	AT2G19170	-3.5934954	AT3G62860	-2.2357414	AT5G62580	1.15760305
AT1G72260	-7.680471	AT3G06430	-1.0177795	AT3G46550	-1.3200583	AT4G26060	1.30000184
AT1G17140	-3.3557218	AT2G21050	-2.210577	AT4G15540	-1.1073864	AT1G19270	1.45229944
AT1G23080	-2.3480972	AT1G50900	-1.2072987	AT5G38360	-1.1123314	AT2G04400	1.32114766
AT1G15820	-2.1716325	AT3G46890	-4.2215648	AT5G23580	-1.2880969	AT5G16360	1.4584376
AT3G26520	-2.7872329	AT5G51890	-1.8487314	AT2G38540	-1.0387818	AT1G07540	3.02394625
AT4G35320	-3.4829485	AT4G18370	-1.0768364	AT4G19985	-1.0853977	AT2G33110	1.47014621
AT3G59010	-3.3445312	AT3G52370	-5.8907461	AT1G77700	-2.845053	AT1G14730	1.15270927
AT3G55500	-4.7120602	AT2G24790	-1.3421163	AT1G65450	-5.5133063	AT4G17720	1.3712331
AT1G74430	-4.1105986	AT3G02020	-2.3548948	AT1G09390	-2.7612441	AT1G32928	1.83114367
AT1G75500	-2.6173489	AT3G63140	-1.1911203	AT1G62540	-1.6675332	AT4G26270	1.51268145
AT5G55730	-5.1317381	AT4G25890	-1.3750953	AT5G15270	-1.167723	AT3G11050	1.86149246
AT5G13140	-5.1887188	AT5G64860	-1.1591352	AT1G60060	-2.4407995	AT5G58730	1.28663818
AT1G13250	-3.9914233	AT5G19940	-1.0517044	AT2G44850	-1.2705605	AT4G01870	2.24872797
AT5G49555	-2.058665	AT3G14420	-1.0075244	AT5G17520	-1.1846385	AT5G14330	5.22055533
AT4G32280	-2.9567478	AT1G24764	-1.1658266	AT5G02060	-1.9189113	AT5G26030	1.08776164
AT4G21650	-3.9791263	AT4G36280	-1.9234277	AT2G01520	-7.1457723	AT1G10740	1.19818776
AT1G69850	-1.7169601	AT2G36870	-2.5509549	AT5G63810	-1.4340262	AT4G30060	1.91909391
AT5G55620	-2.6616415	AT2G25820	-3.466798	AT4G36180	-1.6383649	AT4G11521	2.29318032
AT2G15090	-3.7464477	AT3G27740	-1.2886643	AT5G58520	-1.1878611	AT1G02820	2.08885905
AT4G04340	-1.7364415	AT5G13000	-1.4950868	AT2G37585	-1.1238085	AT5G64080	1.32429215
AT1G19670	-3.7076328	AT5G60210	-1.451056	AT2G21530	-1.4516768	AT1G69550	1.17469653
AT4G10340	-2.4072377	AT3G27030	-2.08721	AT3G05980	-4.1753482	AT3G49210	1.10316197
AT2G04780	-3.8880814	AT5G19770	-1.1167868	AT3G13980	-1.6997494	AT3G53990	1.03402827
AT4G34090	-2.4144248	AT3G22970	-1.4783668	AT5G56500	-1.0769433	AT5G22300	2.19292929
AT4G05180	-2.2675436	AT1G75280	-1.7647311	AT4G27240	-1.2404063	AT1G23280	1.12781595
AT3G21055	-1.9629185	AT5G18020	-4.1181101	AT3G16400	-1.147455	AT5G65980	4.60975445
AT3G12145	-8.1480752	AT5G19670	-1.5464453	AT1G28110	-2.0610679	AT4G34150	1.5843379
AT5G44130	-3.0207717	AT1G54200	-1.8335276	AT2G28315	-3.3450169	AT3G03620	2.48037977
AT1G78970	-4.5147847	AT3G07200	-1.230161	AT4G14096	-1.2603406	AT4G22530	1.7963419
AT2G43530	-4.0733833	AT2G37640	-5.7737196	AT5G38150	-1.0237319	AT5G54710	2.43561822
AT1G43580	-1.9173874	AT1G20840	-1.3280663	AT3G25905	-5.2607341	AT3G27540	1.45189366
AT1G78060	-1.7357324	AT2G41650	-1.0444507	AT4G35350	-2.2866011	AT1G68795	2.38811816
AT1G11850	-4.2552948	AT5G08000	-2.1784401	AT1G60000	-1.1368061	AT1G14520	1.50302244
AT5G03170	-3.3845943	AT1G73760	-1.0347691	AT2G41290	-1.4282049	AT5G57910	1.37896251
AT4G17190	-2.2783216	AT4G37080	-1.2907548	AT1G05200	-1.0658006	AT5G43630	1.82766278
AT4G39330	-3.0204057	AT4G32460	-1.1144152	AT3G57070	-1.0413918	AT1G01480	2.82189665
AT1G56220	-1.3264562	AT4G16340	-1.1320139	AT1G26290	-2.2738227	AT2G20560	1.71386466
AT4G26530	-2.6464484	AT3G58990	-2.5064234	AT2G44210	-1.0598719	AT5G55560	1.52718333
AT5G57340	-2.7211446	AT1G07920	-1.1070377	AT5G04200	-1.3886358	AT3G28340	3.10975034
AT3G55240	-3.4034657	AT1G21050	-2.5631105	AT4G18440	-1.1425646	AT5G51130	1.38703635
AT1G14380	-1.9819054	AT1G03820	-3.0408159	AT3G52770	-1.6303402	AT2G13790	1.31277323
AT1G68520	-2.1605913	AT2G42530	-1.6108136	AT1G29160	-1.3864052	AT5G47050	1.69163405
AT5G12050	-4.6243567	AT3G05470	-5.0689169	AT1G16960	-1.2186237	AT1G17020	1.53397725
AT1G72480	-1.8553759	AT2G36230	-1.3499626	AT5G64550	-1.3425108	AT5G41740	2.61544947
AT4G11320	-6.4660697	AT4G37660	-1.1261458	AT1G61600	-1.7230257	AT1G28190	1.90667113
AT5G46330	-2.2624294	AT5G25980	-1.1816386	AT4G10380	-1.3193114	AT5G11650	1.53072531
AT4G08870	-2.6833736	AT5G18080	-2.5791043	AT4G15210	-2.1705768	AT1G71140	1.52678792
AT1G25440	-2.2458875	AT5G42070	-1.4902602	AT2G40316	-1.0368825	AT2G02060	1.00547448
AT4G28250	-5.0360002	AT3G13690	-1.2440986	AT3G53750	-1.2001712	AT3G15740	3.19091622
AT3G28040	-2.8985825	AT4G30410	-4.1968691	AT1G63295	-1.5970412	AT1G20440	1.26023627
AT4G40060	-1.5695042	AT3G52900	-2.3319124	AT3G49260	-1.3072873	AT3G57450	1.56328102
AT5G19090	-3.5143661	AT2G22430	-1.0933084	AT1G67265	-1.0376714	AT4G20320	1.53879511
AT3G23450	-3.6371821	AT2G43010	-1.2823884	AT1G62660	-1.0321054	AT3G02240	3.80140614
AT1G78150	-1.3462737	AT3G50440	-1.8285135	AT5G11750	-1.1779508	AT5G01600	1.39581296
AT1G70280	-2.440011	AT2G31010	-3.3294699	AT2G18730	-1.2397625	AT1G72900	2.23182807
AT5G15310	-3.3034876	AT3G28070	-1.6931948	AT2G47180	-1.236099	AT5G19080	1.30173124
AT3G08920	-2.0162617	AT1G19835	-1.0353832	AT3G63210	-1.1020586	AT1G19020	2.80093118
AT1G26150	-2.1293934	AT2G22190	-1.8360067	AT1G51440	-1.8768887	AT5G44380	4.94658969
AT1G54690	-1.7892591	AT5G12900	-2.5716636	AT4G10390	-2.6602456	AT3G46680	6.24411721
AT5G01020	-1.4960048	AT3G26650	-1.380473	AT4G25870	-1.4525694	AT1G01340	2.56548475
AT1G24070	-5.7469218	AT4G30400	-2.6283409	AT3G49250	-1.6091899	AT4G14365	2.30655161
AT1G55670	-1.870213	AT5G15970	-1.4877539	AT1G70710	-1.8864722	AT5G55750	2.95959603

AT5G03760	-3.7082518	AT4G37925	-1.3523152	AT5G13460	-1.0273681	AT5G61210	1.17999054
AT5G57180	-1.6959201	AT5G60400	-1.2140871	AT4G03150	-1.0708895	AT1G11310	1.04688295
AT1G43790	-1.669109	AT2G32720	-1.365783	AT5G56990	-2.2073381	AT5G58120	1.15521892
AT1G72610	-3.0382343	AT5G09240	-1.4508183	AT3G61950	-3.3741816	AT1G22340	1.86684478
AT3G20820	-2.3976576	AT5G09870	-1.1096554	AT4G32480	-1.4335811	AT1G50260	1.41113207
AT1G01620	-2.2450382	AT5G03830	-1.3422348	AT3G23480	-1.0058991	AT4G12400	1.56401312
AT1G32540	-3.0054594	AT1G18880	-2.9990353	AT5G08640	-1.5969778	AT3G50970	1.65813915
AT4G36540	-3.6005459	AT5G49215	-1.944715	AT5G46690	-2.7677488	AT1G18300	2.29144149
AT2G32990	-5.2113939	AT5G41920	-1.2273882	AT5G24660	-1.4836487	AT3G59700	1.02621187
AT2G37930	-1.7202616	AT2G45970	-2.0159843	AT4G18970	-2.322715	AT4G33420	2.54034199
AT1G51400	-1.7969417	AT4G22300	-1.287014	AT4G37650	-1.0588318	AT2G36950	1.30153834
AT4G18780	-2.8080676	AT1G29530	-1.5615092	AT1G62990	-1.6557122	AT3G60420	5.39230573
AT1G66150	-1.5238316	AT3G47860	-1.1582892	AT5G48720	-1.0793708	AT1G23480	2.32227771
AT5G23100	-2.6943326	AT3G49930	-4.1143582	AT5G05960	-1.5729807	AT3G11402	2.14982472
AT5G14920	-2.6469985	AT3G14410	-1.1599489	AT3G43960	-5.2165915	AT3G54130	1.45098059
AT2G45340	-2.9029689	AT1G31550	-2.0924069	ATCG01010	-1.2421334	AT1G75000	1.74209248
AT4G34220	-3.3789291	AT3G14150	-1.6174392	AT1G33800	-1.5646867	AT5G56160	1.32203972
AT5G12250	-1.7918676	AT1G60010	-1.1688809	AT3G07540	-2.1833576	AT2G32210	2.74046115
AT5G18460	-1.912236	AT3G17310	-1.1971355	AT5G14200	-1.2019027	AT1G09970	1.25133615
AT3G28130	-2.1660272	AT3G19370	-1.4190207	AT5G62900	-1.0558807	AT3G13600	4.03107305
AT1G74690	-1.8211918	AT5G50010	-6.1253493	AT1G74670	-2.3348234	AT5G54490	2.42700213
AT5G02940	-2.6438613	AT3G18090	-2.6726174	AT1G06960	-1.2761683	AT1G74590	3.25809117
AT3G21550	-3.0075219	AT5G44420	-6.8542885	AT3G51325	-3.8182664	AT2G20320	1.02055761
AT5G55230	-1.7667404	AT2G40130	-1.5027298	AT5G25830	-5.7964232	AT5G02270	1.10433065
AT4G23060	-2.6690455	AT1G31710	-3.1251211	AT5G65730	-2.7091652	AT1G23550	1.80860777
AT1G14280	-1.8552041	AT2G24290	-1.4166929	AT5G15630	-2.2001854	AT1G65690	2.17369499
AT5G50335	-7.3438397	AT2G25060	-3.5932331	AT4G25830	-1.3809995	AT3G55610	1.11299594
AT1G22885	-1.5393236	AT3G43540	-1.2025071	AT5G06050	-1.0142735	AT4G39670	3.57958066
AT3G18080	-1.9474367	AT3G55360	-1.0590986	AT2G47160	-1.5513955	AT1G29680	2.0929568
AT2G38970	-2.1383815	AT2G38170	-1.207255	AT3G25760	-1.7068522	AT1G10990	1.94960843
AT5G21430	-1.7760938	AT2G22980	-1.6764835	AT5G27550	-2.7984396	AT3G28850	1.31938422
AT5G15230	-5.2297696	AT3G59400	-1.7716791	AT5G13220	-2.0050199	AT1G66090	2.66862663
AT3G15530	-1.521338	AT4G31310	-1.0983374	AT2G33330	-3.2450378	AT5G35735	1.69666494
AT2G15050	-2.1338813	AT3G44716	-1.9654338	AT3G44220	-2.7674159	AT3G19970	2.05592147
AT5G42765	-1.4929224	AT1G29500	-2.0245534	AT3G12520	-1.6068436	AT5G67080	2.61589858
AT4G27860	-3.3486724	AT5G63780	-1.785753	AT3G05410	-1.1221179	AT4G04220	2.56172087
AT2G26910	-1.5710788	AT5G21100	-1.9913478	AT5G39790	-1.1535549	AT2G15480	1.2643893
AT1G29930	-1.8000955	AT5G63700	-1.3295223	AT4G17770	-1.4407547	AT4G26940	1.02900633
AT1G52040	-5.7531223	AT1G49010	-1.5363458	AT1G67830	-1.9896721	AT1G80840	2.21904652
AT1G11860	-1.9200093	AT4G37450	-2.5013262	AT1G69420	-1.1629072	AT5G53970	1.12373691
AT4G28706	-1.7228219	AT3G46970	-1.1776597	AT4G19120	-1.1202427	AT3G55630	1.01283144
AT5G06530	-1.7725144	AT4G23690	-4.0077769	AT4G37890	-1.6786581	AT3G13433	3.04777181
AT2G29630	-1.6638345	AT4G00740	-1.2909695	AT2G46300	-3.3880866	AT5G46960	3.9771523
AT1G08380	-1.3287283	AT5G48580	-1.0542515	AT3G20898	-1.8981062	AT1G09500	3.11067005
AT1G21500	-1.6594965	AT5G45670	-5.1898652	AT5G64410	-1.8467641	AT2G36780	3.75365911
AT1G65010	-1.895637	AT1G11680	-1.103777	AT4G23800	-2.2359958	AT4G13510	1.41532035
AT3G09035	-2.2348332	AT3G52750	-1.416623	AT1G77990	-1.3872216	AT4G07408	1.27843299
AT5G16030	-2.026834	AT3G20570	-1.934275	AT1G18620	-1.1877496	AT1G52565	2.41900387
AT1G06680	-1.5503907	AT4G04630	-1.9153708	AT5G63650	-3.1547866	AT3G17010	3.15967046
AT1G70100	-1.4794091	AT2G39280	-1.2356835	AT1G21090	-1.8592679	AT3G04010	1.6223572
AT4G01900	-1.8370037	AT3G28860	-1.3549582	AT3G22120	-1.2266385	AT4G39950	2.61817235
AT2G32690	-1.9362911	AT5G39240	-3.33748	AT1G67710	-1.669796	AT2G41640	1.89425424
AT4G28050	-1.9432785	AT4G32710	-1.9294655	AT2G32860	-1.0366167	AT1G37130	1.70874422
AT2G01910	-1.8008106	AT4G24275	-2.3077136	AT3G48720	-3.1420896	AT4G24400	1.00637768
AT2G29290	-2.9049828	AT4G20360	-1.4176584	AT4G28630	-1.0207755	AT2G36420	1.23972275
AT5G35480	-2.2458061	AT3G56120	-1.7390353	AT4G23820	-1.9913864	AT1G60730	1.47860354
AT5G67070	-1.7827533	AT2G27590	-1.2237631	AT5G42680	-1.4047983	AT3G22600	3.4158589
AT5G24770	-5.7741759	AT3G57785	-1.0854654	AT3G48440	-1.2822848	AT4G33050	1.75934454
AT1G49230	-2.4472759	AT2G20870	-8.0973185	AT4G35335	-1.1006808	AT5G12930	1.6848712
AT3G57062	-1.5255437	AT2G36390	-1.2478431	AT1G29170	-1.5368493	AT2G45220	3.56258282
AT2G46640	-3.2626902	AT2G05160	-2.9052381	AT5G62230	-3.9160273	AT3G49055	3.71668114
AT5G50740	-3.4119027	AT1G77590	-1.4906466	AT5G10150	-1.6584354	AT3G20600	1.29495074
AT3G01500	-2.8548675	AT2G28790	-2.508677	AT1G18650	-1.4290764	AT5G01550	3.6418636
AT3G46780	-2.119763	AT3G25980	-6.1098466	AT4G25100	-1.09004	AT2G02010	3.53354137
AT4G27440	-1.4340185	AT2G23360	-2.4969429	AT1G18710	-1.8037895	AT5G45810	3.35736951
AT2G29510	-1.3387876	AT1G12000	-1.2754565	AT4G28360	-1.1723765	AT2G34580	3.50396954
AT5G28020	-2.3743715	AT2G29125	-3.0473549	AT3G20015	-1.9352589	AT3G53810	1.50970253
AT1G70700	-2.2575164	AT1G25230	-1.760487	AT1G17190	-1.2124176	AT5G56980	1.04187975
AT4G14200	-3.39915	AT1G78490	-1.3719953	AT2G24440	-1.6359818	AT1G75960	2.92361492
AT1G01080	-1.7722808	AT5G42650	-1.6390967	AT2G02100	-1.2961779	AT3G13430	1.42551271
AT5G08330	-1.7099527	AT1G45207	-1.9535525	AT2G47500	-2.3447908	AT4G08545	3.04641442
AT1G10760	-1.5754714	AT1G68560	-1.1063848	AT3G05600	-6.3049486	AT1G36622	3.10884628
AT3G48670	-1.4593429	AT1G12090	-1.2474515	AT2G03500	-1.1472748	AT4G37010	2.65151588
AT4G21960	-2.5627106	AT3G03190	-2.5064371	AT1G57700	-1.4816338	AT1G72680	1.49403598
AT5G08260	-1.5347401	AT5G54530	-4.1126793	AT3G54720	-1.1878888	AT3G11080	1.55281992
AT1G67090	-2.0611712	AT5G66460	-1.2556933	AT4G26540	-2.1926216	AT3G07600	3.51259809

AT3G20470	-3.8590157	AT4G19170	-1.6682452	AT3G28500	-2.0361907	AT5G64430	1.19141404
AT4G08685	-2.3578248	AT4G22290	-1.5462524	AT1G67510	-1.4035489	AT5G51830	1.16476848
AT4G12880	-2.8322895	AT1G72430	-1.2086476	AT2G13690	-1.104659	AT4G39890	1.43037929
AT1G04040	-3.1408856	AT5G24620	-1.2602041	AT4G20940	-5.03142	AT1G60970	1.3087175
AT5G65700	-2.0122579	AT1G76460	-1.1373654	AT5G57100	-1.3397268	AT3G45650	2.39456888
AT1G60230	-1.9446277	AT3G03040	-1.0879722	AT3G04443	-2.1300788	AT5G62480	1.645463
AT3G04290	-6.6944828	AT1G74800	-1.170906	AT4G16590	-6.7075032	AT2G23110	3.08265272
AT5G51550	-2.3454185	AT5G33370	-8.7943766	AT1G68780	-3.1223104	AT1G54100	1.19156921
AT3G14240	-1.9562409	AT5G23820	-3.500542	AT2G35120	-1.2987159	AT1G48370	1.35603025
AT1G05590	-1.9033243	AT1G16920	-1.1694077	AT5G11540	-3.9317478	AT1G78410	2.49270045
AT3G06130	-3.5090316	AT5G21222	-1.1217077	AT2G22770	-3.2961284	AT4G22590	1.34627495
AT5G24420	-5.4607696	AT4G00380	-2.4434825	AT3G05730	-2.6928551	AT2G30770	4.09375165
AT4G26760	-6.8831217	AT2G37230	-1.6049691	AT1G62670	-1.821588	AT3G17420	1.70112412
AT1G49750	-1.7037352	AT2G24350	-2.026083	AT5G24490	-1.356771	AT5G54780	1.3732696
AT2G28760	-2.2900234	AT3G62750	-1.1055374	AT1G19330	-1.3979394	AT1G21790	1.006362
AT4G13100	-1.9672369	AT5G19580	-3.0701379	AT3G56570	-1.4028336	AT3G21690	1.10768349
AT5G60200	-2.4919135	AT1G30380	-1.0602789	AT1G14890	-1.0955219	AT1G69890	1.24639918
AT2G39730	-1.3376897	AT1G12570	-6.9781394	AT5G15780	-1.3443094	AT5G55930	1.74140939
AT5G41600	-1.4168373	AT3G50240	-1.3960063	AT1G10657	-1.745593	AT5G54510	1.6479001
AT5G02120	-1.6186203	AT5G65640	-2.2118614	AT5G66590	-1.2676881	AT2G32030	2.70520246
AT5G66570	-1.4025648	AT4G23790	-1.4013593	AT5G43870	-1.4709928	AT5G17450	1.38376532
AT5G27950	-1.4890639	AT1G29450	-4.020153	AT5G60850	-1.2116175	AT2G29990	1.15002352
AT5G16720	-2.7666348	AT1G12500	-1.1458769	AT3G45850	-1.6231238	AT1G30860	1.54988809
AT4G38840	-2.4169651	AT4G35160	-5.2521422	AT1G10970	-1.4573072	AT2G44450	4.53714043
AT3G27690	-2.3456696	AT1G11350	-1.0790245	AT4G11450	-1.5916765	AT3G56400	2.14233342
AT1G70210	-2.4299663	AT3G14310	-1.3625151	AT5G27360	-3.6346365	AT2G21590	1.08672437
AT2G28660	-2.2237214	AT2G22230	-1.2748685	AT5G61130	-1.0947528	AT5G19850	1.246848
AT4G39350	-1.4702075	AT1G71180	-1.176204	AT5G56590	-1.6278184	AT2G30750	3.24342151
AT3G18890	-1.8377407	AT5G10310	-2.0068135	AT4G38670	-1.2885835	AT4G06746	2.95849118
AT3G19620	-3.0888193	AT1G74880	-1.0723733	AT3G20260	-2.8769873	AT5G13320	3.210036
AT4G30020	-2.7806592	AT1G26100	-2.4905812	AT1G05810	-2.8681265	AT5G22540	1.80073841
AT2G34680	-1.8235668	AT5G62630	-1.3932357	AT5G39320	-1.6293779	AT2G43290	1.20152767
AT4G11211	-3.1224988	AT2G36570	-2.3888296	AT1G27120	-3.6442606	AT1G21240	3.26610173
AT5G54270	-1.710377	AT5G03200	-1.0759303	AT3G06160	-5.2773737	AT1G07000	1.58386902
AT1G19350	-1.8283914	AT5G65390	-3.9835668	AT2G23590	-3.3241477	AT1G02920	2.6522616
AT3G17840	-3.1097182	AT2G27230	-1.2844045	AT2G39980	-1.2919702	AT1G02930	2.19946187
AT5G64260	-2.1722374	AT5G66310	-2.4812576	AT5G44620	-7.0058562	AT4G23250	1.33948673
AT3G08940	-1.5658259	AT2G10940	-3.8108068	AT4G24930	-1.170215	AT5G22060	1.26223752
AT2G36145	-1.5951869	AT5G23860	-1.3925149	AT3G43670	-1.0060773	AT2G32250	1.10278766
AT1G04680	-3.422226	AT5G22740	-1.3093677	AT4G36270	-2.5229183	AT1G53625	3.74550292
AT1G31330	-1.3897521	AT4G16141	-1.7206444	AT1G10030	-1.2791515	AT4G26470	2.59754478
AT5G44030	-2.3436293	AT2G44940	-2.3163233	AT4G24350	-2.2908687	AT5G54650	1.62604452
AT5G57685	-2.8575976	AT2G41340	-2.761662	AT5G38010	-3.5192249	AT5G42050	1.20296786
AT1G11580	-2.0651318	AT5G58600	-1.114825	AT4G01580	-2.3424231	AT2G28890	1.26770403
AT2G45180	-2.4037615	AT2G47240	-1.5686768	AT3G20865	-4.3122664	AT3G17700	1.2683238
AT1G09340	-1.4962893	AT5G58390	-3.4389548	AT5G07560	-6.3443718	AT1G35210	2.27493957
AT3G16370	-1.968117	AT1G74070	-1.4787292	AT5G25475	-1.2349634	AT3G57480	1.15618799
AT1G50280	-6.4063521	AT3G51950	-1.1603791	AT1G34065	-2.4376899	AT5G56150	1.02353661
AT1G51570	-1.2258506	AT2G35780	-1.104466	AT1G48175	-1.3086746	AT1G73805	2.47787068
AT1G27520	-1.196012	AT1G76790	-1.6868095	AT5G15120	-2.1535417	AT4G28290	1.38876714
AT5G09460	-1.432898	AT3G02180	-1.0575914	AT1G27480	-1.1809671	AT4G35070	1.45335892
AT3G16240	-4.1287876	AT3G17070	-1.9025298	AT1G77490	-1.3695035	AT1G32170	1.74098726
AT5G67420	-1.4290286	AT5G21930	-1.5161195	AT1G11440	-1.0631787	AT2G41380	1.45734477
AT1G28290	-5.0394822	AT4G28780	-3.4369812	AT4G14310	-2.1721077	AT5G46520	1.55958022
AT3G18660	-3.4776411	AT5G35170	-1.0312935	AT1G26540	-5.2431617	AT5G38710	2.11545248
AT2G36830	-2.9256127	AT5G22940	-5.6593884	AT4G01080	-2.3760373	AT1G02220	2.9476411
AT1G24020	-4.5851141	AT1G29980	-1.8895723	AT5G60670	-1.0660566	AT3G11773	3.37451939
AT1G51940	-1.8536826	AT1G11220	-4.2720029	AT2G01080	-1.2567553	AT3G47090	1.57349634
AT1G05460	-1.9386369	AT2G42220	-1.7823337	AT1G62030	-1.1821746	AT5G52740	2.62581683
AT1G52000	-5.0376567	AT1G72275	-1.2639406	AT5G65683	-1.6487266	AT4G11550	4.3182132
AT1G20190	-2.5604074	AT4G29020	-1.9600618	AT4G19070	-1.0809674	AT4G03820	1.32945857
AT3G19820	-2.1103178	AT5G67210	-3.4793898	AT3G05910	-1.1127135	AT1G80610	1.12947461
AT4G24780	-2.9064058	AT1G75710	-1.9835843	AT5G66560	-1.4510784	AT3G56710	1.52948004
AT1G20340	-1.4393549	AT1G42970	-1.1062393	AT5G46295	8.92616638	AT2G11810	2.37331417
AT1G74940	-2.0140426	AT2G46890	-1.8878869	AT3G57010	2.40543591	AT1G56060	3.66652219
AT4G12730	-6.3909082	AT1G69080	-3.5809768	AT3G27380	1.88920502	AT2G36790	1.88791958
AT5G50950	-2.4887001	AT5G02200	-3.3482532	AT2G22470	3.27985492	AT3G22910	2.61306579
AT5G10800	-2.4659574	AT1G72450	-1.7813465	AT5G22460	1.86898408	AT1G79680	2.42064598
AT5G50420	-2.1657056	AT5G18060	-5.5870069	AT1G68440	3.06700235	AT1G24140	2.06857901
AT2G42690	-1.9228963	AT3G01440	-1.802942	AT3G22840	3.03989806	AT2G27389	3.85277805
AT1G73660	-1.4359972	AT5G48545	-1.1643866	AT1G27760	1.78802582	AT3G09440	1.74930844
AT4G14440	-1.9970618	AT3G16420	-1.9790256	AT5G25130	2.77335745	AT1G02310	2.20027338
AT4G37800	-5.1940977	AT1G01120	-1.7620789	AT3G24170	1.79169558	AT5G41750	2.06712052
AT1G47670	-2.7271839	AT3G50685	-1.1860797	AT2G20625	7.30951079	AT3G53160	3.60605129
AT1G73870	-2.7102941	AT3G24040	-1.3295652	AT3G07090	1.81700455	AT1G62380	1.33140413
AT2G33860	-1.5528061	AT3G08890	-1.1166065	AT1G32920	2.62324062	AT5G02780	3.53851685

AT1G64390	-2.8129977	AT2G44830	-4.0100724	AT1G15430	2.17985238	AT5G01300	1.41901962
AT2G38080	-2.9959773	AT1G65370	-1.3951452	AT3G22370	2.02486501	AT5G09800	2.68740181
AT5G19151	-1.5265215	AT5G43750	-1.4388482	AT5G27760	1.92286797	AT2G26190	1.51773752
AT3G01810	-1.7923285	AT4G16447	-2.0569041	AT5G64310	3.16088979	AT2G24550	1.10602374
AT1G67750	-4.4393805	AT2G24690	-1.0104718	AT2G33520	3.74819594	AT3G04060	1.32703549
AT5G01790	-3.8641107	AT5G23280	-1.321526	AT4G10040	1.91499752	AT4G33467	1.95268213
AT4G00360	-1.8939697	AT1G65420	-1.3774725	AT1G30620	2.18465584	AT2G36770	2.27395354
AT5G01530	-1.4774209	AT4G15920	-1.2018125	AT5G05220	3.05374413	AT4G03230	1.16072326
AT5G42100	-1.7275616	AT5G14450	-1.371433	AT3G22490	5.3340097	AT2G29750	2.78280107
AT5G07030	-2.5694819	AT4G21326	-1.4979572	AT4G02410	1.82140875	AT3G13790	3.51827974
AT4G21280	-1.6176462	AT1G11800	-1.5004245	AT3G01650	1.90363033	AT5G06730	3.2182106
AT1G06010	-1.3963548	AT2G16750	-3.2413539	AT5G62610	1.33444193	AT5G65300	1.35636347
AT1G26945	-2.8487409	AT1G29840	-1.976952	AT5G46080	2.43489569	AT4G26990	1.28345888
AT5G18210	-1.8670591	AT4G39190	-1.7093293	AT2G41730	3.2343916	AT2G35730	2.85912482
AT1G54020	-5.7593802	AT1G13790	-2.6144769	AT5G15470	1.85356228	AT5G59845	1.51888689
AT5G46700	-3.0461652	AT2G40030	-1.506552	AT2G31570	1.63738975	AT3G21780	1.44012841
AT3G54790	-1.277228	AT1G44110	-5.6002457	AT2G30040	2.47041835	AT2G25000	1.72369892
AT3G17210	-1.3728328	AT2G35620	-1.468146	AT3G52360	2.10821596	AT5G39720	2.05998829
AT3G61100	-2.5698777	AT4G23930	-1.4199982	AT5G08790	2.37602398	AT3G49120	1.21792103
AT1G55360	-1.8809637	AT5G65090	-3.6699788	AT2G18680	2.85420959	AT1G66160	3.04850788
AT3G53850	-1.6563913	AT3G02110	-1.6751167	AT3G23530	3.26229283	AT2G33580	1.60964567
AT2G34490	-4.0287325	AT3G11490	-1.1428256	AT1G03790	4.17788622	AT2G37770	1.74326185
AT2G32280	-3.7295381	AT5G58480	-2.0249207	AT1G78380	1.6695076	AT2G38640	1.23404547
AT5G02190	-2.9909565	AT1G25480	-1.6261141	AT3G57020	2.50397788	AT1G67520	2.71433809
AT2G05070	-2.0586043	AT2G26330	-1.2269617	AT1G30755	2.00140225	AT4G21390	2.87900813
AT4G13500	-1.7198864	AT1G47410	-2.6920734	AT2G01340	2.24838092	AT5G27520	1.05303139
AT1G68220	-1.8392057	AT3G45160	-1.7864216	AT5G62540	1.20904289	AT4G14370	2.91694277
AT4G21910	-2.0893342	AT5G49330	-1.8470737	AT1G66500	1.86425678	AT5G38250	3.21879846
AT1G79500	-2.0298373	AT5G63470	-1.2771682	AT1G69610	1.54895523	AT2G38860	1.73632686
AT1G30260	-1.1912534	AT3G27420	-1.1789469	AT1G23710	1.94678197	AT4G01950	1.63809563
AT3G02170	-2.4581752	AT1G78820	-1.2486861	AT3G06420	1.89759949	AT4G30490	1.06906051
AT5G67150	-2.4555509	AT3G20810	-1.1744961	AT1G27461	3.77715188	AT4G23470	1.29648097
AT2G01760	-2.5663064	AT5G14220	-1.2577282	AT1G74020	2.58156579	AT4G08470	1.00331255
AT4G25080	-1.5308828	AT3G53760	-1.8275011	AT3G15760	2.58697231	AT2G25460	2.53254996
AT3G02050	-1.5256374	AT4G17810	-2.5063676	AT3G07390	2.17182745	AT5G49560	2.54149896
AT1G63300	-3.4657443	AT2G44130	-1.1502782	AT5G66760	1.25491179	AT2G42900	3.73040978
AT4G33220	-2.0935474	AT1G53070	-2.8574839	AT2G33700	1.49580403	AT5G26690	2.71065396
AT3G01690	-1.4099258	AT5G44680	-1.4532433	AT5G11740	1.55188502	AT3G09010	2.28388372
AT3G46990	-2.2280237	AT3G52500	-1.7285512	AT4G31800	2.44992524	AT2G36970	1.32648465
AT3G10080	-3.1544596	AT3G13120	-1.1060659	AT5G58350	1.91575182	AT5G59550	1.01750498
AT2G30424	-3.6270864	AT1G72230	-2.3616429	AT2G41880	1.30021357	AT2G38490	3.42562479
AT5G37790	-3.2746009	AT2G35430	-1.1900451	AT1G09940	1.55161966	AT5G40880	1.87268932
AT3G24770	-1.925884	AT3G57600	-1.8276129	AT1G70740	1.87967384	AT2G26150	2.48061693
AT2G14890	-2.0665455	AT1G11950	-1.6410645	AT3G04210	2.34330989	AT3G51960	1.11179623
AT2G02790	-2.0632137	AT5G26570	-1.052553	AT4G04610	2.31189381	AT2G29460	2.44127155
AT1G75800	-1.6919352	AT3G28840	-2.5306655	AT5G20830	1.92446886	AT1G05680	2.81637111
AT3G17120	-2.4008221	AT1G08660	-1.164137	AT5G22470	3.7490568	AT2G47820	1.4289214
AT5G14060	-1.5123498	AT1G67910	-2.305199	AT4G35090	1.34046545	AT5G17300	1.72274872
AT5G47240	-2.1184255	AT1G21560	-1.8116124	AT2G38470	2.61840908	AT4G16400	1.94329018
AT5G63180	-3.9473579	AT1G72500	-1.1834304	AT2G36630	1.96634901	AT3G25882	2.31108997
AT1G45201	-2.2831951	AT1G04250	-1.6480548	AT3G13520	2.11090276	AT4G23180	1.20369476
AT2G04570	-3.1145969	AT1G68130	-1.4630268	AT2G37940	1.44266123	AT1G61800	2.61376938
AT5G16290	-1.5913833	AT1G60770	-1.0309972	AT1G05340	2.31574729	AT1G67340	1.15196707
AT1G29670	-2.2446283	AT4G14480	-1.2980068	AT3G24503	1.91294818	AT4G21020	2.43357885
AT5G44565	-2.1167494	AT4G16780	-1.6837666	AT1G14330	2.01143657	AT3G62720	1.34666861
AT3G61820	-1.9331445	AT2G40480	-2.2162137	AT5G43450	2.45795858	AT3G19260	1.08289874
AT4G22120	-2.0954862	AT1G13280	-1.1832609	AT3G12620	1.50290054	AT5G61560	1.09984615
AT5G42240	-1.203206	AT1G11120	-3.5162524	AT5G54870	1.0989574	AT4G15270	2.15884288
AT3G59060	-1.7279006	AT4G19020	-1.7045374	AT5G58320	1.93407148	AT1G19440	1.30578628
AT2G32520	-1.2414598	AT5G20450	-1.1385944	AT3G61450	2.23986108	AT1G15670	1.55127488
AT5G62890	-1.4878893	AT5G15580	-2.227256	AT3G46230	2.73712572	AT4G17840	1.04419968
AT5G38410	-2.0284527	AT2G30620	-1.0273276	AT5G22690	1.9829382	AT5G25930	2.08747551
AT4G14890	-1.2811514	AT1G29450	-4.020153	AT5G37550	2.31452613	AT2G41110	1.40962348
AT5G09995	-2.1867507	AT4G35950	-1.1942054	AT3G08720	1.68658453	AT4G33930	6.11598368
AT3G16920	-2.117371	AT5G17420	-2.2205795	AT1G66400	2.98119614	AT5G13330	1.36828908
AT4G03210	-3.2687979	AT1G33240	-1.1000201	AT3G04200	6.22603364	AT5G49450	1.33081519
AT1G26560	-1.4442492	AT3G28100	-1.0749259	AT3G16030	1.58327192	AT1G77890	1.34352568
AT2G25900	-1.5635188	AT5G14410	-1.5424691	AT5G01670	1.32627988	AT5G18350	2.76773189
AT3G56370	-2.754728	AT3G58070	-1.5723453	AT4G20860	2.76740816	AT1G80450	1.4782836
AT1G52190	-2.7681168	AT5G21105	-1.1244995	AT3G06500	1.88896467	AT5G54840	1.32151956
AT1G75820	-1.8914277	AT4G31600	-1.2086104	AT5G43770	2.53646058	AT4G23190	2.05939332
AT1G68530	-1.5415682	AT2G43535	-2.2713137	AT5G47230	2.57608592	AT1G77500	1.43368448
AT3G18490	-1.7497331	AT1G07090	-1.2520301	AT2G37970	1.78917945	AT1G49960	5.73287036
AT3G22790	-3.5255467	AT2G05210	-1.3202737	AT3G23920	1.30461276	AT1G30700	3.91617671
AT3G62820	-1.5332167	AT1G31150	-1.4993104	AT4G20830	3.007338	AT5G64990	1.98948523
AT4G04890	-1.3084299	AT4G00950	-1.6412242	AT5G43620	2.24896121	AT5G13700	2.64980952

AT5G38980	-1.5694478	AT1G76405	-1.3889127	AT3G55430	1.57767353	AT2G27310	1.3105479
AT1G25320	-2.064833	AT1G17110	-1.0002903	AT2G03760	2.73189549	AT1G05575	1.6430212
AT1G01610	-1.1833867	AT4G24750	-1.005102	AT5G05410	1.8315901	AT1G69930	3.87041223
AT1G67050	-1.5935309	AT2G33990	-1.0125065	AT5G13490	2.14253508	AT2G33590	1.0082938
AT1G08980	-1.5726881	AT4G25740	-1.0279568	AT3G03460	2.53002044	AT5G57890	1.62179909
AT4G36230	-4.5423167	AT1G67590	-1.4511815	AT1G18390	1.88340924	AT2G43120	1.90161579
AT3G23830	-1.6969102	AT5G10080	-2.857726	AT5G67600	1.39520024	AT2G31945	2.87016264
AT4G02770	-1.1542517	AT3G50845	-1.5530844	AT5G26340	2.09065542	AT2G46430	1.15274534
AT4G17090	-2.4490205	AT3G56270	-1.3217223	AT2G01180	2.30610677	AT1G19180	1.60234695
AT2G28605	-1.4452166	AT3G10190	-1.3877652	AT1G27730	2.93933073	AT5G17990	1.12082797
AT3G45610	-2.0079311	AT2G35960	-1.4949583	AT1G57990	2.82053832	AT1G17870	1.28043039
AT1G49975	-1.5001461	AT3G08680	-1.6067647	AT2G25735	3.23502783	AT2G45760	3.16712053
AT3G46580	-1.8856409	AT2G41300	-2.9497926	AT5G47730	1.82967703	AT1G20970	1.07484733
AT5G42480	-1.2637158	AT1G02730	-4.2007576	AT5G51630	2.52633466	AT1G53620	4.19757738
AT3G12610	-2.9597406	AT5G14230	-3.0124873	AT5G56350	1.36604436	AT2G01430	3.95290499
AT3G50840	-1.8757975	AT1G74520	-1.2158286	AT1G43160	3.68778442	AT1G09510	5.10680955
AT1G20850	-1.9171085	AT1G58070	-2.1479888	AT5G11110	1.35855561	AT5G24210	1.87920663
AT3G29320	-1.7018234	AT4G02290	-7.302776	AT4G11370	2.00711942	AT3G20490	1.3139143
AT1G60260	-1.6195847	AT3G51450	-1.7901084	AT2G46330	2.22495773	AT5G41610	3.27780097
AT3G57930	-1.1869363	AT3G59320	-2.0255904	AT4G25433	1.69331939	AT1G19025	2.13557165
AT5G18050	-6.1224017	AT4G04750	-1.8648091	AT5G66780	1.56201418	AT4G29950	1.14960141
AT1G56700	-1.1892847	AT5G01840	-3.3131135	AT1G03220	2.56024933	AT1G07620	1.68405543
AT3G57170	-1.5283353	AT1G02205	-1.2808516	AT5G17060	1.76435686	AT3G60450	1.23110485
AT2G41560	-1.6067294	AT3G58650	-5.5355669	AT1G31540	1.56076957	AT4G01360	2.98408779
AT4G12030	-2.6713288	AT2G35700	-2.4456141	AT5G64370	1.1045234	AT2G22860	2.09396617
AT5G57440	-1.6475441	AT5G11550	-2.0765115	AT1G62300	2.50847539	AT5G43260	1.03620766
AT1G67740	-1.3944849	AT5G66530	-1.53005	AT2G39650	1.99693879	AT1G73010	1.503492
AT5G38420	-2.630048	AT5G65810	-1.2376666	AT4G28085	2.13144403	AT2G29120	1.32485591
AT3G54920	-1.8096244	AT2G25270	-5.4379045	AT5G49900	1.55267806	AT1G56140	1.04418931
AT5G14880	-1.2627811	AT1G48600	-1.2935362	AT2G32800	1.42729377	AT5G06860	1.5164885
AT2G39030	-2.7084672	AT3G60380	-1.3542169	AT3G01040	1.39095892	AT1G22180	1.08179389
AT5G65010	-2.1904056	AT3G57800	-1.4884956	AT2G33120	1.24273213	AT4G04490	2.25626821
AT1G68600	-3.0414069	AT1G18730	-1.0090757	AT3G54950	1.72346432	AT3G28480	1.19576346
AT1G78020	-2.3676891	AT3G15380	-1.1803636	AT5G24110	5.9346034	AT5G62520	3.53829357
AT4G29905	-1.4617838	AT5G52100	-1.7382073	AT4G02940	1.52370645	AT2G44500	1.64227863
AT5G64040	-1.3500728	AT5G46600	-2.005316	AT5G24030	2.01259581	AT5G04930	1.0538564
AT2G28410	-2.5303223	AT5G26000	-1.0307696	AT2G19900	1.79978449	AT2G04100	2.52225076
AT3G01920	-1.3484316	AT3G25690	-1.1254696	AT1G61260	1.52881254	AT3G12910	3.71239381
AT4G22560	-2.1823051	AT1G51430	-1.0429039	AT3G55980	2.52992414	AT1G32350	2.841904
AT1G15290	-1.498056	AT2G26580	-1.1421112	AT4G31860	1.21224922	AT1G66580	1.06344902
AT1G29910	-1.4939154	AT1G09750	-1.6239681	AT1G09560	2.21002878	AT5G03610	1.33388487
AT3G28080	-2.78757	AT2G34150	-1.9984302	AT1G09920	1.09182078	AT3G26830	3.04233105
AT4G18670	-2.3176845	AT2G03750	-1.0080652	AT5G40390	1.80437858	AT2G18690	2.84103411
AT3G01860	-1.8235237	AT1G61580	-1.1383729	AT5G48180	2.17209842	AT5G44575	3.38874677
AT3G24890	-1.5998089	AT4G28240	-1.0517975	AT1G29690	1.65824168	AT4G11800	1.11109287
AT1G30280	-3.990246	AT4G33810	-2.0957634	AT2G23810	2.06705077	AT1G74360	2.19601287
AT1G68010	-1.1726635	AT5G04290	-1.0749242	AT1G75600	4.38938481	AT1G26420	2.44562098
AT5G18970	-1.714035	AT1G29430	-3.8232868	AT4G33540	1.20167974	AT4G23810	1.96482865
AT1G12430	-1.4827359	AT2G05920	-1.2918524	AT2G02120	2.55547459	AT4G23700	3.35003197
AT4G27435	-2.0532661	AT3G22142	-3.9473601	AT1G27100	1.34937459	AT5G52810	1.98091325
AT2G45470	-1.8746993	AT1G28570	-1.7982403	AT5G13190	1.59879571	AT4G02520	2.08199167
AT2G33480	-1.2856616	AT1G10060	-1.808908	AT3G01175	4.93169788	AT3G15352	1.31127032
AT4G15440	-3.4891122	AT2G16850	-5.5593516	AT3G21150	3.07482587	AT5G54585	1.25632445
AT1G75090	-2.5863987	AT4G27450	-1.2634287	AT1G54290	1.1913564	AT5G57035	1.05151655
AT2G43360	-2.0983671	AT5G07530	-10.016287	AT2G23320	1.84535103	AT3G03240	2.28283283
AT3G27200	-2.3382316	AT4G38660	-3.8549699	AT2G30020	1.85861508	AT1G69870	1.39241884
AT5G57660	-1.4998579	AT1G15720	-1.4385423	AT3G16800	1.79466205	AT3G07255	3.12831982
AT5G38430	-2.1798252	AT2G35470	-1.0581955	AT1G21120	2.89464785	AT3G02840	3.48479917
AT1G70890	-2.3248004	AT3G14000	-1.6469919	AT5G22350	1.08586739	AT5G25260	3.21928219
AT1G79790	-1.434542	AT4G30180	-3.2123037	AT2G32190	3.34976416	AT4G29780	2.12130346
AT3G16100	-1.3995269	AT2G26640	-1.3416682	AT3G50260	2.45158369	AT3G59080	1.53683816
AT2G03550	-1.6070021	AT1G79460	-1.3468096	AT5G13750	1.56479919	AT3G46670	1.35199652
AT5G13300	-1.3047209	AT2G42610	-1.380055	AT2G17500	2.84670573	AT3G61640	1.11272948
AT3G61470	-1.1457834	AT4G37250	-2.0970353	AT1G53540	2.89522341	AT3G15500	2.131369
AT1G26820	-2.0194072	AT2G40640	-1.6993918	AT3G62990	1.28843587	AT5G04250	1.10630498
AT1G20020	-1.6573433	AT1G05385	-1.1720004	AT2G22500	1.66598194	AT1G33420	1.29169303
AT5G08130	-1.258292	AT3G43800	-1.0971426	AT4G27280	2.29476271	AT4G36990	1.26035381
AT1G60800	-1.7764004	AT2G03350	-1.3140438	AT2G30720	1.28972574	AT1G69490	1.21486225
AT3G18800	-1.5779015	AT2G34430	-1.7800464	AT4G27780	1.15958071	AT5G15260	1.08828942
AT2G06520	-1.1937818	AT1G09660	-1.0774882	AT1G22190	1.21199471	AT1G01180	1.35077178
AT4G10770	-1.7344065	AT1G51080	-1.488209	AT5G50100	1.30688979	AT2G35750	1.35538946
AT1G68190	-1.5162295	AT1G55675	-1.0709867	AT5G39090	2.23736479	AT5G51680	2.42316636
AT2G40320	-6.3609095	AT3G14220	-1.2574752	AT4G33905	1.32094514	AT1G72280	1.27173304
AT1G78915	-1.5197175	AT4G23020	-2.6772511	AT5G18400	1.50878129	AT5G17650	1.10313581
AT2G19460	-1.6402109	AT5G10170	-1.9671628	AT1G71100	1.6689525	AT1G25220	1.60815293
AT1G21590	-1.0289721	AT5G26910	-1.1081043	AT4G20110	1.73267006	AT5G38900	2.76088616

AT5G48830	-2.1284475	AT1G79620	-2.7116886	AT2G40000	2.00194763	AT1G59590	2.39979584
AT3G56160	-2.1358875	AT3G25500	-1.2722997	AT2G17760	1.42796623	AT1G75180	1.10505565
AT5G01920	-1.3699362	AT1G34640	-1.2391532	AT2G24180	1.73637282	AT5G25250	2.02723116
AT3G53420	-1.8383578	AT5G14100	-1.743391	AT5G20960	2.66660278	AT5G07010	1.45202153
AT2G20120	-1.3758635	AT2G46970	-1.8467464	AT2G40095	2.77372793	AT3G09600	1.63148273
AT3G16250	-1.6636267	AT3G25530	-1.1623702	AT1G18570	2.14432227	AT5G13080	3.07948816
AT5G02090	-2.4405814	AT1G26770	-3.2680422	AT4G11570	1.09571313	AT5G52870	1.14384102
AT4G33000	-2.5554788	AT1G15410	-1.5257773	AT1G07135	3.58471418	AT5G14700	1.04882081
AT1G78680	-1.5910845	AT3G43270	-1.0951659	AT3G12320	2.08486148	AT2G46400	2.12954453
AT4G22756	-2.3063473	AT1G66370	-5.6003302	AT3G49130	3.77775399	AT2G26560	2.1064706
AT2G37630	-1.6485887	AT5G10180	-1.0456693	AT1G09740	1.6255452	AT5G23730	1.60164829
AT5G19530	-1.2782485	AT1G26761	-1.6259776	AT5G19440	1.32366492	AT3G11820	1.01201816
AT5G65440	-1.6383919	AT2G18328	-2.2082322	AT2G26740	1.13849988	AT5G48400	2.57341912
AT5G06790	-3.5681553	AT1G30840	-2.3139723	AT1G05894	4.52752216	AT1G26390	3.02245619
AT3G23780	-1.5432266	AT5G26850	-1.7852622	AT1G51340	1.72386725	AT3G05200	1.01201842
AT3G10060	-1.4012478	AT5G13510	-1.0509236	AT4G28460	5.90241456	AT2G27500	1.2743231
AT1G66140	-1.4233652	AT4G13770	-1.5157928	AT3G53120	1.13834464	AT5G22860	1.20254301
AT2G47070	-1.1036865	AT1G72410	-1.100912	AT5G47880	1.80867519	AT4G34340	1.06643523
AT3G61830	-1.1351263	AT1G06640	-1.2149191	AT3G57520	1.79403633	AT4G39270	1.17362459
AT5G23920	-1.2411733	AT5G22430	-8.7237026	AT1G64065	1.78860216	AT3G09480	1.59551964
AT1G75900	-1.713073	AT5G63410	-1.205244	AT1G21080	1.15123084	AT3G14050	1.09420956
AT4G26520	-1.4390657	AT3G10570	-6.2639565	AT3G14470	2.17657515	AT5G52730	5.73971196
AT3G25770	-1.6342098	AT3G49670	-1.6892466	AT5G39785	2.08476955	AT3G29010	1.65835931
AT5G20630	-6.7948483	AT1G62870	-3.5211148	AT4G29810	1.26280873	AT1G01560	2.8684106
AT1G15000	-2.5794743	AT1G63000	-1.0626605	AT4G12005	6.20798563	AT2G47140	3.60157105
AT5G13400	-2.3834243	AT3G53130	-1.140971	AT1G05510	3.48414897	AT1G15110	1.35145654
AT1G09310	-1.6796602	AT1G70760	-1.3749693	AT5G20910	1.2371402	AT2G33380	1.64191438
AT1G13380	-1.2427288	AT2G18910	-1.0995015	AT3G12510	2.26035647	AT1G04280	1.05464548
AT4G17050	-1.170995	AT1G34320	-1.1183482	AT2G38870	2.01634826	AT1G07390	1.21526683
AT4G33790	-3.6902102	AT3G44990	-5.509611	AT5G01540	3.0061948	AT1G75830	5.95941226
AT2G47590	-1.0473672	AT1G20650	-1.1700338	AT2G17270	1.29797957	AT1G63440	1.69278212
AT4G00165	-1.3609899	AT1G33811	-3.8274435	AT2G39210	2.59925935	AT5G64940	1.05330711
AT1G29900	-1.251667	AT1G10180	-1.4305441	AT3G09810	1.44510701	AT4G31550	1.01969999
AT4G31330	-3.4038129	AT5G02160	-1.322029	AT5G07440	2.34882608	AT3G55950	1.6726156
AT2G17230	-2.3987975	AT2G39900	-1.4028508	AT5G04340	1.84116703	AT1G65970	3.36066507
AT1G55265	-1.6090146	AT3G19710	-1.5555497	AT1G76070	1.69353855	AT2G41000	1.27594635
AT1G52510	-1.3018361	AT1G18870	-3.4373688	AT1G71697	1.47816804	AT5G25910	2.50005623
AT3G60390	-2.4201133	AT1G07320	-1.300719	AT5G64840	1.27836735	AT5G64905	4.21862579
AT3G17160	-1.361292	AT5G58090	-1.0673295	AT5G48540	2.55052881	AT5G06230	1.98268554
AT4G29360	-6.1687966	AT1G30690	-1.1031761	AT4G12735	2.71894762	AT5G45340	1.63796431
AT5G61480	-2.2671786	AT4G09640	-1.1579235	AT4G31830	1.81186415	AT4G09600	1.00285462
AT2G47930	-2.5188454	AT1G04430	-1.3789186	AT3G10815	3.09580185	AT1G11925	3.5176886
AT3G10525	-1.2211534	AT4G02630	-1.3980066	AT2G26530	2.3484021	AT4G11860	1.05204062
AT1G80260	-1.5210928	AT1G45130	-2.4064209	AT5G46230	2.60529837	AT3G54150	2.49467511
AT1G15260	-1.6371717	AT1G35180	-5.4360139	AT5G13370	1.48746561	AT2G23321	3.47763345
AT3G54600	-1.9285036	AT5G10020	-1.4422051	AT1G11330	2.5496815	AT1G67856	1.38667237
AT5G19190	-3.3909462	AT2G44230	-1.8266269	AT2G27510	1.2000157	AT1G22570	1.07897059
AT4G32350	-1.3032574	AT1G06240	-1.3199506	AT5G65380	1.38103383	AT5G07380	2.27389484
AT5G48920	-3.8270583	AT1G14700	-2.0398608	AT5G27350	1.66280636	AT3G15518	2.45112328
AT1G11130	-2.0145292	AT5G23660	-1.2293619	AT2G25450	1.88132017	AT2G34340	1.74133496
AT3G50270	-3.3977042	AT4G32295	-1.4048152	AT5G15950	2.06690244	AT1G18890	1.00231915
AT2G42320	-1.3708916	AT2G24645	-1.8913636	AT3G14770	3.42023194	AT5G61600	1.18895378
AT1G52230	-1.2878962	AT2G32180	-1.2704797	AT5G15640	1.61584384	AT1G67810	1.87473005
AT4G27870	-1.3090341	AT1G49130	-1.2143122	AT1G77120	1.72862276	AT2G40340	1.5045702
AT1G32470	-1.5435489	AT1G70230	-1.1151799	AT1G08650	1.49971599	AT1G71000	2.68923685
AT1G71790	-1.3690065	AT3G01680	-1.3663723	AT1G24600	1.71516109	AT5G26920	1.49834018
AT5G60020	-2.6296545	AT2G33850	-3.9782488	AT4G12430	1.60328214	AT1G58340	2.77411967
AT5G26230	-4.8513046	AT5G50160	-1.1966113	AT5G04010	2.33360464	AT3G01830	2.77025262
AT3G59780	-1.6834533	AT1G72310	-1.002916	AT4G16760	1.07505508	AT3G54420	2.00948307
AT1G48330	-2.013446	AT4G17890	-1.0290329	AT3G23240	2.43110373	AT3G14670	3.72832115
AT1G05470	-2.8679687	AT4G19865	-1.0810891	AT4G35110	2.07290087	AT5G09470	3.64871493
AT1G28610	-1.9759737	AT2G34170	-2.8578273	AT5G59820	2.86675102	AT5G47140	1.08238903
AT5G62670	-1.9215318	AT1G64640	-1.8741277	AT3G54810	1.30680062	AT1G19250	3.76446039
AT4G29110	-1.4510912	AT5G24280	-2.5917052	AT5G24120	1.79152778	AT4G25030	1.17427185
AT5G20740	-5.4256281	AT2G01070	-1.1045626	AT1G77840	1.29312433	AT1G02450	2.58671277
AT3G20390	-1.1166213	AT1G78460	-1.3335456	AT2G24100	1.51411266	AT4G00955	1.51310739
AT1G35260	-4.7316213	AT4G12900	-1.5168452	AT3G25610	1.95007189	AT3G57120	1.06110662
AT1G10360	-2.0244697	AT5G03150	-1.9762695	AT3G03310	1.32215866	AT3G53600	3.70078751
AT5G04360	-1.7477947	AT5G49630	-1.7321094	AT4G03110	1.36909952	AT5G18490	1.05581811
AT3G11500	-1.122711	AT5G14090	-2.485333	AT5G57510	5.27158371	AT4G19520	1.02835521
AT5G06870	-3.1859124	AT2G27385	-1.3089472	AT1G10040	1.9823391	AT3G15356	2.23171469
AT2G39930	-1.5319503	AT4G34000	-1.3394721	AT3G05580	1.27585707	AT1G43910	2.1645598
AT4G27900	-1.6750827	AT2G35860	-1.4126089	AT2G24600	2.025539	AT3G11570	2.42469611
AT5G51750	-2.732771	AT1G80170	-1.5043903	AT5G25920	6.65996833	AT3G51750	1.17574226
AT2G28870	-1.5281053	AT4G09810	-1.261543	AT1G78830	1.69482065	AT1G14870	2.0369413
AT5G62690	-1.2042465	AT5G16000	-1.4355299	AT5G67340	2.42459031	AT1G54120	1.1634431

AT3G60740	-1.3744946	AT5G16130	-1.027937	AT3G21700	1.58556488	AT2G40740	4.09850637
AT1G09440	-3.1205612	AT1G24577	-1.5843028	AT2G43000	3.7880239	AT4G26120	1.80624627
AT4G25000	-2.1780984	AT2G24395	-2.3867117	AT1G63720	1.75348242	AT5G18270	2.02652132
AT5G14210	-1.6816958	AT3G06140	-5.3394645	AT1G06430	1.04231215	AT4G20390	2.37554115
AT1G64760	-1.4579396	AT1G15250	-1.014563	AT2G30550	1.43395961	AT2G02350	1.47974938
AT2G30570	-1.1611252	AT1G45010	-2.2187862	AT5G19400	1.03943527	AT4G11000	2.20171359
AT2G04790	-2.6926894	AT1G34245	-4.2113467	AT5G04830	1.05730295	AT1G72660	1.66894086
AT1G28660	-2.0024965	AT1G73600	-2.2277108	AT3G57550	1.93030842	AT1G33700	1.00250144
AT2G40475	-2.1833813	AT4G18480	-1.1423739	AT3G19010	1.83088408	AT5G01100	2.03954749
AT2G34300	-1.692492	AT3G03780	-1.0297059	AT5G04220	1.26467106	AT3G14680	1.79593762
AT5G10745	-1.1595928	AT5G46850	-1.2242892	AT3G22060	2.74358871	AT4G35180	2.93837922
AT4G29080	-1.8907257	AT5G17490	-1.710518	AT5G61010	2.0953724	AT1G52200	2.32120746
AT5G62700	-1.2163602	AT1G74950	-1.121246	AT2G01890	2.62313124	AT3G26440	1.45531163
AT1G69370	-2.165001	AT1G59960	-1.5311907	AT1G22890	2.49931465	AT5G49480	1.30253861
AT1G12380	-2.9825121	AT1G53000	-1.0665145	AT3G26910	1.80646623	AT5G38530	1.06912871
AT1G78370	-1.8133373	AT1G73830	-2.8159363	AT3G26600	1.38927624	AT5G51990	1.73654118
AT5G05250	-3.4447415	AT1G52150	-1.0948051	AT4G17650	1.40691619	AT1G21390	1.09026256
AT5G52780	-1.2914705	AT2G20850	-1.2040414	AT1G54130	1.22346427	AT1G26410	3.57300328
AT3G19515	-1.2897655	AT2G01400	-1.5366215	AT5G24150	1.91364654	AT1G04490	3.36666913
AT3G02640	-6.2276482	AT5G18690	-2.3096708	AT5G45000	2.93475153	AT3G50900	1.04947373
AT3G06035	-2.2109129	AT1G75690	-1.2959582	AT5G06320	1.87927365	AT4G39830	2.45295983
AT2G46820	-1.1775855	AT1G62981	-3.3835921	AT2G41100	2.34740045	AT3G24460	2.80003607
AT2G36120	-2.2484149	AT3G08770	-5.1180363	AT1G11940	1.29113977	AT5G49700	1.38656798
AT1G32060	-1.1006967	AT5G62360	-3.9933637	AT4G14930	1.23665242	AT5G62180	1.75126797
AT4G32330	-1.1079726	AT2G22840	-1.3257348	AT2G27660	3.68254956	AT2G30560	3.50242777
AT4G30690	-1.1855817	AT3G17860	-1.1224585	AT1G70170	3.98016979	AT4G14450	3.34839276
AT1G48420	-1.0802897	AT5G59870	-1.3811794	AT3G29000	3.31820679	AT4G39030	2.31474397
AT3G13750	-2.4190947	AT5G15530	-2.8843576	AT5G24090	1.74548319	AT4G15610	1.84127125
AT1G60810	-1.6582016	AT4G34760	-2.0060468	AT2G40140	1.83137745	AT3G46690	2.6583814
AT1G22060	-1.1681439	AT4G29030	-6.0172741	AT2G17220	1.48178546	AT5G57550	1.57111577
AT3G07460	-1.4961363	AT4G21930	-3.0877209	AT1G07400	2.83507166	AT3G26230	1.25201268
AT2G26730	-1.692268	AT4G38690	-1.0424775	AT5G17380	1.30895114	AT4G22710	2.13451775
AT3G50780	-1.4164092	AT2G15790	-1.1882034	AT4G04960	1.43943749	AT3G60415	1.64720639
AT3G27850	-1.3103365	AT3G05936	-1.2674378	AT4G37370	3.16574861	AT5G15160	1.26018298
AT4G15765	-1.7181187	AT5G23740	-1.1034507	AT5G11520	1.32693203	AT5G43380	1.15161595
AT1G75840	-1.1006946	AT5G49100	-1.994101	AT3G26670	1.54379275	AT1G07610	1.9195383
AT4G27595	-2.504192	AT5G57130	-2.5968028	AT2G20760	1.02967657	AT2G03520	3.85288873
AT3G59110	-1.628635	AT5G40150	-1.5689492	AT4G28350	2.02729174	AT2G38790	1.10760421
AT5G46110	-1.6934518	AT4G35930	-2.3176778	AT5G46910	2.22110501	AT4G16690	1.50068511
AT1G10200	-1.3341563	AT5G46160	-1.2080034	AT5G57560	2.65254372	AT1G18970	7.54218803
AT3G21190	-1.6918946	AT5G19470	-6.1371938	AT4G20110	1.73267006	AT4G32870	1.59582664
AT3G50750	-1.3850763	AT1G18550	-2.8765593	AT3G48640	3.76751364	AT1G74710	2.29752262
AT4G22200	-1.4065985	AT4G16442	-1.151716	AT1G76130	1.50178635	AT1G02400	2.10327005
AT1G20090	-1.2391441	AT5G12440	-1.2341747	AT1G67880	1.03333498	AT4G31240	1.11916498
AT1G02335	-1.7393144	AT4G13710	-4.0477895	AT4G37320	1.03103315	AT5G12030	1.83021401
AT5G66052	-1.2813591	AT5G19160	-1.3366708	AT3G07195	2.33143169	AT1G17147	1.77244347
AT1G32640	-1.5338022	AT4G15810	-1.5579644	AT5G42380	4.00792773	AT4G27410	1.07394522
AT3G01670	-1.7711747	AT2G42740	-1.3870411	AT2G02930	3.02527744	AT1G26200	2.92981071
AT2G26500	-1.0273057	AT1G44920	-1.0547075	AT1G33110	1.43875033	AT1G76650	1.89913998
AT1G79720	-2.4818881	AT5G60970	-1.8442813	AT1G71040	1.13185142	AT5G38940	5.64002655
AT5G43810	-1.3160456	AT1G78995	-1.1015665	AT3G46930	1.97296341	AT1G59910	1.0293349
AT1G01300	-1.7886737	AT2G39470	-1.2872365	AT3G01290	2.35971216	AT1G30750	6.62332178
AT1G60070	-1.0768613	AT3G11700	-1.0788922	AT4G10960	1.60812178	AT2G31141	1.05143192
AT5G03260	-2.4399092	AT2G26010	-7.0986895	AT4G39640	2.06113925	AT3G06370	1.20563598
AT5G11420	-1.2588244	AT4G22010	-2.6251229	ATMG00516	2.35250896	AT1G31750	1.04220967
AT2G28070	-1.3852274	AT2G01630	-1.1554045	AT4G37295	1.986997	AT3G02800	1.6930404
AT2G45960	-1.0047053	AT3G58850	-1.7857801	AT5G57220	3.33315352	AT4G11170	3.63599495
AT5G63140	-3.3848199	AT3G15570	-1.245513	AT5G05190	1.90434861	AT1G13520	3.22232405
AT1G15910	-1.5677697	AT1G29660	-1.6294219	AT2G38400	1.34803788	AT5G22250	1.37527506
AT2G37170	-2.2736734	AT5G42710	-3.5270717	AT5G10695	1.73611449	AT5G52760	1.9803681
AT2G38370	-1.3298452	AT5G03230	-1.5115813	AT1G76680	1.2456396	AT3G15990	1.90034314
AT3G47675	-2.224897	AT4G31820	-1.3550872	AT4G24380	1.46598653	AT2G45570	2.29828744
AT1G22030	-2.0193017	AT4G26580	-5.3865784	AT5G19855	1.20860986	AT3G27440	3.05083765
AT5G65310	-1.3883532	AT5G26622	-1.0333386	AT5G46780	1.2468589	AT1G05010	1.29325484
AT5G56040	-2.0541011	AT3G08600	-1.6656301	AT4G12410	1.66452287	AT2G47000	1.75427837
AT3G59310	-1.6892298	AT4G01130	-1.2494387	AT1G76600	1.54367208	AT1G07985	1.46822028
AT4G14620	-1.1952111	AT1G35780	-1.6011153	AT5G54500	1.15817383	AT1G12320	1.3684656
AT5G54770	-1.3807343	AT1G66180	-1.5312889	AT2G35980	4.0428599	AT1G52560	2.33980197
AT5G06670	-1.640252	AT1G77330	-5.3689257	AT2G22480	1.09563388	AT5G01760	3.16233682
AT5G62350	-1.4570006	AT5G03140	-1.5604515	AT1G52080	1.49186952	AT4G37070	3.05378971
AT2G23350	-1.15435	AT2G25480	-1.3041203	AT3G19580	1.51563727	AT1G59510	1.09133967
AT2G20260	-1.0424006	AT1G69690	-1.3162331	AT1G18030	1.25897724	AT1G16130	1.55257041
AT3G23640	-1.0742668	AT5G48460	-2.4427975	AT5G57480	2.07074129	AT4G05020	1.14391858
AT2G26110	-1.0773748	AT5G02890	-3.7033629	AT4G18010	1.26875041	AT2G27300	2.22214692
AT3G53800	-1.3597809	AT1G80560	-1.2605492	AT4G18170	3.44480627	AT1G29770	3.60137769
AT2G20340	-2.2986079	AT1G56310	-1.3614598	AT3G56790	3.14180489	AT1G67920	1.07680073

AT1G55260	-2.3318471	AT1G12860	-1.278092	AT3G05830	1.42712434	AT5G39050	1.43240154
AT1G26220	-1.5971155	AT4G14740	-1.2042164	AT1G68500	1.56633909	AT4G30850	1.92274987
AT5G27220	-6.9533664	AT3G09070	-1.2912441	AT3G28210	3.4794115	AT2G32765	1.41991622
AT4G19430	-5.7944221	AT4G38950	-3.7939424	AT1G78570	1.5171616	AT1G23040	1.03708201
AT4G34980	-1.7025528	AT1G65295	-1.1534704	AT1G25400	2.56309975	AT3G44450	1.00634453
AT1G73655	-1.3021984	AT4G04570	-1.2157114	AT4G13395	3.62583778	AT5G42010	1.61119928
AT5G62940	-2.3329967	AT1G59720	-3.1217213	AT3G15670	1.53211469	AT5G66650	1.14320386
AT5G04470	-1.3039368	AT5G46270	-1.0164186	AT1G55365	1.83377882	AT2G37750	1.79916023
AT4G14760	-1.0691753	AT3G01940	-3.2501791	AT1G04778	3.66738288	AT3G05550	1.8111082
AT1G04800	-2.7777583	AT3G01510	-1.1090615	AT1G56660	2.25963351	AT5G35660	1.57390879
AT2G35500	-1.278274	AT4G10890	-1.1072193	AT3G53000	1.06108027	AT5G66080	1.54255698
AT4G31060	-1.6191407	AT3G52870	-1.4278256	AT2G43820	2.2885563	AT1G30900	1.99596776
AT1G69700	-1.548421	AT1G68810	-1.3962193	AT3G13080	1.98463824	AT1G20310	2.63385567
AT4G02820	-1.8699989	AT1G59970	-1.0983578	AT3G61190	3.52889632	AT2G41220	1.05014921
AT2G40530	-2.6301565	AT1G56210	-1.517562	AT3G09830	1.12735701	AT5G39040	1.05447574
AT5G13690	-1.2153727	AT2G38995	-2.7669011	AT3G25870	1.09350459	AT1G48405	2.97896868
AT2G34420	-1.1019448	AT4G37750	-3.3604538	AT5G58380	1.00414507	AT5G54730	1.15493316
AT5G23060	-1.7726818	AT5G66000	-1.9206517	AT5G50200	2.02095387	AT4G19810	2.19037668
AT5G45650	-1.8222192	AT1G54730	-1.0003574	AT4G11280	2.7797248	AT5G42830	2.68903202
AT4G22570	-1.5536115	AT2G16660	-1.4182166	AT2G01850	1.41162081	AT5G48530	1.70961526
AT1G46480	-3.7701052	AT4G01460	-1.5747126	AT2G02220	1.39100509	AT4G21380	1.46111671
AT3G14810	-1.3996066	AT5G01370	-3.7431498	AT2G17730	1.48791148	AT5G44910	2.54248278
AT1G28670	-1.6990747	AT2G32290	-2.5407174	AT3G52400	1.91705013	AT4G25390	1.04548705
AT4G18030	-1.3638279	AT1G77460	-1.2741152	AT5G16830	1.0736189	AT1G79450	1.67891797
AT2G37790	-1.633494	AT5G10770	-1.3590213	AT5G16910	1.17329012	AT3G48180	1.56393258
AT4G31840	-4.0716491	AT4G27720	-1.3887569	AT5G41100	1.49582895	AT1G56550	2.03260303
AT3G54910	-2.2151156	ATCG00750	-1.2308357	AT1G68390	4.73557599	AT3G46080	3.14655868
AT1G53840	-1.2947221	AT5G48900	-1.7089468	AT4G12120	1.67352203	AT1G28480	2.14983788
AT3G25717	-1.3954485	AT3G01980	-1.1083487	AT2G29995	1.34139784	AT5G39670	2.13128852
AT2G34655	-1.5882985	AT1G72810	-1.4539231	AT2G42000	3.43689741	AT2G34610	2.85177793
AT1G64200	-2.5135214	AT2G20570	-1.1015202	AT1G55910	1.46011158	AT1G05730	1.2459584
AT3G25030	-1.3069011	AT5G52280	-1.0512694	AT5G53590	1.11977969	AT2G43580	1.05289797
AT2G32560	-1.409124	AT5G14380	-3.8482706	AT4G09030	1.80864049	AT4G30230	2.48463729
AT4G14400	-1.7592194	AT4G18640	-2.1752503	AT1G53470	2.85438161	AT2G39400	1.12144508
AT5G09660	-1.1410141	AT5G41120	-2.1587254	AT5G41990	1.13946734	AT1G57630	2.64844753
AT2G01420	-1.2235304	AT2G37460	-2.0971732	AT1G18740	1.08011389	AT5G60610	2.72267801
AT1G52220	-1.045143	AT1G72030	-1.1817673	AT1G20630	1.13620788	AT3G26630	1.03607737
AT2G01870	-1.4761395	AT4G35880	-1.1407718	AT1G08920	1.54757468	AT4G24570	2.89166251
AT2G29130	-2.7678241	AT2G43910	-1.01535	AT3G17770	1.35967309	AT3G09350	1.21293415
AT4G17880	-1.4577198	AT1G64625	-5.2546759	AT4G22980	1.78656281	AT1G68410	1.06249929
AT3G58120	-4.438764	AT2G37195	-1.0676492	AT1G03740	1.35426606	AT3G23170	1.44272478
AT5G51560	-4.3064367	AT5G48990	-1.0198655	AT3G10930	3.50978865	AT4G32070	1.29225372
AT5G07690	-2.3665314	AT4G27260	-1.8405147	AT2G27150	1.23636021	AT3G29034	2.2881657
AT3G06750	-2.3753632	AT2G37330	-1.15191	AT5G45110	1.55949295	AT2G16900	1.64257431
AT2G45590	-1.0211057	AT5G03204	-2.8477957	AT4G37530	2.13011333		
AT1G29510	-5.9752773	AT3G55330	-1.2508349	AT4G18950	1.68841618		
AT3G47470	-1.0039349	AT2G33810	-1.1002329	AT1G55450	1.38467472		
AT5G21482	-1.9056932	AT2G43610	-5.8489179	AT4G16680	2.2987505		
AT4G24510	-1.4118663	AT1G64770	-1.1421797	AT1G51790	2.48703299		
Col-0_D vs JAR1-OE_D		**Col-0_D vs JAR1-OE_D**		**Col-0_D vs JAR1-OE_D**		**Col-0_D vs JAR1-OE_D**	
AGI code	**logFC**	**AGI code**	**logFC**	**AGI code**	**logFC**	**AGI code**	**logFC**
AT5G66780	-3.6976254	AT1G11440	1.04768612	AT1G06640	1.50311804	AT3G54880	2.45231861
AT4G31830	-5.4029497	AT5G04010	-2.0812518	AT3G06130	1.78529652	AT1G62630	1.33959005
AT2G19900	-4.4663371	AT1G60470	-3.6200843	AT5G56530	1.79961618	AT1G44350	1.18797823
AT4G33905	-3.0707174	AT2G18540	-1.6572259	AT1G59970	1.17662273	AT5G25460	1.42829436
AT4G15910	-3.1417006	AT5G37500	-1.1743745	AT2G32080	1.06044404	AT2G37130	1.92681531
AT5G35660	-5.3884636	AT3G51960	-1.0664206	AT1G55210	1.41940936	AT1G25230	1.37355858
AT5G40382	-2.6281106	AT4G25780	-2.0732574	AT5G55120	1.32151517	AT1G70890	1.84015655
AT3G13784	-4.4555782	AT5G53660	-1.209343	AT5G13100	1.38247698	AT2G29890	2.83816497
AT2G21590	-2.5859697	AT1G67856	-1.4822312	AT2G43550	3.31354423	AT1G21100	2.96492791
AT2G35300	-3.6661704	AT3G21250	-1.180485	AT1G61170	1.60271146	AT3G51230	4.26959552
AT5G01300	-3.4505972	AT4G31354	-1.533256	AT4G11320	3.72277402	AT5G46050	1.81211461
AT1G66390	-4.817681	AT2G20560	-1.4515435	AT2G28410	1.93253137	AT4G30410	1.89295324
AT4G09600	-2.612804	AT2G36970	-1.2724945	AT3G54400	2.52739955	AT3G09940	3.71592697
AT5G44310	-4.451956	AT1G66100	6.50867098	AT1G18250	3.57361194	AT3G24420	1.49186715
AT4G02280	-2.5588873	AT3G16460	3.82698484	AT3G46320	1.6176202	AT4G37750	2.28564578
AT4G27670	-6.8342001	AT4G24780	3.02018822	AT5G02160	1.71750532	AT1G02730	2.47070328
AT5G66110	-2.6052054	AT4G34220	2.65540068	AT1G78370	1.87275016	AT5G23010	1.61652075
AT5G22460	-2.105492	AT4G16980	2.73141268	AT3G19710	2.04704415	AT5G36907	6.0208263
AT3G02480	-3.0396941	AT1G49750	2.68097299	AT4G28030	1.02214799	AT1G35710	1.85313096
AT4G32920	-1.6155178	AT2G18300	3.87426178	AT4G21850	3.58974237	AT4G11080	1.74906385
AT1G30190	-2.0832655	AT1G14250	7.69737496	AT4G08850	1.84861949	AT3G07580	1.51839264
AT1G17870	-2.7431666	AT5G22390	3.08556073	AT4G04570	1.45250995	AT1G19850	1.41207676
AT2G33590	-2.0000167	AT1G31580	3.37498913	AT3G12145	3.16410679	AT3G23090	1.41814179
AT3G50980	-2.3584547	AT5G23820	3.9762119	AT1G52220	1.11146385	AT5G08020	3.05225775
AT3G22840	-3.1853448	AT4G08870	3.5257446	AT4G36540	2.07544341	AT3G14240	1.27065553

AT5G06760	-2.6638905	AT2G34430	4.46498748	AT1G04800	1.92125852	AT1G68780	2.04085392
AT4G25433	-2.4104527	AT4G38660	3.83601578	AT2G32690	1.58916411	AT4G03270	5.78866597
AT3G55880	-2.0293222	AT1G68840	2.71832986	AT1G54020	3.37993056	AT1G52410	2.41690025
AT1G14730	-2.0916721	AT3G16470	4.10128802	AT2G22330	2.00189658	AT1G47290	1.09326107
AT3G44290	-4.1125878	AT1G18620	2.37099927	AT2G39310	6.22274608	AT4G39190	1.26131983
AT4G33150	-1.8657883	AT5G65730	3.32914811	AT3G25130	2.65237352	AT3G06020	2.68966221
AT4G25450	-1.2488334	AT4G14400	3.10246189	AT3G09035	1.3740352	AT4G14815	3.90724271
AT3G12960	-3.9841334	AT1G66970	2.12613708	AT5G58150	1.62667144	AT5G45470	1.43554517
AT3G03620	-5.3521398	AT4G00400	3.14972151	AT2G34490	2.32977849	AT1G26570	2.12882568
AT4G36240	-1.5528589	AT3G53190	4.45335088	AT2G05070	1.85849495	AT3G48040	1.45581563
AT2G12400	-1.4035912	AT2G15080	1.96561846	AT2G34620	1.90861696	AT5G55730	1.93716193
AT3G62990	-2.1392363	AT2G42870	3.56706204	AT2G41800	3.00457997	AT5G16400	1.0322794
AT5G47560	-1.5794236	AT5G63180	2.27894162	AT2G42690	1.61603269	AT5G22880	1.25665826
AT1G57590	-2.8073178	AT2G39330	4.3190086	AT1G80280	2.05690506	AT1G12250	1.08155119
AT1G05340	-2.568833	AT1G65486	3.06324241	AT1G49430	1.48840948	AT1G73870	1.58182418
AT1G14720	-1.3405606	AT4G24350	2.94721834	AT5G60710	1.2031395	AT4G25050	1.23747334
AT2G46940	-1.6805261	AT1G66940	3.19063038	AT5G06290	1.34978489	AT2G05100	1.13628797
AT1G31750	-2.1729428	AT1G73325	5.25582633	AT2G38120	1.27217343	AT3G23730	2.31571592
AT5G26770	-1.3141497	AT3G55630	1.72479108	AT4G03100	2.9533173	AT3G16770	1.33393726
AT1G03106	-2.9837963	AT3G01500	3.53166617	AT5G49630	1.64435415	AT1G14290	1.47713169
AT4G21320	-1.831968	AT2G37170	2.49609012	AT5G56550	1.51046134	AT1G47400	5.58265456
AT4G23493	-1.5845429	AT2G32100	2.69922238	AT3G47470	1.07457825	AT1G74070	1.1998437
AT1G60970	-3.0386244	AT5G25980	1.95768049	AT1G29930	1.44641206	AT2G04780	1.47690771
AT2G42560	-4.584553	AT2G36050	3.0830809	AT2G46810	2.08396759	AT3G07340	2.56931348
AT1G68500	-2.1048096	AT1G26770	3.04393401	AT4G37410	3.60065319	AT5G42650	1.54450321
AT2G42000	-6.7570504	AT4G18440	2.32277619	AT1G20340	1.26150835	AT1G19840	2.22075776
AT5G15250	-3.2313999	AT1G65860	2.84051051	AT1G09340	1.25068811	AT2G23010	1.99539197
AT3G17520	-4.2238034	AT5G06150	3.90558921	AT5G24660	1.56799051	AT3G13560	1.41135056
AT4G12580	-1.9935348	AT1G64200	2.70480514	AT1G14460	1.46672677	AT3G22060	2.2465171
AT1G70800	-1.4152426	AT5G67420	1.65293731	AT2G43535	2.29589981	AT2G21640	1.36346713
AT1G77120	-2.1298474	AT1G54010	4.94327529	AT1G21520	1.45690612	AT5G03390	2.87421796
AT1G50930	-3.3311456	AT5G42530	3.08075293	AT5G18060	2.35661161	AT1G62660	1.09797139
AT5G13370	-1.8962885	AT4G17470	3.33609835	AT1G22330	2.73084482	AT5G44572	1.78155727
AT5G07330	-2.0991338	AT5G16030	2.26394637	AT2G37950	2.29949756	AT3G03190	1.94091649
AT1G29640	-2.0247301	AT1G28400	2.14776275	AT5G16190	3.01561287	AT3G18890	1.17361163
AT3G23000	-1.3050506	AT3G05730	3.71693805	AT5G66570	1.18107154	AT2G34510	1.3872997
AT3G22830	-2.729365	AT1G21500	1.83514774	AT3G23890	3.32384667	AT1G70820	1.2601746
AT4G09610	-2.7975125	AT3G45860	2.5410292	AT3G06080	1.22591792	AT2G13610	1.52600686
AT4G34860	-1.9004933	AT4G12730	2.73830168	AT1G65845	2.97437178	AT1G08980	1.12628011
AT3G21270	-1.3121777	AT3G27690	2.62768527	AT5G65700	1.41059443	AT1G52030	2.45292335
AT5G61820	-1.5581342	AT5G24420	3.89534617	AT3G27400	2.51373145	AT1G10470	1.27812794
AT3G50970	-2.2159142	AT3G26520	2.62169421	AT1G10657	2.01448505	AT4G13500	1.14250361
AT2G37770	-2.7064577	AT3G49670	1.94515292	AT5G43020	2.11186557	AT5G18860	1.44857459
AT5G54585	-1.9306464	AT5G54270	2.0234527	AT1G49870	3.95502604	AT1G52770	1.99556141
AT5G05220	-2.7273439	AT5G44020	3.2189011	AT3G54600	1.72841536	AT3G55330	1.3497546
AT3G57520	-1.9609719	AT3G47380	7.38098533	AT1G11260	2.15354876	AT2G17550	1.22795679
AT1G47570	-1.0661223	AT1G72610	2.9124623	AT5G03885	6.79830856	AT5G51550	1.54859443
AT4G18422	-2.3176962	AT2G29290	2.35159924	AT3G02110	1.47574862	AT2G33850	3.15270804
AT5G25110	-2.7486972	AT3G47340	3.09025657	AT4G39710	1.42824186	AT2G06200	5.51002081
AT4G33540	-1.2703503	AT3G50270	2.26627532	AT5G45650	1.5373834	AT5G58670	1.06605225
AT4G10250	-2.5445973	AT2G23700	2.14299877	AT1G54385	4.89458987	AT4G21590	2.82803016
AT3G44880	-1.3004992	AT3G02120	4.90027678	AT1G17140	1.77561498	AT5G03350	3.25919665
AT2G34850	-1.5869634	AT5G62630	1.58206818	AT5G08760	1.92096503	AT1G77060	1.29540017
AT1G21460	-1.8555644	AT3G22890	1.23860742	AT5G51720	2.03220483	AT2G14750	1.2124051
AT4G30830	-1.7094	AT2G21140	3.98894237	AT5G59360	3.12439342	AT1G78820	1.1257795
AT1G21790	-1.3981496	AT3G02640	3.56881227	AT4G05180	1.58171528	AT4G10340	1.38670053
AT3G23910	-1.3619564	AT1G16630	4.81595356	AT5G09440	1.39594952	AT1G11670	2.0205853
AT1G29680	-4.1599348	AT4G29700	4.24336496	AT3G10080	1.94519739	AT1G18370	4.48129213
AT5G11110	-1.4020952	AT4G14040	1.64819274	AT5G07030	2.03293273	AT4G24970	1.47159235
AT2G39250	-1.5601377	AT2G33480	1.13249903	AT2G42530	1.70093308	AT3G19550	1.83523241
AT3G20300	-1.6592942	AT2G39700	1.94758013	AT5G56850	1.24507883	AT5G67150	1.44908011
AT5G15450	-1.0868319	AT3G14840	1.79462158	AT5G10400	1.69437705	AT1G18140	3.28075147
AT3G53230	-1.3413303	AT4G27860	2.29701973	AT1G64720	1.07814315	AT3G10010	1.39589551
AT1G15310	-1.6458673	AT2G25510	2.40914409	AT4G04630	1.62096469	AT3G48720	2.10886555
AT5G37540	-1.2032852	AT5G10170	2.14734246	AT1G53520	2.9641463	AT5G27060	2.91436053
AT1G46768	-1.3244293	AT2G30766	3.58220193	AT4G18760	1.85966831	AT4G22120	1.213822
AT5G54580	-1.0166587	AT1G76310	3.37905913	AT3G04910	1.01051957	AT2G46140	1.41409235
AT3G45970	-2.756972	AT1G11580	2.16817828	AT5G43750	1.38706621	AT1G52400	2.74062779
AT5G22470	-6.8673453	AT2G36120	2.92128752	AT2G36430	1.24549961	AT1G21810	2.96188203
AT5G66400	-3.0022605	AT5G38420	3.07172751	AT1G74690	1.24678356	AT1G11860	1.21493918
AT3G25870	-1.2878599	AT5G06870	2.76248709	AT3G52060	1.03661258	AT4G15765	1.223741
AT1G78600	-1.1416704	AT5G10180	1.65401909	AT5G23210	1.65134157	AT2G30500	1.12694438
AT1G07720	-1.3241546	AT5G64040	1.64036832	AT5G60800	2.94328513	AT3G07320	1.86992708
AT4G22240	-1.2219376	AT4G39940	1.83796377	AT1G23390	1.40947129	AT5G57130	1.8750466
AT4G35560	-1.5565244	AT5G27290	2.83992901	AT2G32380	1.4719582	AT5G20740	2.86728254
AT3G62660	-1.1165941	AT3G21055	1.82689399	AT3G43800	1.12310681	AT4G00460	5.51214324

AT1G17020	-1.8611635	AT4G13410	5.39913765	AT1G58290	1.08498774	AT2G12462	2.06159897
AT5G54165	-2.2098967	AT1G75180	1.76217348	AT1G76110	1.10940025	AT3G19050	2.84145889
AT3G55610	-1.3402546	AT1G49130	1.90716429	AT5G09240	1.2594394	AT4G29080	1.38119796
AT3G03270	-1.2077695	AT5G56610	1.65594542	AT5G57700	1.59269927	AT1G09390	1.74260937
AT3G46230	-2.5001376	AT1G13260	2.32722736	AT2G39470	1.49685126	AT4G13770	1.51753098
AT3G15670	-1.9639349	AT4G01460	2.13055593	AT3G13750	2.28282659	AT2G46440	1.20577068
AT2G43580	-1.7162151	AT1G65490	1.93832182	AT5G19120	2.52451898	AT4G14330	2.63136112
AT5G50360	-2.2193695	AT3G45140	3.40887837	AT3G19850	1.72722534	AT5G59870	1.32588932
AT1G54120	-1.7974777	AT1G71880	1.62489101	AT4G02770	1.03330766	AT1G29160	1.26496022
AT2G41210	-1.1310895	AT1G09750	2.08642423	AT2G32990	2.34823568	AT3G22231	2.54008681
AT3G57010	-1.495376	AT1G31710	2.86390135	AT3G18080	1.42337109	AT2G31880	1.65424721
AT4G39140	-1.0539115	AT1G19640	3.09550546	AT2G25900	1.29705367	AT5G47330	2.6464826
AT5G08600	-2.2511281	AT1G66280	5.42031748	AT1G29920	1.94588146	AT3G61280	1.24022019
AT4G37295	-3.5811662	AT4G12480	3.6176844	AT1G48480	2.10443624	AT3G51080	1.99555441
AT5G50240	-1.2138696	AT3G50280	3.41161838	AT3G06770	2.37437686	AT1G80850	1.67138188
AT5G43770	-6.0078532	AT4G12490	6.25060293	AT2G40820	1.55257874	AT5G14060	1.00731239
AT2G27300	-4.4174093	AT3G59010	2.08021011	AT1G02800	3.77425617	AT1G15085	2.96675946
AT4G30710	-1.1205556	AT4G27740	1.78662241	AT4G31360	1.40998539	AT1G31690	5.70300218
AT4G03820	-1.6734706	AT3G13510	2.05403314	AT3G19820	1.70700587	AT5G44680	1.29235917
AT2G20770	-1.1752877	AT5G01530	1.62244984	AT3G50750	1.25656354	AT2G34060	2.63517583
AT2G16890	-1.3751994	AT5G26000	1.56816001	AT5G10310	1.33458988	AT5G40150	1.23199835
AT1G33700	-1.6122274	AT1G16410	2.48118639	AT2G30570	1.11427653	AT4G21445	1.45682005
AT3G48240	-1.6687701	AT5G08330	1.54515478	AT3G50240	1.26661355	AT2G25270	1.88945594
AT1G16515	-1.6300987	AT3G50070	2.58796878	AT5G10390	1.55434408	AT3G23880	2.16282114
AT5G15240	-2.1878511	AT1G51400	1.67745623	AT4G13575	1.34194879	AT1G27020	2.98734551
AT4G32690	-1.2994068	AT4G33666	1.94256115	AT5G21170	1.43436967	AT4G18570	1.01158987
AT1G48000	-1.5541053	AT4G15830	3.44507662	AT2G22980	1.4689123	AT4G37110	1.61997884
AT4G34590	-1.2412012	AT5G49170	4.14056866	AT5G42860	2.14893948	AT3G47560	1.26460925
AT2G15480	-1.4433711	AT5G44568	3.11666677	AT4G03210	2.37579165	AT2G38870	1.52645433
AT5G47590	-1.7812617	AT1G09415	1.30611291	AT4G37650	1.12635262	AT5G43060	1.22075663
AT1G10070	-1.2968639	AT3G55500	2.02128934	AT4G02060	1.75038999	AT3G55240	1.75235711
AT3G13672	-1.4362068	AT4G23800	2.85756193	AT3G13437	2.71987534	AT3G50770	1.4841753
AT1G01470	-1.0327525	AT5G45490	1.5790618	AT3G52720	2.78846612	AT5G04190	2.86090166
AT5G61600	-1.6069496	AT2G15090	1.86620905	AT1G73020	1.69950127	AT5G44565	1.23037447
AT1G26210	-1.3512832	AT3G12150	1.77893685	AT1G72060	2.67505579	AT2G36890	3.09870216
AT1G24580	-2.1475744	AT3G28860	1.66535019	AT1G44000	1.2351707	AT3G54920	1.23733538
AT3G03250	-1.2064829	AT5G13630	1.29643644	AT5G55170	1.84547439	AT2G34810	1.26694624
AT4G39210	-1.4334124	AT3G10720	2.33502082	AT1G44110	2.27108959	AT1G15125	2.86345375
AT4G23920	-1.430244	AT2G05790	2.02324171	AT4G35620	3.77298505	AT5G63850	1.13653716
AT1G51090	-1.5359078	AT4G34160	2.9869283	AT1G68520	1.4519189	AT2G28510	1.04747786
AT1G69260	-1.2048901	AT1G03820	2.405952	AT5G42720	1.45700111	AT5G49160	1.50331226
AT5G09640	-3.9761176	AT1G04680	2.64528195	AT4G23170	1.29151482	AT3G27060	1.22465954
AT5G17460	-1.6717522	AT1G77885	2.36761521	AT1G22650	2.48155003	AT2G38760	2.82752805
AT4G24000	-1.6172619	AT2G41090	1.99164355	AT5G66920	1.92332589	AT5G18660	1.47526428
AT1G35720	-1.0937745	AT5G24290	2.86788297	AT5G07660	2.43185637	AT1G20610	3.01864677
AT1G62045	-1.6342438	AT4G36670	2.12643358	AT4G20430	1.80535531	AT5G06790	1.45868055
AT3G61890	-1.5039702	AT2G28950	1.96630841	AT2G22930	3.72686954	AT2G29730	2.02210493
AT4G25990	-1.6108278	AT1G73330	4.76446349	AT1G26761	1.36181521	AT2G36200	2.82843317
AT1G08630	-1.7127749	AT5G14200	1.8066207	AT3G54560	2.2735398	AT1G78995	1.011453
AT3G12955	-2.0682213	AT3G28220	3.59273856	AT3G08920	1.21517845	AT5G54530	1.83435316
AT3G59280	-1.0130161	AT4G15210	3.51593563	AT3G56480	1.50078083	AT2G46535	1.36665569
AT5G23750	-1.786373	AT4G04840	3.91643259	AT2G16850	2.41463158	AT3G07540	1.83780298
AT1G54160	-1.445042	AT2G15760	3.13571442	AT1G65230	1.01061238	AT1G12900	1.01042368
AT2G41190	-1.766374	AT1G15820	1.73789355	AT2G15050	1.41324	AT2G23680	1.16648643
AT5G53400	-1.0058985	AT2G43150	1.84875344	AT4G23130	1.94801102	AT1G15910	1.12922601
AT3G20500	-1.0870339	AT1G67740	1.43734315	AT4G11190	6.66284486	AT4G36230	1.53284
AT2G43780	-1.0408027	AT5G46240	1.96654526	AT1G15830	2.22849783	AT5G40460	4.10221273
AT5G13170	-1.7348987	AT3G20390	1.28851206	AT5G59670	2.17187912	AT1G32470	1.14358201
AT4G12430	-1.5252813	AT1G08380	1.25782483	AT5G25190	3.51594796	AT2G23200	1.09776619
AT5G07080	-1.6023679	AT3G10120	1.54807741	AT5G46330	1.18715377	AT1G47670	1.47399701
AT1G07390	-1.6694548	AT5G38410	2.18439473	AT2G20670	2.48654429	AT2G32010	1.52362024
AT4G19230	-1.5608245	AT4G21830	5.31682206	AT1G67750	2.55920397	AT4G26660	2.70123998
AT3G22560	-1.3695771	AT4G17340	2.00862953	AT4G37260	1.22800795	AT3G51340	2.96948104
AT1G16850	-1.6247271	AT5G24770	5.27151262	AT2G43520	2.3751334	AT4G29360	1.78909992
AT5G42290	-1.5319432	AT2G37640	2.49229188	AT5G25090	3.11022513	AT5G25490	1.90489791
AT5G43330	-1.0449268	AT2G30520	1.44081038	AT2G01420	1.08528503	AT1G48610	1.13464457
AT4G13800	-1.695738	AT1G12010	2.39048206	AT5G05340	2.84355227	AT2G44450	4.25139646
AT2G16720	-1.140721	AT5G60200	1.66548613	AT1G59930	3.17643841	AT3G01710	3.25335552
AT1G20440	-1.2365192	AT1G55670	1.62989292	AT4G23260	1.1656829	AT5G14230	1.87102256
AT1G50020	-1.0080998	AT3G15950	4.05964316	AT5G15580	1.69565301	AT2G03550	1.11592091
AT1G14520	-1.5514043	AT1G29980	2.11318204	AT1G06160	1.87645498	AT4G05190	2.62210476
AT1G68640	-4.2258979	AT3G51740	3.79786422	AT4G28250	2.24391789	AT1G18590	1.15327294
AT2G29380	-4.0890733	AT1G12020	1.60181993	AT1G30600	2.32792297	AT3G16400	1.21098871
AT5G51990	-2.5438698	AT1G54030	1.09149124	AT1G06420	2.59912583	AT4G12420	1.52107736
AT1G50630	-1.1623046	AT2G25060	3.28455543	AT1G69910	1.25032874	AT3G17460	1.31305807
AT1G52690	-3.7986711	AT4G12030	2.34702582	AT5G67385	1.66244305	AT1G65710	3.11983242

AT5G01670	-1.0245382	AT4G04830	2.14771932	AT1G75820	1.32136681	AT2G02950	1.28527588
AT1G62710	-1.4969278	AT3G51450	1.88000752	AT5G40450	1.77704248	AT2G25810	6.27597139
AT5G15190	-1.4510587	AT5G64410	2.21658449	AT5G56860	1.04556532	AT1G75550	3.6199739
AT1G77450	-1.4642483	AT2G38970	1.37450119	AT3G19540	1.03023042	AT5G11410	5.41585336
AT3G11050	-2.0164557	AT3G46780	1.9267021	AT3G44050	2.52964563	AT2G39900	1.2468568
AT1G73880	-1.3643603	AT1G70830	1.65348718	AT1G64390	1.89901889	AT4G32830	3.24184279
AT1G54100	-1.2094398	AT4G16990	1.19726451	AT1G30380	1.10048478	AT5G16720	1.22036776
AT5G15960	-1.8652419	AT5G62280	2.35656977	AT1G28390	2.51364724	AT1G75450	2.19518628
AT3G07810	-1.1065391	AT5G23860	1.66668152	AT3G63140	1.12901842	AT3G54180	2.12254657
AT3G03341	-1.1739589	AT1G52230	1.44721394	AT5G13140	2.14765592	AT5G63780	1.31207456
AT1G07290	-3.0044143	AT1G31330	1.34947699	AT3G20150	2.68413423	AT2G34170	1.5980899
AT4G17530	-1.1594599	AT5G51560	2.5732354	AT4G38770	1.85681384	AT3G22415	1.38065109
AT4G18830	-1.2369992	AT1G03130	1.26954876	AT3G01680	1.42333455	AT3G04630	1.29296946
AT1G55280	-1.0719591	AT5G49100	1.93564844	AT4G03205	1.1908612	AT1G21270	1.0832444
AT4G40080	-1.2306343	AT2G28790	3.0297681	AT3G29631	2.13139264	AT5G23420	1.38872095
AT4G26950	-2.2183407	AT2G32487	2.93737009	AT1G72250	2.17683862	AT2G36355	2.41582448
AT3G49320	-1.6041049	AT3G24982	2.00232006	AT1G52190	1.98629353	AT1G65510	2.14386083
AT1G02700	-3.0113981	AT3G22120	1.94791669	AT5G39860	2.64179784	AT5G04840	2.16782406
AT4G15530	-1.3384252	AT4G28780	2.34687735	AT3G61820	1.38439958	AT1G73620	5.51243741
AT5G28080	-1.9909843	AT3G22210	1.49452832	AT5G22580	2.2592078	AT3G51150	1.13904555
AT4G30150	-1.0204946	AT2G46820	1.33216017	AT5G28020	1.36874061	AT4G12470	5.99922152
AT5G04250	-1.21948	AT5G16250	2.79568657	AT5G58260	1.26891083	AT4G10290	3.40388088
AT2G35760	-1.0016156	AT1G19670	2.71564685	AT4G26520	1.13105977	AT5G18030	1.31731601
AT5G57560	-2.1698402	AT3G28040	1.59539316	AT2G06520	1.0187986	AT5G15350	1.16216902
AT4G17840	-1.0821392	AT5G50740	2.34569966	AT3G27360	1.24519374	AT1G35260	1.9869302
AT3G57780	-1.1716666	AT4G12500	7.47904997	AT5G25440	1.36056511	AT1G67050	1.06784729
AT5G53870	-1.5488433	AT1G01620	1.78099983	AT3G57600	1.3772778	AT3G25730	4.01286854
AT1G02470	-1.7729724	AT1G45201	2.19525537	AT3G54890	1.14734021	AT3G20470	2.17968272
AT1G06570	-1.0031469	AT2G44210	1.42049593	AT1G08560	2.51079864	AT3G30180	1.45302011
AT3G04040	-1.1795111	AT2G18560	1.64185064	AT5G44040	1.81344263	AT4G32290	1.19158846
AT1G60680	-1.7346651	AT3G22142	2.56577733	AT1G20930	2.45365593	AT5G46700	1.58438273
AT5G63350	-1.2411533	AT2G01950	2.24480921	AT1G19990	1.24398179	AT3G26470	2.63141983
AT2G36800	-1.4292108	AT5G02890	2.50386304	AT4G02420	1.45855548	AT1G07610	2.04528022
AT3G10450	-1.2533346	AT1G24100	1.17903704	AT5G52780	1.07189234	AT4G22470	3.15183271
AT5G62480	-1.6367054	AT3G18050	1.78089269	AT5G62710	1.6876332	AT5G59080	1.47186457
AT3G61900	-1.6848866	AT4G31840	2.98890762	AT5G05250	2.63068113	AT1G18810	1.31877405
AT3G49210	-1.0325828	AT4G21280	1.53262877	AT1G06620	2.9266697	AT5G26670	2.7570911
AT3G62090	-1.2100363	AT4G01900	1.27516026	AT1G62520	1.95552497	AT3G15550	3.61921946
AT5G51220	-1.1810894	AT4G04220	3.14372368	AT1G74440	1.57868037	AT1G36675	2.81568899
AT5G53710	-1.1615272	AT3G16420	1.92063904	AT1G29450	1.82181193	AT4G16983	5.22808237
AT1G01250	-1.5977219	AT5G56840	4.71820726	AT1G67090	1.49625166	AT1G72730	2.21213116
AT4G19645	-1.7204238	AT4G00760	1.1956416	AT5G44130	1.7349865	AT3G09960	2.16847786
AT3G48020	-1.6700025	AT3G45930	1.46196175	AT1G19960	2.05156034	AT1G15000	1.25216458
AT5G37670	-1.1791884	AT1G29910	1.54829484	AT1G05210	2.25357439	AT2G05160	1.45363487
AT5G62150	-1.7652327	AT3G62390	2.31123897	AT5G10605	2.58497217	AT3G17840	1.71237173
AT1G22990	-1.5052327	AT2G33400	2.32727608	AT4G22305	1.89746778	AT3G25020	1.53546169
AT1G62570	-1.1960825	AT5G19230	2.52303976	AT2G25200	1.35948381	AT1G69700	1.10514434
AT5G64430	-1.1297926	AT1G50010	1.56992922	AT3G09070	1.25389522	AT4G04610	1.38683011
AT3G54680	-1.0327509	AT1G68560	1.34031368	AT1G50732	1.86745174	AT5G18050	1.50442155
AT5G49700	-1.6906599	AT2G30420	2.87993343	AT4G31500	1.33526	AT2G19460	1.0965165
AT5G05880	-5.5762677	AT1G32060	1.20158922	AT2G26530	1.98568428	AT4G30130	3.27810926
AT1G72660	-2.6290716	AT3G08940	1.44126702	AT1G58225	1.98271267	AT2G43100	1.4500418
AT5G52300	-2.4726923	AT1G75190	1.78342597	AT3G15630	1.96830557	AT1G65985	1.81213201
AT5G25900	-1.0101618	AT1G24147	2.79230748	AT3G06868	2.4657233	AT5G03870	3.67447878
AT4G27010	-1.1918769	AT1G06680	1.34130585	AT5G23020	2.30734028	AT1G31320	2.31824129
AT1G12064	-3.8882251	AT4G28750	1.14818631	AT1G66465	2.93674817	AT4G02330	2.47464392
AT5G47650	-1.0487258	AT1G25510	3.20313318	AT3G03130	4.74843657	AT1G26250	4.11505146
AT2G17680	-2.4825775	AT4G22010	2.63996489	AT3G16250	1.21408431	AT1G78460	1.18253483
AT2G38400	-1.0876347	AT5G24780	3.83878961	AT1G15570	3.17240333	AT1G52140	1.76091123
AT3G15357	-2.0802072	AT2G28620	3.71250138	AT1G14345	1.06540116	AT5G61480	1.29875686
AT4G01985	-1.6820255	AT3G58990	2.19017758	AT3G56370	1.68651426	AT5G38710	1.87678341
AT5G01520	-1.2279928	AT3G02020	2.55906744	AT1G32190	1.84495439	AT3G16660	1.91732163
AT2G28320	-1.0299108	AT2G07180	1.05020048	AT1G17560	2.58672119	AT3G51280	3.82507151
AT2G36750	-2.7704514	AT4G38062	5.1459366	AT5G60930	2.67885269	AT2G38620	3.9759515
AT4G08570	-2.4403266	AT1G69780	2.1846945	AT1G54740	1.28457708	AT1G75690	1.13689932
AT4G36700	-2.8794209	AT1G66870	5.20543034	AT2G25220	2.31614668	AT5G47500	2.42803404
AT5G43840	-1.3902951	AT5G21430	1.24455741	AT5G64260	1.57095384	AT5G10430	1.48957707
AT3G28007	-1.1470979	AT4G27440	1.24166703	AT1G70710	1.7302978	AT3G49570	2.2030686
AT5G24030	-1.4961653	AT4G31820	1.75585346	AT1G29270	6.06122247	AT4G33260	5.23516571
AT1G17830	-1.1936394	AT5G14740	2.42336024	AT2G18730	1.32556243	AT1G76870	1.47472774
AT4G09589	-5.4278451	AT2G34420	1.2208883	AT4G30560	1.61999365	AT1G06360	2.19241744
AT1G15550	-1.8661738	AT4G26530	1.9978277	AT1G66190	1.657538		
AT1G02340	2.1198574	AT1G70470	2.48196248	AT1G14180	2.6330626		

Supplemental Table 4: Gene ontology (GO) of each cluster in the hierarchical clustering to all DEGs among wild-type, *jar1-11* and JAR1-OE as mentioned in Fig. 26C.

Cluster 1_summary_topGO_analysis

GO.ID	Term	p.adj
GO:0006833	water transport	4E-04
GO:0040008	regulation of growth	0.0076
GO:0009734	auxin-activated signaling pathway	0.0088
GO:0006949	syncytium formation	0.0088
GO:0045490	pectin catabolic process	0.0379

Cluster 2_summary_topGO_analysis

GO.ID	Term	p.adj
GO:0009735	response to cytokinin	0
GO:0009768	photosynthesis	9E-04
GO:0006412	translation	0.0036
GO:0018298	protein-chromophore linkage	0.0104
GO:0009773	photosynthetic electron transport in pho...	0.0179
GO:0019344	cysteine biosynthetic process	0.0179
GO:0015995	chlorophyll biosynthetic process	0.0433
GO:0080167	response to karrikin	0.0449
GO:0009645	response to low light intensity stimulus	0.0449

Cluster 3_summary_topGO_analysis

GO.ID	Term	p.adj
GO:0010411	xyloglucan metabolic process	4E-04
GO:0042546	cell wall biogenesis	4E-04
GO:0009861	jasmonic acid and ethylene-dependent sys...	0.0426
GO:0009741	response to brassinosteroid	0.0426

Cluster 4_summary_topGO_analysis

GO.ID	Term	p.adj
GO:0009416	response to light stimulus	0.0027
GO:0015979	photosynthesis	0.0054
GO:0007623	circadian rhythm	0.008
GO:0009744	response to sucrose	0.0205
GO:0019761	glucosinolate biosynthetic process	0.0303
GO:0006468	protein phosphorylation	0.0352
GO:0032259	methylation	0.0352

Cluster 5_summary_topGO_analysis

GO.ID	Term	p.adj
GO:0009414	response to water deprivation	0
GO:0009651	response to salt stress	0
GO:0009737	response to abscisic acid	0
GO:0071456	cellular response to hypoxia	0
GO:0009611	response to wounding	0
GO:0009753	response to jasmonic acid	0
GO:0042542	response to hydrogen peroxide	0
GO:0009409	response to cold	0
GO:0042538	hyperosmotic salinity response	0
GO:0009408	response to heat	0
GO:0009644	response to high light intensity	0
GO:0006979	response to oxidative stress	1E-04
GO:0055114	oxidation-reduction process	4E-04
GO:0009751	response to salicylic acid	5E-04
GO:2000143	negative regulation of DNA-templated tra...	6E-04
GO:0009738	abscisic acid-activated signaling pathwa...	9E-04
GO:0010150	leaf senescence	0.0017
GO:0010200	response to chitin	0.0025
GO:0010286	heat acclimation	0.004
GO:0006572	tyrosine catabolic process	0.0044
GO:0006970	response to osmotic stress	0.0066
GO:0006749	glutathione metabolic process	0.0086
GO:0009723	response to ethylene	0.0102
GO:0080167	response to karrikin	0.0155
GO:0046686	response to cadmium ion	0.0303
GO:0055129	L-proline biosynthetic process	0.0316
GO:0009058	biosynthetic process	0.0374
GO:0009718	anthocyanin-containing compound biosynth...	0.0383
GO:0045893	positive regulation of transcription	0.0479

Supplemental Table 5: List of DEGs up-and downregulated in *myb2* compared to WT plants. (DESeq, adjusted FDR < 0.01 and LogFC ≥ 1)**;** "C" under control conditions; "D" under drought stress. logFC with "+" or"-" sign indicates up- or downregulation respectively.

Col_C-MB_C logFC		**Col_C-MB_C logFC**		**Col_C-MB_C logFC**	
AGI code	**logFC**	**AGI code**	**logFC**	**AGI code**	**logFC**
AT2G47190	-4.3079378	AT5G42180	-6.2794327	AT4G38080	-6.9562308
Col_D-MB_D		**Col_D-MB_D**		**Col_D-MB_D**	
AGI code	**logFC**	**AGI code**	**logFC**	**AGI code**	**logFC**
AT2G47190	-5.5278464	AT2G28950	-2.0644259	AT5G63180	-2.3874995
AT4G38860	-2.8681548	AT4G19430	-7.7955907	AT2G40610	-6.5037155
AT5G60490	-3.1260677	AT5G24780	-3.8283071	AT3G04290	-4.2607931
AT2G24762	-2.1272103	AT5G22580	-2.7760364	AT5G46295	7.1235337
AT5G15230	-4.3196651	AT2G10940	-4.606942	AT2G22470	1.88228668
AT4G18970	-4.1936116	AT1G78970	-2.3737336		
AT3G58120	-6.4800057	AT5G20630	-5.9013309		

Supplemental File 1: Accession numbers mentioned in the thesis

Gene	ID	Gene	ID	Gene	ID	Gene	ID
EXPA3	AT2G37640	*LEA46*	AT5G06760	*ABCG25*	AT1G71960	*JAZ9*	AT1G70700
LTP2	AT2G38530	*ZEP*	AT5G67030	*ABCG40*	AT1G15520	*JAZ10*	AT5G13220
FT	AT1G65480	*ABA2*	AT1G52340	*ABI1*	AT4G26080	*JAZ11*	AT3G43440
LFY	AT5G61850	*ABA3*	AT1G16540	*ABI2*	AT5G57050	*JAZ12*	AT5G20900
APETALA2	AT2G33860	*ABA4*	AT1G67080	*ABI3*	AT3G24650	*JAZ13*	AT3G22275
FLC	AT5G10140	*NCED1*	AT3G63520	*ABI4*	AT2G40220	*MYC2*	AT1G32640
SOC1	AT2G45660	*NCED2*	AT4G18350	*ABI5*	AT2G36270	*MYC3*	AT5G46760
FMO1	AT1G19250	*GCR2*	AT1G52920	*ACX1*	AT4G16760	*NINJA*	AT4G28910
CYP94B3	AT3G48520	*NCED7*	AT2G44990	*AOC1*	AT3G25760	*JAM1*	AT2G46510
CYP94C1	AT2G27690	*NCED8*	AT4G32810	*AOC2*	AT3G25770	*CLH1*	AT1G19670
JOX3	AT3G55970	*NCED9*	AT1G78390	*AOC3*	AT3G25780	*CORI3*	AT4G23600
CYP94B1	AT5G63450	*AAO3*	AT2G27150	*AOC4*	AT1G13280	*ORA59*	AT1G06160
MBP2	AT1G52030	*NCED5*	AT1G30100	*AOS*	AT5G42650	*VSP2*	AT5G24770
GRF5	AT3G13960	*LEA31*	AT3G22490	*BG2*	AT2G32860	*JAZ6*	AT1G72450
GIF1	AT5G28640	*RAB18*	AT5G66400	*BGLU18*	AT1G52400	*JAZ5*	AT1G17380
SYP111	AT1G08560	*LEA7*	AT1G52690	*CYP707A1*	AT4G19230	*JAZ1*	AT1G19180
FBL17	AT3G54650	*LEA18*	AT2G35300	*CYP707A2*	AT2G29090	*JAZ2*	AT1G74950
CYCA3.2	AT1G47210	*RD22*	AT5G25610	*CYP707A3*	AT5G45340	*JAZ3*	AT3G17860
CYCB1.2	AT5G06150	*RD29B*	AT5G52300	*CYP707A4*	AT3G19270	*JAZ4*	AT1G48500
EXPA8	AT2G40610	*SAUR16*	AT4G38860	*GASA4*	AT5G15230	*ADH1*	AT1G77120
SOT15	AT5G07010	*NCED6*	AT3G24220	*HPL*	AT4G15440	*VSP1*	AT5G24780
TKL1	AT3G60750	*TGG1*	AT5G26000	*JAR1*	AT2G46370	*ORA47*	AT1G74930
IAR3	AT1G51760	*RD29A*	AT5G52310	*JASSY*	AT1G70480	*SKP1*	AT1G75950
HIGD2	AT5G27760	*TGG2*	AT5G25980	*JMT*	AT1G19640	*GSH1*	AT4G23100
LHCB2.4	AT3G27690	*EPF2*	AT1G34245	*KAT1*	AT1G04710	*GR1*	AT3G24170
MAF1	AT1G77080	*NCED3*	AT3G14440	*LOX2*	AT3G45140	*MYC4*	AT4G17880
SPL4	AT1G53160	*NCED4*	AT4G19170	*LOX3*	AT1G17420	*PDF1.2A*	AT5G44420
LHCB6	AT1G15820	*MYB124*	AT1G14350	*MFP*	AT3G16000	*DHAR1*	AT1G19570
ILL6	AT1G44350	*ERD7*	AT2G17840	*OPCL1*	AT1G20510	*CUL1*	AT4G02570
COR15B	AT2G42530	*LEA14*	AT1G01470	*OPR3*	AT2G06050	*TPL*	AT1G15750
LHCB6	AT1G15820	*EXPA6*	AT2G28950	*PSAB*	ATCG00340	*MYB2*	AT2G47190
COR47	AT1G20440	*TMM*	AT1G80080	*PXG3/RD20*	AT2G33380	*GSH2*	AT5G27380
LHCB5	AT4G10340	*FLA12*	AT5G60490	*RBCL*	ATCG00490	*CML12*	AT2G41100
LHCB4.2	AT3G08940	*SBT1.2*	AT1G04110	*RBCS1A*	At1g67090	*GR2*	AT3G54660
LHCB1.1	AT1G29920	*ACT2*	AT3G18780	*RBCS1B*	At5g38430	*CaBP-22*	AT2G41090
LHCB2.1	AT2G05100	*LHCB3*	AT5G54270	*RBCS2B*	At5g38420	*CML42*	AT4G20780
LHB1.4	AT2G34430	*PER64*	AT5G42180	*RBCS2B*	At5g38420	*CAM2*	AT2G41110
LHCB2.2	AT2G05070	*LHCB4.1*	AT5G01530	*RBCS3B*	At5g38410	*CML37*	AT5G42380
SYP111	AT1G08560	*DREB2A*	AT5G05410	*UGT71B6*	AT3G21780	*JAZ7*	AT2G34600
CSLD5	AT1G02730	*LEA6*	AT1G32560	*UGT75C1*	AT4G14090	*JAZ8*	AT1G30135

Supplemental File 2: License and official John Wiley and Sons permission for Figure 1.3

JOHN WILEY AND SONS LICENSE
TERMS AND CONDITIONS
Jun 13, 2021

This Agreement between Mr. Sakil Mahmud ("You") and John Wiley and Sons ("John Wiley and Sons") consists of your license details and the terms and conditions provided by John Wiley and Sons and Copyright Clearance Center.

License Number	5075370774413
License date	May 24, 2021
Licensed Content Publisher	John Wiley and Sons
Licensed Content Publication	New Phytologist
Licensed Content Title	A plant's balance of growth and defense – revisited
Licensed Content Author	Claus Wasternack
Licensed Content Date	Aug 3, 2017
Licensed Content Volume	215
Licensed Content Issue	4
Licensed Content Pages	4
Type of use	Dissertation/Thesis
Requestor type	University/Academic
Format	Electronic
Portion	Figure/table
Number of figures/tables	1
Will you be translating?	Yes, including English rights
Number of languages	1
Title	Role of jasmonates in drought stress in Arabidopsis thaliana
Institution name	University of Bonn
Expected presentation date	Aug 2021
Order reference number	https://doi.org/10.1111/nph.14720
Portions	Figure 2
Specific Languages	English
Requestor Location	Mr. Sakil Mahmud Kirschallee 1 Endenich Bonn, NRW 53115 Germany Attn: University of Bonn
Publisher Tax ID	EU826007151
Total	0.00 USD

References

Abe, H., Urao, T., Ito, T., Seki, M., & Shinozaki, K. (2003). Arabidopsis AtMYC2 (bHLH) and AtMYB2 (MYB) Function as Transcriptional Activators in Abscisic Acid Signaling, *15*(January), 63–78. https://doi.org/10.1105/tpc.006130.salt

Acosta, I. F., & Farmer, E. E. (2010). Jasmonates. *The Arabidopsis Book*. 10.1199/tab.0129

Ai, Y., & Zhu, Z. (2018). Melatonin Antagonizes Jasmonate-Triggered Anthocyanin Biosynthesis in Arabidopsis thaliana. *Journal of Agricultural and Food Chemistry*, *66*(21), 5392–5400. https://doi.org/10.1021/acs.jafc.8b01795

Akter, N., Okuma, E., Sobahan, M. A., Uraji, M., Munemasa, S., Nakamura, Y., … Murata, Y. (2013). Negative Regulation of Methyl Jasmonate-Induced Stomatal Closure by Glutathione in Arabidopsis. *Journal of Plant Growth Regulation*, *32*(1), 208–215. https://doi.org/10.1007/s00344-012-9291-7

Alexa, A., & Rahnenfuhrer, J. (2020). topGO: Enrichment Analysis for Gene Ontology. *R Package Version*, *2*(42), 0. https://doi.org/10.18129/B9.bioc.topGO

Ambawat, S., Sharma, P., Yadav, N. R., & Yadav, R. C. (2013). MYB transcription factor genes as regulators for plant responses: An overview. *Physiology and Molecular Biology of Plants*, *19*(3), 307–321. https://doi.org/10.1007/s12298-013-0179-1

Antosiewicz, D. M., Polisensky, D. H., & Braam, J. (1995). Cellular localization of the Ca^{2+}binding TCH3 protein of Arbisopsis. *Plant Journal*, 8(5), 623-636. https://doi.org/10.1046/j.1365-313X.1995.08050623.x

Armezzani, A., Abad, U., Ali, O., Robin, A. A., Vachez, L., Larrieu, A., … Sassi, M. (2018). Transcriptional induction of cell wall remodelling genes is coupled to microtubule-driven growth isotropy at the shoot apex in arabidopsis. *Development (Cambridge)*, *145*(11). https://doi.org/10.1242/dev.162255

Aubert, Y., Widemann, E., Miesch, L., Pinot, F., & Heitz, T. (2015a). CYP94-mediated jasmonoyl-isoleucine hormone oxidation shapes jasmonate profiles and attenuates defence responses to Botrytis cinerea infection. *Journal of Experimental Botany*, *66*(13), 3879–3892. https://doi.org/10.1093/jxb/erv190

Baldoni, E., Genga, A., & Cominelli, E. (2015). Plant MYB transcription factors: Their role in drought response mechanisms. *International Journal of Molecular Sciences*, *16*(7), 15811–15851. https://doi.org/10.3390/ijms160715811

Balfagón, D., Sengupta, S., Gómez-Cadenas, A., Fritschi, F. B., Azad, R. K., Mittler, R., & Zandalinasc, S. I. (2019). Jasmonic acid is required for plant acclimation to a combination

of high light and heat stress. *Plant Physiology*, *181*(4), 1668–1682. https://doi.org/10.1104/pp.19.00956

Barth, C., & Jander, G. (2006). Arabidopsis myrosinases TGG1 and TGG2 have redundant function in glucosinolate breakdown and insect defense. *Plant Journal*, *46*(4), 549–562. https://doi.org/10.1111/j.1365-313X.2006.02716.x

Bell, E., Creelman, R. A., Mullet, J. E., & Zenk, M. H. (1995). A chloroplast lipoxygenase is required for wound-induced jasmonic acid accumulation in Arabidopsis *Communicated by*. *Plant Biology* (Vol. 92).

Benjamini, Y., & Hochberg, Y. (1995). Controlling the False Discovery Rate: A Practical and Powerful Approach to Multiple Testing. *Journal of the Royal Statistical Society.*, *57*(1), 289–300.

Bernal, A. J., Jensen, J. K., Harholt, J., Sørensen, S., Moller, I., Blaukopf, C., … Willats, W. G. T. (2007). Disruption of ATCSLD5 results in reduced growth, reduced xylan and homogalacturonan synthase activity and altered xylan occurrence in Arabidopsis. *Plant Journal*, *52*(5), 791–802. https://doi.org/10.1111/j.1365-313X.2007.03281.x

Bertolino, L. T., Caine, R. S., & Gray, J. E. (2019). Impact of stomatal density and morphology on water-use efficiency in a changing world. *Frontiers in Plant Science*, *10*(March). https://doi.org/10.3389/fpls.2019.00225

Boruc, J., Mylle, E., Duda, M., de Clercq, R., Rombauts, S., Geelen, D., … Russinova, E. (2010). Systematic localization of the Arabidopsis core cell cycle proteins reveals novel cell division complexes. *Plant Physiology*, *152*(2), 553–565. https://doi.org/10.1104/pp.109.148643

Braam, J. (1992). Regulated expression of the calmodulin-related TCH genes in cultured Arabidopsis cells: Induction by calcium and heat shock. *Proceedings of the National Academy of Sciences of the United States of America*, *89*(8), 3213–3216. https://doi.org/10.1073/pnas.89.8.3213

Braam, Janet, & Davis, R. W. (1990). Rain-, wind-, and touch-induced expression of calmodulin and calmodulin-related genes in Arabidopsis. *Cell*, *60*(3), 357–364. https://doi.org/10.1016/0092-8674(90)90587-5

Brioudes, F., Joly, C., Szécsi, J., Varaud, E., Leroux, J., Bellvert, F., … Bendahmane, M. (2009). Jasmonate controls late development stages of petal growth in Arabidopsis thaliana. *Plant Journal*, *60*(6), 1070–1080. https://doi.org/10.1111/j.1365-313X.2009.04023.x

Capella, A., Menossi, M., Arruda, P., & Benedetti, C. (2001). COI1 affects myrosinase activity

and controls the expression of two flower-specific myrosinase-binding protein homologues in Arabidopsis. *Planta*, *213*(5), 691–699. https://doi.org/10.1007/s004250100548

Chae, K., Gonong, B. J., Kim, S. C., Kieslich, C. A., Morikis, D., Balasubramanian, S., & Lord, E. M. (2010). A multifaceted study of stigma/style cysteine-rich adhesin (SCA)-like Arabidopsis lipid transfer proteins (LTPs) suggests diversified roles for these LTPs in plant growth and reproduction. *Journal of Experimental Botany*, *61*(15), 4277–4290. https://doi.org/10.1093/jxb/erq228

Chambers, J. M., Freeny, A., & Heiberger, R. M. (1992). Analysis of variance; designed experiments, *Chapter 5o*.

Chehab, E. W., Yao, C., Henderson, Z., Kim, S., & Braam, J. (2012). Arabidopsis touch-induced morphogenesis is jasmonate mediated and protects against pests. *Current Biology*, *22*(8), 701–706. https://doi.org/10.1016/j.cub.2012.02.061

Chen, H., Fu, T., Yang, S., & Hsieh, H. (2018). FIN219/JAR1 and cryptochrome1 antagonize each other to modulate photomorphogenesis under blue light in Arabidopsis. *PLoS* Genetics, *14*(3), 1–19. https:// doi.org/10.1371/journal.pgen.1007248

Chen, H. Y., Hsieh, E. J., Cheng, M. C., Chen, C. Y., Hwang, S. Y., & Lin, T. P. (2016). ORA47 (octadecanoid-responsive AP2/ERF-domain transcription factor 47) regulates jasmonic acid and abscisic acid biosynthesis and signaling through binding to a novel cis-element. *The New Phytologist*, *211*(2), 599–613. https://doi.org/10.1111/nph.13914

Cheng, C. Y., Krishnakumar, V., Chan, A. P., Thibaud-Nissen, F., Schobel, S., & Town, C. D. (2017). Araport11: a complete reannotation of the Arabidopsis thaliana reference genome. *Plant Journal*, *89*(4), 789–804. https://doi.org/10.1111/tpj.13415

Cheng, W. H., Endo, A., Zhou, L., Penney, J., Chen, H. C., Arroyo, A., … Sheen, J. (2002). A unique short-chain dehydrogenase/reductase in arabidopsis glucose signaling and abscisic acid biosynthesis and functions. *Plant Cell*, *14*(11), 2723–2743. https://doi.org/10.1105/tpc.006494

Chung, H. S., Koo, A. J. K., Gao, X., Jayanty, S., Thines, B., … Howe, G. A. (2008). Regulation and Function of Arabidopsis JASMONATE ZIM -Domain Genes in Response to Wounding. *Plant Physiolog, 146*(March), 952–964.

Claeys, H., & Inzé, D. (2013). The agony of choice: How plants balance growth and survival under water-limiting conditions. *Plant Physiology*, *16*(4), 1768-1779. https://doi.org/10.1104/pp.113.220921

Clauw, P., Coppens, F., Korte, A., Herman, D., Slabbinck, B., Dhondt, S., … Inzé, D. (2016).

Leaf growth response to mild drought: Natural variation in arabidopsis sheds light on trait architecture. *Plant Cell*, *28*(10), 2417–2434. https://doi.org/10.1105/tpc.16.00483

Daszkowska-Golec, A., & Szarejko, I. (2013). Open or close the gate - Stomata action under the control of phytohormones in drought stress conditions. *Frontiers in Plant Science*, *4*(May), 1-16 https://doi.org/10.3389/fpls.2013.00138

de Ollas, C., Arbona, V., & Gómez-Cadenas, A. (2015a). Jasmonic acid interacts with abscisic acid to regulate plant responses to water stress conditions. *Plant Signaling and Behavior*, *10*(12). https://doi.org/10.1080/15592324.2015.1078953

de Ollas, C., Arbona, V., & Gómez-Cadenas, A. (2015b). Jasmonoyl isoleucine accumulation is needed for abscisic acid build-up in roots of Arabidopsis under water stress conditions. *Plant, Cell and Environment*, *38*(10), 2157–2170. https://doi.org/10.1111/pce.12536

Devoto, A., & Turner, J. G. (2005). Jasmonate-regulated Arabidopsis stress signalling network. *Physiologia Plantarum*, *123*(2), 161–172. https://doi.org/10.1111/j.1399-3054.2004.00418.x

Dodd, A. N., Kudla, J., & Sanders, D. (2010). The language of calcium signaling. *Annual Review of Plant Biology*, *61*, 593–620. https://doi.org/10.1146/annurev-arplant-070109-104628

Dombrecht, B., Gang, P. X., Sprague, S. J., Kirkegaard, J. A., Ross, J. J., Reid, J. B., … Kazana, K. (2007). MYC2 differentially modulates diverse jasmonate-dependent functions in Arabidopsis. *Plant Cell*, *19*(7), 2225–2245. https://doi.org/10.1105/tpc.106.048017

Dubos, C., Stracke, R., Grotewold, E., Weisshaar, B., Martin, C., & Lepiniec, L. (2010). MYB transcription factors in Arabidopsis. *Trends in Plant Science*, *15*(10), 573–581. https://doi.org/10.1016/j.tplants.2010.06.005

Durinck, S., Spellman, P. T., Birney, E., & Huber, W. (2009). Mapping identifiers for the integration of genomic datasets with the R/ Bioconductor package biomaRt. *Nature Protocols*, *4*(8), 1184–1191. https://doi.org/10.1038/nprot.2009.97

Edwards, K., Johnstone, C., & Thompson, C. (1991). A simple and rapid method for the preparation of plant genomic DNA for PCR analysis. *Nucleic Acids Research*, *19*(6), 1349. 10.1093/nar/19.6.1349

Fernandez-Calvino, L., Faulkner, C., Walshaw, J., Saalbach, G., Bayer, E., Benitez-Alfonso, Y., & Maule, A. (2011). Arabidopsis plasmodesmal proteome. *PLoS ONE*, *6*(4). https://doi.org/10.1371/journal.pone.0018880

Fernández-Calvo, P., Chini, A., Fernández-Barbero, G., Chico, J. M., Gimenez-Ibanez, S., Geerinck, J., … Solano, R. (2011). The Arabidopsis bHLH transcription factors MYC3

and MYC4 are targets of JAZ repressors and act additively with MYC2 in the activation of jasmonate responses. *Plant Cell*, *23*(2), 701–715. https://doi.org/10.1105/tpc.110.080788

Fisher, R. A. (1925). StatisticalMethods for Research Workers. *Oliver and Boyd (Edinburgh).*, *ISBN 0-05-*.

Förster, S., Schmidt, L. K., Kopic, E., Anschütz, U., Huang, S., Schlücking, K., … Becker, D. (2019). Wounding-Induced Stomatal Closure Requires Jasmonate-Mediated Activation of GORK K + Channels by a Ca 2+ Sensor-Kinase CBL1-CIPK5 Complex. *Developmental Cell*, *48*(1), 87-99.e6. https://doi.org/10.1016/j.devcel.2018.11.014

Gheysen, G., & Mitchum, M. G. (2019). Phytoparasitic nematode control of plant hormone pathways. *Plant Physiology*, *179*(4), 1212–1226. https://doi.org/10.1104/pp.18.01067

Gidda, S. K., Miersch, O., Levitin, A., Schmidt, J., Wasternack, C., & Varin, L. (2003). Biochemical and molecular characterization of a hydroxyjasmonate sulfotransferase from Arabidopsis thaliana. *Journal of Biological Chemistry*, *278*(20), 17895–17900. https://doi.org/10.1074/jbc.M211943200

Glauser, G., Grata, E., Dubugnon, L., Rudaz, S., Farmer, E. E., & Wolfender, J. L. (2008). Spatial and temporal dynamics of jasmonate synthesis and accumulation in Arabidopsis in response to wounding. *Journal of Biological Chemistry*, *283*(24), 16400–16407. https://doi.org/10.1074/jbc.M801760200

Guan, L., Denkert, N., Eisa, A., Lehmann, M., Sjuts, I., Weiberg, A., … Schwenkert, S. (2019). JASSY, a chloroplast outer membrane protein required for jasmonate biosynthesis. *Proceedings of the National Academy of Sciences of the United States of America*, *116*(21), 10568–10575. https://doi.org/10.1073/pnas.1900482116

Guo, Q., Yoshida, Y., Major, I. T., Wang, K., Sugimoto, K., Kapali, G., … Howe, G. A. (2018). JAZ repressors of metabolic defense promote growth and reproductive fitness in Arabidopsis. *Proceedings of the National Academy of Sciences of the United States of America*, *115*(45), E10768–E10777. https://doi.org/10.1073/pnas.1811828115

Gupta, A., Rico-Medina, A., & Caño-Delgado, A. I. (2020). The physiology of plant responses to drought. *Science*, *368*(6488), 266–269. https://doi.org/10.1126/science.aaz7614

Guranowski, A., Miersch, O., Staswick, P. E., Suza, W., & Wasternack, C. (2007). Substrate specificity and products of side-reactions catalyzed by jasmonate : amino acid synthetase (JAR1). *FEBS Letters*, *581*, 815–820. https://doi.org/10.1016/j.febslet.2007.01.049

Gutscher, M.., Pauleau, A., Marty, L., Brach, T., Wabnitz, G. H., Samstag, Y., Meyer, A. J. & Dick, T. P. (2008). Real-time imaging of the intracellular glutathione redox potential.

Nature Methods, *5*(6), 553-559. DOI:10.1038/NMETH.1212

Han, X., Hu, Y., Zhang, G., Jiang, Y., Chen, X., & Yu, D. (2018). Jasmonate negatively regulates stomatal development in arabidopsis cotyledons. *Plant Physiology*, *176*(4), 2871–2885. https://doi.org/10.1104/pp.17.00444

Harb, A., Krishnan, A., Ambavaram, M. M. R., & Pereira, A. (2010). Molecular and physiological analysis of drought stress in arabidopsis reveals early responses leading to acclimation in plant growth. *Plant Physiology*, *154*(3), 1254–1271. https://doi.org/10.1104/pp.110.161752

Hartigan, J. A., & Wong, M. A. (1979). Algorithm AS 136: A K-Means Clustering Algorithm Author (s): J . A . Hartigan and M . A . Wong Published by : Blackwell Publishing for the Royal Statistical Society Stable URL : http://www.jstor.org/stable/2346830. *Journal of the Royal Statistical Society. Series C (Applied Statistics)*, *28*(1), 100–108.

Xie, D., Feys, B. F., James, S., Nieto-rostro, M., & Turner, J. G. (1998). COl1: An Arabidopsis gene required for jasmonate-regulated defense and fertility. *Science*, *280*, 1091-1094. 10.1126/science.280.5366.1091

Hickman, R., Van Verk, M. C., Van Dijken, A. J. H., Mendes, M. P., Vroegop-Vos, I. A., Caarls, L., … Van Wees, S. C. M. (2017). Architecture and dynamics of the jasmonic acid gene regulatory network. *Plant Cell*, *29*(9), 2086–2105. https://doi.org/10.1105/tpc.16.00958

Hoeren, F. U., Dolferus, R., Wu, Y., Peacock, W. J., & Dennis, E. S. (1998). Evidence for a role for AtMYB2 in the induction of the arabidopsis alcohol dehydrogenase gene (ADH1) by low oxygen. *Genetics*, *149*(2), 479–490.

Howard, B. E., Hu, Q., Babaoglu, A. C., Chandra, M., Borghi, M., Tan, X., … Heber, S. (2013). High-Throughput RNA Sequencing of Pseudomonas-Infected Arabidopsis Reveals Hidden Transcriptome Complexity and Novel Splice Variants. *PLoS ONE*, *8*(10). https://doi.org/10.1371/journal.pone.0074183

Howe, G. A., Major, I. T., & Koo, A. J. (2018). Modularity in Jasmonate Signaling for Multistress Resilience. *Annual Review of Plant Biology*, *69*, 387–415. https://doi.org/10.1146/annurev-arplant-042817-040047

Huang, D., Wu, W., Abrams, S. R., & Cutler, A. J. (2008). The relationship of drought-related gene expression in Arabidopsis thaliana to hormonal and environmental factors. *Journal of Experimental Botany*, *59*(11), 2991–3007. https://doi.org/10.1093/jxb/ern155

Islam, M. M., Tani, C., Watanabe-Sugimoto, M., Uraji, M., Jahan, M. S., Masuda, C., … Murata, Y. (2009). Myrosinases, TGG1 and TGG2, redundantly function in ABA and

MeJA signaling in arabidopsis guard cells. *Plant and Cell Physiology*, *50*(6), 1171–1175. https://doi.org/10.1093/pcp/pcp066

Jacq, A., Pernot, C., Martinez, Y., Domergue, F., Payré, B., Jamet, E., … Pacquit, V. B. (2017). The Arabidopsis lipid transfer protein 2 (AtLTP2) is involved in cuticle-cell wall interface integrity and in etiolated hypocotyl permeability. *Frontiers in Plant Science*, *8*(February), 1–17. https://doi.org/10.3389/fpls.2017.00263

Jaquinod, M., Villiers, F., Kieffer-Jaquinod, S., Hugouvieux, V., Bruley, C., Garin, J., & Bourguignon, J. (2007). A proteomics dissection of Arabidopsis thaliana vacuoles isolated from cell culture. *Molecular and Cellular Proteomics*, *6*(3), 394–412. https://doi.org/10.1074/mcp.M600250-MCP200

Katsir, L., Schilmiller, A. L., Staswick, P. E., Sheng, Y. H., & Howe, G. A. (2008). COI1 is a critical component of a receptor for jasmonate and the bacterial virulence factor coronatine. *Proceedings of the National Academy of Sciences of the United States of America*,*105*(19), 7100-7105. https://doi.org/10.1073/pnas.0802332105

Kazan, K., & Lyons, R. (2016). The link between flowering time and stress tolerance. *Journal of Experimental Botany*. *67*(1), 47–60. https://doi.org/10.1093/jxb/erv441

Kenney, A. M., Mckay, J. K., Richards, J. H., & Juenger, T. E. (2014). Direct and indirect selection on flowering time, water-use efficiency (WUE, δ13C), and WUE plasticity to drought in Arabidopsis thaliana. *Ecology and Evolution*, *4*(23), 4505–4521. https://doi.org/10.1002/ece3.1270

Kim, J. H., & Kende, H. (2004). A transcriptional coactivator, AtGIF1, is involved in regulating leaf growth and morphology in Arabidopsis. *Proceedings of the National Academy of Sciences of the United States of America*, *101*(36), 13374-13379.

Kim, M. C., Chung, W. S., Yun, D. J., & Cho, M. J. (2009). Calcium and calmodulin-mediated regulation of gene expression in plants. *Molecular Plant*, *2*(1), 13–21. https://doi.org/10.1093/mp/ssn091

Knight, H., Trewavas, A. J., & Knight, M. R. (1997). Calcium signalling in Arabidopsis thaliana responding to drought and salinity. *Plant Journal*, *12*(5), 1067–1078. https://doi.org/10.1046/j.1365-313X.1997.12051067.x

Koo, A. J. (2018). Metabolism of the plant hormone jasmonate: a sentinel for tissue damage and master regulator of stress response. *Phytochemistry Reviews*, *17*(1), 51–80. https://doi.org/10.1007/s11101-017-9510-8

Koo, A. J. K., Gao, X., Jones, A. D., Howe, G. A., Lansing, E., Lansing, E., & Lansing, E. (2009). A rapid wound signal activates the systemic synthesis of bioactive jasmonates in

Arabidopsis. *The Plant Journal*, *59*, 974–986. https://doi.org/10.1111/j.1365-313X.2009.03924.x

Kudla, J., Becker, D., Grill, E., Hedrich, R., Hippler, M., Kummer, U., … Schumacher, K. (2018). Advances and current challenges in calcium signaling. *New Phytologist*, *218*(2), 414–431. https://doi.org/10.1111/nph.14966

Kurusu, T., Kuchitsu, K., Nakano, M., Nakayama, Y., & Iida, H. (2013). Plant mechanosensing and Ca^{2+} transport. *Trends in Plant Science*, *18*(4), 227–233. https://doi.org/10.1016/j.tplants.2012.12.002

Kyhse-Andersen, J. (1984). Electroblotting of multiple gels: a simple apparatus without buffer tank for rapid transfer of proteins from polyacrylamide to nitrocellulose. *Journal of Biochemical and Biophysical Methods*, *10*, 203-209.

Lackman, P., González-guzmán, M., Carqueijeiro, I., & Cuéllar, A. (2011). Jasmonate signaling involves the abscisic acid receptor PYL4 to regulate metabolic reprogramming in Arabidopsis and tobacco, *6*(24), 25–27. https://doi.org/10.1073/pnas.1103010108

Laemmli, U. K. (1970). Cleavage of Structural Proteins during the Assembly of the Head of Bacteriophage T4. *Nature*, *227*, 680–685.

Laudert, D., Schaller, F., & Weiler, E. W. (2000). Transgenic Nicotiana tabacum and Arabidopsis thaliana plants overexpressing allene oxide synthase. *Planta*, *211*(1), 163–165. https://doi.org/10.1007/s004250000316

Lee, T. A. & Bailey-Serres, J. (2019). Integrative Analysis from the Epigenome to Translatome Uncovers Patterns of Dominant Nuclear Regulation during Transient Stress. *The Plant Cell*, *31*(11), 2573-2595. 10.1105/tpc.19.00463

Lee, B. H., Ko, J. H., Lee, S., Lee, Y., Pak, J. H., & Kim, J. H. (2009). The Arabidopsis GRF-Interacting Factor gene family performs an overlapping function in determining organ size as well as multiple. *Plant Physiology*, *151*(2), 655–668. https://doi.org/10.1104/pp.109.141838

Leuzinger, K., Dent, M., Hurtado, J., Stahnke, J., Lai, H., Zhou, X., & Chen, Q. (2013). Efficient agroinfiltration of plants for high-level transient expression of recombinant proteins. *Journal of Visualized Experiments*, (77), 1–9. https://doi.org/10.3791/50521

Liu, N., & Avramova, Z. (2016). Molecular mechanism of the priming by jasmonic acid of specific dehydration stress response genes in Arabidopsis. *Epigenetics & Chromatin*, 1–23. https://doi.org/10.1186/s13072-016-0057-5

Liu, X., Yue, Y., Li, B., Nie, Y., Li, W., Wu, W. H., & Ma, L. (2007). A G protein-coupled receptor is a plasma membrane receptor for the plant hormone abscisic acid. *Science*,

315(5819), 1712–1716. https://doi.org/10.1126/science.1135882

Liu, Z., Li, N., Zhang, Y., & Li, Y. (2020). Transcriptional repression of GIF1 by the KIX-PPD-MYC repressor complex controls seed size in Arabidopsis. *Nature Communications*, *11*(1). https://doi.org/10.1038/s41467-020-15603-3

Marquis, V., Smirnova, E., Poirier, L., Zumsteg, J., Schweizer, F., Reymond, P., & Heitz, T. (2020). Stress- and pathway-specific impacts of impaired jasmonoyl-isoleucine (JA-Ile) catabolism on defense signalling and biotic stress resistance. *Plant Cell and Environment*, *43*(6), 1558–1570. https://doi.org/10.1111/pce.13753

Marty, L., Bausewein, D., Müller, C., Bangash, S. A. K., Moseler, A., Schwarzländer, M., … Meyer, A. J. (2019). Arabidopsis glutathione reductase 2 is indispensable in plastids, while mitochondrial glutathione is safeguarded by additional reduction and transport systems. *New Phytologist*, *224*(4), 1569–1584. https://doi.org/10.1111/nph.16086

McAinsh, M. R. & Pittman, J. K. (2009). Shaping the calcium signature. *New Phytologist*, *181*: 275–294. 10.1111/j.1469-8137.2008.02682.x

McBride, Z., Chen, D., Reick, C., Xie, J., & Szymanski, D. B. (2017). Global analysis of membrane-associated protein oligomerization using protein correlation profiling. *Molecular and Cellular Proteomics*, *16*(11), 1972–1989. https://doi.org/10.1074/mcp.RA117.000276

McCormack, E., Tsai, Y. C., & Braam, J. (2005). Handling calcium signaling: Arabidopsis CaMs and CMLs. *Trends in Plant Science*, *10*(8), 383–389. https://doi.org/10.1016/j.tplants.2005.07.001

Mehlmer, N., Parvin, N., Hurst, C. H., Knight, M. R., Teige, M., & Vothknecht, U. C. (2012). A toolset of aequorin expression vectors for in planta studies of subcellular calcium concentrations in Arabidopsis thaliana. *Journal of Experimental Botany*, *63*(4), 1751–1761. https://doi.org/10.1093/jxb/err406

Meyer, A. J., Brach, T., Marty, L., Kreye, S., Rouhier, N., Jacquot, J. P., & Hell, R. (2007). Redox-sensitive GFP in Arabidopsis thaliana is a quantitative biosensor for the redox potential of the cellular glutathione redox buffer. *Plant Journal*, *52*(5), 973–986. https://doi.org/10.1111/j.1365-313X.2007.03280.x

Mhamdi, A., Hager, J., Chaouch, S., Queval, G., Han, Y., Taconnat, L., … Noctor, G. (2010). Arabidopsis GLUTATHIONE REDUCTASE1 plays a crucial role in leaf responses to intracellular hydrogen peroxide and in ensuring appropriate gene expression through both salicylic acid and jasmonic acid signaling pathways. *Plant Physiology*, *153*(3), 1144–1160. https://doi.org/10.1104/pp.110.153767

Michaels, S. D., & Amasino, R. M. (2001). Loss of FLOWERING LOCUS C activity eliminates the late-flowering phenotype of FRIGADA and autonomous pathway mutations but not responsiveness to vernalization. *Plant Cell* (Vol. 13). https://doi.org/10.1105/tpc.13.4.935

Miersch, O., Neumerkel, J., Dippe, M., Stenzel, I., Wasternack, C., & Wasternack, C. (2008). Hydroxylated jasmonates are commonly occurring metabolites of jasmonic acid and contribute to a partial switch-off in jasmonate signaling. *New Phytologist*, *177*, 114–127. 10.1111/j.1469-8137.2007.02252.x

Monroe, J. G., Powell, T., Price, N., Mullen, J. L., Howard, A., Evans, K., … McKay, J. K. (2018). Drought adaptation in nature by extensive genetic loss-of-function. *BioRxiv*. https://doi.org/10.1101/372854

Mousavi, A. R. S. (2013). Long-Distance Wound Signalling In Arabidopsis, 139.

Munemasa, S., Oda, K., Watanabe-Sugimoto, M., Nakamura, Y., Shimoishi, Y., & Murata, Y. (2007). The coronatine-insensitive 1 mutation reveals the hormonal signaling interaction between abscisic acid and methyl jasmonate in Arabidopsis guard cells. Specific impairment of ion channel activation and second messenger production. *Plant Physiology*, *143*(3), 1398–1407. https://doi.org/10.1104/pp.106.091298

Murata, Y., Pei, Z.-M., Mori, I. C., & Schroeder, J. (2001). Abscisic Acid Activation of Plasma Membrane Ca 2+ Channels in Guard Cells Requires Cytosolic NAD(P)H and Is Differentially Disrupted Upstream and Downstream of Reactive Oxygen Species Production in abi1-1 and abi2-1 Protein Phosphatase 2C Mutants . *The Plant Cell*, *13*(11), 2513–2523. https://doi.org/10.1105/tpc.010210

Misyura, M., Colasanti, J., & Rothstein, S. J. (2012). Physiological and genetic analysis of *Arabidopsis thaliana* anthocyanin biosynthesis mutants under chronic adverse environmental conditions. *Journal of Experimental Botany, 64*(1), 229-240. https://doi.org/10.1093/jxb/ers328

Neff, M. M., & Chory, J. (1998). Genetic interactions between phytochrome A, phytochrome B, and cryptochrome 1 during arabidopsis development. *Plant Physiology*, *118*(1), 27–36. https://doi.org/10.1104/pp.118.1.27

Nietzel, T., Elsässer, M., Ruberti, C., Steinbeck, J., ...Schwarzländer, M. (2019). The fluorescent protein sensor roGFP2-Orp1 monitors in vivo H 2 O 2 and thiol redox integration and elucidates intracellular H 2 O 2 dynamics during elicitor-induced oxidative burst in Arabidopsis. *New Phytologist*, *221*(3), 1649–1664. https://doi.org/10.1111/nph.15550

Noctor, G., Mhamdi, A., & Foyer, C. H. (2014). The roles of reactive oxygen metabolism in drought: Not so cut and dried. *Plant Physiology*, *164*(4), 1636–1648. https://doi.org/10.1104/pp.113.233478

Noir, S., Bömer, M., Takahashi, N., Ishida, T., Tsui, T. L., Balbi, V., … Devoto, A. (2013). Jasmonate controls leaf growth by repressing cell proliferation and the onset of endoreduplication while maintaining a potential stand-by mode. *Plant Physiolog*, *161*(4), 1930–1951. https://doi.org/10.1104/pp.113.214908

Park, J. H., Halitschke, R., Kim, H. B., Baldwin, I. T., Feldmann, K. A., & Feyereisen, R. (2002). A knock-out mutation in allene oxide synthase results in male sterility and defective wound signal transduction in Arabidopsis due to a block in jasmonic acid biosynthesis. *Plant Journal*, *31*(1), 1–12. https://doi.org/10.1046/j.1365-313X.2002.01328.x

Pauwels, L., Morreel, K., De Witte, E., Lammertyn, F., Van Montagu, M., Boerjan, W., … Goossens, A. (2008). Mapping methyl jasmonate-mediated transcriptional reprogramming of metabolism and cell cycle progression in cultured Arabidopsis cells. *Proceedings of the National Academy of Sciences of the United States of America* (Vol. 105). https://doi.org/10.1073/pnas.0711203105

Pérez, C. A., Nagels Durand, A., Vanden Bossche, R., De Clercq, R., Persiau, G., Van Wees, S. C. M., … Pauwels, L. (2014). The non-JAZ TIFY protein TIFY8 from Arabidopsis thaliana is a transcriptional repressor. *PLoS ONE*, *9*(1). https://doi.org/10.1371/journal.pone.0084891

Poovaiah, B. W., Du, L., Wang, H., & Yang, T. (2013). Recent advances in calcium/calmodulin-mediated signaling with an emphasis on plant-microbe interactions. *Plant Physiology*, *163*(2), 531–542. https://doi.org/10.1104/pp.113.220780

Porra, R. J., Thompson, W. A., & Kriedemann, P. E. (1989). Determination of accurate extinction coefficients and simultaneous equations for assaying chlorophylls a and b extracted with four different solvents: verification of the concentration of chlorophyll standards by atomic absorption spectroscopy. *Biochimica et Biophysica Acta (BBA) - Bioenergetics, 975***,** 384-394.

Poudel, A. N., Holtsclaw, R. E., Kimberlin, A., Sen, S., Zeng, S., Joshi, T., … Koo, A. J. (2019). 12-Hydroxy-Jasmonoyl-l-Isoleucine Is an Active Jasmonate That Signals through CORONATINE INSENSITIVE 1 and Contributes to the Wound Response in Arabidopsis. *Plant and Cell Physiology*, *60*(10), 2152–2166. https://doi.org/10.1093/pcp/pcz109

Ralhan, A., Schöttle, S., Thurow, C., Iven, T., Feussner, I., Polle, A., & Gatz, C. (2012). The vascular pathogen Verticillium longisporum requires a jasmonic acid-independent COI1 function in roots to elicit disease symptoms in Arabidopsis shoots. *Plant Physiology*, *159*(3), 1192–1203. https://doi.org/10.1104/pp.112.198598

Ranty, B., Aldon, D., & Galaud, J.-P. (2006). Plant calmodulins and calmodulin-related proteins: multifaceted relays to decode calcium signals. *Plant Signaling & Behavior*, *1*(3), 96–104. https://doi.org/10.4161/psb.1.3.2998

Ratcliffe, O. J., Nadzan, G. C., Reuber, T. L., & Riechmann, J. L. (2001). Regulation of Flowering in Arabidopsis by an FLC Homologue. *Plant Physiology, 126*(1), 122-132. Retrieved from http://www.arabidopsis.org/

Reymond, P., Weber, H., Damond, M., & Farmer, E. E. (2000). Differential gene expression in response to mechanical wounding and insect feeding in Arabidopsis. *Plant Cell*, *12*(5), 707–719. https://doi.org/10.1105/tpc.12.5.707

Rhaman, M. S., Nakamura, T., Nakamura, Y., Munemasa, S., & Murata, Y. (2020). The Myrosinases TGG1 and TGG2 Function Redundantly in Reactive Carbonyl Species Signaling in Arabidopsis Guard Cells. *Plant and Cell Physiology*, *61*(5), 967–977. https://doi.org/10.1093/pcp/pcaa024

Richter, R., Kinoshita, A., Vincent, C., Martinez-Gallegos, R., Gao, H., van Driel, A. D., … Coupland, G. (2019). Floral regulators FLC and SOC1 directly regulate expression of the B3-type transcription factor TARGET of FLC and SVP 1 at the Arabidopsis shoot apex via antagonistic chromatin modifications. *PLoS Genetics*, *15*(4). https://doi.org/10.1371/journal.pgen.1008065

Robinson, M. D., McCarthy, D. J., & Smyth, G. K. (2009). edgeR: A Bioconductor package for differential expression analysis of digital gene expression data. *Bioinformatics*, *26*(1), 139–140. https://doi.org/10.1093/bioinformatics/btp616

Robinson, M. D., & Oshlack, A. (2010). Deseq2论文附录. *Genome Biology*, *11*(3), 1–9. Retrieved from http://genomebiology.com/2010/11/3/R25

Rojas-Murcia, N., Hématy, K., Lee, Y., Emonet, A., Ursache, R., Fujita, S., … Geldner, N. (2020). High-order mutants reveal an essential requirement for peroxidases but not laccases in Casparian strip lignification. *Proceedings of the National Academy of Sciences of the United States of America*, *117*(46), 29166–29177. https://doi.org/10.1073/pnas.2012728117

Sasaki-Sekimoto, Y., Taki, N., Obayashi, T., Aono, M., Matsumoto, F., Sakurai, N., … Ohta,

H. (2005). Coordinated activation of metabolic pathways for antioxidants and defence compounds by jasmonates and their roles in stress tolerance in Arabidopsis. *Plant Journal*, *44*(4), 653–668. https://doi.org/10.1111/j.1365-313X.2005.02560.x

Savchenko, T., Kolla, V. A., Wang, C., Nasa, Z., Hicks, D. R., Phadungchob, B., … Biology, P. (2014). Functional Convergence of Oxylipin and Abscisic Acid Pathways Controls Stomatal Closure in Response to Drought. *Plant Physiology*, *164*(March), 1151–1160. https://doi.org/10.1104/pp.113.234310

Savchenko, T. V., Rolletschek, H., & Dehesh, K. (2019). Jasmonates-Mediated Rewiring of Central Metabolism Regulates Adaptive Responses. *Plant and Cell Physiology*, *60*(12), 2613–2620. https://doi.org/10.1093/pcp/pcz181

Schmalenbach, I., Zhang, L., Reymond, M., Jiménez-gómez, J. M., & Lovell, J. T. (2014). The relationship between flowering time and growth responses to drought in the Arabidopsis Landsberg erecta x Antwerp-1 population. *Frontiers in Plant Science 5*(November), 1–9. https://doi.org/10.3389/fpls.2014.00609

Schmid, M., Uhlenhaut, N. H., Godard, F., Demar, M., Bressan, R., Weigel, D., & Lohman, J. U. (2003). Dissection of floral induction pathways using global expression analysis. *Development*, *130*(24), 6001–6012. https://doi.org/10.1242/dev.00842

Scholz, S. S., Vadassery, J., Heyer, M., Reichelt, M., Bender, K. W., Snedden, W. A., … Mithöfer, A. (2014). Mutation of the arabidopsis calmodulin-like protein CML37 deregulates the jasmonate pathway and enhances susceptibility to herbivory. *Molecular Plant*, *7*(12), 1712–1726. https://doi.org/10.1093/mp/ssu102

Schwenk, A. J. (1984). Venn Diagram for Five Sets. *Mathematics Magazine*, *57*(5), 297. https://doi.org/10.2307/2689606

Seigneurin-Berny, D., Salvi, D., Dorne, A. J., Joyard, J., & Rolland, N. (2008). Percoll-purified and photosynthetically active chloroplasts from Arabidopsis thaliana leaves. *Plant Physiology and Biochemistry*, *46*(11), 951–955. https://doi.org/10.1016/j.plaphy.2008.06.009

Shan, X., Wang, J., Chua, L., Jiang, D., Peng, W., & Xie, D. (2011). The role of arabidopsis rubisco activase in jasmonate-induced leaf senescence. *Plant Physiology*, *155*(2), 751–764. https://doi.org/10.1104/pp.110.166595

Shepherd, T. (2006). Tansley review. *New Phytologist*, (2008), 469–499.

Sistrunk, M. L., Antosiewicz, D. M., Purugganan, M. M., Braam, J., The, S., Cell, P., … Braam, J. (1994). Arabidopsis TCH3 Encodes a Novel Ca^{2+} Binding Protein and Shows Environmentally Induced and Tissue-Specific Regulation. The Plant Cell, *6*(11), 1553–

1565.

Smirnova, E., Marquis, V., Poirier, L., Aubert, Y., Zumsteg, J., Ménard, R., … Heitz, T. (2017). Jasmonic Acid Oxidase 2 Hydroxylates Jasmonic Acid and Represses Basal Defense and Resistance Responses against Botrytis cinerea Infection. *Molecular Plant*, *10*(9), 1159–1173. https://doi.org/10.1016/j.molp.2017.07.010

Snedden, W. A. (1998). Proteins and Plant Responses To the. *Science*, *3*(8), 299–304.

Stamm, P., Topham, A. T., Mukhtar, N. K., Jackson, M. D. B., Tomé, D. F. A., Beynon, J. L., & Bassel, G. W. (2017). The transcription factor ATHB5 affects GA-mediated plasticity in hypocotyl cell growth during seed germination. *Plant Physiology*, *173*(1), 907–917. https://doi.org/10.1104/pp.16.01099

Staswick, P. E., Su, W., & Howell, S. H. (1992). Methyl jasmonate inhibition of root growth and induction of a leaf protein are decreased in an Arabidopsis thaliana mutant. *Proceedings of the National Academy of Sciences of the United States of America* (Vol. 89). https://doi.org/10.1073/pnas.89.15.6837

Staswick, P. E., & Tiryaki, I. (2004). The oxylipin signal jasmonic acid is activated by an enzyme that conjugate it to isoleucine in Arabidopsis W inside box sign. *Plant Cell*, *16*(8), 2117–2127. https://doi.org/10.1105/tpc.104.023549

Staswick, P. E., Tiryaki, I., & Rowe, M. L. (2002). Jasmonate response locus JAR1 and several related Arabidopsis genes encode enzymes of the firefly luciferase superfamily that show activity on jasmonic, salicylic, and indole-3-acetic acids in an assay for adenylation. *Plant Cell*, *14*(6), 1405–1415. https://doi.org/10.1105/tpc.000885

Staswick, P. E., Yuen, G. Y., & Lehman, C. C. (1998). Jasmonate signaling mutants of Arabidopsis are susceptible to the soil fungus Pythium irregulare. *Plant Journal*, *15*(6), 747–754. https://doi.org/10.1046/j.1365-313X.1998.00265.x

Suza, W. P., Rowe, M. L., Hamberg, M., & Staswick, P. E. (2010). A tomato enzyme synthesizes (+)-7-iso-jasmonoyl-L-isoleucine in wounded leaves. *Planta*, *231*(3), 717–728. https://doi.org/10.1007/s00425-009-1080-6

Suza, W. P., & Staswick, P. E. (2008). The role of JAR1 in Jasmonoyl-l-isoleucine production during Arabidopsis wound response. *Planta*, *227*(6), 1221–1232. https://doi.org/10.1007/s00425-008-0694-4

Swain, S., Jiang, H., & Hsieh, H. (2017). FAR-RED INSENSITIVE 219 / JAR1 Contributes to Shade Avoidance Responses of Arabidopsis Seedlings by Modulating Key Shade Signaling Components, *8*(November), 1–14. https://doi.org/10.3389/fpls.2017.01901

Świątek, A., Azmi, A., Stals, H., Inzé, D., & Van Onckelen, H. (2004). Jasmonic acid prevents

the accumulation of cyclin B1;1 and CDK-B in synchronized tobacco BY-2 cells. *FEBS Letters*, *572*(1–3), 118–122. https://doi.org/10.1016/j.febslet.2004.07.018

Takahashi, N., Ogita, N., Takahashi, T., Taniguchi, S., Tanaka, M., Seki, M., & Umeda, M. (2019). A regulatory module controlling stress-induced cell cycle arrest in arabidopsis. *ELife*, *8*, 1–27. https://doi.org/10.7554/eLife.43944

Thines, B., Katsir, L., Melotto, M., Niu, Y., Mandaokar, A., Liu, G., … Browse, J. (2007). JAZ repressor proteins are targets of the SCFCOI1 complex during jasmonate signalling. *Nature*, *448*(7154), 661–665. https://doi.org/10.1038/nature05960

Thorndike, R. L. (1953). Who belongs in the family? *Psychometrika*, *18*(4), 267–276. https://doi.org/10.1007/BF02289263

Tukey, J. W. . (1949). Comparing Individual Means in the Analysis of Variance. *International Biometric Society*, *5*(2), 99–114. https://doi.org/http://www.jstor.org/stable/3001913

Turner, J. G., Ellis, C., & Devoto, A. (2002). The Jasmonate Signal Pathway. *The Plant Cell*, 153–165. https://doi.org/10.1105/tpc.000679.S154

Ullah, C., Tsai, C. J., Unsicker, S. B., Xue, L., Reichelt, M., Gershenzon, J., & Hammerbacher, A. (2019). Salicylic acid activates poplar defense against the biotrophic rust fungus Melampsora larici-populina via increased biosynthesis of catechin and proanthocyanidins. *New Phytologist*, *221*(2), 960–975. https://doi.org/10.1111/nph.15396

Urao, T. (1993). An Arabidopsis myb Homolog Is Induced by Dehydration Stress and Its Gene Product Binds to the Conserved MYB Recognition Sequence. *The Plant Cell Online*, *5*(11), 1529–1539. https://doi.org/10.1105/tpc.5.11.1529

Vadassery, J., Reichelt, M., Hause, B., Gershenzon, J., Boland, W., & Mithöfer, A. (2012). CML42-mediated calcium signaling coordinates responses to Spodoptera herbivory and abiotic stresses in Arabidopsis. *Plant Physiology*, *159*(3), 1159–1175. https://doi.org/10.1104/pp.112.198150

Vahala, T., Stabel, P., & Eriksson, T. (1989). Genetic transformation of willows (Salix spp.) by Agrobacterium tumefaciens. *Plant Cell Reports*, *8*(2), 55–58. https://doi.org/10.1007/BF00716837

Verma, V., Ravindran, P., & Kumar, P. P. (2016). Plant hormone-mediated regulation of stress responses. *BMC Plant Biology*, *16*(1). https://doi.org/10.1186/s12870-016-0771-y

Wakuta, S., Hamada, S., Ito, H., Matsuura, H., Nabeta, K., & Matsui, H. (2010). Identification of a β-glucosidase hydrolyzing tuberonic acid glucoside in rice (Oryza sativa L.). *Phytochemistry*, *71*(11–12), 1280–1288.

Wang, J., Song, L., Gong, X., Xu, J., & Li, M. (2020). Functions of jasmonic acid in plant

regulation and response to abiotic stress. *International Journal of Molecular Sciences*. MDPI AG. https://doi.org/10.3390/ijms21041446

Wasternack, C., & Hause, B. (2013, June). Jasmonates: Biosynthesis, perception, signal transduction and action in plant stress response, growth and development. An update to the 2007 review in Annals of Botany. *Annals of Botany*. https://doi.org/10.1093/aob/mct067

Wasternack, Claus. (2017). A plant's balance of growth and defense – revisited. *New Phytologist*, *215*(4), 1291–1294. https://doi.org/10.1111/nph.14720

Wasternack, Claus, & Song, S. (2017). Jasmonates: Biosynthesis, metabolism, and signaling by proteins activating and repressing transcription. *Journal of Experimental Botany*, *68*(6), 1303–1321. https://doi.org/10.1093/jxb/erw443

Wu, G., & Poethig, R. S. (2006). Temporal regulation of shoot development in Arabidopsis thaliana by miRr156 and its target SPL3. *Development*, *133*(18), 3539–3547. https://doi.org/10.1242/dev.02521

Xiang, C., & Oliver, D. J. (1998). Glutathione metabolic genes coordinately respond to heavy metals and jasmonic acid in arabidopsis. *Plant Cell* (Vol. 10). https://doi.org/10.1105/tpc.10.9.1539

Xiao, Y., & Offringa, R. (2020). PDK1 regulates auxin transport and Arabidopsis vascular development through AGC1 kinase PAX. *Nature Plants*, *6*(5), 544–555. https://doi.org/10.1038/s41477-020-0650-2

Yadav, V., Mallappa, C., Gangappa, S. N., Bhatia, S., & Chattopadhyay, S. (2005). A basic helix-loop-helix transcription factor in Arabidopsis, MYC2, acts as a repressor of blue light-mediated photomorphogenic growth. *Plant Cell*, *17*(7), 1953–1966. https://doi.org/10.1105/tpc.105.032060

Yamaguchi-Shinozaki, K., Urao, T., & Shinozaki, K. (1995). Regulation of genes that are induced by drought stress in Arabidopsis thaliana. *Journal of Plant Research*, *108*(1), 127–136. https://doi.org/10.1007/BF02344316

Yan, J., Zhang, C., Gu, M., Bai, Z., Zhang, W., Qi, T., … Xie, D. (2009). The arabidopsis CORONATINE INSENSITIVE1 protein is a jasmonate receptor. *Plant Cell*, *21*(8), 2220–2236. https://doi.org/10.1105/tpc.109.065730

Yang, D., Yao, J., Mei, C., Tong, X., Zeng, L., Li, Q., & Xiao, L. (2012). Plant hormone jasmonate prioritizes defense over growth by interfering with gibberellin signaling cascade, *109*(19).

Yang, J., Duan, G., Li, C., Liu, L., Han, G., Zhang, Y., & Wang, C. (2019). The Crosstalks

Between Jasmonic Acid and Other Plant Hormone Signaling Highlight the Involvement of Jasmonic Acid as a Core Component in Plant Response to Biotic and Abiotic Stresses. *Frontiers in Plant Science*, *10*(October), 1–12. https://doi.org/10.3389/fpls.2019.01349

Yang, S., Vanderbeld, B., Wan, J., & Huang, Y. (2010). Narrowing down the targets: Towards successful genetic engineering of drought-tolerant crops. *Molecular Plant*. Oxford University Press. https://doi.org/10.1093/mp/ssq016

Yates, A. D., Achuthan, P., Akanni, W., Allen, J., Allen, J., Alvarez-Jarreta, J., … Flicek, P. (2020). Ensembl 2020. *Nucleic Acids Research*, *48*(D1), D682–D688. https://doi.org/10.1093/nar/gkz966

Yoo, J. H., Chan, Y. P., Jong, C. K., Won, D. H., Mi, S. C., Hyeong, C. P., … Moo, J. C. (2005). Direct interaction of a divergent CaM isoform and the transcription factor, MYB2, enhances salt tolerance in Arabidopsis. *Journal of Biological Chemistry*, *280*(5), 3697–3706. https://doi.org/10.1074/jbc.M408237200

Zander, M., Lewsey, M. G., Clark, N. M., Yin, L., Bartlett, A., Saldierna Guzmán, J. P., … Ecker, J. R. (2020). Integrated multi-omics framework of the plant response to jasmonic acid. *Nature Plants*, *6*(3), 290–302. https://doi.org/10.1038/s41477-020-0605-7

Zeng, H., Xu, L., Singh, A., Wang, H., Du, L., & Poovaiah, B. W. (2015). Involvement of calmodulin and calmodulin-like proteins in plant responses to abiotic stresses. *Frontiers in Plant Science*, *6*(August), 600. https://doi.org/10.3389/fpls.2015.00600

Zhai, Q., Zhang, X., Wu, F., Feng, H., Deng, L., Xu, L., … Li, C. (2015). Transcriptional Mechanism of Jasmonate Receptor COI1-Mediated Delay of Flowering Time in Arabidopsis, *27*(October), 2814–2828. https://doi.org/10.1105/tpc.15.00619

Zhang, Y., & Turner, J. G. (2008a). Wound-induced endogenous jasmonates stunt plant growth by inhibiting mitosis. *PLoS ONE*, *3*(11). https://doi.org/10.1371/journal.pone.0003699

Züst, T., & Agrawal, A. A. (2017). Trade-Offs Between Plant Growth and Defense Against Insect Herbivory: An Emerging Mechanistic Synthesis. *Annual Review of Plant Biology*, *68*, 513–534. https://doi.org/10.1146/annurev-arplant-042916-040856

Acknowledgments

I would like to express my heartfelt gratitude to my respected PhD supervisor Prof. Dr. Ute C. Vothknecht for allowing me to work with the wonderful team of Plant Cell Biology Lab. I learned much from her, not only does she have a detailed understanding of molecular biology and plant science but she also has a pragmatic perspective on science as a social enterprise, a most useful perspective. By offering me the opportunity to attend conferences and courses and to supervise several students she helped me improve my knowledge and strengthen my skills.

I express my sincere thanks to the German Academic Exchange Service (DAAD) for granting me a PhD scholarship for accomplishing my PhD project.

Special thanks to Dr. Fatima Chigri for her valuable pieces of advice, critiques of this research work, theoretical, technical support and generous proofreading of my thesis and manuscript during my entire research project.

Some special words of gratitude go to my friends who have always been a major source of support and they always managed to make me feel special and encourage me: Nilou and Maya. Thanks dear friends for always being there for me.

I acknowledge the excellent assistance of our lab technicians Claudia and Ursula for the introduction of the lab rules, chemical handling, and providing lab materials. I wish to acknowledge the previous and current lab members- PD Dr. Frantisek Baluska, Gelareh, Ahlem, Ammar, Annelotte, Christina, Mariam. Special thanks to Sabarna and Ioana for the generous proofreading of my thesis and for helping me finish my research work. I would like to offer my gratitude to the members of the IZMB for valuable criticism, support and exchange of materials during my research work.

I am also grateful to our collaborators i) Dr. Chhana Ullah and Prof. Dr. Jonathan Gershenzon, Department of Biochemistry, Max Planck Institute for Chemical Ecology, Germany for hormone analysis and ii) Annika Kortz, Dr. Peng Yu and Prof. Dr. Frank Hochholdingher, INRES, University of Bonn, Germany for RNA-seq analysis. I acknowledge the NGS Core Facility, University of Bonn for providing the RNA-seq service. Special gratitude to Dr. Stefanie Müller, INRES for introduction to the ratiometric analysis and Prof. Dr, Markus Schwarzländer, University of Münster for providing the seeds of roGFP2 and YC3.6 lines. Also, thanks to Prof. Edward Farmer, University of Lausanne; Prof. Dr. Remko Offringa, Leiden University and Dr. Alain Goossens, VIB, Belgium for the generous gift of the seeds. Heartfelt thanks to Prof. Dr. Gitta Coaker including her lab technician- Tanya, University of California and Dr. Wan-Hsing Cheng, IPMB, Taiwan for kindly sending the α-CML12 antibody and *aba2-1* mutant seeds respectively. Also, grateful to Prof. Dr. Gabriel Shaaf for allowing the use of their RT-PCR machine at the beginning.

Last but not least I feel my proud privilege to mention the feelings of obligation towards my parents and brothers for their affection, who supported me morally.

Finally, I must thanks to my beloved wife Afsana for her continuous support throughout the PhD journey and well wishes.